

MULTI-USER COMMUNICATION SYSTEMS:
CAPACITY, DUALITY, AND COOPERATION

A DISSERTATION
SUBMITTED TO THE DEPARTMENT OF ELECTRICAL ENGINEERING
AND THE COMMITTEE ON GRADUATE STUDIES
OF STANFORD UNIVERSITY
IN PARTIAL FULFILLMENT OF THE REQUIREMENTS
FOR THE DEGREE OF
DOCTOR OF PHILOSOPHY

Nihar Jindal
July 2004

© Copyright by Nihar Jindal 2004
All Rights Reserved

I certify that I have read this dissertation and that, in my opinion, it is fully adequate in scope and quality, as a dissertation for the degree of Doctor of Philosophy.

Andrea J. Goldsmith
(Principal Adviser)

I certify that I have read this dissertation and that, in my opinion, it is fully adequate in scope and quality, as a dissertation for the degree of Doctor of Philosophy.

Thomas Cover

I certify that I have read this dissertation and that, in my opinion, it is fully adequate in scope and quality, as a dissertation for the degree of Doctor of Philosophy.

Abbas El Gamal

Approved for the University Committee on Graduate Studies.

Abstract

In this thesis we investigate the capacity of multi-user wireless communication channels. We first establish a duality relationship between the Gaussian broadcast and multiple-access channels. This relationship allows us to characterize the capacity region of the Gaussian broadcast channel in terms of the dual Gaussian multiple-access channel, and vice versa. This relationship holds for constant, fading, and multiple antenna channels. We also extend this duality to a class of deterministic, discrete memoryless channels.

We then consider multiple-antenna multi-user channels, for which the capacity region is known only for the multiple-access channel. A duality is established between the dirty paper coding achievable region of the broadcast channel, which is a lower bound to the capacity region, and the true capacity region of the multiple-access channel. We use duality to prove that dirty paper coding achieves the sum rate capacity of the multiple-antenna broadcast channel. Next, we provide an efficient and provably convergent algorithm that computes the sum rate capacity. Finally, we analytically upper bound the advantage that dirty paper coding provides over the sub-optimal technique of time division.

Next we consider power allocation for time-varying wireless channels. We propose the concept of minimum rate capacity, in which average rates are maximized subject to the constraint that a minimum rate must be maintained for each user in all fading states. We explicitly characterize the minimum rate capacity and the corresponding optimal power allocation policies for the fading broadcast channel. We then use duality to characterize the minimum rate capacity of the dual fading multiple-access channel. Finally, we find the optimal power allocation policies that maximize ergodic capacity of a fading broadcast channel with both independent messages and a common, or multicast, message.

In the final chapter, we study the benefits of cooperative communication in an ad-hoc network. In such a network there are multiple transmitters and multiple receivers. We consider cooperation schemes within the transmitting and receiving clusters. Using our earlier work on multiple antenna multi-user channels, we compare achievable rates to those achievable without cooperation.

Acknowledgments

There are a number of people I wish to thank for making my experience as a graduate student one of the most rewarding periods of my life. First off, I would like to thank my advisor Prof. Andrea Goldsmith for her continual support and guidance over the years. Her seemingly boundless energy, continual encouragement, and loyalty to her students has been truly inspirational. Prof. Goldsmith always showed great faith in my abilities and allowed me to work quite independently, but at the same time provided invaluable guidance at the necessary times.

I am also grateful to Prof. Thomas Cover for serving as my associate advisor. Prof. Cover has always been a wonderful reference and I will surely miss his passion and his encyclopedia-like knowledge. In addition, his colorful information theory courses will serve as continual inspiration in any future teaching endeavors. I would also like to thank Professors Abbas El Gamal and Arogyaswami Paulraj. Prof. El Gamal served on my orals committee and reading committee and has also been a wonderful resource and teacher. His course on multi-user information theory was eye-opening to me and many others at Stanford and has already led to the development of similar courses at other universities. Prof. Paulraj served as chairman of my orals committee and also taught a course on space-time communication that greatly broadened my depth of knowledge of the field.

I am also deeply indebted to current and past members of the Wireless Systems Lab, including Sriram Vishwanath, Syed Jafar, Xiangheng Liu, Tim Holliday, Taesang Yoo, Kevin Yu, Shuguang Cui, Stavros Toumpis, Rajiv Agarwal, Hrishikesh Mandyam, and Neelesh Mehta. I will sorely miss our lively blackboard discussions, particularly with Sriram and Syed, and the many hours we passed together both inside and outside of Packard. I am also thankful to my co-authors Sriram Vishwanath, Urbashi Mitra, Syed Jafar, Wonjong Rhee, and Lifang Li, without whom much of this thesis would not be possible. In addition, I would like to thank all those I interacted with while interning in the Wireless Research Lab at Bell Labs. Jerry Foschini was an excellent mentor and role model, and I will always remember Reinaldo Valenzuela's passionate leadership.

Of course, I have to thank my friends, inside and outside of Stanford, for making the years so enjoyable. I would also like to thank my parents for inspiring a love of learning, particularly in math and science. I can't imagine coming so far without their love and

dedication. Finally, I am particularly indebted to my wife Bharti. We met only a year before I came to Stanford, and my experience here would not have been the same without her in my life. She has brought so much love to my life and has been a constant source of support throughout the ups and downs of my studies.

Contents

| | |
|-------------------------------------------------------------|-----------|
| Abstract | iv |
| Acknowledgments | v |
| List of Tables | xi |
| List of Figures | xii |
| 1 Introduction | 1 |
| 1.1 Background and Motivation | 1 |
| 1.2 Overview of Contributions | 5 |
| 2 Capacity of Broadcast and Multiple-Access Channels | 10 |
| 2.1 Discrete Memoryless Channels | 10 |
| 2.1.1 Multiple-Access Channel | 11 |
| 2.2 Gaussian Channels | 11 |
| 2.2.1 AWGN Broadcast Channel | 11 |
| 2.2.2 AWGN Multiple-Access Channel | 13 |
| 2.2.3 Fading Broadcast Channel | 14 |
| 2.2.4 Fading Multiple-Access Channel | 15 |
| 2.2.5 MIMO Broadcast Channel | 16 |
| 2.2.6 MIMO Multiple-Access Channel | 18 |
| 2.3 Summary | 20 |
| 3 Duality of Broadcast and Multiple-Access Channels | 21 |
| 3.1 Gaussian Channels | 22 |
| 3.1.1 AWGN MAC and BC | 22 |
| 3.1.2 Fading MAC and BC | 30 |
| 3.1.3 Outage Capacity | 36 |
| 3.1.4 MIMO MAC and BC | 37 |
| 3.1.5 Multi-Terminal Networks | 42 |
| 3.2 Deterministic Channels | 43 |
| 3.2.1 Deterministic Broadcast Channels | 45 |
| 3.2.2 Deterministic Multiple-Access Channels | 46 |

| | | |
|----------|---------------------------------------------------------------------|-----------|
| 3.2.3 | Duality for $M = aN$ | 46 |
| 3.2.4 | Duality for $N < M < 2N$ | 49 |
| 3.2.5 | Duality Counter-example | 51 |
| 3.2.6 | Deterministic vs. Non-deterministic Channels | 53 |
| 3.3 | Summary | 56 |
| 3.4 | Appendix | 57 |
| 3.4.1 | Power-Preserving Property of MAC-BC Transformations | 57 |
| 3.4.2 | Proof of Corollary 3.8 | 58 |
| 3.4.3 | Proof of Theorem 3.2 | 60 |
| 3.4.4 | Verification of Rate Region Conditions | 65 |
| 3.4.5 | Equivalent Covariance Matrix for Flipped Channel | 66 |
| 3.4.6 | Trace-Preserving Property of MIMO MAC-BC Transformations | 67 |
| 4 | Multiple-Antenna Broadcast Channels | 69 |
| 4.1 | System Model | 70 |
| 4.2 | Sum Rate Capacity | 71 |
| 4.2.1 | Numerical Examples | 77 |
| 4.3 | Computation of Sum Rate Capacity | 81 |
| 4.3.1 | Iterative Water-Filling with Individual Power Constraints | 82 |
| 4.3.2 | Sum Power Iterative Water-Filling | 84 |
| 4.3.3 | Convergence Proof | 85 |
| 4.4 | DPC and TDMA Comparison | 89 |
| 4.4.1 | Definition of DPC Gain | 90 |
| 4.4.2 | Bounds on Sum-Rate Capacity and DPC Gain | 92 |
| 4.4.3 | Asymptotic DPC Gain | 94 |
| 4.4.4 | Tightness of Bound in Rayleigh Fading | 97 |
| 4.4.5 | Rate Region Bounds | 103 |
| 4.4.6 | Frequency Selective Broadcast Channels | 104 |
| 4.4.7 | Transmitter Beamforming | 104 |
| 4.4.8 | Bound on Sum-Rate Gain of Successive Decoding for Uplink | 105 |
| 4.5 | Summary | 107 |
| 4.6 | Appendix | 107 |
| 4.6.1 | Lagrangian Dual Problem | 107 |
| 4.6.2 | Uniqueness of Water-Filling Solution | 109 |
| 4.6.3 | Proof of Theorem 4.5 | 110 |
| 4.6.4 | Proof of Theorem 4.6 | 111 |

| | | |
|----------|-----------------------------------------------------------------------------|------------|
| 5 | Fading Multi-User Channels | 113 |
| 5.1 | Broadcast Channels with Minimum Rate Constraints | 114 |
| 5.1.1 | System Model | 116 |
| 5.1.2 | Ergodic & Zero Outage Capacity Regions | 117 |
| 5.1.3 | Minimum Rate Capacity Region | 118 |
| 5.1.4 | Explicit Characterization of Minimum Rate Capacity Region | 122 |
| 5.1.5 | Alternative Constraints on Transmitted Power | 130 |
| 5.1.6 | Minimum Rate Outage Capacity | 133 |
| 5.1.7 | Numerical Results | 135 |
| 5.1.8 | Multiple-Access Channel with Minimum Rate Constraints | 137 |
| 5.2 | Broadcast Channels with Common Messages | 140 |
| 5.2.1 | System Model | 141 |
| 5.2.2 | Capacity Region Characterization | 141 |
| 5.2.3 | Formulation of Optimization | 142 |
| 5.2.4 | Maximization of Lagrangian | 144 |
| 5.2.5 | Optimal Lagrange Multipliers | 147 |
| 5.2.6 | Numerical Results | 148 |
| 5.2.7 | MIMO Channels | 148 |
| 5.3 | Summary | 151 |
| 5.4 | Appendix | 152 |
| 5.4.1 | Proof of Excess and Effective Power Relationship | 152 |
| 5.4.2 | Proof that Excess to Effective Power Transformation is One-to-One | 152 |
| 5.4.3 | Proof that Noise to Effective Noise Transformation is One-to-One | 153 |
| 5.4.4 | Proof of Effective Noise Ordering Equivalence | 153 |
| 5.4.5 | Proof of Theorem 5.1 | 154 |
| 6 | Capacity of Cooperative Ad-Hoc Networks | 163 |
| 6.1 | System Model | 164 |
| 6.2 | Broadcast and Multiple-Access Channel Background | 166 |
| 6.3 | Non-Cooperative Transmission | 167 |
| 6.4 | Transmitter Cooperation | 167 |
| 6.5 | Receiver Cooperation | 168 |
| 6.6 | Transmitter Cooperation & Receiver Cooperation | 169 |
| 6.7 | Upper Bounds | 171 |
| 6.8 | Numerical Results | 172 |
| 6.8.1 | Bandwidth Assumption 1 | 172 |
| 6.8.2 | Bandwidth Assumption 2 | 174 |
| 6.9 | Summary | 175 |

List of Tables

1.1 Table of abbreviations. 9

List of Figures

| | | |
|------|--------------------------------------------------------------------------------------------------------------------|-----|
| 1.1 | Cellular channel model | 2 |
| 1.2 | Ad-hoc network | 3 |
| 1.3 | Rate region of a two user broadcast channel | 3 |
| 1.4 | Traditional network stack | 5 |
| 2.1 | System Models | 12 |
| 2.2 | System models of the MIMO BC(left) and the MIMO MAC (right) channels | 16 |
| 3.1 | Constant BC capacity in terms of the dual MAC | 26 |
| 3.2 | Scaled dual channels | 27 |
| 3.3 | Constant MAC capacity in terms of the dual BC | 30 |
| 3.4 | Duality of the fading MAC and BC | 31 |
| 3.5 | Capacity regions for the dual fading MAC and BC | 33 |
| 3.6 | MAC capacity region optimization | 34 |
| 3.7 | Multi-Terminal Gaussian Network | 42 |
| 3.8 | Discrete memoryless MAC and BC. | 44 |
| 3.9 | Capacity region of MAC and BC for $M = aN$ | 48 |
| 3.10 | Deterministic BC and MAC capacity regions for $M = 5, N = 3$ | 51 |
| 3.11 | Closeup of deterministic BC and MAC capacity regions for $M = 8, N = 3$. | 53 |
| 3.12 | BSC and an equivalent finite-state channel | 54 |
| 4.1 | Dirty paper broadcast region: $K = 2, M = 2, r_1 = r_2 = 1, H_1 = [1 \ .4], H_2 =$ $[.4 \ 1], P = 10$ | 76 |
| 4.2 | Achievable region and Sato upper bound for Example 1 | 78 |
| 4.3 | Channel Parameters for Example 2 | 79 |
| 4.4 | Algorithm comparison for convergent scenario | 88 |
| 4.5 | Algorithm comparison for divergent scenario | 88 |
| 4.6 | DPC and TDMA rate regions for a 2 user system with 2 transmit antennas | 91 |
| 4.7 | Plots of DPC gain and sum rate for a 2 user, 2 transmit antenna, 1 receive antenna channel | 96 |
| 4.8 | Plots of DPC gain and sum rate for a 2 user, 2 transmit antenna, 2 receive antenna channel | 97 |
| 4.9 | DPC Gain as a function of SNR for a 10 user system | 100 |

| | | |
|------|----------------------------------------------------------------------------------------------------------------------|-----|
| 4.10 | DPC Gain as a function of M for a system with 3 users at 10 dB | 101 |
| 4.11 | DPC Gain as a function of # of users for a system with 4 TX antennas and 1 RX antenna | 102 |
| 4.12 | DPC Gain as a function of SNR for a 10 user system with 1 RX antenna . . | 103 |
| 5.1 | Ergodic, zero-outage, and minimum rate capacity regions for small (left) and large (right) minimum rates. | 121 |
| 5.2 | Ergodic capacity of effective channel and minimum rate capacity region . . | 126 |
| 5.3 | Water-filling diagram for two-user channel with minimum rates | 128 |
| 5.4 | Water-filling diagram for a single-user channel | 129 |
| 5.5 | Capacity of symmetric channel with 40 dB difference in SNR | 137 |
| 5.6 | Capacity of symmetric channel with 20dB difference in SNR | 137 |
| 5.7 | Rician fading with $K = 1$, Average SNR = 10 dB | 138 |
| 5.8 | Rician fading with $K = 5$, Average SNR = 10 dB | 138 |
| 5.9 | Rician fading with $K = 1$, Average SNR = 10 dB, Asymmetric Minimum Rates | 138 |
| 5.10 | MAC Minimum Rate (200 Kbps Min Rate), Ergodic, and Zero-Outage Ca- pacity Regions | 140 |
| 5.11 | Utility Functions for a sample channel with $\mu_2 = 0$ | 145 |
| 5.12 | Plot of capacity region channel with 20 dB SNR difference between the two users | 149 |
| 5.13 | Plot of capacity region channel with 10 dB SNR difference between the two users | 150 |
| 6.1 | System Model | 165 |
| 6.2 | Upper bounds and achievable rates for SNR = 0 dB, G = 10 dB | 173 |
| 6.3 | Upper bounds and achievable rates for SNR = 0 dB, G = 20 dB | 173 |
| 6.4 | Plot of rate vs. gain for SNR = 10 dB | 174 |
| 6.5 | Upper bounds and achievable rates for SNR = 0 dB, G = 10 dB | 175 |
| 6.6 | Upper bounds and achievable rates for SNR = 0 dB, G = 20 dB | 175 |
| 6.7 | Plot of rate vs. gain for SNR = 0 dB, BW assumption 2 | 176 |

Chapter 1

Introduction

Over the last decade or so, wireless communication has transformed from a niche technology into an indispensable part of life. Spectacular growth is still occurring in cellular telephony and wireless networking, with no apparent end in sight. The combination of ubiquitous cellular phone service and rapid growth of the Internet has created an environment where consumers desire seamless, high quality connectivity at all times and from virtually all locations. Though perhaps unrealistic, this is, in essence, a desire to replicate, and perhaps even surpass, the wired experience in a wireless fashion.

In addition to the traditional network usage of wireless technology, many new applications of wireless have emerged over the years. Most notably is the idea of distributed sensing, in which large numbers of cheap, wireless nodes sense some ongoing process and wirelessly communicate with each other and wired access points. Environmental detection, surveillance, and health monitoring are just a few of the innumerable potential uses of distributed sensor networks.

With these visions comes a need for substantial technological improvements. This thesis studies the fundamental limits of wireless networks, and along the way provides suggestions for improvements that may allow us to bring many of these visions to fruition. The remainder of this chapter provides necessary background material and outlines the specific contributions of this thesis.

1.1 Background and Motivation

In this work we study the fundamental system limits, or channel capacity, of wireless communication systems. The notion of channel capacity was first developed by Claude E. Shannon in his landmark 1948 paper “A mathematical theory of communication” [59]. Channel capacity is defined to be the maximum achievable communication rate with arbitrarily small probability of error. Channel capacity is defined with no limits on computational complexity or delay, and thus is a truly fundamental measure of the performance limits of any

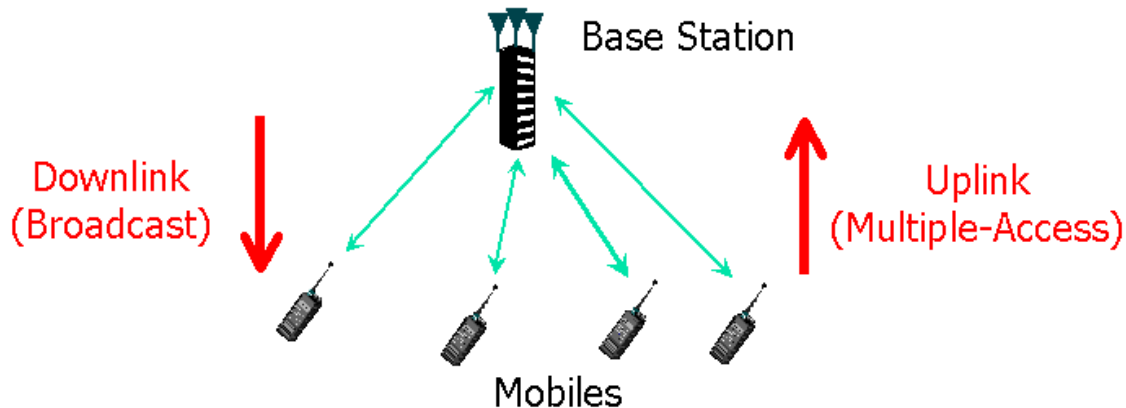


Figure 1.1: Cellular channel model

communication system. The additive white Gaussian noise channel is perhaps the simplest example of a point-to-point channel. In such a channel, the output, denoted by y , is equal to the sum of the input x and additive Gaussian noise n :

$$y = x + n. \quad (1.1)$$

Here the inputs and outputs could be voltages in communication circuitry, and the additive noise could be thermal noise in the circuitry. By Shannon's results, the capacity of such a channel is equal to

$$\mathcal{C} = \log(1 + \text{SNR}) \quad (1.2)$$

where the SNR is equal to the ratio of the power of the input signal to the power of the noise. Thus, asymptotically error-free communication at rates below $\log(1 + \text{SNR})$ is possible, while transmission at any rate larger than $\log(1 + \text{SNR})$ is guaranteed to have errors.

In this thesis we focus exclusively on multi-user communication networks. Most traditional wireless systems are based on the cellular methodology, where the area to be covered is broken into geographical cells. A wired base station or access point is placed in each cell, and the wireless users in each cell communicate exclusively with the corresponding base station, which acts as a gateway to the rest of the network. Cellular telephone systems and wireless local area networks are organized in this manner. Though neighboring cells do generally interact with one another, it is standard to model interference from neighboring cells as an additional source of noise. Thus, we concentrate on the single cell model shown in Figure 1.1, in which there is a single base station and multiple mobile devices.

When the base station is transmitting messages to the mobiles, the channel is referred to as a downlink or broadcast channel. In the context of a wireless network, the base station could be transmitting a different voice call to a number of mobiles while simultaneously transferring data files to other users. Notice that this differs from a TV or radio broadcast, in

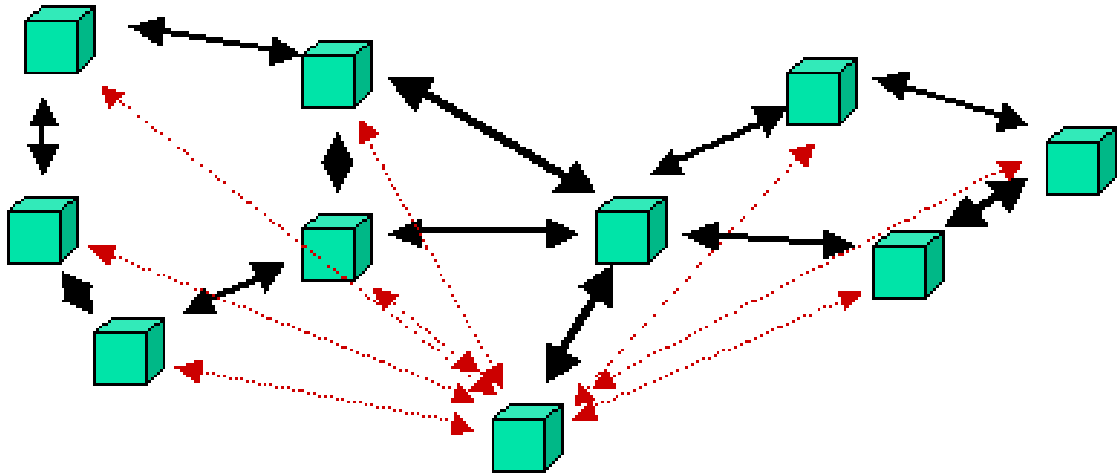


Figure 1.2: Ad-hoc network

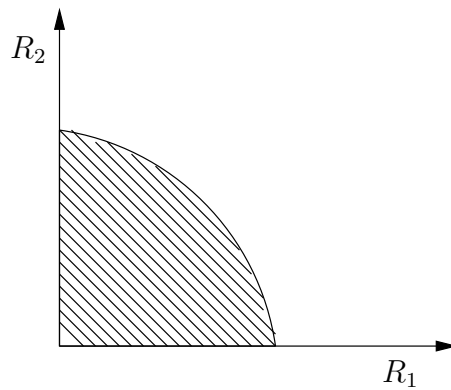


Figure 1.3: Rate region of a two user broadcast channel

which the transmitter sends the same message to each receiver. We are in general interested in transmission of different messages to each mobile. Conversely, when the mobiles are transmitting messages to the base station, the channel is referred to as an uplink or multiple-access channel. Similar to the downlink channel, we are interested in the scenario where each mobile is transmitting a different message to the base station.

In both point-to-point channels and multi-user channels, using multiple antennas at the transmitters and/or receivers has been shown to significantly increase data rates [16] [61] [5]. We thus consider the broadcast and multiple-access channels with and without multiple antennas. In general, the multiple antenna scenario is not nearly as well understood as the single antenna scenario.

In addition to studying cellular systems, we also study ad-hoc and sensor networks in which there are many wireless nodes and no wired infrastructure. Such a network is shown

in Figure 1.2. In these networks, any node can communicate with any other node. When wireless sensors are placed in an environment and need to communicate with each other such infrastructure-less networks are required.

In point-to-point systems, the channel capacity is a single number that dictates the maximum data rate from transmitter to receiver. In a multi-user system such as the broadcast channel in Figure 1.1, the transmitter can simultaneously transmit to more than one user. Thus, the channel capacity is the set of all simultaneously achievable rate vectors. The capacity region of a two user broadcast channel is shown in Figure 1.3. Notice that the axes are R_1 and R_2 , or the transmission rates to receivers 1 and 2 respectively. Here, the capacity region is the set of all achievable rate pairs (R_1, R_2) . Any rate pair not in the capacity region is not achievable, i.e. transmission at a rate pair not in the region will lead to errors. Similarly, the rate region for a K -user broadcast channel or a K -user multiple-access channel is a K -dimensional region. In a K -node ad-hoc network the capacity region is in fact $K(K - 1)$ -dimensional since the K nodes can each communicate with $K - 1$ other nodes.

In this work we study the capacity region of the broadcast channel and multiple-access channel, and consider the capacity of an ad-hoc network when cooperation between nodes is allowed. There are a number of motivations for studying channel capacity. First off, channel capacity by definition establishes limits on the performance of practical communication systems. These limits provide system benchmarks and allow engineers to easily see how much improvement is theoretically possible. Second, the process of studying channel capacity often provides motivation for practical transmission strategies. A prime example of this is in the development of coding theory for wireline telephone channels. Shannon's early channel capacity results established that the capacity of telephone channels was orders of magnitudes greater than the data rates previously thought feasible. Thus, it became a goal of engineers to develop practical communication systems that came close to Shannon's limits, primarily in the form of advanced channel coding techniques. Over the years, theoretical ideas such as random coding have influenced the design of practical systems, and telephone modems have recently approached the channel capacity. Without Shannon's ideas, engineers would have no concrete goal to aim at, nor would they have known when their systems could no longer be significantly improved upon.

A final motivation for the study of channel capacity can be found by examining the entire network stack (shown in Figure 1.4), which traditionally consists of an application layer, followed by the transport and network layers, and finally the physical layer. Channel capacity establishes fundamental limits of the physical/MAC layer of the network architecture. In previous decades, engineers used the network stack architecture to abstract out the functionality of each layer and study each layer independently. In wireless systems, however, the prevailing view is that such abstraction is not possible and that the entire

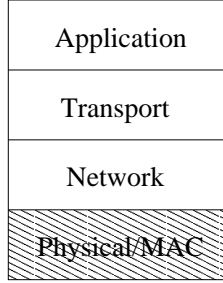


Figure 1.4: Traditional network stack

communication and network system design needs to be thought of simultaneously, which is referred to as cross-layer design. From this viewpoint, it is essential to thoroughly understand performance limits and tradeoffs in the physical layer. Thus, channel capacity is tremendously valuable from a broad network perspective.

1.2 Overview of Contributions

We address the following specific questions in this thesis:

1. Are the multiple-access channel and broadcast channel related?
2. What are the fundamental capacity limits of the multiple antenna broadcast channel?
3. How should rate and power be optimally allocated for fading multi-user channels?
4. Can cooperation provide significant gains in terms of data rate in an ad-hoc network?

We begin by providing the fundamental capacity results known for the multiple-access channel and the broadcast channel in Chapter 2. We define the precise system models for both channels, and present expressions for the capacity regions for both discrete memoryless channels and Gaussian channels. Within the class of Gaussian channels, we consider constant, or AWGN channels, fading channels, and multiple-antenna channels.

The broadcast channel was first introduced by Cover in the 1970's [9], whereas the multiple-access channel dates back to the days of Shannon [58, pp. 641]. While the capacity region of the general multiple-access channel is known [1] [44], the same cannot be said for the broadcast channel. The capacity region of the general broadcast channel remains unknown, but the capacity region of the single antenna Gaussian noise broadcast channel, which we study extensively, was determined by Bergmans [2].

In Chapter 3 we derive a fundamental result relating the broadcast channel and the multiple-access channel. Though the capacity regions for the Gaussian versions of these channels have been known for years, no previous relationship has been established between the uplink and downlink channels. We first consider Gaussian channels and show that

the capacity region of the broadcast channel can be characterized in terms of the capacity region of what we refer to as the *dual* multiple-access channel, and vice versa. The dual multiple-access channel is arrived at by converting the transmitter in the broadcast channel into a receiver and by converting all receivers in the broadcast channel into transmitters. In addition, the dual multiple-access channel has the same channel gains as the broadcast channel and the noise power at the multiple-access receiver is the same as the noise power in each of the broadcast channel receivers. If the uplink and downlink channels in Figure 1.1 are operated on the same frequencies, we would expect them to be duals of each other.

We first establish a capacity region relationship for AWGN broadcast and multiple-access channels and then show it can be extended to fading channels. We then consider Gaussian multiple-antenna broadcast and multiple-access channels. We establish a duality relationship between a lower bound to the capacity region of the multiple-antenna broadcast channel and the actual capacity region of the multiple-antenna multiple-access channel. We later see that this result is crucial in establishing the sum rate capacity of the multiple-antenna broadcast channel. We also attempt to generalize this duality result by considering discrete memoryless broadcast and multiple-access channels. We propose a framework for a duality between discrete memoryless broadcast and multiple-access channels, and we establish a duality relationship between a limited class of deterministic, or noiseless, channels. However, we also prove a negative result by providing an example of a broadcast channel for which no dual multiple-access channel exists within our framework.

In Chapter 4 we consider a multiple antenna broadcast channel, for which the capacity region was previously unknown. Multiple-antenna point-to-point channels were first studied by Foschini and Gans [16] and Telatar [61] in the mid 1990's. In their seminal work, it was shown that adding multiple transmit and receive antennas can lead to spectacular increases in capacity without increasing either power or bandwidth. In fact, capacity grows approximately linearly with the number of antennas. Thus, doubling the number of receive and transmit antennas can theoretically double data rates without an increase in power. This spectacular result has attracted a great deal of interest in industry and in the research community. In our work, we consider the use of multiple antennas in a multiple-user setting instead of a point-to-point setting.

The single-antenna broadcast channel falls into the class of degraded broadcast channels, for which the capacity region is known. Roughly speaking, a broadcast channel is degraded if the users can be absolutely ordered in terms of received signal quality. The multiple-antenna broadcast channel, however, is not a degraded broadcast channel because the channels of each user is described by a matrix of channel gains instead of a single scalar value. Caire and Shamai first applied the concept of dirty paper coding [8] to the multiple antenna broadcast channel [5]. Dirty paper coding is a technique that reduces interference seen at each receiver by pre-subtracting interference at the transmitter. Using dirty paper coding,

Caire and Shamai established an achievable rate region, which is a lower bound to the capacity region by definition, and showed that this rate region actually achieves the sum rate capacity of the multiple antenna broadcast channel for a two user channel in which only the transmitter has multiple antennas.

In this thesis, we extend and build upon this work in a number of different ways. First, we establish a duality between the capacity region of the multiple-access channel and the dirty paper coding achievable rate region of the broadcast channel. We then use this duality to show that dirty paper coding achieves the sum rate capacity of the multiple antenna broadcast channel with an arbitrary number of users and an arbitrary number of transmit and receive antennas. From this result, the sum rate capacity is characterized in terms of a high-dimensional maximization problem. We then propose an efficient and provably convergent algorithm that computes the sum rate capacity of the multiple antenna broadcast channel and the corresponding optimal transmission strategy. Finally, we compare the sum rate capacity of the multiple antenna broadcast channel, achievable through use of dirty paper coding, to the maximum sum rate achievable using time-division multiple-access, a sub-optimal but more practical transmission scheme. This allows us to quantify the advantage that the complex but capacity achieving strategy of dirty paper coding provides over simpler schemes.

In Chapter 5 we consider the problem of optimally allocating rate and power to a fading broadcast channel. Goldsmith and Varaiya first characterized the optimal power allocation policy for a fading single-user channel in [20]. The optimal power policy maximizes the long-term average rates achievable in this channel when both the transmitter and receiver are able to perfectly track the instantaneous channel conditions. This work was extended to the fading broadcast channel in [41, 63] and to the multiple-access channel in [62]. As intuition would suggest, the optimal rate and power policy allocates a large amount of rate to users with strong channels. An unfortunate consequence of focusing exclusively on average rate is that users with poor channels may be allocated very little (or possibly even zero) rate. This is unacceptable for certain delay-sensitive applications such as video, which require a non-negligible instantaneous rate. We therefore find the optimal rate and power allocation policy for the broadcast channel that maximizes long-term average rates subject to a minimum rate constraint for each user in every fading state. This ensures that some minimum level of service can be guaranteed to each user, regardless of channel conditions, while at the same time taking advantage of channel variation. We term this the minimum rate capacity region. Furthermore, we are able to show that the minimum rate capacity achieving power policy can be interpreted in terms of the ergodic capacity (i.e. long-term average rates only) achieving power policy of a related channel.

Finding the optimal rate and power policy for the same performance metric for the fading multiple-access channel seems very difficult. However, we are able to circumvent

this difficulty by using the duality relationship established in Chapter 3 to characterize the minimum rate capacity region of the multiple-access channel in terms of the minimum rate capacity region of the dual broadcast channel.

We also consider fading broadcast channels in which the transmitter wishes to send a common, i.e. multicast, message in addition to independent messages to each user. A common message must be decodable by all users. A fading broadcast channel is essentially a parallel set of broadcast channels, one for each fading state. Each of these broadcast channels is a degraded broadcast channel, for which we know the capacity region. However, in general, the same user does not have the strongest channel in every fading state. Thus, the channel is not degraded in the same direction in each fading state. Such a channel is referred to as a mismatched broadcast channel or a reversely degraded broadcast channel. El Gamal derived the capacity region (with respect only to average rates) of such a channel in the late 1970's in [18]. The given expression for the capacity region is quite difficult to manipulate. In our work, we derive an alternative formulation for the capacity region that is much more amenable to optimization and then find the optimal power allocation policies that maximize average rates. We find the optimal solution to be quite different than the optimal power allocation policies found in [41, 63] when there is no common message. In addition, we also consider multiple antenna broadcast channels with common messages. The capacity of such a channel is unknown, but we propose a dirty-paper coding based achievable region. This region is an intuitive extension of the dirty paper coding region, but it appears quite difficult to determine whether the region is actually the capacity region.

In Chapter 6 we consider an ad-hoc network in which there are multiple transmitters and multiple receivers. We measure the performance gain of using cooperation in such an environment, i.e. we quantify the increase in data rates possible by allowing the transmitters and/or receivers to cooperate. Sendonaris et. al. [57] considered the rates achievable in a channel with two cooperative transmitters and a single receiver. Laneman, Tse, and Wornell considered a model similar to ours, but studied only the effect of cooperation on channel outage, instead of channel capacity, in a fading environment [40]. Host-Madsen has also analyzed a two transmitter, two receiver channel in terms of channel capacity, but only with respect transmitter cooperation [24]. In our work, we study cooperation at both the transmitter and receiver sides in a non-fading environment in terms of data rate increases. We consider different cooperation schemes and show that using transmitter cooperation can yield significant data rate increases over non-cooperation.

Finally, we discuss conclusions and possible extensions of this thesis in Chapter 7. The following table lists some abbreviations used throughout the thesis.

| | |
|------|---------------------------------------------------|
| AWGN | Additive White Gaussian Noise |
| MAC | Multiple-Access Channel |
| BC | Broadcast Channel |
| DMC | Discrete Memoryless Channel |
| MIMO | Multiple Input Multiple Output (Multiple Antenna) |
| DPC | Dirty Paper Coding |
| TDMA | Time-Division Multiple Access |
| CSI | Channel State Information |
| TX | Transmitter |
| RX | Receiver |

Table 1.1: Table of abbreviations.

Chapter 2

Capacity of Broadcast and Multiple-Access Channels

This chapter introduces the two most heavily studied multi-user channels: the broadcast channel and the multiple-access channel. The broadcast channel was introduced by Cover in the early 1970's [9], whereas the multiple-access channel dates back to Shannon [58, pp. 641]. We state the basic system models for both discrete memoryless and Gaussian broadcast and multiple-access channels, along with known capacity results.

2.1 Discrete Memoryless Channels

In the broadcast channel, there is a single transmitter and multiple receivers. The transmitter wishes to send a separate message to each of the receivers¹. For simplicity, we consider only two user broadcast channels in this section. A two-user discrete memoryless broadcast channel consists of three finite sets X, Y, Z and probability distributions $p(y, z|x)$ on $Y \times Z$ for every $x \in X$.

The capacity region of the general broadcast channel remains unknown, and the best known achievable region was given by Marton [50]. However, the capacity region is known for a number of classes of broadcast channels. Of particular interest for this thesis is the class of degraded broadcast channels. A broadcast channel is degraded if there exists a channel $p'(z|y)$ such that Z can be written as the output of a composite channel from Y to Z , i.e. $p(z|x) = \sum_{y \in Y} p(y|x)p'(z|y)$. The capacity region of a degraded broadcast channel was shown by Gallager [17] to equal the closure of the convex hull of all (R_1, R_2) that satisfy:

$$R_1 \leq I(X; Y|U) \tag{2.1}$$

$$R_2 \leq I(U; Z) \tag{2.2}$$

¹In Chapter 5 we also consider the scenario where the transmitter also sends a common message that must be decoded by every receiver.

for some distribution $p(u)p(x|u)p(y, z|x)$ [13]. Rate vectors in the capacity region can be achieved through use of superposition coding, which was first proposed in [9]. In superposition coding, codewords are first chosen for Receiver Z via the auxiliary random variable U , and codewords for Receiver Y (the stronger of the two receivers) are superimposed on U via the distribution $p(x|u)$. Receiver Z decodes only the codeword intended for him, while Receiver Y first decodes the Z codeword and then decodes the codeword intended for himself.

2.1.1 Multiple-Access Channel

A multiple-access channel is a channel in which multiple transmitters wish to send independent messages to a single receiver. Such a channel consists of three finite alphabets X_1, X_2, Y and probability distributions $p(y|x_1, x_2)$ on Y for each $(x_1, x_2) \in X_1 \times X_2$. In [1] and [44], the capacity region of the multiple-access channel was shown to equal the closure of the convex hull of all rate pairs (R_1, R_2) that satisfy

$$R_1 \leq I(X_1; Y|X_2) \quad (2.3)$$

$$R_2 \leq I(X_2; Y|X_1) \quad (2.4)$$

$$R_1 + R_2 \leq I(X_1, X_2; Y) \quad (2.5)$$

for some product distribution $p(x_1)p(x_2)$ [13]. Each input distribution $p(x_1)p(x_2)$ corresponds to a pentagon region, described by the above inequalities, and corner points of the pentagon can be achieved by using successive decoding at the receiver, i.e. by decoding the codeword from one of the users first, and then decoding the other codeword.

2.2 Gaussian Channels

Throughout this thesis we consider discrete-time Gaussian channels, which are continuous input-continuous output channels where the received signal is equal to a scaled version of the transmitted signal and additive Gaussian noise. We consider both the broadcast and multiple-access versions of the Gaussian channel, which are commonly used to model the downlink and uplink channels, respectively, of cellular systems.

2.2.1 AWGN Broadcast Channel

In the Gaussian broadcast channel, the transmitter sends independent information to each receiver by broadcasting a complex signal $X[i]$ to K different receivers simultaneously. Here i denotes the time index. Notice that $X[i]$ contains information for all K receivers, i.e. some part of it is intended for user 1, another part for user 2, etc. Each receiver is assumed to suffer from flat-fading, i.e. the desired signal $X[i]$ is multiplied by a channel gain h_j , and

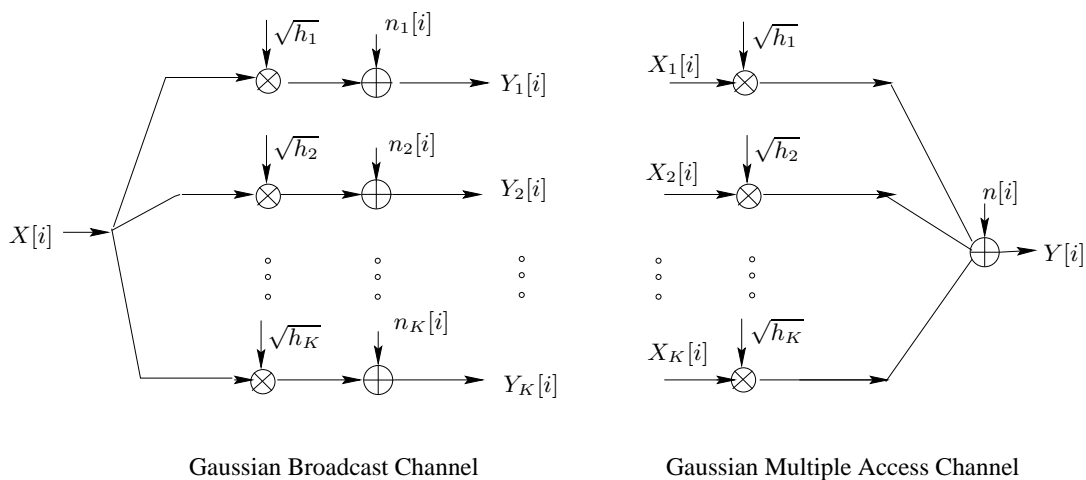


Figure 2.1: System Models

white Gaussian noise $n_j[i]$ is added to the received signal. It is easy to show that the capacity region of the single-antenna broadcast channel only depends on the norm of the channel gain h_j . Thus, for simplicity we will assume that all channel gains are real in the single antenna scenario for both the broadcast channel and multiple-access channel. We let $\mathbf{h} = (h_1, \dots, h_K)$ denote the vector of channel gains, which are fixed for all time. Mathematically, the j -th received signal in the broadcast channel can be described by:

$$Y_j[i] = \sqrt{h_j}X[i] + n_j[i] \quad j = 1, \dots, K$$

where $n_j[i]$ is normally distributed with unit variance². The broadcast channel is illustrated in the left side of Fig. 2.1. The transmitter is subject to an average power constraint \bar{P} , i.e. the input signal $X[i]$ must satisfy $E[X^2] \leq \bar{P}$.

In [2], Bergmans showed that the capacity region of the Gaussian BC with channel gains $\mathbf{h} = (h_1, \dots, h_K)$ and power constraint \bar{P} , denoted $\mathcal{C}_{BC}(\mathbf{h}, \bar{P})$, is given by the rate vectors satisfying

$$R_j \leq \log \left(1 + \frac{h_j P_j^B}{1 + h_j \sum_{k=1}^K P_k^B \mathbf{1}[h_k > h_j]} \right) \quad j = 1, \dots, K \quad (2.6)$$

for any power allocation P_1^B, \dots, P_K^B satisfying $\sum_{j=1}^K P_j^B = \bar{P}$. Additionally, any rate vector taking the form of (2.6) with equality lies on the boundary of the capacity region.

Any set of rates in the capacity region is achievable using successive decoding, in which

²Throughout this work we assume additive Gaussian noise has variance one for simplicity. If the noise variance is not equal to one, the channel gains can be normalized such that the noise variance is unity.

users decode and subtract out signals intended for other users before decoding their own signal. To achieve the boundary points of the BC capacity region, the signals are encoded such that the strongest user can decode all users' signals, the second strongest user can decode all users' signals except for the strongest user's signal, etc. The "strongest" user refers to the user with the largest channel gain h_i .

As seen in [81], the capacity region of the broadcast channel is also achievable via "dirty-paper coding", in which the transmitter "pre-subtracts" (similar to pre-coding for inter-symbol interference mitigation) certain users' codewords instead of receivers decoding and subtracting out other users' signals. When users are encoded in order of increasing channel gains, this technique achieves capacity and is equivalent to successive decoding. Though sub-optimal, dirty paper coding can be performed using any other encoding order as well³. Assuming encoding order $(\pi(1), \pi(2), \dots, \pi(K))$ in which the codeword of User $\pi(1)$ is encoded first, the rates achieved in the BC are:

$$R_{\pi(j)}^B = \frac{1}{2} \log \left(1 + \frac{h_{\pi(j)} P_{\pi(j)}^B}{1 + h_{\pi(j)} \sum_{i=j+1}^K P_{\pi(i)}^B} \right). \quad (2.7)$$

Clearly these rates are achievable and thus are in the BC capacity region. In fact, any rates of the form of (2.7) for any encoding order $\pi(\cdot)$ and any power allocation such that $\sum_{i=1}^N P_i^B = \bar{P}$ lie in $\mathcal{C}_{BC}(\mathbf{h}, \bar{P})$. We will make extensive use of this fact in proofs in Chapter 3. Note that if $\pi(\cdot)$ is in order of increasing channel gains, then the rate vector (2.7) lies on the boundary of the capacity region.

2.2.2 AWGN Multiple-Access Channel

In the Gaussian multiple-access channel, each transmitter transmits a complex-valued input (subject to an average power constraint) and the received signal is equal to the sum of the transmitted signals and additive Gaussian noise. Similar to the broadcast channel, each user is assumed to suffer from flat-fading, i.e. the j -th transmit signal X_j is multiplied by $\sqrt{h_j}$. As noted in the earlier description of the AWGN broadcast channel in Chapter 2.2.1, without loss of generality we assume that each of the channel gains is purely real. Mathematically, the received signal in the multiple-access channel is equal to:

$$Y[i] = \sum_{j=1}^K \sqrt{h_j} X_j[i] + n[i] \quad (2.8)$$

³Note that with successive decoding, when a sub-optimal decoding order is used it must be ensured that all users who are supposed to decode and subtract out a certain user's signal have a large enough channel gain to do so. This limits the rates achievable using successive decoding with a sub-optimal decoding order.

where $n[i]$ is normally distributed with unit variance. Here i again represents the time index. The multiple-access channel is illustrated in the right side of Fig. 2.1. Each transmitter is subject to an average power constraint \bar{P}_j , i.e. the input signal $X_j[i]$ must satisfy $E[X_j^2] \leq \bar{P}_j$ for $j = 1, \dots, K$. From [13], the capacity region of a Gaussian multiple-access channel with channel gains $\mathbf{h} = (h_1, \dots, h_K)$ and power constraints $\bar{\mathbf{P}} = (\bar{P}_1, \dots, \bar{P}_K)$, denoted by $\mathcal{C}_{MAC}(\mathbf{h}, \bar{\mathbf{P}})$ is given by:

$$\mathcal{C}_{MAC}(\mathbf{h}, \bar{\mathbf{P}}) = \left\{ \mathbf{R} : \sum_{j \in S} R_j \leq \log \left(1 + \sum_{j \in S} h_j \bar{P}_j \right) \quad \forall S \subseteq \{1, \dots, K\} \right\}. \quad (2.9)$$

The capacity region of the constant MAC is a K -dimensional polyhedron, and successive decoding with interference cancellation can achieve all corner points of the capacity region [13]. There are $K!$ corner points in the capacity region, and every decoding order corresponds to a different corner point of the capacity region. Given a decoding order $(\pi(1), \pi(2), \dots, \pi(K))$ in which User $\pi(1)$ is decoded first, User $\pi(2)$ is decoded second, etc., the rates of the corresponding corner point are:

$$R_{\pi(j)} = I(X_{\pi(j)}; Y | X_{\pi(1)}, \dots, X_{\pi(j-1)}) \quad (2.10)$$

$$= \log \left(1 + \frac{h_{\pi(j)} \bar{P}_{\pi(j)}}{1 + \sum_{i=j+1}^K h_{\pi(i)} \bar{P}_{\pi(i)}} \right) \quad j = 1, \dots, K. \quad (2.11)$$

We will use this form of the rates throughout this work. The capacity region of the MAC is in fact equal to the convex hull of these $K!$ corner points and all other rate vectors that lie below this convex hull (i.e. are component-wise less than or equal to a rate vector in the convex hull).

2.2.3 Fading Broadcast Channel

In a flat-fading broadcast channel, the channel gains $h_j[i]$ vary over time according to some jointly stationary and ergodic fading process $\mathbf{H} = (\mathbf{H}_1, \dots, \mathbf{H}_K)$. The mathematical description therefore is:

$$Y_j[i] = \sqrt{h_j[i]} X[i] + n_j[i] \quad j = 1, \dots, K.$$

The only difference from the AWGN model in (2.6) is that the channel gain $h_j[i]$ changes according to an ergodic fading process. We consider the scenario where the transmitter and all receivers have perfect CSI (channel state knowledge), i.e. each transmitter and receiver has perfect and instantaneous knowledge of the fading state $\mathbf{h}[i] = (h_1[i], \dots, h_K[i])$.

In order to determine the *ergodic capacity* of this channel, which is the set of all achievable long-term average rates, we must consider power policies. A power policy \mathcal{P}_{BC} is a

function that maps from a joint fading state $\mathbf{h} = (h_1, \dots, h_K)$ to the transmitted power $P_j^B(\mathbf{h})$ for each user. Let \mathcal{F}_{BC} denote the set of all power policies satisfying the average power constraint: $\mathcal{F}_{BC} = \{\mathcal{P}_{BC} : \mathbb{E}_{\mathbf{H}}[\sum_{j=1}^K P_j^B(\mathbf{h})] \leq \bar{P}\}$. From Theorem 1 of [41], the ergodic capacity region of the BC with perfect CSI and power constraint \bar{P} is the union over all power policies in \mathcal{F}_{BC} :

$$\mathcal{C}_{BC}(\mathbf{H}, \bar{P}) = \bigcup_{\mathcal{P}_{BC} \in \mathcal{F}_{BC}} \mathcal{C}_{BC}(\mathbf{H}, \mathcal{P}_{BC}) \quad (2.12)$$

where $\mathcal{C}_{BC}(\mathbf{H}, \mathcal{P}_{BC})$ are the rates achievable using power policy \mathcal{P}_{BC} :

$$\mathcal{C}_{BC}(\mathbf{H}, \mathcal{P}_{BC}) = \left\{ \mathbf{R} : R_j \leq \mathbb{E}_{\mathbf{H}} \left[\log \left(1 + \frac{h_j P_j^B(\mathbf{h})}{1 + h_j \sum_{k=1}^K P_k^B(\mathbf{h}) \mathbf{1}[h_k > h_j]} \right) \right], j = 1, \dots, K \right\}.$$

From this definition it follows that a rate vector \mathbf{R} is in $\mathcal{C}_{BC}(\mathbf{H}, \bar{P})$ if and only if there exists a mapping from joint fading states to rate vectors $\mathbf{R}(\mathbf{h})$ and a power policy $\mathbf{P}^B(\mathbf{h})$ in \mathcal{F}_{BC} such that $\mathbf{R} \leq \mathbb{E}_{\mathbf{H}}[\mathbf{R}(\mathbf{h})]$ with $\mathbf{R}(\mathbf{h}) \in \mathcal{C}_{BC}(\sum_{i=1}^K \mathbf{P}_i^B(\mathbf{h}); \mathbf{h})$ for all fading states \mathbf{h} .

2.2.4 Fading Multiple-Access Channel

In a flat-fading multiple-access channel, the channel gains $h_j[i]$ vary according to a jointly stationary and ergodic fading process $\mathbf{H} = (\mathbf{H}_1, \dots, \mathbf{H}_K)$. The received signal therefore is given by:

$$Y[i] = \sum_{j=1}^K \sqrt{h_j[i]} X_j[i] + n[i]. \quad (2.13)$$

The only difference from the AWGN model in (2.8) is that the channel gain $h_j[i]$ changes according to an ergodic fading process. We consider the scenario where the transmitter and all receivers have perfect CSI, i.e. each transmitter and receiver has perfect and instantaneous knowledge of the fading state $\mathbf{h}[i] = (h_1[i], \dots, h_K[i])$.

In order to determine the *ergodic capacity* of the fading MAC, we must consider power policies. Similar to the fading broadcast channel, a power policy \mathcal{P}_{MAC} is a map from fading states $\mathbf{h} = (h_1, \dots, h_K)$ to the transmitted power $P_j^M(\mathbf{h})$ for each user. Let \mathcal{F}_{MAC} denote the set of all power policies satisfying the K individual average power constraints: $\mathcal{F}_{MAC} = \{\mathcal{P}_{MAC} : \mathbb{E}_{\mathbf{H}}[P_j^M(\mathbf{h})] \leq \bar{P}_j \quad 1 \leq j \leq K\}$.

From Theorem 2.1 of [62], the ergodic capacity region of the multiple-access channel with perfect CSI and power constraints $\bar{\mathbf{P}} = (\bar{P}_1, \dots, \bar{P}_K)$ is:

$$\mathcal{C}_{MAC}(\mathbf{H}, \bar{\mathbf{P}}) = \bigcup_{\mathcal{P}_{MAC} \in \mathcal{F}_{MAC}} \mathcal{C}_{MAC}(\mathbf{H}, \mathcal{P}_{MAC}), \quad (2.14)$$

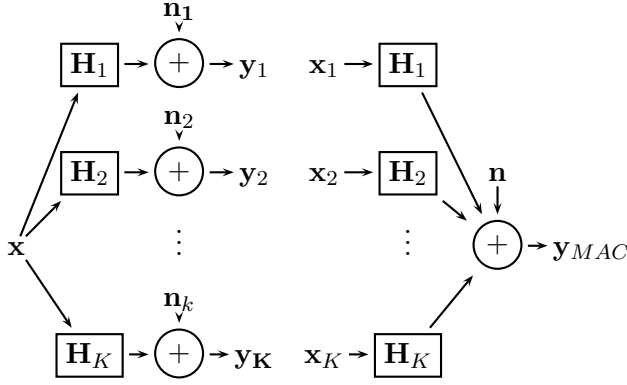


Figure 2.2: System models of the MIMO BC(left) and the MIMO MAC (right) channels

where $\mathcal{C}_{MAC}(\mathbf{H}, \mathcal{P}_{MAC})$ is defined as:

$$\mathcal{C}_{MAC}(\mathbf{H}, \mathcal{P}_{MAC}) = \left\{ \mathbf{R} : \sum_{j \in S} R_j \leq \mathbb{E}_{\mathbf{H}} \left[\log \left(1 + \sum_{j \in S} h_j \bar{P}_j \right) \right] \quad \forall S \subseteq \{1, \dots, K\} \right\}.$$

By Lemma 3.8 of [62], $\mathcal{C}_{MAC}(\mathbf{H}, \mathcal{P}_{MAC})$ can alternatively be defined as:

$$\mathcal{C}_{MAC}(\mathbf{H}, \mathcal{P}_{MAC}) = \{ \mathbb{E}_{\mathbf{H}}[\mathbf{R}(\mathbf{h})] : \mathbf{R}(\mathbf{h}) \in \mathcal{C}_{MAC}(\mathbf{P}^M(\mathbf{h}); \mathbf{h}) \quad \forall \mathbf{h} \}. \quad (2.15)$$

where $\mathbf{R}(\mathbf{h})$ is the rate vector of all K users as a function of the joint fading state and $\mathcal{C}_{MAC}(\mathbf{h}, \mathbf{P}^M(\mathbf{h}))$ is the constant MAC capacity region.

2.2.5 MIMO Broadcast Channel

In a multiple-input, multiple-output (MIMO) broadcast channel, the transmitter and the receivers have multiple antennas. We also loosely use the term MIMO to refer to the case where the transmitter has multiple antennas and the receivers may each only have single antennas. This channel differs from the AWGN broadcast channel described in Chapter 2.2.1 in that the input is vector-valued and the received signal is equal to the product of the channel gain *matrix* and the vector input, plus additive Gaussian noise on each receive antenna component. We consider a MIMO broadcast channel with an M transmit antennas and K receivers with r_1, \dots, r_K receive antennas, respectively. As in the AWGN channel, the transmitter sends independent information to each receiver. The broadcast channel is the system on the left in Fig. 2.2.

Let $\mathbf{x} \in \mathbb{C}^{M \times 1}$ be the transmitted vector signal and let $\mathbf{H}_k \in \mathbb{C}^{r_k \times M}$ be the channel matrix of receiver k where $\mathbf{H}_k(i, j)$ represents the channel gain from transmit antenna j

to antenna i of receiver k . Unlike the scalar broadcast and multiple-access channel, we cannot assume without loss of generality that the channel matrix is purely real. Thus, we explicitly deal with complex quantities throughout all discussions of MIMO channels. The circularly symmetric complex Gaussian noise at receiver k is represented by $\mathbf{n}_k \in \mathbb{C}^{r_k \times 1}$ where $\mathbf{n}_k \sim N(0, \mathbf{I})$. Notice that *each* receive antenna component suffers from additive complex Gaussian noise of variance one. Let $\mathbf{y}_k \in \mathbb{C}^{r_k \times 1}$ be the received signal at receiver k . The received signals are given by:

$$\begin{bmatrix} \mathbf{y}_1 \\ \vdots \\ \mathbf{y}_K \end{bmatrix} = \mathbf{H}\mathbf{x} + \begin{bmatrix} \mathbf{n}_1 \\ \vdots \\ \mathbf{n}_k \end{bmatrix} \quad \text{where} \quad \mathbf{H} = \begin{bmatrix} \mathbf{H}_1 \\ \vdots \\ \mathbf{H}_K \end{bmatrix}. \quad (2.16)$$

The matrix \mathbf{H} represents the channel gains of all receivers. The covariance matrix of the input signal is $\Sigma_x \triangleq \mathbb{E}[\mathbf{x}\mathbf{x}^\dagger]$. The transmitter is subject to an average power constraint P , which implies $\text{Tr}(\Sigma_x) \leq P$. We assume the channel matrix \mathbf{H} is constant and is known perfectly at the transmitter and at all receivers.

Unlike the scalar AWGN broadcast channel described earlier, the MIMO broadcast channel is in general not a degraded broadcast channel. For the scalar channel, users can be absolutely ordered in terms of their channel norms. For the MIMO case, it is not in general possible to order all channels. Thus, the capacity region of the MIMO broadcast channel is not known in general.

An achievable region for the MIMO BC was first obtained in [5]. In [81], the region was extended to the more general multiple-user, multiple-antenna case using the following extension of dirty paper coding [8] to the vector case:

Lemma 2.1 [Yu, Cioffi] *Consider a channel with $\mathbf{y}_k = \mathbf{H}_k\mathbf{x}_k + \mathbf{s}_k + \mathbf{n}_k$, where \mathbf{y}_k is the received vector, \mathbf{x}_k the transmitted vector, \mathbf{s}_k the vector Gaussian interference, and \mathbf{n}_k the vector white Gaussian noise. If \mathbf{s}_k and \mathbf{n}_k are independent and non-causal knowledge of \mathbf{s}_k is available at the transmitter but not at the receiver, then the capacity of the channel is the same as if \mathbf{s}_k is not present.*

In the MIMO BC, this result can be applied at the transmitter when choosing codewords for different receivers. The transmitter first picks a codeword for receiver 1. The transmitter then chooses a codeword for receiver 2 with full (non-causal) knowledge of the codeword intended for receiver 1. Therefore receiver 2 does not see the codeword intended for receiver 1 as interference. Similarly, the codeword for receiver 3 is chosen such that receiver 3 does not see the signals intended for receivers 1 and 2 as interference. This process continues for all K receivers. Receiver 1 subsequently sees the signals intended for all other users as interference, Receiver 2 sees the signals intended for Users 3 through K as interference, etc. Since the ordering of the users clearly matters in such a procedure, the following is an

achievable rate vector:

$$R_{\pi(i)} = \log \frac{\left| \mathbf{I} + \mathbf{H}_{\pi(i)} \left(\sum_{j \geq i} \boldsymbol{\Sigma}_{\pi(j)} \right) \mathbf{H}_{\pi(i)}^\dagger \right|}{\left| \mathbf{I} + \mathbf{H}_{\pi(i)} \left(\sum_{j > i} \boldsymbol{\Sigma}_{\pi(j)} \right) \mathbf{H}_{\pi(i)}^\dagger \right|}} \quad i = 1, \dots, K. \quad (2.17)$$

where π is any permutation of $1, \dots, K$. The rate in (2.17) corresponds to the rates achieved by encoding user $\pi(1)$ first, followed by $\pi(2)$, etc. Thus, user $\pi(i)$ employs dirty paper coding to eliminate interference from the codewords intended for users $\pi(1)$ through $\pi(i-1)$. However, the codewords intended for user $\pi(i+1)$ through $\pi(K)$ are treated as interference at receiver $\pi(i)$. Thus, the effective noise (i.e. noise plus interference) at receiver $\pi(i)$ has covariance $\mathbf{I} + \mathbf{H}_{\pi(i)} \left(\sum_{j > i} \boldsymbol{\Sigma}_{\pi(j)} \right) \mathbf{H}_{\pi(i)}^\dagger$, while the intended signal has covariance $\mathbf{H}_{\pi(i)} \boldsymbol{\Sigma}_{\pi(i)} \mathbf{H}_{\pi(i)}^\dagger$. By whitening the effective noise, it is apparent that the transmission rate to receiver $\pi(i)$ is given by:

$$R_{\pi(i)} = \log \left| \mathbf{I} + \left(\mathbf{I} + \mathbf{H}_{\pi(i)} \left(\sum_{j > i} \boldsymbol{\Sigma}_{\pi(j)} \right) \mathbf{H}_{\pi(i)}^\dagger \right)^{-1} \mathbf{H}_{\pi(i)} \boldsymbol{\Sigma}_{\pi(i)} \mathbf{H}_{\pi(i)}^\dagger \right|, \quad (2.18)$$

which by simple manipulation is equal to the expression in (2.17).

The dirty-paper region $\mathcal{C}_{\text{DPC}}(\mathbf{H}_1, \dots, \mathbf{H}_K, P)$ is defined to equal the convex hull of the union of all such rates vectors over all positive semi-definite covariance matrices $\boldsymbol{\Sigma}_1, \dots, \boldsymbol{\Sigma}_K$ such that $\text{Tr}(\boldsymbol{\Sigma}_1 + \dots + \boldsymbol{\Sigma}_K) = \text{Tr}(\boldsymbol{\Sigma}_x) \leq P$ and over all permutations π :

$$\mathcal{C}_{\text{DPC}}(\mathbf{H}_1, \dots, \mathbf{H}_K, P) \triangleq \text{Co} \left(\bigcup_{\pi, \boldsymbol{\Sigma}_i} \mathbf{R}(\pi, \boldsymbol{\Sigma}_i) \right) \quad (2.19)$$

where $\mathbf{R}(\pi, \boldsymbol{\Sigma}_i)$ is given by (2.17). The transmitted signal is $\mathbf{x} = \mathbf{x}_1 + \dots + \mathbf{x}_K$ and the input covariance matrices are of the form $\boldsymbol{\Sigma}_i = \mathbb{E}[\mathbf{x}_i \mathbf{x}_i^\dagger]$. The dirty paper-coding procedure yields statistically independent signals $\mathbf{x}_1, \dots, \mathbf{x}_K$, from which it follows that $\boldsymbol{\Sigma}_x = \boldsymbol{\Sigma}_1 + \dots + \boldsymbol{\Sigma}_K$.

One important feature to notice about the dirty paper rate equations in (2.17) is that the rate equations are neither a concave nor convex function of the covariance matrices $\boldsymbol{\Sigma}_1, \dots, \boldsymbol{\Sigma}_K$. This makes finding the dirty paper region very difficult, because generally the entire space of covariance matrices which meet the power constraint must be searched over. In this thesis we consider the dirty paper region subject to a transmit power constraint. Recent work [39] has characterized the dirty paper region subject to individual rate constraints (i.e. minimizing the transmit power required to achieve a certain set of rates).

2.2.6 MIMO Multiple-Access Channel

In a MIMO multiple-access channel, each of the transmitters and the receiver possibly have multiple antennas. We consider a MAC where the j -th transmitter has r_j antennas, and

the receiver has M antennas.

Let $\mathbf{x}_k \in \mathbb{C}^{r_k \times 1}$ denote the transmitted signal of transmitter k . Let $\mathbf{y}_{MAC} \in \mathbb{C}^{M \times 1}$ be the received signal and $\mathbf{n} \in \mathbb{C}^{M \times 1}$ the noise vector where $\mathbf{n} \sim N(0, \mathbf{I})$. We also use $\mathbf{H}_k \in \mathbb{C}^{M \times r_k}$ to denote the channel matrix from the k -th transmitter to the receiver (notice that the channel matrix dimensions are opposite those in the MIMO broadcast channel). The received signal is mathematically represented as

$$\begin{aligned} \mathbf{y}_{MAC} &= \mathbf{H}_1 \mathbf{x}_1 + \dots + \mathbf{H}_K \mathbf{x}_K + \mathbf{n} \\ &= \mathbf{H} \begin{bmatrix} \mathbf{x}_1 \\ \vdots \\ \mathbf{x}_K \end{bmatrix} + \mathbf{n} \quad \text{where } \mathbf{H} = [\mathbf{H}_1 \dots \mathbf{H}_K]. \end{aligned}$$

Each transmitter is subject to an individual power constraint of P_1, \dots, P_K . The channel matrices $\mathbf{H}_1, \dots, \mathbf{H}_K$ are assumed to be fixed and known at all transmitters and receivers. The MIMO MAC is shown in the right half of Fig. 2.2.

The capacity region of the MIMO MAC, which we denote as $\mathcal{C}_{MAC}(\mathbf{H}_1, \dots, \mathbf{H}_K, P_1, \dots, P_K)$, was obtained in [61, 66, 83]:

$$\begin{aligned} \mathcal{C}_{MAC}(\mathbf{H}_1, \dots, \mathbf{H}_K, P_1, \dots, P_K) &\triangleq \bigcup_{\{\mathbf{Q}_i \geq 0, \text{Tr}(\mathbf{Q}_i) \leq P_i \quad \forall i\}} \left\{ (R_1, \dots, R_K) : \right. & (2.20) \\ &\left. \sum_{i \in S} R_i \leq \log \left| \mathbf{I} + \sum_{i \in S} \mathbf{H}_i \mathbf{Q}_i \mathbf{H}_i^\dagger \right| \quad \forall S \subseteq \{1, \dots, K\} \right\}. \end{aligned}$$

For each set of covariance matrices $\mathbf{Q}_1, \dots, \mathbf{Q}_K$ the set of achievable rates is equal to a K -dimensional polyhedron that is similar in shape to the AWGN MAC capacity region. Successive decoding with interference cancellation can achieve all corner points of the polyhedron. Every decoding order corresponds to a different corner point of the capacity region, and consequently there are $K!$ corner points in the polyhedron. Given a decoding order $(\pi(1), \pi(2), \dots, \pi(K))$ in which User $\pi(1)$ is decoded first, User $\pi(2)$ is decoded second, etc., the rates of the corresponding corner point are:

$$\begin{aligned} R_{\pi(j)} &= I(X_{\pi(j)}; Y | X_{\pi(1)}, \dots, X_{\pi(j-1)}) \\ &= \log \left| \mathbf{I} + \sum_{i=j}^K (\mathbf{H}_i \mathbf{Q}_i \mathbf{H}_i^\dagger) \right| - \log \left| \mathbf{I} + \sum_{i=j+1}^K (\mathbf{H}_i \mathbf{Q}_i \mathbf{H}_i^\dagger) \right| \\ &= \log \left| \mathbf{I} + \left(\mathbf{I} + \sum_{i=j+1}^K (\mathbf{H}_i \mathbf{Q}_i \mathbf{H}_i^\dagger) \right)^{-1} \mathbf{H}_j \mathbf{Q}_j \mathbf{H}_j^\dagger \right| & (2.21) \end{aligned}$$

These successive decoding rate vectors correspond to the corner points of the K -dimension polyhedron, and can be used to fully characterize the region. Unlike the scalar MAC, the

capacity region of the MIMO MAC is equal to a *union* of such polyhedrons, where the union is taken over all input covariance matrices, each corresponding to a different polyhedron.

Later in this thesis we deal heavily with the sum rate capacity of the MIMO multiple-access channel, denoted C_{MAC}^{sumrate} , which is defined as:

$$\begin{aligned}
 C_{MAC}^{\text{sumrate}}(\mathbf{H}_1, \dots, \mathbf{H}_K, P_1, \dots, P_K) &\triangleq \max_{R_1, \dots, R_K \in \mathcal{C}_{MAC}(\mathbf{H}_1, \dots, \mathbf{H}_K, P_1, \dots, P_K)} \sum_{i=1}^K R_i \\
 &= \max_{\text{Tr}(\mathbf{Q}_i) \leq P_i} \log \left| \mathbf{I} + \sum_{i=1}^K \mathbf{H}_i \mathbf{Q}_i \mathbf{H}_i^\dagger \right| \quad (2.22)
 \end{aligned}$$

2.3 Summary

In this chapter we reviewed known results about the broadcast channel and the multiple-access channel. We purposely studied these channels in a parallel fashion to emphasize the natural symmetry in the two channel models. In the following chapter, we will see that the Gaussian broadcast and multiple-access channels are closely related through their capacity regions, and that there may be a more fundamental relationship between general discrete memoryless broadcast and multiple-access channels.

Chapter 3

Duality of Broadcast and Multiple-Access Channels

In this chapter we establish a fundamental relationship between the multiple-access channel and the broadcast channel. We first examine Gaussian channels (AWGN, fading, and MIMO versions) and show that the broadcast and multiple-access channel capacity regions are exactly equal for what we term *dual* channels, subject to a slight change in the power constraint structure for the multiple-access channel. We then attempt to generalize this notion of multiple-access/broadcast duality to the broader class of discrete memoryless channels. We focus on deterministic, or noiseless, broadcast and multiple-access channels, and show that we can establish a notion of duality for a limited class of deterministic channels. However, we also describe a broadcast channel for which no dual multiple-access channel can exist within our framework.

Establishing a relationship between the multiple-access and broadcast channels is significant for a number of different reasons. First off, establishing such a relationship gives us insight into fundamental connections in multi-user information theory. A connection between channel coding and rate distortion [10] has been known for many decades, and there are a number of other interesting dualities in information theory [52] [13, Section 14.5]. Exploring these connections adds to our general understanding of information theory, and secondly, can also allow us to establish new information theoretic results. This is perhaps the most significant aspect of the MAC-BC duality established in this chapter. In Chapter 3.1.4, a duality is established between the MIMO broadcast and MAC. In Chapter 4.2 of this thesis, this duality result is used to establish the sum rate capacity of a general MIMO broadcast channel, which was previously unknown. In addition, there turn out to be a number of numerical advantages to the dual MIMO MAC, which are further explored in Chapter 4.3. The work in Chapter 3.1 is also published in [35] [36] [38] [68] [69]. Many of the results of Chapter 3.2 appear in [37].

3.1 Gaussian Channels

In this section we show that an inherent duality exists between the Gaussian multiple-access and broadcast channel. Given a broadcast channel, we define the *dual* multiple-access channel to be the same channel with all transmitters converted into receivers and all receivers converted into transmitters, and with the same noise power at the multiple-access channel receiver as in each of the broadcast channel receivers. We can similarly consider the dual of a multiple-access channel, and it is easy to see that this relationship is reciprocal, i.e. that the dual to the dual of a broadcast channel is the original broadcast channel. For AWGN and fading channels, the dual broadcast and multiple-access channels have exactly the same channel gains. For MIMO channels, the channel matrices describing the dual channel are the transpose of the channel matrices describing the original channel.

We show that the capacity regions of the dual channels as defined above are intimately related. First, we show that the broadcast channel capacity region is equal to the union of the capacity regions of the dual multiple-access channel, where the union is taken over all power constraint vectors that sum up to the broadcast channel power constraint. Secondly, we show that the capacity region of the multiple-access channel is equal to the intersection of the capacity regions of the dual broadcast channels, where the intersection is taken over different scaled versions of the dual broadcast channel. We are able to prove this duality relationship for AWGN channels, fading channels for ergodic and outage capacity, and MIMO channels. For the case of the MIMO broadcast channel, we work with the dirty paper coding achievable region instead of the capacity region.

In the following sections, we first state and prove duality results for AWGN broadcast and multiple-access channels. We then consider flat-fading channels, which can essentially be decomposed into an infinite set of AWGN channels, one for each fading state. This decomposition allows us to use the duality of the AWGN channels to prove duality holds for fading channels, both for ergodic capacity and outage capacity. Next, we consider MIMO channels, for which the proofs of duality are significantly more involved than for AWGN channels, but the basic methodology is quite similar. Finally, we address the possible extension of duality to multi-terminal Gaussian networks.

3.1.1 AWGN MAC and BC

In this section we establish a duality connection between the AWGN MAC and BC, which are described in Section 2.2.1 and 2.2.2, respectively. We consider a broadcast channel with fixed channel gains $\mathbf{h} = h_1, \dots, h_K$ and power constraint P . The dual multiple-access channel, which is arrived at by converting all transmitters into receivers and all receivers into transmitters, also has channel gains $\mathbf{h} = h_1, \dots, h_K$. The dual channels can mathematically

be expressed as:

$$\begin{aligned} \text{BC: } Y_j[i] &= \sqrt{h_j}X[i] + n_j[i], \quad j = 1, \dots, K \\ \text{MAC: } Y[i] &= \sum_{j=1}^K \sqrt{h_j}X_j[i] + n[i], \end{aligned}$$

where n_i and n are unit variance Gaussian noise components. In this section we relate the capacity regions of the two channels described above.

Though our motivation for considering the dual multiple-access channel is theoretical, it is interesting to note that the dual broadcast and multiple-access channels can be viewed as the uplink and downlink of a time-division duplexed cellular system. In such a system, the channel is used in a downlink fashion (base station to mobiles, or broadcast channel) for some fraction of time and is used in an uplink fashion (mobiles to base station, or multiple-access channel) for the remaining period of time, and the channel gains are assumed to be fixed over time. Since the same carrier frequency is used for the uplink and downlink in a time-division duplexed system, the channel gains on the uplink and downlink are the same. The assumption of noise powers being the same in all receivers (i.e. unit variance) also seems reasonable assuming that similar receiver structures are used in all devices.

In Theorem 3.1, we show that the capacity region of the AWGN broadcast channel can be characterized simply in terms of the capacity region of the dual multiple-access channel. Then, in Theorem 3.3, we show that the capacity region of the AWGN multiple-access channel can be characterized in terms of the capacity region of the dual broadcast channel.

Theorem 3.1 *The capacity region of a constant Gaussian BC with power constraint \bar{P} is equal to the union of capacity regions of the dual MAC with power constraints (P_1, \dots, P_K) such that $\sum_{j=1}^K P_j = \bar{P}$:*

$$\mathcal{C}_{BC}(\mathbf{h}, \bar{P}) = \bigcup_{\{\mathbf{P}: \mathbf{1} \cdot \mathbf{P} = \bar{P}\}} \mathcal{C}_{MAC}(\mathbf{h}, \mathbf{P}). \quad (3.1)$$

Proof: We first show that every corner point of the dual MAC capacity region for every set of powers is in the dual BC capacity region with the same sum power. Since the capacity region of the MAC is equal to the convex hull of the corner points of the region (see Chapter 2.2.2), this suffices to prove $\bigcup_{\{\mathbf{P}: \mathbf{1} \cdot \mathbf{P} = \bar{P}\}} \mathcal{C}_{MAC}(\mathbf{h}, \mathbf{P}) \subseteq \mathcal{C}_{BC}(\mathbf{h}, \bar{P})$. We then show that every point on the boundary of the BC capacity region is a corner point of the dual MAC capacity region for some set of powers with the same sum power, which gives us the inequality in the other direction and leads to the final result.

Let us consider the successive decoding point of the MAC with power constraints (P_1^M, \dots, P_K^M) corresponding to decoding order $(\pi(1), \dots, \pi(K))$ for some permutation $\pi(\cdot)$

of $(1, \dots, K)$. The rate of User $\pi(j)$ in the MAC at this successive decoding point is

$$R_{\pi(j)}^M = \log \left(1 + \frac{h_{\pi(j)} P_{\pi(j)}^M}{1 + \sum_{i=j+1}^K h_{\pi(i)} P_{\pi(i)}^M} \right).$$

Assuming that the *opposite* encoding order is used in the BC (i.e. User $\pi(1)$ encoded last, etc.), the rate of User $\pi(j)$ in the dual BC when powers (P_1^B, \dots, P_K^B) are used is

$$R_{\pi(j)}^B = \log \left(1 + \frac{h_{\pi(j)} P_{\pi(j)}^B}{1 + h_{\pi(j)} \sum_{i=1}^{j-1} P_{\pi(i)}^B} \right).$$

By defining A_j and B_j as

$$A_j = 1 + h_{\pi(j)} \sum_{i=1}^{j-1} P_{\pi(i)}^B, \quad B_j = 1 + \sum_{i=j+1}^K h_{\pi(i)} P_{\pi(i)}^M, \quad (3.2)$$

we can rewrite the rates in the MAC and BC as

$$R_{\pi(j)}^M = \log \left(1 + \frac{h_{\pi(j)} P_{\pi(j)}^M}{B_j} \right) \quad (3.3)$$

$$R_{\pi(j)}^B = \log \left(1 + \frac{h_{\pi(j)} P_{\pi(j)}^B}{A_j} \right). \quad (3.4)$$

Thus, if the powers satisfy

$$\frac{P_{\pi(j)}^B}{A_j} = \frac{P_{\pi(j)}^M}{B_j}, \quad j = 1, \dots, K \quad (3.5)$$

then the rates in the MAC using powers (P_1^M, \dots, P_K^M) and decoding order $(\pi(1), \dots, \pi(K))$ are the same as the rates in the BC using powers (P_1^B, \dots, P_K^B) and encoding order $(\pi(K), \dots, \pi(1))$. In Chapter 3.4.1 we show that if the powers satisfy (3.5), then $\sum_{j=1}^K P_j^M = \sum_{j=1}^K P_j^B$.

We now need only show that given a set of MAC powers and a MAC decoding order, there exist a set of BC powers satisfying (3.5), and vice versa. To compute BC powers from MAC powers, the relationship in (3.5) must be evaluated in numerical order, starting with

user $\pi(1)$:

$$\begin{aligned}
P_{\pi(1)}^B &= P_{\pi(1)}^M \frac{1}{1 + \sum_{i=2}^K h_{\pi(i)} P_{\pi(i)}^M} \\
P_{\pi(2)}^B &= P_{\pi(2)}^M \frac{1 + h_{\pi(2)} P_{\pi(1)}^B}{1 + \sum_{i=3}^K h_{\pi(i)} P_{\pi(i)}^M} \\
&\dots \\
P_{\pi(K)}^B &= P_{\pi(K)}^M \left(1 + h_{\pi(K)} \sum_{i=1}^{K-1} P_{\pi(i)}^B \right). \tag{3.6}
\end{aligned}$$

Notice that $P_{\pi(1)}^B$ depends only on the MAC powers, $P_{\pi(2)}^B$ depends on the MAC powers and $P_{\pi(1)}^B$, etc. Therefore, any successive decoding point of the MAC region for any set of powers (P_1^M, \dots, P_K^M) with $\sum_{i=1}^K P_i^M = P$ is in the dual BC capacity region.

Similarly, MAC powers can be derived from BC powers starting with User $\pi(K)$ downwards:

$$\begin{aligned}
P_{\pi(K)}^M &= P_{\pi(K)}^B \frac{1}{1 + h_{\pi(K)} \sum_{i=1}^{K-1} P_{\pi(i)}^B} \\
P_{\pi(K-1)}^M &= P_{\pi(K-1)}^B \frac{1 + h_{\pi(K)} P_{\pi(K)}^M}{1 + h_{\pi(K-1)} \sum_{i=1}^{K-2} P_{\pi(i)}^B} \\
&\dots \\
P_{\pi(1)}^M &= P_{\pi(K)}^B \left(1 + \sum_{i=2}^K h_{\pi(i)} P_{\pi(i)}^M \right). \tag{3.7}
\end{aligned}$$

If we consider only permutations corresponding to encoding in order of increasing channel gain, we see that any point on the boundary of the BC capacity region is in the dual MAC region for some set of MAC powers with the same sum power. \square

Note that we refer to (3.6) and (3.7) as the MAC-BC transformations and BC-MAC transformations, respectively,

Corollary 3.1 *The capacity region of a constant Gaussian MAC with power constraints $\mathbf{P} = (P_1, \dots, P_K)$ is a subset of the capacity region of the dual BC with power constraint $P = \mathbf{1} \cdot \mathbf{P}$:*

$$\mathcal{C}_{MAC}(\mathbf{h}, \mathbf{P}) \subseteq \mathcal{C}_{BC}(\mathbf{h}, \mathbf{1} \cdot \mathbf{P}). \tag{3.8}$$

Furthermore, the boundaries of the two regions intersect at exactly one point if the channel gains of all K users are distinct ($h_i \neq h_j$ for all $i \neq j$).

Proof: See Chapter 3.4.2. \square

Theorem 3.1 is illustrated in Fig. 3.1, where $\mathcal{C}_{MAC}(h_1, h_2, P_1, P - P_1)$ is plotted for different values of P_1 . The BC capacity region boundary is shown in bold in the figure. Notice that each MAC capacity region boundary touches the BC capacity region boundary

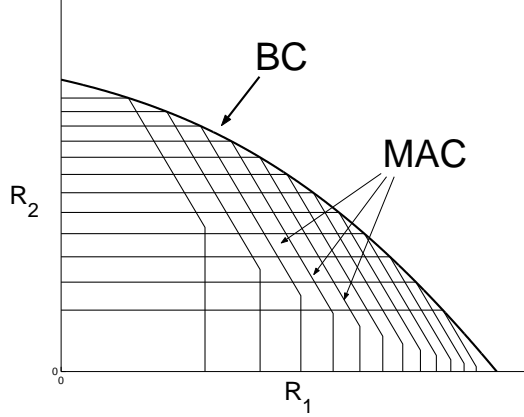


Figure 3.1: Constant BC capacity in terms of the dual MAC

at a *different* point, as specified by Corollary 3.1.

If we carefully examine the union expression in the characterization of the BC in terms of the dual MAC in (3.1), it is easy to see that the union of MAC's is equal to the capacity region of the MAC with a *sum* power constraint $P = \sum_{i=1}^K P_i$ instead of *individual* power constraints (P_1, \dots, P_K) . This is the channel where the transmitters are not allowed to transmit cooperatively (i.e each transmitter transmits an independent message) but the transmitters are allowed to draw from a common power source. Therefore, Theorem 3.1 implies that *the capacity region of the MAC with sum power constraint P equals the capacity region of the dual BC with power constraint P .*

Though the capacity regions of the sum power constraint uplink (MAC) and downlink (BC) are equivalent, the optimal decoding orders on the downlink and uplink are the opposite of each other. From the BC-MAC transformations and from Theorem 3.1, we discover that boundary points of the BC capacity region are achievable in the MAC using successive decoding in order of *decreasing* channel gains. In the BC, it is optimal to give maximum priority (i.e. encode last) to the strongest user, whereas in the sum power MAC, it is optimal to give priority (i.e. decode last) to the weakest user.

We now show that the multiple-access capacity region with individual power constraints can be expressed in terms of the capacity region of the dual broadcast channel. In order to establish this relationship, we make use of a concept called *channel scaling*. Since h_j and P_j always appear as a product in the constant MAC capacity expression (2.9), we can scale h_j by any positive constant α_j and scale P_j by the inverse of α_j without affecting the capacity region. Therefore, $\mathcal{C}_{MAC}(\mathbf{h}, \mathbf{P}) = \mathcal{C}_{MAC}(\boldsymbol{\alpha}\mathbf{h}, \frac{\mathbf{P}}{\boldsymbol{\alpha}})$ for any vector of positive constants $\boldsymbol{\alpha} > 0$. The scaled dual channels are shown in Fig. 3.2. The scaling of the channel and the power constraints clearly negate each other in the multiple-access channel. However, the dual BC is affected by channel scaling and the capacity region of the scaled BC is a function of $\boldsymbol{\alpha}$ since channel scaling affects the power constraint as well as the channel gains of each user

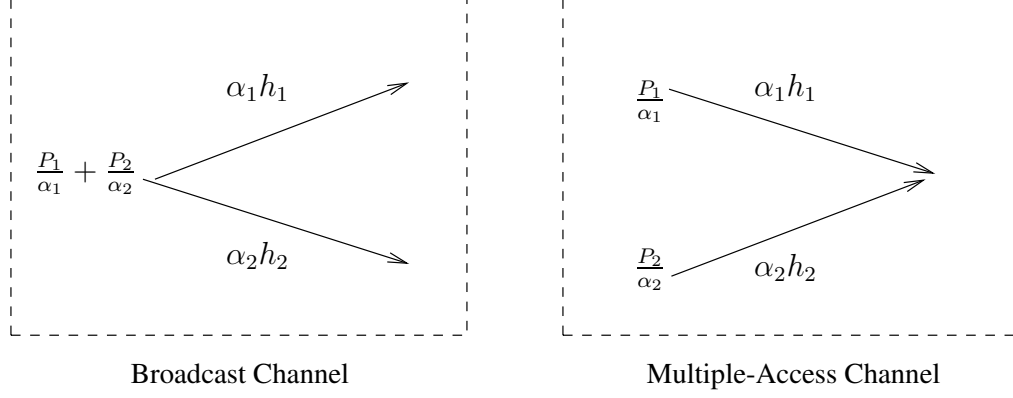


Figure 3.2: Scaled dual channels

relative to all other users. By applying Corollary 3.1 to the scaled MAC and the scaled BC, we find that

$$\mathcal{C}_{MAC}(\mathbf{h}, \mathbf{P}) = \mathcal{C}_{MAC}\left(\boldsymbol{\alpha}\mathbf{h}, \frac{\mathbf{P}}{\boldsymbol{\alpha}}\right) \subseteq \mathcal{C}_{BC}\left(\boldsymbol{\alpha}\mathbf{h}, \mathbf{1} \cdot \frac{\mathbf{P}}{\boldsymbol{\alpha}}\right) \quad \forall \boldsymbol{\alpha} > 0 \quad (3.9)$$

and the boundaries of the MAC capacity region and each scaled BC capacity region intersect. In fact, $\mathcal{C}_{MAC}(\mathbf{h}, \mathbf{P})$ and $\mathcal{C}_{BC}(\boldsymbol{\alpha}\mathbf{h}, \mathbf{1} \cdot \frac{\mathbf{P}}{\boldsymbol{\alpha}})$ intersect at the corner point of the MAC corresponding to decoding in decreasing order of scaled gains $\alpha_i h_i$, opposite the optimal decoding order of the *scaled* BC.

In order to characterize the capacity region of the MAC in terms of the BC, we first establish a general theorem (Theorem 3.2 below) that characterizes *individual transmit power constraint* rate regions of a Gaussian multiple-access channel in terms of *sum transmit power constraint* rate regions. We could directly establish a relationship between the MAC and the scaled BC for the constant channel. However, we present a more general theorem here that is applicable to fading channels as well. Before stating the theorem, we first define the notion of a rate region and the conditions that the rate regions must satisfy in order for the theorems to hold.

Definition 3.1 Let a K -dimensional rate vector be written as $\mathbf{R} = (R_1, \dots, R_K)$ where R_j is the rate of transmitter j . Let $\mathbf{P} = (P_1, \dots, P_K)$ be the vector of transmit power constraints and let $\boldsymbol{\alpha} = (\alpha_1, \dots, \alpha_K)$ be a vector of scaling constants. We define a rate region $R(\mathbf{P})$ as a mapping from a power constraint vector \mathbf{P} to a set in \mathcal{R}_+^K that satisfies the conditions stated in Definition 3.2 below. The $\boldsymbol{\alpha}$ -scaled version of the channel is the channel in which the channel gain from transmitter i to the receiver is scaled by α_i . We denote the rate region of the scaled channel as $R_{\boldsymbol{\alpha}}(\mathbf{P})$.

Definition 3.2 We consider K -dimensional rate regions $R(\mathbf{P}) \subseteq \mathcal{R}_+^K$ that satisfy the following conditions:

1. $R(\mathbf{P}) = R_{\alpha}(\frac{\mathbf{P}}{\alpha}) \forall \alpha > 0, \mathbf{P} > 0$.
2. $S = \{(\mathbf{R}, \mathbf{P}) | \mathbf{P} \in \mathcal{R}_+^K, \mathbf{R} \in R(\mathbf{P})\}$ is a convex set.
3. For all $\mathbf{P} \in \mathcal{R}_+^K$, $R(\mathbf{P})$ is a closed, convex region.
4. If $\mathbf{P}_1 \geq \mathbf{P}_2$ then $R(\mathbf{P}_1) \supseteq R(\mathbf{P}_2)$.
5. If $(R_1, \dots, R_K) \in R(P_1, P_2, \dots, P_K)$, then for any i ,
 $(R_1, \dots, R_{i-1}, 0, R_{i+1}, \dots, R_K) \in R(P_1, \dots, P_{i-1}, 0, P_{i+1}, \dots, P_K)$.
6. If $\mathbf{R} \in R(\mathbf{P})$ and $\mathbf{R}' \leq \mathbf{R}$, then $\mathbf{R}' \in R(\mathbf{P})$.
7. $R(\mathbf{P})$ is unbounded in every direction as \mathbf{P} increases, or $\max_{R_j \in R(\mathbf{P})} R_j \rightarrow \infty$ as $P_j \rightarrow \infty$ for all j .
8. $R(\mathbf{P})$ is finite for all $\mathbf{P} > 0$.

These conditions on the rate region $R(\mathbf{P})$ are very general and are satisfied by nearly any capacity region or rate region. Finally, we define the notion of a sum power constraint rate region.

Definition 3.3 For any scaling α , we define the sum power constraint rate region $R_{\alpha}^{sum}(P_{sum})$ as:

$$R_{\alpha}^{sum}(P_{sum}) \triangleq \bigcup_{\{\mathbf{P} | \mathbf{P} \in \mathcal{R}_+^K, \mathbf{1} \cdot \mathbf{P} \leq P_{sum}\}} R_{\alpha}(\mathbf{P}). \quad (3.10)$$

Having established these definitions, we now state a theorem about rate regions and channel scaling.

Theorem 3.2 Any rate region $R(\mathbf{P})$ satisfying the conditions of Definition 3.2 is equal to the intersection over all strictly positive scalings of the sum power constraint rate regions for any strictly positive power constraint vector \mathbf{P} :

$$R(\mathbf{P}) = \bigcap_{\alpha > 0} R_{\alpha}^{sum} \left(\mathbf{1} \cdot \frac{\mathbf{P}}{\alpha} \right). \quad (3.11)$$

Proof: See Chapter 3.4.3. \square

We now apply Theorem 3.2 to the capacity region of the constant MAC:

Theorem 3.3 The capacity region of a constant Gaussian MAC is equal to the intersection of the capacity regions of the scaled dual BC over all possible channel scalings:

$$\mathcal{C}_{MAC}(\mathbf{h}, \mathbf{P}) = \bigcap_{\alpha > 0} \mathcal{C}_{BC} \left(\alpha \mathbf{h}, \mathbf{1} \cdot \frac{\mathbf{P}}{\alpha} \right). \quad (3.12)$$

Proof: In Chapter 3.4.4 we show that the region $\mathcal{C}_{MAC}(\mathbf{P}; \mathbf{h})$ satisfies the conditions of Definition 3.2. Therefore, by Theorem 3.2 we get:

$$\mathcal{C}_{MAC}(\mathbf{P}; \mathbf{h}) = \bigcap_{\alpha > 0} \mathcal{C}_{MAC}^{sum} \left(\mathbf{1} \cdot \frac{\mathbf{P}}{\alpha}; \alpha \mathbf{h} \right). \quad (3.13)$$

By Theorem 3.1, $\mathcal{C}_{MAC}^{sum} \left(\alpha \mathbf{h}, \mathbf{1} \cdot \frac{\mathbf{P}}{\alpha} \right) = \mathcal{C}_{BC} \left(\alpha \mathbf{h}, \mathbf{1} \cdot \frac{\mathbf{P}}{\alpha} \right)$ for any $\alpha > 0$. Thus, the result follows. \square

Theorem 3.3 is illustrated for a 2-user channel in Fig. 3.3. Although we consider channel scaling of all K users in Theorem 3.2, scaling $K - 1$ users is sufficient because scaling by $\alpha = (\alpha_1, \dots, \alpha_{K-1}, \alpha_K)$ is equivalent to scaling by $(\frac{\alpha_1}{\alpha_K}, \dots, \frac{\alpha_{K-1}}{\alpha_K}, 1)$. We therefore let $\alpha_2 = 1$ and only let α_1 (denoted by α in the figure) vary. In the figure we plot $\mathcal{C}_{BC}(\alpha h_1, h_2, \frac{P_1}{\alpha} + P_2)$ for a range of values of $\alpha > 0$. Since the constant MAC region is a pentagon, the BC characterized by $\alpha = (h_2/h_1)$ and the limit of the broadcast channels as $\alpha \rightarrow 0$ and $\alpha \rightarrow \infty$ are sufficient to form the pentagon. When $\alpha = (h_2/h_1)$, the channel gains of both users are the same and the BC capacity region is bounded by a straight line segment because the capacity region can be achieved by time-sharing between single-user transmission. This line segment corresponds exactly with the forty-five degree line bounding the MAC capacity region. As $\alpha \rightarrow 0$, the total transmit power $\frac{P_1}{\alpha} + P_2$ tends to infinity but the channel gain of User 1 goes to zero. These effects negate each other and cause $R_1 \rightarrow \log(1 + h_1 P_1)$ and $R_2 \rightarrow \infty$. As $\alpha \rightarrow \infty$, the total amount of power converges to P_2 and the channel gain of User 1 becomes infinite. This causes $R_1 \rightarrow \infty$ and $R_2 \rightarrow \log(1 + h_2 P_2)$. These two limiting capacity regions bound the vertical and horizontal line segments, respectively, of the MAC capacity region boundary.

Additionally, by Corollary 3.1, all scaled BC capacity regions except the channel corresponding to $\alpha = (h_2/h_1)$ intersect the MAC at exactly one of the two corner points of the MAC region. Scaled BC capacity regions with $\alpha > (h_2/h_1)$ intersect the MAC at the point where user 2 is decoded last in the MAC (i.e. upper left corner), and all scaled BC capacity regions with $\alpha < (h_2/h_1)$ intersect the MAC at the corner point where user 1 is decoded last (i.e. the lower right corner).

A general K -user constant MAC capacity region is the intersection of $2^K - 1$ hyperplanes, each corresponding to a different subset of $\{1, \dots, K\}$. Therefore, in general, only $2^K - 1$ different scaled BC capacity regions are needed to get the MAC capacity region. One of these regions corresponds to α such that $\alpha_i h_i = \alpha_j h_j$ for all i, j . The other necessary scalings correspond to limiting capacity regions as one or more of the components of α are taken to infinity.

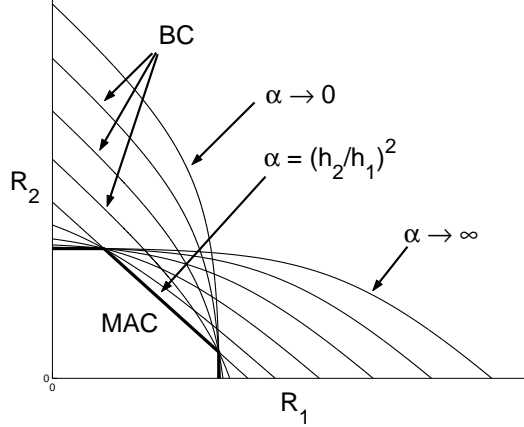


Figure 3.3: Constant MAC capacity in terms of the dual BC

3.1.2 Fading MAC and BC

In this section we show that the duality relationship established for the AWGN broadcast and multiple-access channels also extends to the ergodic capacity of flat-fading broadcast and multiple-access channels. Expressions for the ergodic capacity region of the broadcast and multiple-access channel are given in Chapters 2.2.3 and 2.2.4, respectively. Flat-fading channels can be decomposed into an infinite set of parallel, independent channels, one for each joint fading state. The ergodic capacity for both the MAC and the BC is roughly equal to the average of the capacities of each of these independent channels. We can then use the duality of the MAC and BC for each fading state to show that duality holds for the ergodic capacity region as well.

We consider a fading broadcast channel where the channel gains $(h_1[i], \dots, h_K[i])$ change according to some ergodic and stationary fading process denoted by $\mathbf{H} = (\mathbf{H}_1, \dots, \mathbf{H}_K)$. The dual fading multiple-access channel has channel gains that also vary according to the process \mathbf{H} . Mathematically, we have

$$\begin{aligned} \text{BC: } Y_j[i] &= \sqrt{h_j[i]}X[i] + n_j[i], \quad j = 1, \dots, K \\ \text{MAC: } Y[i] &= \sum_{j=1}^K \sqrt{h_j[i]}X_j[i] + n[i], \end{aligned}$$

where the processes governing the fading gains $\mathbf{h}[i]$ in the MAC and BC are the same. We now show that Theorems 3.1 and 3.3, which applied to AWGN channels, can be extended to flat-fading channels.

Theorem 3.4 *The ergodic capacity region of a fading Gaussian BC with power constraint \bar{P} is equal to the union of ergodic capacity regions of the dual MAC with power constraints*

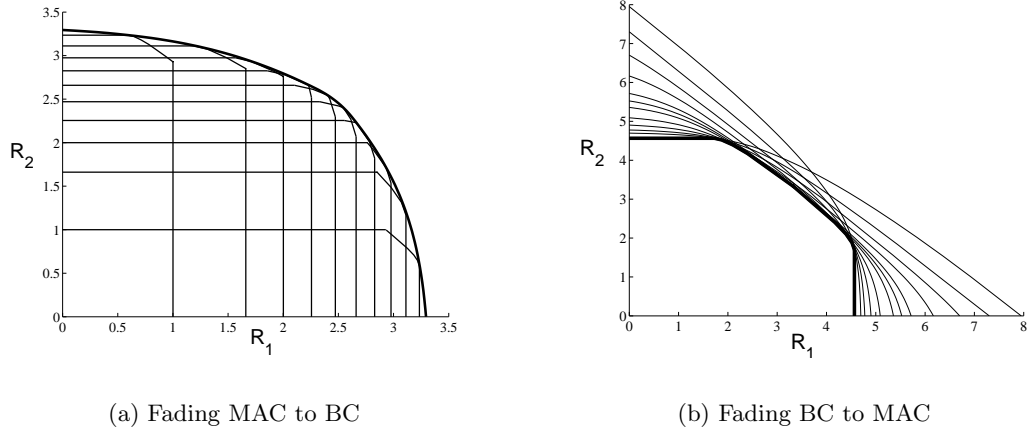


Figure 3.4: Duality of the fading MAC and BC

(P_1, \dots, P_K) such that $\mathbf{1} \cdot \mathbf{P} = \bar{P}$:

$$\mathcal{C}_{BC}(\mathbf{H}, \bar{P}) = \bigcup_{\mathbf{1} \cdot \mathbf{P} = \bar{P}} \mathcal{C}_{MAC}(\mathbf{H}, \mathbf{P}). \quad (3.14)$$

Proof: We show that any rate vector in the union of MAC regions is in the dual BC capacity region, and vice versa. By the definition of $\mathcal{C}_{MAC}(\mathbf{H}, \mathbf{P})$, a rate vector \mathbf{R} is in the ergodic capacity region of the MAC if and only if $\mathbf{R} = \mathbb{E}_{\mathbf{H}}[\mathbf{R}(\mathbf{h})]$ for some $\mathbf{R}(\mathbf{h})$ such that $\mathbf{R}(\mathbf{h}) \in \mathcal{C}_{MAC}(\mathbf{h}, \mathbf{P}^M(\mathbf{h}))$ for all \mathbf{h} . By Theorem 3.1, $\mathbf{R}(\mathbf{h}) \in \mathcal{C}_{MAC}(\mathbf{h}, \mathbf{P}^M(\mathbf{h}))$ implies $\mathbf{R}(\mathbf{h}) \in \mathcal{C}_{BC}(\mathbf{h}, \sum_{i=1}^K \mathbf{P}_i^M(\mathbf{h}))$ for all \mathbf{h} . Therefore, by the definition of $\mathcal{C}_{BC}(\mathbf{H}, \bar{P})$, $\mathbf{R} \in \mathcal{C}_{BC}(\mathbf{H}, \bar{P})$.

Similarly, a rate vector \mathbf{R} is in the ergodic capacity region of the BC if and only if there exists $\mathbf{R}(\mathbf{h})$ such that $\mathbf{R} \leq \mathbb{E}_{\mathbf{H}}[\mathbf{R}(\mathbf{h})]$ with $\mathbf{R}(\mathbf{h}) \in \mathcal{C}_{BC}(\mathbf{h}, \sum_{i=1}^K \mathbf{P}_i^B(\mathbf{h})) \quad \forall \mathbf{h}$ for some $\mathbf{P}^B(\mathbf{h})$ in \mathcal{F}_{BC} . Applying Theorem 3.1 to each fading state, we get that $\mathbf{R}(\mathbf{h}) \in \mathcal{C}_{MAC}(\mathbf{h}, \mathbf{P}^M(\mathbf{h}))$ for some $\mathbf{P}^M(\mathbf{h})$ such that $\sum_{i=1}^K \mathbf{P}_i^M(\mathbf{h}) = \sum_{i=1}^K \mathbf{P}_i^B(\mathbf{h})$ for each \mathbf{h} . Therefore, $\mathbb{E}_{\mathbf{H}}[\sum_{i=1}^K \mathbf{P}_i^M(\mathbf{h})] = \mathbb{E}_{\mathbf{H}}[\sum_{i=1}^K \mathbf{P}_i^B(\mathbf{h})] = \bar{P}$. If we let $Q_i = \mathbb{E}_{\mathbf{H}}[\mathbf{P}_i^M(\mathbf{h})]$, then $\mathbf{R} \in \mathcal{C}_{MAC}(Q_1, \dots, Q_K; \mathbf{H}) \in \bigcup_{\mathbf{1} \cdot \mathbf{P} = \bar{P}} \mathcal{C}_{MAC}(\mathbf{H}, \mathbf{P})$ since $\sum_{i=1}^K Q_i = \bar{P}$. \square

Intuitively, for any MAC power policy, we can use the MAC-BC transformations in each fading state to find a BC power policy that achieves the same rates in each fading state, and therefore the same average rates, using the same sum power in each state. Alternatively, for any BC power policy, we can find a dual MAC power policy that achieves the same rates in each fading state while using the same sum power.

Fig. 3.4(a) illustrates Theorem 3.4. The pentagon-like regions are the dual MAC ergodic capacity regions, while the region denoted with a bold line is the BC ergodic capacity region. As we saw for constant channels, we find that the ergodic capacity region of the MAC with a *sum* power constraint P equals the ergodic capacity region of the dual BC with power

constraint P .

Corollary 3.2 *The ergodic capacity region of a flat-fading Gaussian MAC with power constraints $\bar{\mathbf{P}} = (\bar{P}_1, \dots, \bar{P}_K)$ is a subset of the ergodic capacity region of the dual BC with power constraint $P = \mathbf{1} \cdot \bar{\mathbf{P}}$:*

$$\mathcal{C}_{MAC}(\mathbf{H}, \bar{\mathbf{P}}) \subseteq \mathcal{C}_{BC}(\mathbf{H}, \mathbf{1} \cdot \bar{\mathbf{P}}). \quad (3.15)$$

Proof: This result is a direct consequence of Theorem 3.4. We conjecture that the boundaries of the ergodic capacity region of the MAC and of the dual BC meet at one point, as they do for the constant channel case (Corollary 3.1). We are able to show this for the $K = 2$ case, but not for arbitrary K . \square

Fig. 3.5 illustrates the subset relationship established in Corollary 3.2 for the ergodic capacity regions of the dual flat-fading MAC and BC for a 2-user channel. Due to the fading, the ergodic capacity region of the MAC is bounded by straight line segments connected by a curved section as opposed to the pentagon-like capacity region of the constant MAC. The BC and MAC intersect in the curved portion of the MAC boundary.

We now establish a characterization of the ergodic capacity region of the MAC in terms of the ergodic capacity region of the dual BC. In order to do so, we again use channel scaling. Channel scaling by the factor α for fading channels refers to the ergodic capacity of a channel with power constraints $\frac{P}{\alpha}$ and the fading distribution defined as $\tilde{\mathbf{H}} = \alpha \mathbf{H}$. It is easy to see that channel scaling does not affect the ergodic capacity region of a fading MAC, or that $\mathcal{C}_{MAC}(\mathbf{H}, \mathbf{P}) = \mathcal{C}_{MAC}(\alpha \mathbf{H}, \frac{\mathbf{P}}{\alpha})$ for all $\alpha > 0$. Using Theorem 3.2, we can find an expression for the ergodic capacity region of the MAC in terms of the dual BC.

Theorem 3.5 *The ergodic capacity region of a fading MAC is equal to the intersection of the ergodic capacity regions of the dual BC over all scalings:*

$$\mathcal{C}_{MAC}(\mathbf{H}, \mathbf{P}) = \bigcap_{\alpha > 0} \mathcal{C}_{BC} \left(\alpha \mathbf{H}, \mathbf{1} \cdot \frac{\mathbf{P}}{\alpha} \right) \quad (3.16)$$

Proof: The proof of this is identical to the proof for the constant channel version of this in Theorem 3.3. The fact that the ergodic capacity region of the MAC satisfies the conditions of Theorem 3.2 can be verified by the same arguments used for the constant MAC capacity region in Chapter 3.4.4. \square

Theorem 3.5 is illustrated in Figure 3.4(b). The MAC ergodic capacity region cannot be characterized by a finite number of BC regions as was the case for the AWGN MAC capacity region in Chapter 3.1.1. The BC capacity regions where $\alpha \rightarrow 0$ and $\alpha \rightarrow \infty$ still limit the vertical and horizontal line segments of the MAC ergodic capacity region. The curved section of the MAC boundary, however, is intersected by many different scaled BC ergodic capacity regions.

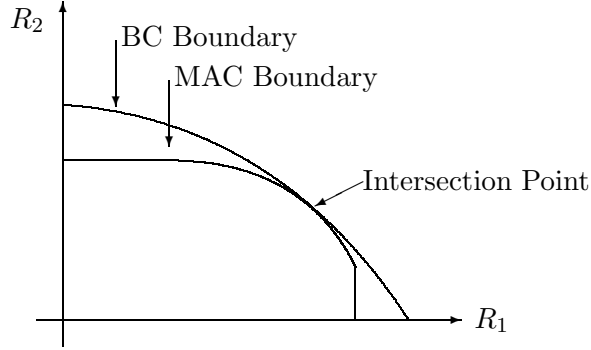


Figure 3.5: Capacity regions for the dual fading MAC and BC

Convex Optimization Interpretation

If we consider the boundary points of $\mathcal{C}_{MAC}(\mathbf{H}, \mathbf{P})$ from a convex optimization viewpoint, we can gain some additional insight into the MAC-BC duality and Theorem 3.5. Since the region $\mathcal{C}_{MAC}(\mathbf{H}, \mathbf{P})$ is closed and convex, we can fully characterize the region by the following convex maximization:

$$\max_{\mathbf{R} \in \mathcal{C}_{MAC}(\mathbf{H}, \mathbf{P})} \boldsymbol{\mu} \cdot \mathbf{R} \quad \text{such that: } \mathbf{P} \leq \bar{\mathbf{P}} \quad (3.17)$$

over all non-negative priority vectors $\boldsymbol{\mu} = (\mu_1, \dots, \mu_K)$ such that $\boldsymbol{\mu} \cdot \mathbf{1} = 1$. Since (3.17) is a convex problem, we know that the solution to the original optimization also maximizes the Lagrangian function $\boldsymbol{\mu} \cdot \mathbf{R} - \sum_{i=1}^K \lambda_i (P_i - \bar{P}_i)$ for the *optimal* Lagrangian multipliers $\boldsymbol{\lambda}^* = (\lambda_1^*, \dots, \lambda_K^*)$. The optimal Lagrange multipliers $\boldsymbol{\lambda}^*$ can be interpreted as the power prices of the K users, or alternatively λ_i^* is the sensitivity of the maximum of $\boldsymbol{\mu} \cdot \mathbf{R}$ to a change in the power constraint \bar{P}_i .

For each non-negative priority vector $\boldsymbol{\mu}$, there exists an optimum Lagrange multiplier $\boldsymbol{\lambda}^*$. If for some $\boldsymbol{\mu}$ we have $\lambda_1^* > \lambda_2^*$, then constraint \bar{P}_1 is more restrictive than constraint \bar{P}_2 . In this scenario, increasing \bar{P}_1 while decreasing \bar{P}_2 by the same amount would lead to an increase in the maximum weighted sum rate $\boldsymbol{\mu} \cdot \mathbf{R}$. On the other hand, if $\lambda_1^* = \lambda_2^* = \dots = \lambda_K^*$, then each power constraint is equally “hard” and no trade-off of power between different users would increase the maximum. Thus, the solution is sum-power optimal in the sense that having individual power constraints $(\bar{P}_1, \dots, \bar{P}_K)$ is no more restrictive than having a sum power constraint $\sum_{i=1}^K \bar{P}_i$. Therefore, the maximum value of $\boldsymbol{\mu} \cdot \mathbf{R}$ in the sum power constraint MAC capacity region and in the individual power constraint MAC capacity region are *equal* for any $\boldsymbol{\mu}$ such that the optimal Lagrangian multipliers are all equal. Since the capacity regions of the sum power constraint MAC and the dual BC are equivalent as established in Theorem 3.4, this implies that the boundaries of the MAC (with individual power constraints) and the dual BC touch at any point on the MAC boundary where $\lambda_1^* = \lambda_2^* = \dots = \lambda_K^*$.

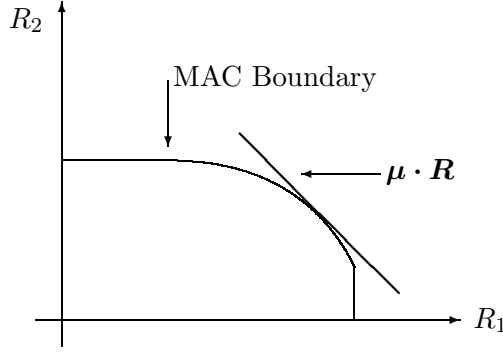


Figure 3.6: MAC capacity region optimization

By scaling the channel gains, we can force the Lagrangians to be equal. If λ^* is the optimal Lagrange multiplier for some priority vector μ for the unscaled MAC, then $\alpha\lambda^*$ is the optimal Lagrange multiplier for the MAC scaled by α . Therefore we can scale the channel appropriately so that $\alpha_i\lambda_i^*$ are equal for all i . Using this method, every point on the boundary of $\mathcal{C}_{MAC}(\mathbf{H}, \mathbf{P})$ can be shown to be on the boundary of the sum power MAC (and therefore of the dual BC) for some scaling vector. The proof of Theorem 3.2 in Chapter 3.4.3 is based on this idea.

If we examine the points where the MAC and BC capacity region boundaries touch, we find that there is also a fundamental relationship between the power policies used to achieve these points. The optimal power policies (i.e. boundary achieving power policies) for the fading MAC and BC are established in [62] and [41] respectively. Given a priority vector μ , it is possible to find the optimal power policy that maximizes $\mu \cdot \mathbf{R}$ in both the MAC and the BC. Due to the duality of these channels, the optimal power policies derived independently for the BC and MAC are related by the MAC-BC (3.6) and BC-MAC (3.7) transformations at the points where the BC and MAC capacity region boundaries touch.

Optimal MAC/BC Decoding Order

The duality of the flat-fading MAC and BC leads to some interesting observations about the optimum decoding order in the BC and MAC. By duality, any point on the boundary of the BC ergodic capacity region is also on the boundary of the MAC ergodic capacity region for some set of power constraints whose sum equals the BC power constraint. Additionally, it is easy to show from the proof of Theorem 3.2 that the MAC and BC ergodic capacity regions are “tangential” at the point where the boundaries touch in the sense that the weighted rate sum $\mu \cdot \mathbf{R}$ at the intersection point is equal to the maximum of $\mu \cdot \mathbf{R}$ in $\mathcal{C}_{MAC}(\mathbf{H}, \mathbf{P})$ and in $\mathcal{C}_{BC}(\mathbf{H}, \mathbf{P})$ for the same μ .

From results on the ergodic capacity region of the MAC [62,67], it is optimal to decode users in order of increasing priority μ_i in all fading states. Therefore, a fixed decoding order in all fading states is optimal for the MAC. Suppose we consider a point on the boundary

of the BC capacity region that is also a boundary point of a dual MAC capacity region. The optimal MAC and BC power policies will be related by the power transformations given earlier. Additionally, the decoding order in the BC and the MAC are opposite in each fading state. Therefore, by duality, we see that boundary points can be achieved in the BC by decoding in order of *decreasing* priority. From basic results on the BC, however, users should be decoded in order of increasing channel gain in every fading state. This apparent inconsistency is resolved by the fact that a user is allocated power in the BC only if all users with larger priority have smaller channel gains. Thus, decoding in order of decreasing priority is equivalent to decoding in order of increasing channel gain for the optimal BC power allocation policy.

Using duality in the form of Theorem 3.3, every boundary point of the MAC is also a boundary point of a scaled BC. In the α -scaled BC, users are decoded in increasing order of $\alpha_i h_i$. Since $\alpha_i = \frac{\lambda_K^*}{\lambda_i^*}$ for the correct scaling (see proof of Theorem 3.2 for justification), users are decoded in order of *increasing* $\frac{h_i}{\lambda_i^*}$ in the BC. By duality, the opposite decoding order should be used in the MAC. Thus, users should be decoded in order of *decreasing* $\frac{h_i}{\lambda_i^*}$. Again, the apparent inconsistency with decoding users in the MAC in order of increasing priority is resolved by the optimal power allocation policy.

Symmetric Channels

If the joint fading distribution is symmetric and all K transmitters in the MAC have the same power constraint, then the optimal Lagrange multipliers corresponding to the sum rate capacity of the MAC (the maximum of $\boldsymbol{\mu} \cdot \mathbf{R}$ where $\mu_1 = \mu_2 = \dots = \mu_K = \frac{1}{K}$) are all equal by symmetry. As discussed in Section 3.1.2, this implies that the unscaled MAC and the unscaled BC (i.e. $\boldsymbol{\alpha} = \mathbf{1}$) ergodic capacity regions meet at the maximum sum rate point of their capacities. In this scenario the optimal power policies in the dual channels are identical, since only the user with the largest fading gain transmits in each fading state [41] [62]. For asymmetric fading distributions and/or power constraints, the uplink sum rate capacity is generally strictly less than the downlink sum rate capacity.

Frequency Selective Channels

Duality easily extends to frequency selective (ISI) channels as well. Broadcast and multiple-access channels with time-invariant, finite-length impulse responses and additive Gaussian noise were considered in [7] [21]. The dual channels have the same impulse response on the uplink and downlink, and the same noise power at each receiver. Similar to flat-fading channels, frequency-selective channels can be decomposed into a set of parallel independent channels, one for each frequency. Using the duality of each of these independent channels, it is easy to establish that the capacity region of the BC is equal to the capacity region of the dual MAC with a sum power constraint. Furthermore, it is also straightforward to

verify that the conditions of Theorem 3.2 hold, and thus the capacity region of the MAC is equal to an intersection of scaled BC capacity regions¹.

3.1.3 Outage Capacity

In this section we show that duality holds for the outage capacity of fading channels. The outage capacity region (denoted $\mathcal{C}_{MAC}^{out}(\mathbf{H}, \bar{\mathbf{P}}, \mathbf{P}^{out})$ and $\mathcal{C}_{BC}^{out}(\mathbf{H}, \bar{\mathbf{P}}, \mathbf{P}^{out})$) is defined as the set of rates that can be maintained for user j for a fraction P_j^{out} of the time, or in all but P_j^{out} of the fading states [42, 43]. Outage capacity is concerned with situations in which each user (in either the BC or MAC) desires a constant rate a certain percentage of the time. The zero-outage capacity² [22, 42] is a special case of outage capacity where a constant rate must be maintained in *all* fading states, or where $\mathbf{P}^{out} = 0$.

By definition, a rate vector \mathbf{R} is in $\mathcal{C}_{MAC}^{out}(\mathbf{H}, \bar{\mathbf{P}}, \mathbf{P}^{out})$ if and only if there exists a power policy $\mathbf{P}(\mathbf{h})$ satisfying the power constraints $\bar{\mathbf{P}}$ and a rate function $\mathbf{R}(\mathbf{h})$ such that $\mathbf{R}(\mathbf{h}) \in \mathcal{C}_{MAC}(\mathbf{h}, \mathbf{P}(\mathbf{h}))$ for all \mathbf{h} and $Pr[\mathbf{R}_j(\mathbf{h}) \geq \mathbf{R}_j] \geq 1 - P_j^{out}$. The BC outage capacity region is defined similarly, except that the power policy must only satisfy a sum power constraint and $\mathbf{R}(\mathbf{h})$ must be in $\mathcal{C}_{BC}(\mathbf{h}, \sum_{i=1}^K \mathbf{P}_i(\mathbf{h}))$ for all \mathbf{h} . By applying duality to each fading state, it is clear that every rate vector in the MAC outage capacity region is achievable in the dual BC, and vice versa. Thus, the outage capacity region of the BC is equal to the sum power constraint outage capacity region of the MAC, with the same outage vector \mathbf{P}^{out} :

$$\mathcal{C}_{BC}^{out}(\mathbf{H}, \bar{\mathbf{P}}, \mathbf{P}^{out}) = \bigcup_{\{\mathbf{P}: \mathbf{1} \cdot \mathbf{P} = \bar{\mathbf{P}}\}} \mathcal{C}_{MAC}^{out}(\mathbf{H}, \mathbf{P}, \mathbf{P}^{out}). \quad (3.18)$$

Using Theorem 3.2, it also follows that the MAC outage capacity region is equal to the intersection of the scaled BC outage capacity regions:

$$\mathcal{C}_{MAC}^{out}(\mathbf{H}, \mathbf{P}, \mathbf{P}^{out}) = \bigcap_{\alpha > 0} \mathcal{C}_{BC}^{out}\left(\alpha \mathbf{H}, \mathbf{1} \cdot \frac{\mathbf{P}}{\alpha}, \mathbf{P}^{out}\right). \quad (3.19)$$

Though the outage capacity region has been characterized for both the BC and MAC [42, 43], the MAC region can be quite difficult to find numerically. Duality, however, allows the region to easily be found numerically via the dual BC outage capacity region.

There is also a more stringent notion of outage capacity in which outages must be declared simultaneously for all users (referred to as common outage). In this situation there is only one outage probability (for all users). It is also straightforward to show that

¹Interestingly, the authors of [7] used the concept of channel scaling in order to find the optimal power allocation policy of the frequency-selective MAC. This turns out to be the same channel scaling that is used to characterize the MAC in terms of the dual BC.

²Zero-outage capacity is referred to as *delay-limited capacity* in [22].

duality extends to common outage as well.

3.1.4 MIMO MAC and BC

In this section we show that the capacity region of the MIMO MAC with a sum power constraint of P for the K transmitters is the same as the dirty paper region of the dual MIMO BC with power constraint P . In other words, any rate vector that is achievable in the dual MAC with power constraints (P_1, \dots, P_K) is in the dirty paper region of the dual BC with power constraint $\sum_{i=1}^K P_i$. Conversely, any rate vector that is in the dirty paper region of the BC is also in the dual MIMO MAC region with the same total power constraint. Expressions for the dirty paper rate region of the MIMO BC and the capacity region of the MIMO MAC are given in Chapters 2.2.5 and 2.2.6, respectively.

Theorem 3.6 *The dirty paper region of a MIMO broadcast channel with power constraint P is equal to the capacity region of the dual MIMO MAC with sum power constraint P .*

$$\mathcal{C}_{\text{DPC}}(\mathbf{H}_1, \dots, \mathbf{H}_K, P) = \bigcup_{\mathbf{1} \cdot \mathbf{P} \leq P} \mathcal{C}_{\text{MAC}}(\mathbf{H}_1^\dagger, \dots, \mathbf{H}_K^\dagger, \mathbf{P}) \quad (3.20)$$

Proof: We first prove $\mathcal{C}_{\text{DPC}}(\mathbf{H}_1, \dots, \mathbf{H}_K, P) \supseteq \bigcup_{\mathbf{P}} \mathcal{C}_{\text{MAC}}(\mathbf{H}_1^\dagger, \dots, \mathbf{H}_K^\dagger, \mathbf{P})$ by showing that every rate vector achieved by successive decoding in the MAC is also in the dirty paper region of the dual MIMO BC. More specifically, we show by the MAC to BC transformations below that for every set of MAC covariance matrices $\mathbf{Q}_1, \dots, \mathbf{Q}_K$ and any decoding order in the MAC, there exist BC covariance matrices $\mathbf{\Sigma}_1, \dots, \mathbf{\Sigma}_K$ using the same sum power as the MAC (i.e. $\sum_{i=1}^K \text{Tr}(\mathbf{Q}_i) = \sum_{i=1}^K \text{Tr}(\mathbf{\Sigma}_i)$) such that the MAC rates are achievable in the BC using dirty paper coding. Each set of MAC covariance matrices corresponds to a K -dimensional polyhedron, as described in (2.20), with the $K!$ corner points of the polyhedron corresponding to performing successive decoding at the receiver in one of the $K!$ possible decoding orders. By the convexity of the dirty paper region (due to the convex hull operation), it is sufficient to show that the corner points of all polyhedrons (i.e. the successive decoding points) corresponding to all MAC covariance matrices are in the dirty paper region of the dual MIMO BC. Thus, with the MAC to BC transformations described below, this implies $\mathcal{C}_{\text{DPC}}(\mathbf{H}_1, \dots, \mathbf{H}_K, P) \supseteq \bigcup_{\mathbf{P}} \mathcal{C}_{\text{MAC}}(\mathbf{H}_1^\dagger, \dots, \mathbf{H}_K^\dagger, \mathbf{P})$.

We complete the proof by showing $\mathcal{C}_{\text{DPC}}(\mathbf{H}_1, \dots, \mathbf{H}_K, P) \subseteq \bigcup_{\mathbf{P}} \mathcal{C}_{\text{MAC}}(\mathbf{H}_1^\dagger, \dots, \mathbf{H}_K^\dagger, \mathbf{P})$. We prove this by showing, via the BC to MAC transformations below, that for every set of BC covariance matrices and any encoding order there exist MAC covariance matrices that achieve the same set of rates using the same sum power. The convexity of the MIMO MAC sum power constraint region thus implies that $\mathcal{C}_{\text{DPC}}(\mathbf{H}_1, \dots, \mathbf{H}_K, P) \subseteq \bigcup_{\mathbf{P}} \mathcal{C}_{\text{MAC}}(\mathbf{H}_1^\dagger, \dots, \mathbf{H}_K^\dagger, \mathbf{P})$. This completes the proof, provided we have the transformations given below that map the MAC covariances to the BC covariances and vice versa.

□

Next, we explain some terminology used in the transformations, followed by the actual transformations. It is important to point out that the transformations require a reverse decoding/encoding order of the users in the dual MAC/BC channel. In other words, if User 1 is decoded first in the MAC (i.e. User 1 suffers interference of all other users' signals), then we must encode User 1's signal *last* (i.e. no interference from other users) in the BC to achieve the same rates using these transformations. Also, notice that the proof of duality only requires *existence* of BC covariance matrices that satisfy the rates achieved by a set of MAC covariance matrices, and vice versa. However, the below transformations actually provide equations for the transformed BC covariances as a function of the MAC covariances, and vice versa.

Terminology

First, we explain the terms *effective channel* and *flipped channel*. A single user MIMO system Θ with channel matrix \mathbf{H} , additive Gaussian noise with covariance \mathbf{X} , and additive independent Gaussian interference with covariance \mathbf{Z} is said to have an effective channel of $(\mathbf{X} + \mathbf{Z})^{-1/2}\mathbf{H}$. The set of rates achievable by Θ and a different system with channel matrix equal to the effective channel and with additive white noise of unit variance and no interference are the same. Also, the capacity of a system Θ_1 with effective channel matrix \mathbf{Y} and the capacity of system Θ_2 with effective channel matrix \mathbf{Y}^\dagger , termed the flipped channel, are the same [61]. In other words, for every transmit covariance Σ in Θ_1 , there exists a $\bar{\Sigma}$ in Θ_2 with $\text{Tr}(\bar{\Sigma}) \leq \text{Tr}(\Sigma)$ such that the rate achieved by $\bar{\Sigma}$ in Θ_2 is equal to the rate achieved by Σ in Θ_1 . In Chapter 3.4.5 we show that $\bar{\Sigma} = \mathbf{F}\mathbf{G}^\dagger\Sigma\mathbf{G}\mathbf{F}^\dagger$ meets this criterion where the Singular Value Decomposition (SVD) of \mathbf{Y} is $\mathbf{Y} = \mathbf{F}\mathbf{\Lambda}\mathbf{G}^\dagger$, where $\mathbf{\Lambda}$ is square and diagonal³. Next, we describe the covariance transformations.

MAC to BC Transformation

In this section we derive a transformation that takes as inputs a set of MAC covariance matrices and a decoding order and outputs a set of BC covariances with the same sum power as the MAC covariances that achieve rates equal to the rates achieved in the MAC using the MAC covariance matrices and successive decoding with the specified decoding order. Note that this is the MIMO analogue of the MAC-BC transformation for scalar channels given in (3.6).

Since the numbering of the users is arbitrary, we assume that User 1 is decoded first, User 2 second, and so on at the MAC receiver. Let $\mathbf{A}_j \triangleq (\mathbf{I} + \mathbf{H}_j(\sum_{l=1}^{j-1} \Sigma_l)\mathbf{H}_j^\dagger)$ and $\mathbf{B}_j \triangleq (\mathbf{I} + \sum_{l=j+1}^K \mathbf{H}_l^\dagger\mathbf{Q}_l\mathbf{H}_l)$. The rate achieved by User j in the MAC for some arbitrary

³Note that the standard SVD command in MATLAB does not always return a square and diagonal matrix of singular values, so modification may be necessary to generate the flipped matrix correctly.

set of positive semi-definite covariance matrices $(\mathbf{Q}_1, \dots, \mathbf{Q}_K)$ is given in (2.21) and can be simplified as:

$$\begin{aligned}
R_j^M &= \log \frac{\left| \mathbf{I} + \sum_{i=j}^K (\mathbf{H}_i^\dagger \mathbf{Q}_i \mathbf{H}_i) \right|}{\left| \mathbf{I} + \sum_{i=j+1}^K (\mathbf{H}_i^\dagger \mathbf{Q}_i \mathbf{H}_i) \right|} \\
&= \log \left| \mathbf{I} + \left(\mathbf{I} + \sum_{i=j+1}^K (\mathbf{H}_i^\dagger \mathbf{Q}_i \mathbf{H}_i) \right)^{-1} \mathbf{H}_j^\dagger \mathbf{Q}_j \mathbf{H}_j \right| \\
&= \log \left| \mathbf{I} + \mathbf{B}_j^{-1} \mathbf{H}_j^\dagger \mathbf{Q}_j \mathbf{H}_j \right|. \tag{3.21}
\end{aligned}$$

Notice that \mathbf{B}_j represents the interference experienced by User j in the MAC. To simplify, we take the square root of \mathbf{B}_j^{-1} and use the property $|\mathbf{I} + \mathbf{A}\mathbf{B}| = |\mathbf{I} + \mathbf{B}\mathbf{A}|$. We also introduce $\mathbf{A}_j^{-1/2} \mathbf{A}_j^{1/2} = \mathbf{I}$ into the expression to get

$$R_j^M = \log \left| \mathbf{I} + \mathbf{B}_j^{-1/2} \mathbf{H}_j^\dagger \mathbf{A}_j^{-1/2} \mathbf{A}_j^{1/2} \mathbf{Q}_j \mathbf{A}_j^{1/2} \mathbf{A}_j^{-1/2} \mathbf{H}_j \mathbf{B}_j^{-1/2} \right|. \tag{3.22}$$

Treating $\mathbf{B}_j^{-1/2} \mathbf{H}_j^\dagger \mathbf{A}_j^{-1/2}$ as the effective channel of the system, we flip the channel and find $\overline{\mathbf{A}_j^{1/2} \mathbf{Q}_j \mathbf{A}_j^{1/2}}$ such that

$$\begin{aligned}
&\overline{\text{Tr}(\mathbf{A}_j^{1/2} \mathbf{Q}_j \mathbf{A}_j^{1/2})} \leq \text{Tr}(\mathbf{A}_j^{1/2} \mathbf{Q}_j \mathbf{A}_j^{1/2}) \\
R_j^M &= \log \left| \mathbf{I} + \mathbf{A}_j^{-1/2} \mathbf{H}_j \mathbf{B}_j^{-1/2} \overline{\mathbf{A}_j^{1/2} \mathbf{Q}_j \mathbf{A}_j^{1/2}} \mathbf{B}_j^{-1/2} \mathbf{H}_j^\dagger \mathbf{A}_j^{-1/2} \right|.
\end{aligned}$$

Now consider the rate of User j in the BC assuming that the opposite encoding order is used (i.e. User 1 is encoded last, User 2 second to last, etc.)

$$\begin{aligned}
R_j^B &= \log \frac{\left| \mathbf{I} + \sum_{i=1}^j (\mathbf{H}_j \mathbf{\Sigma}_i \mathbf{H}_j^\dagger) \right|}{\left| \mathbf{I} + \sum_{i=1}^{j-1} (\mathbf{H}_j \mathbf{\Sigma}_i \mathbf{H}_j^\dagger) \right|} \\
&= \log \left| \mathbf{I} + \mathbf{A}_j^{-1} \mathbf{H}_j \mathbf{\Sigma}_j \mathbf{H}_j^\dagger \right| \\
&= \log \left| \mathbf{I} + \mathbf{A}_j^{-1/2} \mathbf{H}_j \mathbf{\Sigma}_j \mathbf{H}_j^\dagger \mathbf{A}_j^{-1/2} \right|. \tag{3.23}
\end{aligned}$$

Here \mathbf{A}_j represents the interference experienced by User j in the BC. If we choose the BC

covariances as

$$\mathbf{\Sigma}_1 = \mathbf{B}_1^{-1/2} \overline{\mathbf{Q}_1} \mathbf{B}_1^{-1/2} \quad (3.24)$$

\vdots

$$\mathbf{\Sigma}_j = \mathbf{B}_j^{-1/2} \overline{\mathbf{A}_j^{1/2} \mathbf{Q}_j \mathbf{A}_j^{1/2}} \mathbf{B}_j^{-1/2} \quad (3.25)$$

\vdots

$$\mathbf{\Sigma}_K = \overline{\mathbf{A}_K^{1/2} \mathbf{Q}_K \mathbf{A}_K^{1/2}} \quad (3.26)$$

clearly we see $R_j^M = R_j^B$. Additionally, it is easy to show that the resulting covariance matrices are all symmetric and positive semi-definite. In Chapter 3.4.6, we show that the transformations given by (3.24)-(3.26) satisfy the sum trace constraint, or that $\sum_{i=1}^K \text{Tr}(\mathbf{\Sigma}_i) \leq \sum_{i=1}^K \text{Tr}(\mathbf{Q}_i)$. Note that $\mathbf{\Sigma}_j$ depends only on $\mathbf{\Sigma}_1, \dots, \mathbf{\Sigma}_{j-1}$, and hence the $\mathbf{\Sigma}_j$ can be computed sequentially in increasing order. By doing this for all K users, we find covariance matrices for the BC that achieve the same rate as in the MAC. If we substitute in the expression generating the flipped channel, the expression for the BC covariance matrix of the j -th user in (3.25) can be expanded as:

$$\mathbf{\Sigma}_j = \mathbf{B}_j^{-1/2} \mathbf{F}_j \mathbf{G}_j^\dagger \mathbf{A}_j^{1/2} \mathbf{Q}_j \mathbf{A}_j^{1/2} \mathbf{G}_j \mathbf{F}_j^\dagger \mathbf{B}_j^{-1/2} \quad (3.27)$$

where the effective channel $\mathbf{B}_j^{-1/2} \mathbf{H}_j^\dagger \mathbf{A}_j^{-1/2}$ is decomposed using the SVD as $\mathbf{B}_j^{-1/2} \mathbf{H}_j^\dagger \mathbf{A}_j^{-1/2} = \mathbf{F}_j \mathbf{\Lambda}_j \mathbf{G}_j^\dagger$, where $\mathbf{\Lambda}_j$ is a square and diagonal matrix.

BC to MAC transformation

In this section we derive a transformation that, given a set of BC covariance matrices and an encoding order, outputs a set of MAC covariances with the same sum power as the BC covariances that achieve MAC rates (using successive decoding) equal to the rates achieved in the BC using the BC covariance matrices. These transformations are almost identical to the MAC-to-BC transformations given in the previous section, and are the MIMO analogue of the scalar BC-MAC transformation given in (3.7). For the dirty paper encoding at the BC, we assume that User K is encoded first, User $K - 1$ second, and so on in decreasing order. Along the same lines as the MAC-BC transformation, we treat $\mathbf{A}_j^{-1/2} \mathbf{H}_j \mathbf{B}_j^{-1/2}$ as the effective channel and $\mathbf{B}_j^{1/2} \mathbf{\Sigma}_j \mathbf{B}_j^{1/2}$ as the covariance matrix. By flipping the effective

channel, we obtain $\overline{\mathbf{B}_j^{1/2} \boldsymbol{\Sigma}_j \mathbf{B}_j^{1/2}}$ and obtain the transformation

$$\mathbf{Q}_K = \mathbf{A}_K^{-1/2} \overline{\boldsymbol{\Sigma}_K} \mathbf{A}_K^{-1/2} \quad (3.28)$$

\vdots

$$\mathbf{Q}_j = \mathbf{A}_j^{-1/2} \overline{\mathbf{B}_j^{1/2} \boldsymbol{\Sigma}_j \mathbf{B}_j^{1/2}} \mathbf{A}_j^{-1/2} \quad (3.29)$$

\vdots

$$\mathbf{Q}_1 = \overline{\mathbf{B}_1^{1/2} \boldsymbol{\Sigma}_1 \mathbf{B}_1^{1/2}}. \quad (3.30)$$

As before, if we use the opposite decoding order in the MAC (i.e. User 1 decoded first, etc.), this transformation ensures that the rates of all users in the BC and MAC are equivalent along with the total power used in the BC and MAC. Also note that we can sequentially compute the \mathbf{Q}_j 's in decreasing numerical order. If we substitute in the expression generating the flipped channel, the expression for the MAC covariance matrix of the j -th user in (3.29) can be expanded as:

$$\mathbf{Q}_j = \mathbf{A}_j^{-1/2} \mathbf{F}_j \mathbf{G}_j^\dagger \mathbf{B}_j^{1/2} \boldsymbol{\Sigma}_j \mathbf{B}_j^{1/2} \mathbf{G}_j \mathbf{F}_j^\dagger \mathbf{A}_j^{-1/2} \quad (3.31)$$

where the effective channel $\mathbf{A}_j^{-1/2} \mathbf{H}_j \mathbf{B}_j^{-1/2}$ is decomposed using the SVD as $\mathbf{A}_j^{-1/2} \mathbf{H}_j \mathbf{B}_j^{-1/2} = \mathbf{F}_j \boldsymbol{\Lambda}_j \mathbf{G}_j^\dagger$, where $\boldsymbol{\Lambda}_j$ is a square and diagonal matrix.

MIMO MAC with Individual Power Constraints

We can also obtain the capacity region of a MIMO MAC with individual power constraints from the dirty paper region of the dual MIMO BC. By Theorem 3.2, we can characterize the individual power constraint MIMO MAC capacity region as an intersection of sum power constraint MIMO MAC capacity regions. By duality, we know that the sum power constraint MIMO MAC capacity region is equal to the dirty paper achievable region of the dual MIMO BC.

Corollary 3.3 *The capacity region of a MIMO MAC is the intersection of the scaled dirty paper regions of the MIMO BC. Mathematically, this is stated as:*

$$\mathcal{C}_{\text{MAC}}(\mathbf{H}_1, \dots, \mathbf{H}_K, P_1, \dots, P_K) = \bigcap_{\boldsymbol{\alpha} > 0} \mathcal{C}_{\text{DPC}} \left(\sqrt{\alpha_1} \mathbf{H}_1^\dagger, \dots, \sqrt{\alpha_K} \mathbf{H}_K^\dagger, \sum_{i=1}^K \frac{P_i}{\alpha_i} \right). \quad (3.32)$$

Proof: This result can be obtained by a straightforward application of Theorem 3.2 to the MIMO MAC capacity region and the duality developed in Theorem 3.6. The scaled MIMO BC here refers to the channel where the matrix of each receiver \mathbf{H}_i^\dagger is scaled by $\sqrt{\alpha_i}$. \square

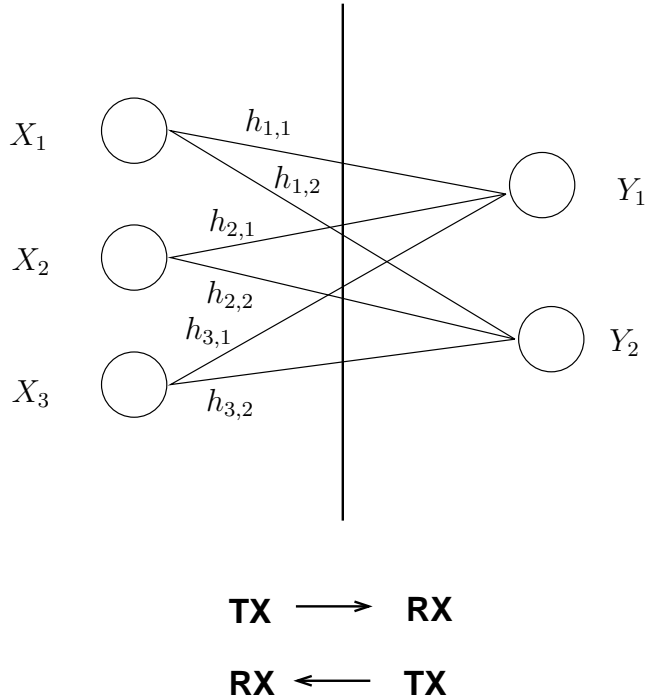


Figure 3.7: Multi-Terminal Gaussian Network

3.1.5 Multi-Terminal Networks

The focus of this section has been to characterize the duality of Gaussian multiple-access and broadcast channels. There are, however, many possible directions in which duality can be extended. In this section we discuss the possibility of a duality for a broader class of Gaussian channels. The Gaussian MAC and BC can be generalized to a model in which there are multiple transmitters *and* multiple receivers, each subject to additive Gaussian noise. Such networks are referred to as Gaussian multi-terminal networks [13, Section 14.10]. In this section we discuss networks in which nodes can either be transmitters or receivers, but not both simultaneously.

In Figure 3.7, a three-transmitter, two receiver channel is shown, if transmission is considered from left-to-right. We define the dual channel for this network as the channel associated with transmission from right-to-left (i.e. two transmitters, three receivers) with the *same channel gains* $h_{i,j}$ between all nodes. As before, we assume that every receiver suffers from Gaussian noise with the same power.

The dual broadcast and multiple-access channels can be seen as a specialization of multi-terminal networks in which there is only a single node on the left. If transmission occurs from left to right, then the channel is a two-user broadcast channel and if the nodes on the right transmit then the channel is a two-user multiple access channel. Theorem 3.1 states that the capacity regions of the BC and the dual sum power constraint MAC are the same. This is equivalent to stating that the capacity regions for left to right communication

(BC) and right to left communication (MAC) are the same if the same sum transmit power constraint is applied to both channels.

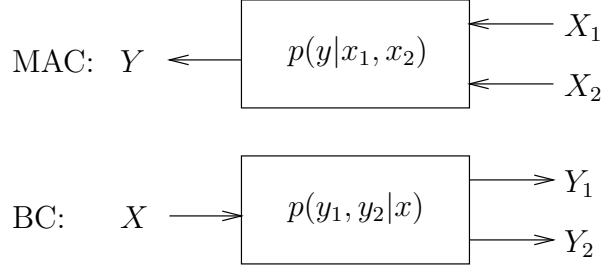
In the general multi-terminal setting we consider, any transmitter is allowed to communicate with any receiver. In the channel shown in Figure 3.7, the capacity region is six-dimensional because there are six possible receiver-transmitter pairs. It is then tempting to conjecture that Theorem 3.1 extends to general Gaussian multi-terminal networks, or that the six-dimensional capacity region governing transmission from left-to-right when sum power constraint P is imposed on the three transmitters on the left is the same as the capacity region for transmission from right-to-left when the same sum power constraint P is imposed on the two transmitters on the right. Unfortunately, this conjecture cannot be confirmed since the capacity region of a general multi-terminal network is not known. Interestingly, Theorem 3.2 can easily be extended to multiple-receiver channels. This allows characterization of a multiple-transmitter/multiple-receiver rate region (with individual transmitter power constraints) in terms of the sum transmit power constraint capacity regions.

If the nodes on the left and right were considered to be multiple-antennas of single users (i.e. a single transmitter with 3 antennas communicating to a receiver with 2 antennas, or vice versa), then duality holds due to the reciprocity of multiple-antenna Gaussian links [61]. By the reciprocity result we know that the capacity of a channel with gain matrix \mathbf{H} is equal to the capacity of the channel with gain matrix equal to the transpose (or conjugation transpose since conjugation of the channel matrix has no effect) of \mathbf{H} . This hints that a broader duality may hold for general Gaussian networks, but this has yet to be confirmed.

3.2 Deterministic Channels

In the previous section, a *duality* was established between the Gaussian multiple-access channel and the Gaussian broadcast channel. The dual channels considered had the same noise power and the same channel gains on the uplink and downlink. The capacity region of the Gaussian broadcast channel was found to equal a union of capacity regions of the dual Gaussian multiple-access channel. A natural question to ask given this result is the following: does a dual multiple-access channel exist for every broadcast channel? In the strongest form, duality would mean that the capacity region of any discrete memoryless (DM) broadcast channel is equal to the union of multiple-access channel capacity regions, where the union is over a set of dual multiple-access channels that are meaningfully related to the original broadcast channel. It is not known if such a relationship exists, and the fact that the capacity region of the general broadcast channel is not known makes it extremely difficult to prove a duality for the most general case.

We consider a two-user discrete memoryless broadcast channel consisting of an input alphabet \mathcal{X} of cardinality M , output alphabets \mathcal{Y}_1 and \mathcal{Y}_2 each of cardinality N , and a



$$|\mathcal{Y}| = |\mathcal{X}| = M, |\mathcal{X}_1| = |\mathcal{X}_2| = |\mathcal{Y}_1| = |\mathcal{Y}_2| = N$$

Figure 3.8: Discrete memoryless MAC and BC.

probability transition function $p(y_1, y_2|x)$. Similarly, we consider a multiple-access channel consisting of input alphabets \mathcal{X}_1 and \mathcal{X}_2 each of cardinality N , an output alphabet \mathcal{Y} of cardinality M , and a probability transition function $p(y|x_1, x_2)$. A simple model for these channels is shown in Figure 3.8. In the broadcast channel we consider the situation where the transmitter sends independent information to each receiver, and in the multiple-access channel we consider the situation where each transmitter sends independent information to the receiver. Our ultimate goal is to discover if there is a fundamental connection between the broadcast and multiple-access channel beyond the obvious symmetries in the channel models. Since the capacity region of the general broadcast channel remains unknown, we explore this duality by considering *deterministic* channels, for which the BC capacity region is known. Deterministic channels are channels in which the outputs are uniquely defined by the input. Alternatively, all entries in the probability transition matrix are either 0 or 1 for a deterministic channel.

When the alphabet sizes satisfy $M = aN$, where a is an integer greater than or equal to 1, we find that a duality can be established between the capacity region of the broadcast and multiple-access channel. More explicitly, we find that the convex hull of the capacity regions of all deterministic broadcast channels (with the given input/output alphabets) is equal to the convex hull of the capacity regions of all deterministic multiple-access channels. We also conjecture that this capacity region equivalence holds for any $N < M < 2N$. However, we are able to show that this duality *does not exist* for $M = 8$ and $N = 3$, i.e. there is a deterministic BC with a capacity region *strictly* larger than the capacity region of any dual deterministic MAC.

We also consider non-deterministic MAC's and BC's from a deterministic point of view. We decompose a non-deterministic channel into a finite-state channel in which the channel is deterministic in each state. This decomposition allows us to upper bound the the capacity region of any non-deterministic BC by a convex hull of deterministic BC capacity regions. This upper bound then allows us to prove that there is a deterministic BC for $M = 8$ and $N = 3$ with a capacity region strictly larger than the capacity region of *any* dual MAC

(deterministic or non-deterministic), i.e there is not always a dual MAC in our given setup.

The remainder of this section is structured as follows. In Chapter 3.2.1 we state the capacity region of the deterministic BC. In Chapter 3.2.3, we establish a duality between the BC and MAC for the case where $M = aN$. In Chapter 3.2.4 we extend this duality to a slightly broader class, and we provide a counter-example to this duality in Chapter 3.2.5. Finally, in Chapter 3.2.6 we upper bound the capacity region of a random BC by the capacity region of a series of related deterministic broadcast channels.

3.2.1 Deterministic Broadcast Channels

Deterministic broadcast channels are discrete memoryless multi-user channels in which entries in the probability transition matrix $p(y_1, y_2|x)$ are either 1 or 0, which implies that every input maps deterministically to a *single* output pair. The transmitter in the broadcast channel is assumed to have alphabet $\mathcal{X} = \{1, \dots, M\}$ and *each* receiver is assumed to have alphabet $\mathcal{Y}_i = \{1, \dots, N\}$. The input to the channel is denoted by x . The deterministic nature of the channel allows us to write the channel output as a function (i.e. deterministic mapping) of the channel input:

$$(y_1, y_2) = f(x). \quad (3.33)$$

Here, the channel transition matrix is entirely captured by the function $f(\cdot)$ which is a mapping from an input in \mathcal{X} to an output pair in $\mathcal{Y}_1 \times \mathcal{Y}_2$.

Determining the capacity region of a noiseless channel may seem like a trivial exercise, but in a broadcast channel there is still the problem of determining how to embed two independent messages in a single codeword. The Blackwell channel (see [14]) is the classical example of such a channel with $M = 3$ and $N = 2$ and the following channel function:

$$f(1) = (1, 1), \quad f(2) = (2, 2), \quad f(3) = (2, 1). \quad (3.34)$$

The capacity region of this specific channel was found in [19] and the capacity region of the general deterministic broadcast channel was later derived in [51] and [49].

For a two-user deterministic broadcast channel, the capacity region $\mathcal{C}_{BC}(f(x))$ is given by:

$$\mathcal{C}_{BC}(f(x)) = Cl \left(\bigcup_{p(x)} \{R_1, R_2 : R_1 \leq H(Y_1), R_2 \leq H(Y_2), R_1 + R_2 \leq H(Y_1, Y_2)\} \right) \quad (3.35)$$

where $Cl(\cdot)$ denotes the convex closure operation. Each input distribution $p(x)$ corresponds to a pentagon region, and the capacity region is the closure of the convex hull of all such pentagons. If multiple inputs map to the same output pair, then the inputs are identical.

Thus, we only consider channels for which each input maps to a different output pair (i.e. $f(a) \neq f(b) \forall a \neq b$). Therefore it follows that $H(Y_1, Y_2) = H(X)$.

Since the deterministic BC is fully characterized by the mapping from input to output pair, we characterize the channel by an input/output table, in which the location of an input in the table indicates the output pair (y_1, y_2) that it maps to. Notice that no two inputs correspond to the same output pair by our earlier assumption, so exactly M of the N^2 output pairs in the table contain inputs. The Blackwell channel in (3.34) is described by the following channel table:

$$x \mapsto (y_1, y_2) : \begin{array}{c|c|c} & y_1, y_2 & \\ \hline & 1 & 2 \\ \hline 1 & 1 & \\ \hline 2 & 3 & 2 \\ \hline \end{array} \quad (3.36)$$

3.2.2 Deterministic Multiple-Access Channels

The deterministic multiple-access channel has a very similar structure as the deterministic broadcast channel. The deterministic nature of the channel allows us to write the output of the channel as a function of the two channel inputs:

$$y = g(x_1, x_2). \quad (3.37)$$

We also use an input/output table to characterize the MAC. In the MAC, the table entries correspond to the outputs of each input pair (x_1, x_2) . Notice that in the MAC every input pair correspond to an output.

An expression for the capacity region of the general discrete memoryless MAC is given in Chapter 2.1.1. For the deterministic MAC, the capacity region can be expressed as:

$$\mathcal{C}_{MAC}(g(x_1, x_2)) = Cl \left(\bigcup_{p(x_1)p(x_2)} \{R_1, R_2 : R_1 \leq H(Y|X_2), R_2 \leq H(Y|X_1), R_1 + R_2 \leq H(Y)\} \right). \quad (3.38)$$

3.2.3 Duality for $M = aN$

In this section we show that there exists a duality between the deterministic BC and MAC for $M = aN$, where a is an integer and $1 \leq a \leq N$. By first principles, it follows that in the BC, R_1 and R_2 are each bounded by $\log(N)$ and $R_1 + R_2 \leq \log(M) = \log(aN)$ for *any* deterministic (or non-deterministic) probability transition matrix. Thus, the region shown in Fig. 3.9 is an upper bound to *any* BC capacity region with the given alphabet sizes.

Consider the BC channel function such that *every* row and *every* column has exactly a entries in it. If we map inputs $\{1, \dots, a\}$ to $y_1 = 1$ and $y_2 = \{1, \dots, a\}$, inputs $\{a+1, \dots, 2a\}$

to $y_1 = 2$ and $y_2 = \{2, \dots, a + 1\}$ (where the column y_2 is assumed to wrap-around for values larger than N), then this condition is satisfied. For the $M = 6, N = 3$ channel, this corresponds to the following channel function:

$$x \mapsto (y_1, y_2) : \begin{array}{c|c|c|c} y_1, y_2 & 1 & 2 & 3 \\ \hline 1 & 1 & 2 & \\ \hline 2 & & 3 & 4 \\ \hline 3 & 6 & & 5 \end{array} \quad (3.39)$$

If $p(x)$ is chosen to be the uniform distribution over the input alphabet, then we have $H(X) = \log(M) = \log(6)$ and $H(Y_1) = H(Y_2) = \log(N) = \log(3)$. Thus, the upper bound is achievable. For arbitrary N and a , the region

$$\mathcal{R}_{\text{pentagon}} = \{(R_1, R_2) : R_1 \leq \log(N), R_2 \leq \log(N), R_1 + R_2 \leq \log(aN)\} \quad (3.40)$$

is achievable if the channel matrix has exactly a entries in every row and column and the input x is chosen equiprobably on $\{1, \dots, M\}$. This region coincides exactly with the upper bound on the capacity region of any BC with input alphabet M and output alphabet N . Thus, the capacity region of the deterministic BC with the channel function satisfying the above condition is equal to $\mathcal{R}_{\text{pentagon}}$. Since $\mathcal{R}_{\text{pentagon}}$ is an upper bound to any capacity region for the given input/output alphabets, the union of capacity regions over *all* channel functions is equal to $\mathcal{R}_{\text{pentagon}}$.

For the dual MAC, it is again easy to see that R_1 and R_2 are bounded by $\log(N)$ and $R_1 + R_2 \leq \log(M) = \log(aN)$. Consider the channel function defined by:

$$y = \begin{cases} a(x_1 - 1) + x_2 & x_2 \leq a \\ 1 & x_2 > a \end{cases}. \quad (3.41)$$

For the $M = 6, N = 3$ channel, this corresponds to the following channel function:

$$(x_1, x_2) \mapsto y : \begin{array}{c|c|c|c} x_1, x_2 & 1 & 2 & 3 \\ \hline 1 & 1 & 2 & 1 \\ \hline 2 & 3 & 4 & 1 \\ \hline 3 & 5 & 6 & 1 \end{array} \quad (3.42)$$

If x_1 is chosen uniformly on $\{1, \dots, N\}$ and x_2 is chosen uniformly on $\{1, \dots, a\}$ (notice x_2 doesn't use all possible inputs), then the receiver will always be able to determine which symbols were sent by both users. Thus, the rate vector $(R_1 = \log(N), R_2 = \log(a))$ can be achieved. The capacity region of this channel is denoted by $C_{MAC,1}$ in Fig. 3.9. By reversing the roles of Users 1 and 2 in the channel function, the rate vector $(R_1 = \log(a), R_2 = \log(N))$

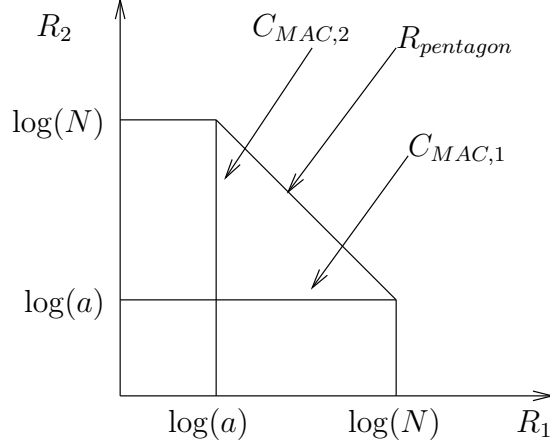


Figure 3.9: Capacity region of MAC and BC for $M = aN$

can also be achieved. The corresponding capacity region is denoted by $C_{MAC,2}$ in Fig. 3.9. It follows then that the convex hull of the capacity regions corresponding to these two channels equals the region $\mathcal{R}_{pentagon}$. Thus, $\mathcal{R}_{pentagon}$ is equal to the convex hull of the union of MAC capacity regions over all transition matrices. We therefore have the following:

Theorem 3.7 *When the alphabet sizes satisfy $|\mathcal{X}| = a|\mathcal{Y}_1| = a|\mathcal{Y}_2|$ for some integer a , the convex hull of the union of BC capacity regions over all deterministic mappings equals the convex hull of the union of MAC capacity regions over all deterministic mappings:*

$$Co \left(\bigcup_{f(x)} \mathcal{C}_{BC}(f(x)) \right) = Co \left(\bigcup_{g(x_1, x_2)} \mathcal{C}_{MAC}(g(x_1, x_2)) \right), \quad (3.43)$$

where $f(x)$ is any map from \mathcal{X} to $(\mathcal{Y}_1 \times \mathcal{Y}_2)$, $g(x_1, x_2)$ is any map from $(\mathcal{X}_1 \times \mathcal{X}_2)$ to \mathcal{Y} , and $Co(\cdot)$ denotes the convex hull operation.

The equivalence in Theorem 3.7 can in fact be strengthened to hold when the union is taken over deterministic and non-deterministic channels (i.e. over all $p(y_1, y_2|x)$ for the BC and all $p(y|x_1, x_2)$ for the MAC) as well, because the region $\mathcal{R}_{pentagon}$ is an upper bound to the capacity region of the BC or MAC for *any* probability transition function, deterministic or not. This relationship then leads to a few interesting questions:

1. Does Theorem 3.7 hold for arbitrary alphabet sizes M and N ?
2. Similarly, does Theorem 3.7 hold for arbitrary alphabet sizes when the union is taken over deterministic and non-deterministic channels?
3. Can a deterministic channel achieve any rate vector achievable by a non-deterministic channel?

We address Question 1 in the next two sections. We first establish a limited version of this relationship for $N < M < 2N$, but then we provide a counter-example for which this duality does not hold. In Chapter 3.2.6, we answer Question 3 by relating the capacity regions of the deterministic and non-deterministic BC (and of the MAC) and we find that Questions 1 and 2 are entirely equivalent because non-deterministic channels can never have a larger capacity region than deterministic channels for the same input/output alphabets.

3.2.4 Duality for $N < M < 2N$

In this section we show a limited duality between deterministic broadcast and multiple-access channels for $N < M \leq 2N$. More explicitly, we show that the convex hull of the union of BC capacity regions, where the union is over a specific class of BC functions, is equal to the convex hull of the union of MAC capacity regions, where the union is over a related class of MAC channel functions.

We consider the class of *balanced* BC functions, by which we mean channel functions such that no output in \mathcal{Y}_1 or in \mathcal{Y}_2 has more than 2 channel inputs that map to it. In terms of the channel function, this corresponds to having no row or column with more than 2 channel inputs in it. Of course, as before, we require that every channel input goes to a different channel output. The Blackwell channel defined in (3.36) is an example of a balanced BC.

Since $M \leq 2N$, it is clear that with such a channel function, $M - N$ of the outputs of each user will have 2 inputs mapping to it, while the remaining $2N - M$ outputs of each user will have only a single input mapping to it. For the $M = 5, N = 3$ channel, the following channel function is *balanced*:

$$x \mapsto (y_1, y_2) : \begin{array}{c|c|c|c} y_1, y_2 & 1 & 2 & 3 \\ \hline 1 & 1 & 2 & \\ \hline 2 & & 3 & 4 \\ \hline 3 & & & 5 \end{array} \quad (3.44)$$

Notice that no row or column has more than 2 inputs in it. A similar channel function can be defined for other values of M and N by using the same procedure of placing inputs along the main diagonal and the upper off-diagonal. If we consider the rate achieved by User 1 in a balanced BC, at one corner point of the pentagon region (for a fixed $p(x)$) we have $R_1 = H(Y_1)$ and $R_2 = H(Y_1, Y_2) - H(Y_1) = H(Y_2|Y_1)$. Thus the rate of User 1 is equal to the received entropy of User 1, while the rate of User 2 is equal to the conditional entropy of each *row* of the channel matrix, which can be no larger than one since each row has no more than 2 inputs in it.

Analogously, we consider *balanced* MAC channel functions in which exactly $M - N$ inputs of User 1 have two possible outputs and $2N - M$ inputs of User 1 have only one

possible output each. For the $M - N$ inputs of User 1 which have two possible outputs, the $x_2 = 1$ output is assumed to be the smaller of the two outputs, while all other values of x_2 correspond to the larger of the two outputs. For the $M = 5, N = 3$ channel, the following channel function is *balanced*:

$$(x_1, x_2) \mapsto y : \begin{array}{c|c|c|c} x_1, x_2 & 1 & 2 & 3 \\ \hline 1 & 1 & 2 & 2 \\ \hline 2 & 3 & 4 & 4 \\ \hline 3 & 5 & 5 & 5 \end{array} \quad (3.45)$$

We also consider the transposes of such matrices, or the situation where the roles of Users 1 and 2 are reversed. It can be shown that the rate vector $(R_1 = H(Y|X_2), R_2 = H(Y|X_1))$ can be achieved for any input product distribution. For the channel described above, $R_1 = H(Y|X_2) = H(X_1)$ is the input entropy of User 1 and $R_2 = H(Y|X_1)$ is the conditional entropy of each row of the channel matrix.

Theorem 3.8 *When the alphabet sizes satisfy $N < M < 2N$, the convex hull of the union of BC capacity regions over all balanced BC deterministic mappings equals the convex hull of the union of MAC capacity regions over all balanced MAC deterministic mappings:*

$$Co \left(\bigcup_{f(x)} \mathcal{C}_{BC}(f(x)) \right) = Co \left(\bigcup_{g(x_1, x_2)} \mathcal{C}_{MAC}(g(x_1, x_2)) \right), \quad (3.46)$$

where $f(x)$ is any balanced map from \mathcal{X} to $(\mathcal{Y}_1 \times \mathcal{Y}_2)$, $g(x_1, x_2)$ is any balanced map from $(\mathcal{X}_1 \times \mathcal{X}_2)$ to \mathcal{Y} , and $Co(\cdot)$ denotes the convex hull operation.

Proof: We first show that for a given input BC distribution $p(x)$, the rate vectors achievable in the BC are also achievable in the dual balanced MAC. By the definition of the deterministic BC capacity region in (3.35), the upper right corner of the pentagon region corresponding to $p(x)$ has $R_1 = H(Y_1)$ and $R_2 = H(Y_2|Y_1) \leq 1$, where the inequality is due to the balanced structure of the BC. In the dual MAC, the rate vector $(R_1 = H(Y|X_2) = H(X_1), R_2 = H(Y|X_1))$ is achievable. By choosing the MAC input X_1 to have the same distribution as the output BC distribution of Y_1 and $P(x_2 = 1) = \frac{1}{2}$, clearly the BC rate vector can also be achieved since $H(X_1) = H(Y_1)$ and $H(Y_2|Y_1) = H(Y|X_1)$. The upper left corner of the pentagon region corresponding to BC input $p(x)$ can also similarly be achieved in the dual balanced MAC by considering the MAC with the roles of users 1 and 2 reversed. Since both the BC and MAC regions are convex, this is sufficient to prove that the LHS of (3.46) is a subset of the RHS of (3.46).

Now consider the rate vector $(R_1 = H(Y|X_2) = H(X_1), R_2 = H(Y|X_1))$ achievable in the MAC. Similarly, any rate vector achievable in the MAC can be achieved in the BC

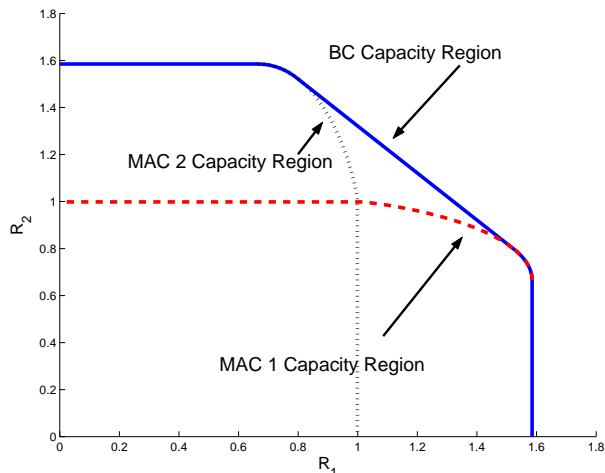


Figure 3.10: Deterministic BC and MAC capacity regions for $M = 5$, $N = 3$

by choosing the BC input distribution $p(x)$ such that $H(Y_1) = H(X_1)$ and such that the conditional entropy $H(Y_2|Y_1) = H(Y|X_1)$. \square

Note that this differs from Theorem 3.7 in that the union is only taken over balanced broadcast and multiple-access channels. We conjecture that the relationship holds when the union is taken over all deterministic channels, but we have been unable to show this as of yet.

Fig. 3.10 shows the capacity region of the balanced deterministic broadcast channel for $M = 5$, $N = 3$ along with the capacity region of the two balanced MAC's. Notice that the convex hull of the MAC regions is equal to the BC capacity region.

3.2.5 Duality Counter-example

In this section we provide a simple counter-example showing that the duality between the deterministic MAC and BC does not always exist. Consider a deterministic BC with $M = 8$ and $N = 3$, with each input going to a unique output (Y_1, Y_2) pair. It is easy to verify that any such deterministic BC mapping is equivalent for this choice of M and N . Clearly, by choosing x uniformly over the input alphabet, we can achieve $H(Y_1, Y_2) = \log(8) = 3$. Thus, the maximum sum rate for the deterministic BC is 3 bits/use. In the dual MAC, with $M = 8$ and $N = 3$, we will show that for any choice of deterministic MAC, the output entropy (i.e. $H(Y)$) is *strictly* less than 3. Therefore, the deterministic BC capacity region cannot be written in terms of dual MAC capacity regions.

We now prove that the output entropy $H(Y)$ for a deterministic MAC is strictly upper bounded by $\log(8)$. In order for $H(Y) = \log(8)$, we require the outputs of the channel to be equiprobable for some given input product distributions $p(x_1)$ and $p(x_2)$ and some channel function. Since every MAC output (i.e. $1, \dots, 8$) must correspond to at least one of the

$N^2 = 9$ input pairs, without loss of generality we assume the first 8 outputs are mapped as follows:

$$(x_1, x_2) \mapsto y : \begin{array}{c|c|c|c} x_1, x_2 & 1 & 2 & 3 \\ \hline 1 & 1 & 2 & 3 \\ \hline 2 & 4 & 5 & 6 \\ \hline 3 & 7 & 8 & ? \end{array} \quad (3.47)$$

and the bottom right output is not yet chosen. We are free to choose any output for $(x_1 = 3, x_2 = 3)$. Since numbering of inputs and outputs is arbitrary, rows and columns can be arbitrarily interchanged as well as output numbers. Thus, there are only two choices for the output in question: we can either place an output that also appears in the same row or column as the bottom right input pair (i.e. 3, 6, 7, or 8), or an output that is not in the same row or column (i.e. 1, 2, 4, or 5).

Assume we choose to map $(x_1 = 3, x_2 = 3)$ to $y = 3$. We show by contradiction that $H(Y) < 3$. Clearly the output entropy $H(Y) = 3$ if and only if $P(Y = i) = \frac{1}{8}$ for $i = 1, \dots, 8$. Since outputs 4, 5, and 6 appear only once, in order for $P(y = 4) = P(y = 5) = P(y = 6) = \frac{1}{8}$ we need $P(x_2 = 1) = P(x_2 = 2) = P(x_2 = 3) = \frac{1}{3}$ and $P(x_1 = 2) = \frac{3}{8}$. Similarly, to have $P(y = 1) = P(y = 7) = \frac{1}{8}$, we need $P(x_1 = 1) = P(x_1 = 3) = \frac{3}{8}$, which is a contradiction. Thus, for any choice of $p(x_1)p(x_2)$ we have $H(Y) < 3$ for this choice of a MAC channel. The maximum output entropy in this configuration is given by: $\max_{p(x_1), p(x_2)} H(Y)$. Since $H(Y)$ is a continuous function of the input distribution $p(x_1)p(x_2)$ and the maximization is taken over a closed set, the maximum is achieved by some $p(x_1)p(x_2)$ because the maximum of any continuous function over a compact set is achieved [48, Chapter 4.4]. Therefore, the maximum output entropy is also strictly smaller than 3.

Now consider the other possible MAC, where we choose to map $(x_1 = 3, x_2 = 3)$ to 1. Then by the same argument as above we need $P(x_2 = 1) = P(x_2 = 2) = P(x_2 = 3) = \frac{1}{3}$. This again implies $P(x_1 = 1) = P(x_1 = 2) = P(x_1 = 3) = \frac{3}{8}$, which is a contradiction. Thus, we see that $H(Y) < \log(8)$ for any channel map. It is also easy to see by the same argument as above that the maximum output entropy in this configuration is also strictly smaller than 3.

Since the maximum entropy in either configuration is strictly smaller than 3, the maximum $H(Y)$ for *any* deterministic MAC is equal to $3 - \epsilon$ for some $\epsilon > 0$. Thus, the convex hull of all deterministic MAC capacity regions is upper bounded by $R_1 + R_2 \leq 3 - \epsilon$, and thus the convex hull of the deterministic MAC capacity regions is strictly smaller than the capacity region of the deterministic BC. Thus, Theorem 3.7 does *not* extend to arbitrary M and N , and therefore Question 1 in Chapter 3.2.3 can be answered negatively.

In Fig. 3.11, a closeup of the deterministic BC capacity region and the convex hull of the MAC capacity regions for $M = 8, N = 3$ is shown. For this case, there are only 2 different deterministic MAC channels (corresponding to the two possible choices for the

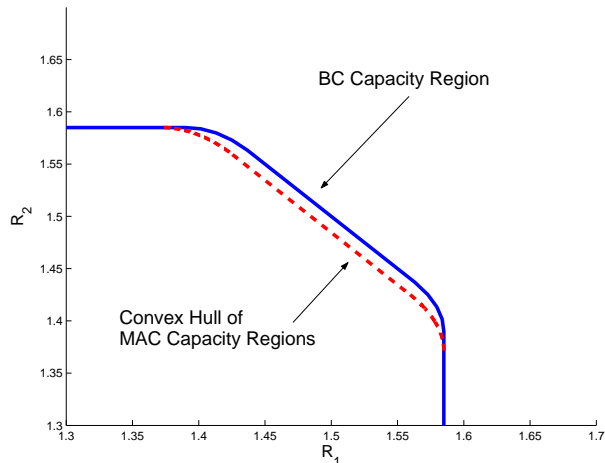


Figure 3.11: Closeup of deterministic BC and MAC capacity regions for $M = 8$, $N = 3$

($x_1 = 3, x_2 = 3$) output), so the convex hull of the regions is easy to compute numerically. We see that there is a slight gap between the sum rate achievable in the MAC and BC, but a picture of the entire capacity regions would show that the capacity regions differ only very slightly. Using the same methodology, we believe that the deterministic BC is in general larger than any deterministic MAC channel for $M > 2N$, but this claim has yet to be proven.

3.2.6 Deterministic vs. Non-deterministic Channels

In this section we explore the relationship between the capacity region of deterministic and non-deterministic broadcast channels. As before, the transmitter alphabet is assumed to have cardinality M and both receivers are assumed to have alphabets of size N . The capacity region of the general broadcast channel is not known, but we still are able to relate the capacity region of the non-deterministic channel to that of the deterministic channel. We do so by decomposing a non-deterministic broadcast channel into a *finite-state broadcast channel*, where in each state the channel is *deterministic*. The probabilistic nature of the channel is captured by the state probabilities.

We first perform this decomposition on a single-user channel to illustrate this idea. Consider a finite-state channel defined by $p(y|x, s)$ where s is an auxiliary random variable unknown to either the transmitter or the receiver and independent of the channel inputs and outputs that is chosen according to some distribution $p(s)$ defined on $\{1, \dots, k\}$. If the channel state is not known by the transmitter nor receiver, the channel probability transition function can be written as $p(y|x) = \sum_{i=1}^k p(y|x, s = i)p(s = i)$. Thus the capacity of any channel with probability transition function $p(y|x)$ is equal to the capacity of a finite-state channel defined by $p(y|x, s)$ in which neither the transmitter nor the receiver know the

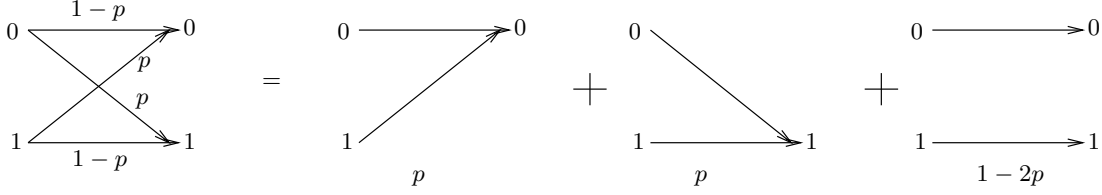


Figure 3.12: BSC and an equivalent finite-state channel

state and $p(y|x) = \sum_{i=1}^k p(y|x, s = i)p(s = i)$. Clearly, the capacity of the finite-state channel where neither the transmitter nor receiver knows the state s is upper-bounded by the capacity of the finite-state channel where both the transmitter and receiver know s . Mathematically, this can be stated as

$$C(p(y|x)) \leq \sum_{i=1}^k C(p(y|x, s = i)) \quad (3.48)$$

for any decomposition $p(y|x, s = i)$ satisfying $p(y|x) = \sum_{i=1}^k p(y|x, s = i)p(s = i)$. Here we have used the fact that capacity of a channel in which both the transmitter and receiver have knowledge of the state is equal to the statistical average over all states of the corresponding capacity in each state [79].

To illustrate this upper bound, let us decompose a single-user binary symmetric channel (BSC) into a finite-state channel, where the channel is strictly deterministic in each state. Consider a standard BSC with crossover probability p , i.e. $p(y = 1|x = 0) = p(y = 0|x = 1) = p$. The BSC can be decomposed into two states: an error-free state ($s = 1$, w.p. $1 - p$), where $y = x$, and an error state ($s = 2$, w.p. p) where y equals the complement of x . Clearly, the capacity in either state is 1, so the upper bound on capacity is 1. An alternative method of decomposing the channel is the following. When $s = 1$ (w.p. p), $p(y = 0|x = 0) = p(y = 0|x = 1) = 1$. When $s = 2$ (w.p. p), $p(y = 1|x = 0) = p(y = 1|x = 1) = 1$. Finally, when $s = 3$ (w.p. $1 - 2p$), $y = x$. This decomposition is illustrated in Fig. 3.12. The capacity of the channel when $s = 1$ or $s = 2$ is clearly 0 and $C(s = 3) = 1$. Thus the upper bound to capacity is $p(s = 1)C(s = 1) + p(s = 2)C(s = 2) + p(s = 3)C(s = 3) = 1 - 2p$, which is strictly greater than the capacity of the original channel (equal to $1 - H(p)$) except when $p = 0$ or $p = .5$.

We can similarly decompose any DM broadcast channel into a finite-state broadcast channel, where in each state the broadcast channel is *deterministic*⁴. We will refer to such a channel as a finite-state deterministic BC. It can be shown that the capacity region of a finite-state deterministic BC where the transmitter and receivers know the state is equal to the weighted “sum” of the capacity region of each state, where the weights are

⁴It is easy to show that a decomposition into a finite-state deterministic channel is always possible for a single or multi user channel with finite input and output alphabets.

equal to the probability of each state. Below we more precisely define the notion of a sum of regions. Again, this is clearly an upper bound to the channel where neither the transmitter nor receivers know the state. As we saw with the BSC, there are many different ways of decomposing a channel into a finite-state deterministic channel. Each of these decompositions may yield a different upper bound to the capacity of the original channel. Thus, we take the intersection of all of these upper bounds to get the following theorem:

Theorem 3.9 *The capacity region of a DM broadcast channel $(\mathcal{X}, \mathcal{Y}_1, \mathcal{Y}_2, p(y_1|x), p(y_2|x))$ is upper bounded by the intersection of capacity regions of finite-state deterministic BC's where the transmitter and receivers know the state:*

$$\mathcal{C}_{BC} \subseteq \bigcap_{p(s), p(y_1, y_2|x, s)} \mathcal{C}_{BC}(p(s), p(y_1, y_2|x, s)) \quad (3.49)$$

where the intersection is taken over deterministic $p(y_1, y_2|x, s)$ that satisfy $\sum_{i=1}^k p(y_1|x, s=i)p(s=i) = p(y_1|x)$ and $\sum_{i=1}^k p(y_2|x, s=i)p(s=i) = p(y_2|x)$, where k is assumed to be the cardinality of the state variable s . Here we use $\mathcal{C}_{BC}(p(s), p(y_1, y_2|x, s))$ to indicate the capacity region of the finite-state deterministic channel with transmitter and receiver knowledge of the state, given by:

$$\mathcal{C}_{BC}(p(s), p(y_1, y_2|x, s)) = p_1 C(s=1) + \dots + p_k C(s=k) \quad (3.50)$$

where $C(s=k)$ is the capacity region of the deterministic broadcast channel when $s=k$ and the sum is defined as element-by-element addition of rate vectors (i.e. a sum of sets).

Proof: The bound given in (3.49) follows obviously from the fact that both the transmitter and receiver can ignore information about the state s . The capacity region of a finite-state deterministic BC can be shown to equal the expression given in (3.50) by bounding $H(Y_1)$, $H(Y_2)$ and $H(Y_1, Y_2)$ in the probabilistic channel by considering the entropies while in each channel state. If we were to consider the n outputs of the channel Y_1 and the length n state sequence, denoted Y_1^n and S^n , respectively, using Fano's inequality and standard information theoretic arguments:

$$nR_1 = H(W_1) \quad (3.51)$$

$$= H(W_1|Y_1^n, S^n) + I(W_1; Y_1^n, S^n) \quad (3.52)$$

$$\leq n\epsilon_n + I(W_1; Y_1^n|S^n) \quad (3.53)$$

$$\leq I(X^n(W_1, W_2, S^n); Y_1^n|S^n) + n\epsilon_n \quad (3.54)$$

$$= H(Y_1^n|S^n) + n\epsilon_n \quad (3.55)$$

$$\leq \sum_{i=1}^n H(Y_1(i)|S(i)) + n\epsilon_n \quad (3.56)$$

where $Y_1(i)$ denotes the output at receiver 1 at the i -th instant and $S(i)$ denotes the i -th state. Thus, since we consider large n and assume the state $S(i)$ is chosen iid, we have $R_1 \leq \sum_{i=1}^k p(S=i) \max_{p(x|s=i)} H(Y_1|S=i)$. We can show similar inequalities for R_2 and $R_1 + R_2$ to give the result. \square

From the definition of the convex hull, it follows that $\mathcal{C}_{BC}(p(s), p(y_1, y_2|x, s))$ lies in the convex hull of the union of $C(s=1), \dots, C(s=k)$. Thus, any rate vector in the capacity region of a non-deterministic broadcast channel lies in the convex hull of capacity regions of deterministic channels with the same input/output alphabets. Thus, we conclude that, similar to single-user channels, *randomness* never helps in broadcast channels in the sense that any rate vector achievable with a random channel is also achievable (at least in the convex hull sense) by deterministic channels. Theorem 3.9 can also be extended to multiple-access channels. Interestingly, for either multiple-access channels or single-user channels, the finite-state upper bound can equivalently be shown using the convexity of mutual information in the channel law [13, Chapter 2].

We can use Theorem 3.9 applied to the MAC to strengthen the duality counter-example presented in Chapter 3.2.5. In the counter-example, we found that the convex hull of the capacity regions of all deterministic MAC's is strictly smaller than the capacity region of the deterministic BC. Since Theorem 3.9 implies that non-deterministic channels are not better than deterministic channels, we can now state that for the $M=8, N=3$ case, no MAC, deterministic *or* non-deterministic, can achieve the capacity region of the deterministic BC described in Chapter 3.2.5. This answers Question 2 posed in Chapter 3.2.3. Furthermore, we can state unequivocally that every discrete memoryless broadcast channel does not have a set of dual multiple-access channels with the same alphabet sizes for which the union of the MAC capacity regions equals the capacity region of the broadcast channel. Of course, this does not preclude a general MAC-BC relationship existing in which the BC and MAC are not forced to have the same alphabet sizes. Intuitively speaking, it seems it may be useful to allow the MAC to have a larger alphabet than the BC when trying to derive a general duality relationship.

3.3 Summary

In this chapter we established a duality relationship between the multiple-access channel and the broadcast channel. For Gaussian channels, we proved that the capacity region of the BC and the MAC are identical if the MAC is formed by reversing the roles of all transmitters and receivers in the BC and if the multiple-access transmitters are subject to a sum power constraint equal to the power constraint in the BC. This relationship holds for AWGN channels, fading channels, and MIMO channels. Furthermore, we considered the general class of discrete memoryless broadcast and multiple-access channels and established a somewhat similar duality for a class of deterministic channels.

Duality is an exciting new concept that gives great insight into the similarities between the MAC and BC. Furthermore, the duality of the Gaussian MAC and BC is particularly useful in deriving new results, as we illustrate in some of the following chapters. In Chapter 5 we use duality and an explicit characterization of the minimum rate capacity of the fading BC to find the minimum rate capacity of the fading MAC. In Chapter 4, we use duality to find the sum rate capacity of the multiple-antenna broadcast channel. We also use duality to develop an efficient numerical algorithm to calculate the sum rate capacity and the corresponding optimal transmission strategy for the MIMO broadcast channel. Finally, duality is used in Chapter 4.4 to analytically compare the sum-rate capacity of the MIMO BC to rates achievable using time-division multiple-access (TDMA), a sub-optimal transmission strategy.

3.4 Appendix

3.4.1 Power-Preserving Property of MAC-BC Transformations

We show that if $P_j^M A_j = P_j^B B_j$ for all j , where A_j and B_j are defined as

$$A_j = 1 + h_j \sum_{i=1}^{j-1} P_i^B, \quad B_j = 1 + \sum_{i=j+1}^K h_i P_i^M,$$

then $\sum_{i=1}^K P_i^M = \sum_{i=1}^K P_i^B$. For notational simplicity we assume $\pi(i) = i$ in this section. We prove the result by inductively showing that

$$\sum_{i=1}^j P_i^B = \frac{1}{B_j} \sum_{i=1}^j P_i^M. \quad (3.57)$$

The base case ($j = 1$) holds by definition: $P_1^B = \frac{A_1 P_1^M}{B_1} = \frac{1}{B_1} P_1^M$. Assume (3.57) holds for j . For $j + 1$ we get:

$$\begin{aligned}
\sum_{i=1}^{j+1} P_i^B &= \sum_{i=1}^j P_i^B + \frac{A_{j+1} P_{j+1}^M}{B_{j+1}} \\
&= \sum_{i=1}^j P_i^B + \frac{P_{j+1}^M (1 + h_{j+1} \sum_{i=1}^j P_i^B)}{B_{j+1}} \\
&= \frac{P_{j+1}^M + (P_{j+1}^M h_{j+1} + B_{j+1}) \sum_{i=1}^j P_i^B}{B_{j+1}} \\
&= \frac{P_{j+1}^M + B_j \sum_{i=1}^j P_i^B}{B_{j+1}} \\
&\stackrel{(a)}{=} \frac{P_{j+1}^M + \sum_{i=1}^j P_i^M}{B_{j+1}} \\
&= \frac{\sum_{i=1}^{j+1} P_i^M}{B_{j+1}},
\end{aligned}$$

where (a) follows from the inductive hypothesis. By using (3.57) for $j = K$ and the fact that $B_K = 1$, we get $\sum_{i=1}^K P_i^B = \sum_{i=1}^K P_i^M$ as desired.

3.4.2 Proof of Corollary 3.8

The fact that $\mathcal{C}_{MAC}(\mathbf{h}, \mathbf{P}) \subseteq \mathcal{C}_{BC}(\mathbf{1}, \mathbf{h}, \mathbf{P})$ follows trivially from Theorem 3.1. Also, the fact that the boundaries of the regions meet at the point where users are decoded in order of decreasing channel gains in the MAC follows from the MAC-BC transformations and the fact that the opposite decoding order is used in the BC. It only remains to show that the MAC and dual BC capacity region boundaries meet at only this point if the channel gains of all K users are distinct⁵ and that all other corner points of the MAC capacity region lie strictly in the interior of the dual BC capacity region.

We show this by proving that every successive decoding point other than the one corresponding to decoding in order of decreasing channel gains lies strictly in the interior of the sum power constraint MAC capacity region (i.e. the dual BC capacity region). We show that the sum power needed to achieve any strictly positive rate vector \mathbf{R} using the decoding order in which the weakest user is last is *strictly less* than the sum power needed to achieve the same rate vector using any other decoding order at the receiver. This implies that points on the boundary of the sum power MAC can only be achieved by successive decoding in order of decreasing channel gain. Therefore all corner points of the individual power constraint MAC other than the optimal decoding order point are in the interior of the dual BC capacity region.

⁵If all channel gains are not distinct, then the MAC and BC boundaries will meet along a hyperplane.

Assume there exist i and j such that $h_i < h_j$ but User i is decoded directly *before* User j . This is easily seen to be true if and only if decoding is not done in order of decreasing channel gains. We will show that the sum power needed to achieve any strictly positive rate vector is strictly less if User i is decoded directly *after* User j . Users i and j do not affect users decoded after them because their signals are subtracted out, but they do contribute interference $h_i P_i + h_j P_j$ to all users decoded before them. All users that are decoded after Users i and j are seen as interference to both Users i and j . We denote this interference by I . The rates of Users i and j then are

$$\begin{aligned} R_i &= \log \left(1 + \frac{h_i P_i}{h_j P_j + 1 + I} \right) \\ R_j &= \log \left(1 + \frac{h_j P_j}{1 + I} \right) \end{aligned}$$

if User i is decoded before User j . The power required by Users i and j to achieve their rates are

$$P_i = \frac{h_j P_j + 1 + I}{h_i} (e^{R_i} - 1), \quad P_j = \frac{1 + I}{h_j} (e^{R_j} - 1)$$

and the sum of their powers is

$$\begin{aligned} P_i + P_j &= \frac{1 + I}{h_i} (e^{R_i} - 1) + \frac{1 + I}{h_j} (e^{R_j} - 1) \\ &\quad + \frac{1 + I}{h_i} (e^{R_i} - 1) (e^{R_j} - 1). \end{aligned}$$

If User i is decoded directly after User j instead of before him, then the required sum power is

$$\begin{aligned} P'_i + P'_j &= \frac{1 + I}{h_i} (e^{R_i} - 1) + \frac{1 + I}{h_j} (e^{R_j} - 1) \\ &\quad + \frac{1 + I}{h_j} (e^{R_i} - 1) (e^{R_j} - 1). \end{aligned}$$

Clearly $P_i + P_j - P'_i - P'_j = (\frac{1+I}{h_i} - \frac{1+I}{h_j})(e^{R_i} - 1)(e^{R_j} - 1) > 0$ since $h_i < h_j$ and $R_i, R_j > 0$ by assumption. Therefore we have $P_i + P_j > P'_i + P'_j$. This fact means that Users i and j can achieve the same rates using *less sum power* by switching the decoding order of Users i and j and switching their powers from P_i and P_j to P'_i and P'_j . The rates of users decoded after i and j are unaffected by such a switch. However, as noted above, Users i and j do contribute interference to all users decoded before them. If we expand the interference contribution of Users i and j , we find

$$h_i P_i + h_j P_j = (1 + I)(e^{2(R_i + R_j)} - 1) = h_i P'_i + h_j P'_j,$$

so the rates of all users decoded earlier are unaffected. Therefore by switching the decoding order of Users i and j and changing the powers to P'_i and P'_j (but not altering the rest of the decoding order or power allocations), we can achieve the same set of rates for all K users using *strictly less* sum power. Thus the point lies in the interior of the sum power constraint MAC and therefore is not on the boundary of the dual BC capacity region.

3.4.3 Proof of Theorem 3.2

We wish to show that for any strictly positive⁶ power constraint $\bar{\mathbf{P}} = (\bar{P}_1, \dots, \bar{P}_K) > 0$

$$R(\bar{\mathbf{P}}) = \bigcap_{\alpha > 0} R_{\alpha}^{sum} \left(\mathbf{1} \cdot \frac{\bar{\mathbf{P}}}{\alpha} \right), \quad (3.58)$$

where the sum power constraint capacity region is defined as

$$R_{\alpha}^{sum}(P_{sum}) \triangleq \bigcup_{\{\mathbf{P} \mid \mathbf{P} \in \mathcal{R}_+^K, \mathbf{1} \cdot \mathbf{P} \leq P_{sum}\}} R_{\alpha}(\mathbf{P}). \quad (3.59)$$

Before beginning the proof, we first restate the conditions required of $R(\mathbf{P})$:

1. $R(\mathbf{P}) = R_{\alpha}(\frac{\mathbf{P}}{\alpha}) \forall \alpha > 0, \mathbf{P} > 0$.
2. $S = \{(\mathbf{R}, \mathbf{P}) \mid \mathbf{P} \in \mathcal{R}_+^K, \mathbf{R} \in R(\mathbf{P})\}$ is a convex set.
3. For all $\mathbf{P} \in \mathcal{R}_+^K$, $R(\mathbf{P})$ is a closed, convex region.
4. If $\mathbf{P}_1 \geq \mathbf{P}_2$ then $R(\mathbf{P}_1) \supseteq R(\mathbf{P}_2)$.
5. If $(R_1, \dots, R_K) \in R(P_1, P_2, \dots, P_K)$, then for any i ,
 $(R_1, \dots, R_{i-1}, 0, R_{i+1}, \dots, R_K) \in R(P_1, \dots, P_{i-1}, 0, P_{i+1}, \dots, P_K)$.
6. If $\mathbf{R} \in R(\mathbf{P})$ and $\mathbf{R}' \leq \mathbf{R}$, then $\mathbf{R}' \in R(\mathbf{P})$.
7. $R(\mathbf{P})$ is unbounded in every direction as \mathbf{P} increases, or $\forall j, \max_{R_j \in R(\mathbf{P})} R_j \rightarrow \infty$ as $P_i \rightarrow \infty$.
8. $R(\mathbf{P})$ is finite for all $\mathbf{P} > 0$.

From condition 1 and the definition of the sum power constraint capacity region (3.59), it is clear that $R(\bar{\mathbf{P}}) = R_{\alpha}(\frac{\bar{\mathbf{P}}}{\alpha}) \subseteq R_{\alpha}^{sum}(\mathbf{1} \cdot \frac{\bar{\mathbf{P}}}{\alpha}) \forall \alpha > 0$. This implies that $R(\bar{\mathbf{P}}) \subseteq \bigcap_{\alpha > 0} R_{\alpha}^{sum}(\mathbf{1} \cdot \frac{\bar{\mathbf{P}}}{\alpha})$. To complete the proof, we must show that this inequality also holds in the opposite direction.

⁶If the power constraint of some transmitter is zero, then we can eliminate the user and consider the $K - 1$ user problem.

Since $R(\bar{\mathbf{P}})$ is a closed and convex region, it is completely characterized by the following maximization [45, p. 135]

$$\max_{\mathbf{R}} \boldsymbol{\mu} \cdot \mathbf{R} \quad \text{s.t.} \quad \mathbf{R} \in R(\bar{\mathbf{P}}) \quad (3.60)$$

over priorities $\boldsymbol{\mu} = (\mu_1, \dots, \mu_K)$ such that $\boldsymbol{\mu} \geq 0$ and $\mathbf{1} \cdot \boldsymbol{\mu} = 1$. Since at least one component of $\boldsymbol{\mu}$ must be strictly positive for $\mathbf{1} \cdot \boldsymbol{\mu} = 1$ to hold, without loss of generality we assume $\mu_K > 0$. For every $\boldsymbol{\mu} \geq 0$, we show⁷

$$\max_{\mathbf{R} \in R(\bar{\mathbf{P}})} \boldsymbol{\mu} \cdot \mathbf{R} \geq \sup_{\mathbf{R} \in \bigcap_{\alpha > 0} R_{\alpha}^{sum} \left(\mathbf{1} \cdot \frac{\bar{\mathbf{P}}}{\alpha} \right)} \boldsymbol{\mu} \cdot \mathbf{R}. \quad (3.61)$$

This implies $R(\bar{\mathbf{P}}) \supseteq \bigcap_{\alpha > 0} R_{\alpha}^{sum} \left(\mathbf{1} \cdot \frac{\bar{\mathbf{P}}}{\alpha} \right)$ because $R(\bar{\mathbf{P}})$ is completely characterized by $\max \boldsymbol{\mu} \cdot \mathbf{R}$ (3.60). We essentially show that for every $\boldsymbol{\mu}$ (or roughly every point on the boundary of $R(\bar{\mathbf{P}})$) there exists an α such that the boundaries of $R_{\alpha}^{sum} \left(\mathbf{1} \cdot \frac{\bar{\mathbf{P}}}{\alpha} \right)$ and $R(\bar{\mathbf{P}})$ meet at the point where $\boldsymbol{\mu} \cdot \mathbf{R}$ is maximized.

The optimization in (3.60) is equivalent to

$$\max_{(\mathbf{R}, \mathbf{P}) \in S} \boldsymbol{\mu} \cdot \mathbf{R} \quad \text{s.t.} \quad \mathbf{P} \leq \bar{\mathbf{P}}. \quad (3.62)$$

where the set S is defined in condition 2. Consider the above maximization for some fixed $\boldsymbol{\mu}$. Since the objective function is linear and the set S is convex, this is a convex optimization problem (see [4] for a general reference on convex optimization and Lagrangian duality). Furthermore, the maximization takes on some optimal value p^* by the feasibility of the constraint set. The optimal value is finite due to the assumption that $R(\bar{\mathbf{P}})$ is finite. The Lagrangian is formed by adding the weighted sum of the constraints to the objective function:

$$L(\mathbf{R}, \mathbf{P}, \boldsymbol{\lambda}) = \boldsymbol{\mu} \cdot \mathbf{R} - \lambda_1(P_1 - \bar{P}_1) - \dots - \lambda_K(P_K - \bar{P}_K)$$

where the weights $\boldsymbol{\lambda} = (\lambda_1, \dots, \lambda_K)$ are the Lagrangian multipliers. The Lagrangian dual function is

$$g(\boldsymbol{\lambda}) = \sup_{(\mathbf{R}, \mathbf{P}) \in S} L(\mathbf{R}, \mathbf{P}, \boldsymbol{\lambda}).$$

By the above definition, for any $(\mathbf{R}, \mathbf{P}) \in S$ satisfying $\mathbf{P} \leq \bar{\mathbf{P}}$ and $\boldsymbol{\lambda} \geq 0$, we have $\boldsymbol{\mu} \cdot \mathbf{R} \leq L(\mathbf{R}, \mathbf{P}, \boldsymbol{\lambda}) \leq g(\boldsymbol{\lambda})$. This implies $p^* \leq g(\boldsymbol{\lambda})$ for any $\boldsymbol{\lambda} \geq 0$. Notice that the supremum is taken over the entire set S *without* taking the power constraints into effect. Additionally, the dual function $g(\boldsymbol{\lambda})$ is a convex function of $\boldsymbol{\lambda}$ since $g(\boldsymbol{\lambda})$ is the pointwise supremum of affine, and therefore convex, functions of $\boldsymbol{\lambda}$.

⁷We take a sup instead of a max over the sum power constraint capacity region because we have not verified that it is a closed region.

By minimizing the dual function over all non-negative Lagrange multipliers, we get an upper bound d^* on the optimal value p^* . Due to the convexity and feasibility of the problem, this bound is tight [4] [45]:

$$d^* \triangleq \min_{\lambda \geq 0} g(\lambda) \triangleq g(\lambda^*) = p^* \quad (3.63)$$

where $\lambda^* = (\lambda_1^*, \dots, \lambda_K^*)$ are the optimum Lagrange multipliers that lead to d^* . Below we show that λ_i^* is finite and strictly positive if $\mu_i > 0$ and λ_i^* is zero if $\mu_i = 0$.

First consider i such that $\mu_i > 0$. If $\lambda_i = \infty$, then with $\mathbf{R} = \mathbf{P} = 0$ we get $L(\mathbf{R}, \mathbf{P}, \lambda) \geq \lambda_i \bar{P}_i$. Thus $g(\lambda) = \infty$, which implies that λ_i^* must be finite. Now assume $\lambda_i = 0$. Choose $P_j = \bar{P}_j$ for all $j \neq i$ and let P_i be arbitrarily large. Additionally, choose all rates to be zero except for R_i . For this choice of (\mathbf{R}, \mathbf{P}) , we have $L(\mathbf{R}, \mathbf{P}, \lambda) = \mu_i R_i$. Due to the unbounded condition on $R(\mathbf{P})$, letting P_i be arbitrarily large implies R_i can be made arbitrarily large while still maintaining $(\mathbf{R}, \mathbf{P}) \in S$. This in turn implies $g(\lambda) = \infty$. Since $p^* = g(\lambda^*)$ is finite, we must have $\lambda_i^* \neq 0$.

We now show that $\mu_i = 0$ implies $\lambda_i^* = 0$. Since $g(\lambda)$ is the supremum of the Lagrangian and because $\mu_i = 0$, it follows from condition 5 that $R_i = P_i = 0$ to achieve $g(\lambda)$ if $\lambda_i > 0$. Thus, for any λ with $\lambda_i > 0$ and any (\mathbf{R}, \mathbf{P}) with $R_i = P_i = 0$, we have

$$\begin{aligned} L(\mathbf{R}, \mathbf{P}, \lambda) &= \boldsymbol{\mu} \cdot \mathbf{R} - \sum_{j \neq i} \lambda_j P_j + \sum_j \lambda_j \bar{P}_j \\ &> \boldsymbol{\mu} \cdot \mathbf{R} - \sum_{j \neq i} \lambda_j P_j + \sum_{j \neq i} \lambda_j \bar{P}_j \\ &= L(\mathbf{R}, \mathbf{P}, \lambda') \end{aligned}$$

where $\lambda' = \lambda$ except that $\lambda'_i = 0$. Thus $g(\lambda) > g(\lambda')$, which implies that $\lambda_i^* = 0$.

Now consider the *scaled* MAC with α_i defined as

$$\alpha_i = \begin{cases} \frac{\lambda_K^*}{\lambda_i^*} & \text{if } \lambda_i^* > 0 \\ c & \text{if } \lambda_i^* = 0 \end{cases} \quad (3.64)$$

for $i = 1, \dots, K$ and where $c > 0$ is some positive constant. Notice that α is an implicit function of c by this definition. Since $\lambda_K^* > 0$ due to the fact that $\mu_K > 0$, we have $\alpha_i > 0$ for all i . We will now consider the sum power constraint capacity region of the scaled MAC with α as defined above. Consider the following optimization on the scaled MAC:

$$\sup_{\mathbf{R}} \boldsymbol{\mu} \cdot \mathbf{R} \quad \text{s.t.} \quad \mathbf{R} \in R_{\alpha}^{sum} \left(\mathbf{1} \cdot \frac{\bar{\mathbf{P}}}{\alpha} \right). \quad (3.65)$$

By the definition of the sum power constraint capacity region, $\mathbf{R} \in R_{\alpha}^{sum} \left(\mathbf{1} \cdot \frac{\bar{\mathbf{P}}}{\alpha} \right)$ is equivalent to $\mathbf{R} \in R_{\alpha}(\mathbf{P})$ for any \mathbf{P} satisfying $\mathbf{1} \cdot \mathbf{P} \leq \mathbf{1} \cdot \frac{\bar{\mathbf{P}}}{\alpha}$. The above maximization (3.65) can

thus be rewritten as

$$\sup_{\mathbf{P} \in R_K^+, \mathbf{R} \in R_\alpha(\mathbf{P})} \boldsymbol{\mu} \cdot \mathbf{R} \quad \text{s.t.} \quad \mathbf{1} \cdot \mathbf{P} \leq \mathbf{1} \cdot \frac{\bar{\mathbf{P}}}{\boldsymbol{\alpha}}. \quad (3.66)$$

We denote the solution to this by d_α^* . Because there is a sum power constraint, there is only one Lagrange multiplier and the Lagrangian therefore is:

$$\begin{aligned} H_\alpha(\mathbf{R}, \mathbf{P}, \nu) &= \boldsymbol{\mu} \cdot \mathbf{R} - \nu \left(\mathbf{1} \cdot \mathbf{P} - \mathbf{1} \cdot \frac{\bar{\mathbf{P}}}{\boldsymbol{\alpha}} \right) \\ &= \boldsymbol{\mu} \cdot \mathbf{R} - \nu \left(P_1 - \frac{\bar{P}_1}{\alpha_1} \right) - \dots \\ &\quad - \nu \left(P_K - \frac{\bar{P}_K}{\alpha_K} \right) \\ &= \boldsymbol{\mu} \cdot \mathbf{R} - \frac{\nu}{\alpha_1} (\alpha_1 P_1 - \bar{P}_1) - \dots \\ &\quad - \frac{\nu}{\alpha_K} (\alpha_K P_K - \bar{P}_K) \end{aligned}$$

and the corresponding Lagrangian dual function is:

$$f_\alpha(\nu) = \sup_{\mathbf{P} \in R_K^+, \mathbf{R} \in R_\alpha(\mathbf{P})} H_\alpha(\mathbf{R}, \mathbf{P}, \nu).$$

Again, the dual function satisfies $f_\alpha(\nu) \geq d_\alpha^*$ for all $\nu \geq 0$. Due to the fact that $R_\alpha(\mathbf{P}) = R(\alpha\mathbf{P})$ and $\boldsymbol{\alpha} > 0$, we can simplify the dual function as:

$$\begin{aligned} f_\alpha(\nu) &= \sup_{\alpha\mathbf{P} \in R_K^+, \mathbf{R} \in R(\alpha\mathbf{P})} \boldsymbol{\mu} \cdot \mathbf{R} - \frac{\nu}{\alpha_1} (\alpha_1 P_1 - \bar{P}_1) - \dots \\ &\quad - \frac{\nu}{\alpha_K} (\alpha_K P_K - \bar{P}_K) \\ &= \sup_{\mathbf{P} \in R_K^+, \mathbf{R} \in R(\mathbf{P})} \boldsymbol{\mu} \cdot \mathbf{R} - \frac{\nu}{\alpha_1} (P_1 - \bar{P}_1) - \dots \\ &\quad - \frac{\nu}{\alpha_K} (P_K - \bar{P}_K) \\ &= g\left(\frac{\nu}{\boldsymbol{\alpha}}\right) \end{aligned}$$

where g is the Lagrangian dual function of the individual power constraint unscaled MAC.

If we evaluate the dual function with $\nu = \lambda_K^*$, we get

$$f_\alpha(\lambda_K^*) = g\left(\frac{\lambda_K^*}{\boldsymbol{\alpha}}\right) = g\left(\frac{\lambda_K^*}{\alpha_1}, \dots, \frac{\lambda_K^*}{\alpha_K}\right).$$

Having established this, there are now two cases to consider: (a) $\mu_i > 0$ for all i ; (b) $\mu_i = 0$ for some i .

If $\mu_i > 0$ for all i , then $\alpha_i = \frac{\lambda_i^*}{\lambda_i^*}$ for all i . Thus

$$f_{\alpha}(\lambda_K^*) = g\left(\frac{\lambda_K^*}{\alpha_1}, \dots, \frac{\lambda_K^*}{\alpha_K}\right) = g(\lambda_1^*, \dots, \lambda_K^*) = p^*.$$

Since $f_{\alpha}(\lambda_K^*)$ is an upper bound to d_{α}^* , we have $d_{\alpha}^* \leq p^*$. This implies

$$\begin{aligned} \max_{\mathbf{R} \in R(\bar{\mathbf{P}})} \boldsymbol{\mu} \cdot \mathbf{R} &\geq \sup_{\mathbf{R} \in R_{\alpha}^{sum}(\mathbf{1} \cdot \frac{\bar{\mathbf{P}}}{\alpha})} \boldsymbol{\mu} \cdot \mathbf{R} \\ &\geq \sup_{\mathbf{R} \in \cap_{\alpha > 0} R_{\alpha}^{sum}(\mathbf{1} \cdot \frac{\mathbf{P}}{\alpha})} \boldsymbol{\mu} \cdot \mathbf{R} \end{aligned}$$

where the second inequality follows from $R_{\alpha}^{sum}(\mathbf{1} \cdot \frac{\bar{\mathbf{P}}}{\alpha}) \supseteq \cap_{\alpha > 0} R_{\alpha}^{sum}(\mathbf{1} \cdot \frac{\mathbf{P}}{\alpha})$.

If $\mu_i = 0$ for some i , we must consider α -scalings for *different* values of c . Assume without loss of generality that $\mu_i = 0$ for $i = 1, \dots, L$ and $\mu_i > 0$ for $i = L + 1, \dots, K$. We established earlier that $\mu_i = 0$ implies $\lambda_i^* = 0$. Therefore, we have $p^* = g(\lambda_1^*, \dots, \lambda_L^*, \lambda_{L+1}^*, \dots, \lambda_K^*) = g(0, \dots, 0, \lambda_{L+1}^*, \dots, \lambda_K^*)$. Using the fact that $f_{\alpha}(\nu) = g(\frac{\nu}{\alpha}) \forall \alpha > 0$, we have

$$\begin{aligned} f_{\alpha}(\lambda_K^*) &= g\left(\frac{\lambda_K^*}{\alpha}\right) \\ &= g\left(\frac{\lambda_K^*}{c}, \dots, \frac{\lambda_K^*}{c}, \frac{\lambda_K^*}{\alpha_{L+1}}, \dots, \frac{\lambda_K^*}{\alpha_K}\right) \\ &= g\left(\frac{\lambda_K^*}{c}, \dots, \frac{\lambda_K^*}{c}, \lambda_{L+1}^*, \dots, \lambda_K^*\right). \end{aligned}$$

Here $f_{\alpha}(\lambda_K^*)$ is a function of the constant c because α depends on c , as defined in (3.64). For a fixed α (i.e. a fixed c), the optimum value of the sum power constraint region satisfies $d_{\alpha}^* \leq f_{\alpha}(\lambda_K^*)$.

We now show the desired result by contradiction. Assume

$$\sup_{\mathbf{R} \in \cap_{\alpha > 0} R_{\alpha}^{sum}(\mathbf{1} \cdot \frac{\mathbf{P}}{\alpha})} \boldsymbol{\mu} \cdot \mathbf{R} > \max_{\mathbf{R} \in R(\bar{\mathbf{P}})} \boldsymbol{\mu} \cdot \mathbf{R}. \quad (3.67)$$

Since $R_{\alpha}^{sum}(\mathbf{1} \cdot \frac{\bar{\mathbf{P}}}{\alpha}) \supseteq \cap_{\alpha > 0} R_{\alpha}^{sum}(\mathbf{1} \cdot \frac{\mathbf{P}}{\alpha}) \forall \alpha > 0$, this implies that for some $\epsilon > 0$,

$$\left(\sup_{\mathbf{R} \in R_{\alpha}^{sum}(\mathbf{1} \cdot \frac{\bar{\mathbf{P}}}{\alpha})} \boldsymbol{\mu} \cdot \mathbf{R} \right) \geq \left(\max_{\mathbf{R} \in R(\bar{\mathbf{P}})} \boldsymbol{\mu} \cdot \mathbf{R} \right) + \epsilon,$$

for all $\alpha > 0$. This implies that for all $\alpha > 0$, $d_{\alpha}^* \geq p^* + \epsilon = g(0, \dots, 0, \lambda_{L+1}^*, \dots, \lambda_K^*) + \epsilon$. However, earlier we established that $d_{\alpha}^* \leq f_{\alpha}(\lambda_K^*) = g\left(\frac{\lambda_K^*}{c}, \dots, \frac{\lambda_K^*}{c}, \lambda_{L+1}^*, \dots, \lambda_K^*\right)$ for all $c > 0$. Thus we have that $g\left(\frac{\lambda_K^*}{c}, \dots, \frac{\lambda_K^*}{c}, \lambda_{L+1}^*, \dots, \lambda_K^*\right) \geq g(0, \dots, 0, \lambda_{L+1}^*, \dots, \lambda_K^*) + \epsilon$

for all c . Since g is a convex function, $g(\beta, \dots, \beta, \lambda_{L+1}^*, \dots, \lambda_K^*)$ must lie *beneath* the line between $g(0, \dots, 0, \lambda_{L+1}^*, \dots, \lambda_K^*)$ and $g(1, \dots, 1, \lambda_{L+1}^*, \dots, \lambda_K^*)$ (which is finite) for $0 \leq \beta \leq 1$. This contradicts

$$g\left(\frac{\lambda_K^*}{c}, \dots, \frac{\lambda_K^*}{c}, \lambda_{L+1}^*, \dots, \lambda_K^*\right) \geq g(0, \dots, 0, \lambda_{L+1}^*, \dots, \lambda_K^*) + \epsilon \quad \forall c \geq \lambda_K^*.$$

In other words, the convexity of g implies that as c becomes large, the value of $g\left(\frac{\lambda_K^*}{c}, \dots, \frac{\lambda_K^*}{c}, \lambda_{L+1}^*, \dots, \lambda_K^*\right)$ must become arbitrarily close to $g(0, \dots, 0, \lambda_{L+1}^*, \dots, \lambda_K^*)$. Thus (3.67) must be false and therefore

$$\max_{\mathbf{R} \in R(\bar{\mathbf{P}})} \boldsymbol{\mu} \cdot \mathbf{R} \geq \sup_{\mathbf{R} \in \bigcap_{\alpha > 0} R_{\alpha}^{\text{sum}}\left(1, \frac{P}{\alpha}\right)} \boldsymbol{\mu} \cdot \mathbf{R} \quad (3.68)$$

for all $\boldsymbol{\mu}$ such that $\mu_i = 0$ for some i .

We have now shown that the above relationship (3.68) holds for *all* $\boldsymbol{\mu} \geq 0$ and the proof is complete.

3.4.4 Verification of Rate Region Conditions

In this section we show that capacity region of the constant MAC $\mathcal{C}_{MAC}(\mathbf{h}, \bar{\mathbf{P}})$ meets the conditions specified in Theorem 3.2. All conditions are satisfied by any reasonable definition of a capacity region, but we explicitly verify them for this case.

1. The scaling property of $\mathcal{C}_{MAC}(\mathbf{h}, \bar{\mathbf{P}})$ follows from the definition of the capacity region in (2.9).
2. The set S is convex if for any $x, y \in S$ and $\theta \in [0, 1]$, $\theta x + (1 - \theta)y \in S$. Let $\mathbf{r} \in \mathcal{C}_{MAC}(\bar{\mathbf{P}})$ and $\mathbf{t} \in \mathcal{C}_{MAC}(\bar{\mathbf{Q}})$. We wish to show that $\theta \mathbf{r} + (1 - \theta)\mathbf{t} \in \mathcal{C}_{MAC}(\theta \bar{\mathbf{P}} + (1 - \theta)\bar{\mathbf{Q}})$. By time-sharing between the schemes used to achieve \mathbf{r} and \mathbf{t} , we use power $\theta \bar{\mathbf{P}} + (1 - \theta)\bar{\mathbf{Q}}$ and achieve rate $\theta \mathbf{r} + (1 - \theta)\mathbf{t}$, which verifies the convexity of the set.
3. The region $\mathcal{C}_{MAC}(\mathbf{h}, \bar{\mathbf{P}})$ is closed by definition and is convex due to a time-sharing argument.
4. $\mathcal{C}_{MAC}(\mathbf{h}, \bar{\mathbf{P}})$ is an increasing function of power because any rate achievable with a smaller power constraint is also achievable with a larger power constraint because all power need not be used.
5. If some set of rates are achievable by transmitters 2 through K while transmitter 1 is also sending information, then those same rates are achievable in the absence of transmitter 1's signal because each user transmits an independent message.

6. If transmission is halted for some fraction of time, then any smaller rate vector can be achieved.
7. Additional power allows for additional rate on any link by transmitting a codeword that can be decoded (and thus subtracted off) by all K receivers, even when treating the rest of the received signal as noise.
8. $\mathcal{C}_{MAC}(\mathbf{h}, \overline{\mathbf{P}})$ is bounded by the individual capacities of each link (i.e. each transmitter-receiver pair), which are finite due to the basic properties of Gaussian channels.

3.4.5 Equivalent Covariance Matrix for Flipped Channel

Given a covariance matrix Σ for some channel \mathbf{H} , we wish to find a covariance matrix $\overline{\Sigma}$ such that $\text{Tr}(\overline{\Sigma}) \leq \text{Tr}(\Sigma)$ and

$$\log |\mathbf{I} + \mathbf{H}\Sigma\mathbf{H}^\dagger| = \log |\mathbf{I} + \mathbf{H}^\dagger\overline{\Sigma}\mathbf{H}|. \quad (3.69)$$

If the SVD of \mathbf{H} is $\mathbf{H} = \mathbf{F}\mathbf{\Lambda}\mathbf{G}^\dagger$ where $\mathbf{\Lambda}$ is square and diagonal, then we propose $\overline{\Sigma} = \mathbf{F}\mathbf{G}^\dagger\Sigma\mathbf{G}\mathbf{F}^\dagger$. Using the identity $|\mathbf{I} + \mathbf{A}\mathbf{B}| = |\mathbf{I} + \mathbf{B}\mathbf{A}|$ and the fact that $\mathbf{F}^\dagger\mathbf{F} = \mathbf{I}$ and $\mathbf{G}^\dagger\mathbf{G} = \mathbf{I}$ we can write the capacity of the unflipped channel as:

$$\begin{aligned} \log |\mathbf{I} + \mathbf{H}\Sigma\mathbf{H}^\dagger| &= \log |\mathbf{I} + \mathbf{F}\mathbf{\Lambda}\mathbf{G}^\dagger\Sigma\mathbf{G}\mathbf{\Lambda}\mathbf{F}^\dagger| \\ &= \log |\mathbf{I} + \mathbf{\Lambda}\mathbf{G}^\dagger\Sigma\mathbf{G}\mathbf{\Lambda}|. \end{aligned} \quad (3.70)$$

We can similarly write the capacity of the flipped channel with our candidate covariance matrix $\overline{\Sigma}$ as:

$$\begin{aligned} \log |\mathbf{I} + \mathbf{H}^\dagger\overline{\Sigma}\mathbf{H}| &= \log |\mathbf{I} + \mathbf{G}\mathbf{\Lambda}\mathbf{F}^\dagger\mathbf{F}\mathbf{G}^\dagger\Sigma\mathbf{G}\mathbf{F}^\dagger\mathbf{F}\mathbf{\Lambda}\mathbf{G}^\dagger| \\ &= \log |\mathbf{I} + \mathbf{G}\mathbf{\Lambda}\mathbf{G}^\dagger\Sigma\mathbf{G}\mathbf{\Lambda}\mathbf{G}^\dagger| \\ &= \log |\mathbf{I} + \mathbf{\Lambda}\mathbf{G}^\dagger\Sigma\mathbf{G}\mathbf{\Lambda}|. \end{aligned} \quad (3.71)$$

Therefore the rate achieved by $\overline{\Sigma}$ in the flipped channel is the same as the rate achieved by the original covariance matrix Σ in the unflipped channel. It thus only remains to show that $\text{Tr}(\overline{\Sigma}) \leq \text{Tr}(\Sigma)$. To do so, we make use of the identity $\text{Tr}(\mathbf{A}\mathbf{B}) = \text{Tr}(\mathbf{B}\mathbf{A})$. Clearly, we can write

$$\text{Tr}(\overline{\Sigma}) = \text{Tr}(\mathbf{F}\mathbf{G}^\dagger\Sigma\mathbf{G}\mathbf{F}^\dagger) = \text{Tr}(\mathbf{G}^\dagger\Sigma\mathbf{G}) = \text{Tr}(\Sigma\mathbf{G}\mathbf{G}^\dagger). \quad (3.72)$$

We then use Gram-Schmidt to expand \mathbf{G} into a full unitary matrix:

$$\tilde{\mathbf{G}} = [\mathbf{G} \quad \overline{\mathbf{G}}] \quad (3.73)$$

such that $\tilde{\mathbf{G}}\tilde{\mathbf{G}}^\dagger = \tilde{\mathbf{G}}^\dagger\tilde{\mathbf{G}} = \mathbf{I}$. Using this unitary matrix, we can write

$$\begin{aligned}\text{Tr}(\boldsymbol{\Sigma}) &= \text{Tr}(\boldsymbol{\Sigma}\tilde{\mathbf{G}}\tilde{\mathbf{G}}^\dagger) \\ &= \text{Tr}(\boldsymbol{\Sigma}\mathbf{G}\mathbf{G}^\dagger) + \text{Tr}(\boldsymbol{\Sigma}\overline{\mathbf{G}}\overline{\mathbf{G}}^\dagger) \\ &\geq \text{Tr}(\boldsymbol{\Sigma}\mathbf{G}\mathbf{G}^\dagger).\end{aligned}\tag{3.74}$$

To get (3.74), we used the fact that the matrix $\overline{\mathbf{G}}^\dagger\boldsymbol{\Sigma}\overline{\mathbf{G}}$ is positive semi-definite, which implies $\text{Tr}(\boldsymbol{\Sigma}\overline{\mathbf{G}}\overline{\mathbf{G}}^\dagger) = \text{Tr}(\overline{\mathbf{G}}^\dagger\boldsymbol{\Sigma}\overline{\mathbf{G}}) \geq 0$.

3.4.6 Trace-Preserving Property of MIMO MAC-BC Transformations

In this section, we show that the MAC-BC transformations obtained in (3.24)-(3.26) satisfy the sum trace requirement. Since $\boldsymbol{\Sigma}_K = \mathbf{A}_K^{1/2}\mathbf{Q}_K\mathbf{A}_K^{1/2}$

$$\begin{aligned}\text{Tr}(\boldsymbol{\Sigma}_K) &\leq \text{Tr}(\mathbf{A}_K^{1/2}\mathbf{Q}_K\mathbf{A}_K^{1/2}) \\ &= \text{Tr}(\mathbf{A}_K\mathbf{Q}_K) \\ &= \text{Tr}(\mathbf{Q}_K) + \sum_{i=1}^{K-1} \text{Tr}(\boldsymbol{\Sigma}_i\mathbf{H}_K^\dagger\mathbf{Q}_K\mathbf{H}_K).\end{aligned}$$

By adding $\sum_{i=1}^{K-1} \text{Tr}(\boldsymbol{\Sigma}_i)$ to both sides we get

$$\sum_{i=1}^K \text{Tr}(\boldsymbol{\Sigma}_i) \leq \text{Tr}(\mathbf{Q}_K) + \sum_{i=1}^{K-1} \text{Tr}(\boldsymbol{\Sigma}_i(\mathbf{I} + \mathbf{H}_K^\dagger\mathbf{Q}_K\mathbf{H}_K)).$$

By the definition of $\boldsymbol{\Sigma}_j$, we get

$$\begin{aligned}\text{Tr}(\boldsymbol{\Sigma}_j(\mathbf{I} + \sum_{i=j+1}^K \mathbf{H}_i^\dagger\mathbf{Q}_i\mathbf{H}_i)) &= \text{Tr}(\boldsymbol{\Sigma}_j\mathbf{B}_j) \\ &\leq \text{Tr}(\mathbf{A}_j\mathbf{Q}_j) \\ &= \text{Tr}(\mathbf{Q}_j) + \sum_{i=1}^{j-1} \text{Tr}(\boldsymbol{\Sigma}_i\mathbf{H}_j^\dagger\mathbf{Q}_j\mathbf{H}_j).\end{aligned}$$

Using this expression for $j = K - 1$ we get

$$\begin{aligned}\sum_{i=1}^K \text{Tr}(\boldsymbol{\Sigma}_i) &\leq \sum_{l=K-1}^K \text{Tr}(\mathbf{Q}_l) + \\ &\quad \sum_{i=1}^{K-2} \text{Tr}(\boldsymbol{\Sigma}_i(\mathbf{I} + \sum_{l=K-1}^K \mathbf{H}_l^\dagger\mathbf{Q}_l\mathbf{H}_l)).\end{aligned}$$

By induction, we can further show that

$$\sum_{i=1}^K \text{Tr}(\boldsymbol{\Sigma}_i) \leq \sum_{l=j}^K \text{Tr}(\mathbf{Q}_l) + \sum_{i=1}^{j-1} \text{Tr}(\boldsymbol{\Sigma}_i(\mathbf{I} + \sum_{l=j}^K \mathbf{H}_l^\dagger \mathbf{Q}_l \mathbf{H}_l)),$$

for any j . For $j = 1$, we get

$$\sum_{i=1}^K \text{Tr}(\boldsymbol{\Sigma}_i) \leq \sum_{l=1}^K \text{Tr}(\mathbf{Q}_l).$$

The same proof method can be used to show that the BC-MAC transformations in (3.28)-(3.30) also satisfy the trace constraints.

Chapter 4

Multiple-Antenna Broadcast Channels

Multiple input multiple output (MIMO) systems have received a great deal of attention as a method to achieve very high data rates over wireless links. The capacity of single-user MIMO Gaussian channels was first studied by Foschini [16] and Telatar [61]. This work has also been extended to the MIMO multiple-access channel (MAC) [61, 66, 83]. In this chapter we study multiple-antenna broadcast channels in which the transmitter and each of the receivers may employ multiple antennas. Such channels are not well understood because they fall into the class of non-degraded broadcast channels, for which the capacity region is unknown. Note that the multiple-antenna broadcast channel is an excellent model for current cellular systems in which multiple antennas are deployed at the base station. Thus, understanding the fundamental limits of such channels is of critical importance.

In pioneering work by Caire and Shamai [5], an achievable rate region for the MIMO broadcast channel was obtained by applying the “dirty paper” result [8] at the transmitter (or alternatively using the coding for non-causally known interference technique [15]). Caire and Shamai also showed that the sum rate capacity of the MIMO BC equals the maximum sum rate of this achievable region for the two user broadcast channel with an arbitrary number of transmit antennas and one receive antenna at each receiver. However, computing this region is extremely complex and the approach used in [5] to prove the optimality of dirty-paper coding for sum rate does not appear to work for more than two users and multiple receive antennas.

In this chapter we develop three new results related to the sum rate capacity of the MIMO BC. First, we generalize the results of [5] and show that dirty paper coding achieves the sum rate capacity of the MIMO BC for an arbitrary number of users, transmit antennas, and receive antennas. We prove that an upper bound to the sum rate capacity of the MIMO BC is equal to the sum rate capacity of the *dual* MIMO multiple-access channel. Using the equivalence of the MIMO MAC capacity region and the MIMO BC dirty paper achievable

region, established in Chapter 3.1.4, this proves the result. Next, we propose an efficient algorithm that numerically computes the sum rate capacity of the MIMO BC and the corresponding optimal transmission policies. This algorithm in fact finds the sum capacity of the dual MIMO multiple-access channel and provably converges. Finally, we compare the sum rate capacity of the MIMO BC, again using the MAC-BC duality, to the maximum sum rate achievable using single-user transmission, i.e. using time-division multiple-access (TDMA), to characterize the gain that dirty paper coding provides over simpler transmission techniques. It is interesting to note that the MAC-BC duality is a crucial component of all three results in this section.

The remainder of this chapter is organized as follows. In Chapter 4.1 we describe the MIMO BC and the dual MIMO MAC. In Chapter 4.2 we find the sum-rate capacity of the MIMO BC, followed by a corresponding numerical algorithm in Chapter 4.3. Finally, we compare the sum-capacity achieving technique of dirty paper coding to the sub-optimal technique of time-division multiple-access in Chapter 4.4. Some of the work in this chapter is also published in [68] [69] [33] [71] [31] [28].

4.1 System Model

We consider a MIMO broadcast channel with an M -antenna transmitter and K receivers with r_1, \dots, r_K receive antennas, respectively, as described in Chapter 2.2.5. In order to facilitate reading of this thesis, we copy the mathematical description of this channel from Chapter 2.2.5. Let $\mathbf{x} \in \mathbb{C}^{M \times 1}$ be the transmitted vector signal and let $\mathbf{H}_k \in \mathbb{C}^{r_k \times M}$ be the channel matrix of receiver k where $\mathbf{H}_k(i, j)$ represents the channel gain from transmit antenna j to antenna i of receiver k . The circularly symmetric complex Gaussian noise at receiver k is represented by $\mathbf{n}_k \in \mathbb{C}^{r_k \times 1}$ where $\mathbf{n}_k \sim N(0, \mathbf{I})$. Notice that *each* receive antenna component suffers from additive complex Gaussian noise of variance one. Let $\mathbf{y}_k \in \mathbb{C}^{r_k \times 1}$ be the received signal at receiver k . The received signal is mathematically represented as:

$$\begin{bmatrix} \mathbf{y}_1 \\ \vdots \\ \mathbf{y}_K \end{bmatrix} = \mathbf{H}\mathbf{x} + \begin{bmatrix} \mathbf{n}_1 \\ \vdots \\ \mathbf{n}_K \end{bmatrix} \quad \text{where} \quad \mathbf{H} = \begin{bmatrix} \mathbf{H}_1 \\ \vdots \\ \mathbf{H}_K \end{bmatrix}. \quad (4.1)$$

The matrix \mathbf{H} represents the channel gains of all receivers. The covariance matrix of the input signal is $\boldsymbol{\Sigma}_x \triangleq \mathbb{E}[\mathbf{x}\mathbf{x}^\dagger]$. The transmitter is subject to an average power constraint P , which implies $\text{Tr}(\boldsymbol{\Sigma}_x) \leq P$. We assume the channel matrix \mathbf{H} is constant and is known perfectly at the transmitter and at all receivers.

Throughout this chapter we also extensively consider the *dual* multiple-access channel, i.e. a K -transmitter multiple-access channel in which the j -th transmitter has r_j antennas

and the receiver has M antennas. This channel is described in Chapter 2.2.6, but for ease of reading we repeat the mathematical description. Let $\mathbf{x}_k \in \mathbb{C}^{r_k \times 1}$ denote the transmitted signal of transmitter k . Let $\mathbf{y}_{MAC} \in \mathbb{C}^{M \times 1}$ be the received signal and $\mathbf{n} \in \mathbb{C}^{M \times 1}$ the noise vector where $\mathbf{n} \sim N(0, \mathbf{I})$. We also use $\mathbf{H}_k \in \mathbb{C}^{M \times r_k}$ to denote the channel matrix from the k -th transmitter to the receiver. Notice that the channel matrix dimensions are opposite those in the MIMO broadcast channel. The received signal is mathematically represented as

$$\begin{aligned} \mathbf{y}_{MAC} &= \mathbf{H}_1 \mathbf{x}_1 + \dots + \mathbf{H}_K \mathbf{x}_K + \mathbf{n} \\ &= \mathbf{H} \begin{bmatrix} \mathbf{x}_1 \\ \vdots \\ \mathbf{x}_K \end{bmatrix} + \mathbf{n} \quad \text{where} \quad \mathbf{H} = [\mathbf{H}_1 \ \dots \ \mathbf{H}_K]. \end{aligned}$$

In the dual MAC, each transmitter is subject to an individual power constraint of P_1, \dots, P_K . We also assume perfect knowledge of the channel at the transmitters and the receiver in the dual MAC.

Lastly, we define the *cooperative system* to be the same as the broadcast channel, but with all receivers coordinating to perform joint detection. If the receivers are allowed to cooperate, the broadcast channel reduces to a single-user $M \times (\sum_{j=1}^K r_j)$ multiple-antenna system described by

$$\mathbf{y} = \mathbf{H}\mathbf{x} + \mathbf{z} \tag{4.2}$$

where $\mathbf{y} = \begin{bmatrix} \mathbf{y}_1 \\ \vdots \\ \mathbf{y}_K \end{bmatrix}$ and $\mathbf{z} = \begin{bmatrix} \mathbf{n}_1 \\ \vdots \\ \mathbf{n}_K \end{bmatrix}$. We call the capacity of this system, denoted $C_{\text{coop}}(\mathbf{H}, P)$, the *cooperative capacity*.

We use boldface to denote matrices and vectors. $|\mathbf{S}|$ denotes the determinant and \mathbf{S}^{-1} the inverse of a square matrix \mathbf{S} . For any general matrix \mathbf{M} , \mathbf{M}^\dagger denotes the conjugate transpose and $\text{Tr}(\mathbf{M})$ denotes the trace. \mathbf{I} denotes the identity matrix and $\text{diag}(\lambda_i)$ denotes a diagonal matrix with the (i, i) entry equal to λ_i .

4.2 Sum Rate Capacity

In this section, we prove that dirty paper coding achieves the sum rate capacity of the multiple-antenna broadcast channel. If we let $C_{BC}^{\text{region}}(\mathbf{H}_1, \dots, \mathbf{H}_K, P)$ denote the capacity region of the MIMO BC, the sum rate capacity of the channel, denoted $C_{BC}(\mathbf{H}_1, \dots, \mathbf{H}_K, P)$, is given by:

$$C_{BC}(\mathbf{H}_1, \dots, \mathbf{H}_K, P) \triangleq \max_{R_1, \dots, R_K \in C_{BC}^{\text{region}}(\mathbf{H}_1, \dots, \mathbf{H}_K, P)} \sum_{i=1}^K R_i. \tag{4.3}$$

We can similarly define the maximum sum rate achievable using dirty paper coding, denoted $C_{DPC}^{\text{sumrate}}(\mathbf{H}_1, \dots, \mathbf{H}_K, P)$, by:

$$C_{DPC}^{\text{sumrate}}(\mathbf{H}_1, \dots, \mathbf{H}_K, P) \triangleq \max_{R_1, \dots, R_K \in C_{DPC}(\mathbf{H}_1, \dots, \mathbf{H}_K, P)} \sum_{i=1}^K R_i. \quad (4.4)$$

where the dirty paper rate region $C_{DPC}(\mathbf{H}_1, \dots, \mathbf{H}_K, P)$ is defined in (2.19).

In [55], Sato presented an upper bound on the capacity region of general BCs. This bound utilizes the capacity of the *cooperative system* as defined in Chapter 4.1. Since the cooperative system is the same as the BC, but with receiver coordination, the capacity of the cooperative system ($\mathcal{C}_{\text{coop}}(\mathbf{H}, P)$) is an upper bound on the BC sum rate capacity, i.e. $C_{BC}(\mathbf{H}_1, \dots, \mathbf{H}_K, P) \leq \mathcal{C}_{\text{coop}}(\mathbf{H}, P)$. This bound is not tight in general, but Sato tightened this bound by using the fact that the capacity region of a general BC depends only on the marginal transition probabilities of the channel (i.e. $p(y_i|x)$) and not on the joint distribution $p(y_1, \dots, y_K|x)$ [13, Theorem 14.6.1]. Thus, if the joint distribution is modified while keeping the marginal distributions fixed, the capacity region of the broadcast channel, and therefore the sum rate capacity, is unaffected. However, the capacity of the cooperative system is affected by the joint distribution, and thus the joint distribution can be modified to yield the lowest cooperative capacity.

For the MIMO BC, the marginal distribution is governed only by the fixed channel matrices and the additive Gaussian noise at each receiver, and is unaffected by any correlation between the noise at *different receivers* of the BC. Such correlation does, however, affect the capacity of the cooperative system, which is still an upper bound on the sum rate of the BC. Therefore we retain $\mathbb{E}(\mathbf{n}_i \mathbf{n}_i^\dagger) = \mathbf{I}$, $1 \leq i \leq K$ as before (i.e. noise components at the multiple receive antennas within a single receiver are uncorrelated) and let $\mathbb{E}(\mathbf{n}_i \mathbf{n}_j^\dagger) \triangleq \mathbf{X}_{i,j} \prec \mathbf{I}$. Let \mathbf{Z} denote the noise covariance matrix in the cooperative system (i.e. $\mathbf{Z} = E[\mathbf{z}\mathbf{z}^T]$ where $\mathbf{z} = [\mathbf{n}_1^T \dots \mathbf{n}_K^T]^T$) and define the set S to be all *non-singular* (or strictly positive definite) noise covariance matrices satisfying the Sato upper bound conditions

$$S = \left\{ \mathbf{Z} : \mathbf{Z} > 0, \mathbf{Z} = \begin{bmatrix} \mathbf{I} & \dots & \mathbf{X}_{K,1}^\dagger \\ \vdots & \vdots & \vdots \\ \mathbf{X}_{K,1} & \dots & \mathbf{I} \end{bmatrix} \right\}. \quad (4.5)$$

Then for any $\mathbf{Z} \in S$, the cooperative capacity is an upper bound to $\mathcal{C}_{BC}(\mathbf{H}_1, \dots, \mathbf{H}_K, P)$. Noise correlation colors the noise of the joint receiver, and it is easy to see that the capacity of the cooperative system with channel \mathbf{H} and Gaussian noise with covariance \mathbf{Z} is equal to $\mathcal{C}_{\text{coop}}(\mathbf{Z}^{-1/2}\mathbf{H}, P)$. Thus, the Sato upper bound is equal to the capacity of the cooperative

system for the worst case \mathbf{Z} :

$$\begin{aligned} \mathcal{C}_{\text{Sato}}(\mathbf{H}_1, \dots, \mathbf{H}_K, P) &\triangleq \inf_{\mathbf{Z} \in \mathcal{S}} \mathcal{C}_{\text{coop}}(\mathbf{Z}^{-1/2} \mathbf{H}, P) \\ &= \inf_{\mathbf{Z} \in \mathcal{S}} \max_{\boldsymbol{\Sigma} \geq 0, \text{Tr}(\boldsymbol{\Sigma}) \leq P} \log \left| \mathbf{I} + \mathbf{Z}^{-1/2} \mathbf{H} \boldsymbol{\Sigma} \mathbf{H}^\dagger \mathbf{Z}^{-1/2} \right|, \end{aligned} \quad (4.6)$$

where the cooperative capacity is given in [61] as:

$$\mathcal{C}_{\text{coop}}(\mathbf{Z}^{-1/2} \mathbf{H}, P) = \max_{\boldsymbol{\Sigma} \geq 0, \text{Tr}(\boldsymbol{\Sigma}) \leq P} \log \left| \mathbf{I} + \mathbf{Z}^{-1/2} \mathbf{H} \boldsymbol{\Sigma} \mathbf{H}^\dagger \mathbf{Z}^{-1/2} \right|.$$

Of course, as noted before, the sum rate capacity of the MIMO BC can be no larger than the Sato upper bound:

$$\mathcal{C}_{\text{BC}}(\mathbf{H}_1, \dots, \mathbf{H}_K, P) \leq \mathcal{C}_{\text{Sato}}(\mathbf{H}_1, \dots, \mathbf{H}_K, P). \quad (4.7)$$

Next, we show that this statement holds with equality, or that the sum rate capacity of the MIMO BC actually equals the Sato upper bound.

Theorem 4.1 *The sum rate capacity of the MIMO BC equals the Sato upper bound. Furthermore, the dirty paper coding strategy achieves the sum rate capacity of the MIMO BC*

$$\mathcal{C}_{\text{BC}}(\mathbf{H}_1, \dots, \mathbf{H}_K, P) = \mathcal{C}_{\text{DPC}}^{\text{sumrate}}(\mathbf{H}_1, \dots, \mathbf{H}_K, P) = \mathcal{C}_{\text{Sato}}(\mathbf{H}_1, \dots, \mathbf{H}_K, P). \quad (4.8)$$

Proof: Since the sum rate capacity of the MIMO BC can be no larger than the Sato upper bound, it is sufficient to show that the Sato upper bound is actually achievable in the MIMO BC using dirty paper coding. By Theorem 3.6 we have $\mathcal{C}_{\text{DPC}}(\mathbf{H}_1, \dots, \mathbf{H}_K, P) = \bigcup_{\mathbf{1} \cdot \mathbf{P} \leq P} \mathcal{C}_{\text{MAC}}(\mathbf{H}_1^\dagger, \dots, \mathbf{H}_K^\dagger, \mathbf{P})$. Thus, if we define $\mathcal{C}_{\text{union}}^{\text{sumrate}}(\mathbf{H}_1^\dagger, \dots, \mathbf{H}_K^\dagger, P)$ as:

$$\mathcal{C}_{\text{union}}^{\text{sumrate}}(\mathbf{H}_1^\dagger, \dots, \mathbf{H}_K^\dagger, P) \triangleq \max_{P_1, \dots, P_K: \sum_{i=1}^K P_i \leq P} \mathcal{C}_{\text{MAC}}^{\text{sumrate}}(\mathbf{H}_1^\dagger, \dots, \mathbf{H}_K^\dagger, P_1, \dots, P_K) \quad (4.9)$$

then clearly we have $\mathcal{C}_{\text{DPC}}^{\text{sumrate}}(\mathbf{H}_1, \dots, \mathbf{H}_K, P) = \mathcal{C}_{\text{union}}^{\text{sumrate}}(\mathbf{H}_1^\dagger, \dots, \mathbf{H}_K^\dagger, P)$. Therefore it is sufficient to show

$$\mathcal{C}_{\text{union}}^{\text{sumrate}}(\mathbf{H}_1^\dagger, \dots, \mathbf{H}_K^\dagger, P) \geq \mathcal{C}_{\text{Sato}}(\mathbf{H}_1, \dots, \mathbf{H}_K, P). \quad (4.10)$$

to get the result. Note that the expression for the MAC sum rate given in (2.22) gives

$$\mathcal{C}_{\text{union}}^{\text{sumrate}}(\mathbf{H}_1^\dagger, \dots, \mathbf{H}_K^\dagger, P) = \max_{\{\mathbf{Q}_j \geq 0, \sum_{i=1}^K \text{Tr}(\mathbf{Q}_i) \leq P\}} \log \left| \mathbf{I} + \sum_{i=1}^K \mathbf{H}_i^\dagger \mathbf{Q}_i \mathbf{H}_i \right|. \quad (4.11)$$

We prove (4.10) by using Lagrangian duality to express both the Sato upper bound and the MIMO MAC sum rate capacity in different forms. Specifically, as shown in Chapter

4.6.1, we can alternatively write the Sato upper bound defined in (4.6) as:

$$\begin{aligned}
\mathcal{C}_{\text{Sato}}(\mathbf{H}_1, \dots, \mathbf{H}_K, P) &= \inf_{\mathbf{Z} \in \mathcal{S}} \min_{\mathbf{A}, \lambda} -\log |\mathbf{A}| + \text{Tr}(\mathbf{A}) + \lambda P - M \\
&\quad \text{such that} \\
&\quad \lambda \geq 0, \mathbf{A} \geq 0 \\
&\quad \lambda \mathbf{Z} \geq \mathbf{H} \mathbf{A} \mathbf{H}^\dagger,
\end{aligned} \tag{4.12}$$

and the MIMO MAC sum rate capacity (4.11) as:

$$\begin{aligned}
\mathcal{C}_{\text{union}}^{\text{sumrate}}(\mathbf{H}_1^\dagger, \dots, \mathbf{H}_K^\dagger, P) &= \min_{\mathbf{A}, \lambda} -\log |\mathbf{A}| + \text{Tr}(\mathbf{A}) + \lambda P - M \\
&\quad \text{such that} \\
&\quad \lambda \geq 0, \mathbf{A} \geq 0, \\
&\quad \lambda \mathbf{I} \geq \mathbf{H}_i \mathbf{A} \mathbf{H}_i^\dagger \quad \forall i.
\end{aligned} \tag{4.13}$$

Notice that the objective functions of (4.12) and (4.13) are the same, but the variables and constraints are different. We will show that $\mathcal{C}_{\text{union}}^{\text{sumrate}}(\mathbf{H}_1^\dagger, \dots, \mathbf{H}_K^\dagger, P) \geq \mathcal{C}_{\text{Sato}}(\mathbf{H}_1, \dots, \mathbf{H}_K, P)$ by constructing a feasible solution to the Sato upper bound dual problem from an optimal solution to the MIMO MAC sum rate dual problem.

Let $\lambda = \lambda_0$, $\mathbf{A} = \mathbf{A}_0$ be an optimizing solution to (4.13), i.e. $\mathcal{C}_{\text{union}}^{\text{sumrate}}(\mathbf{H}_1^\dagger, \dots, \mathbf{H}_K^\dagger, P) = -\log |\mathbf{A}_0| + \text{Tr}(\mathbf{A}_0) + \lambda_0 P - M$. Since (4.13) is a minimization of a convex function over a closed set, we know that the minimum is achieved and the minimizing pair $(\lambda_0, \mathbf{A}_0)$ exists. We prove (4.10) by explicitly constructing a feasible set of variables $(\lambda, \mathbf{A}, \mathbf{Z})$ for the Sato upper bound (4.12) such that the objective functions in (4.13) and (4.12) are equal.

Let us first consider the choice of values of $(\lambda, \mathbf{A}, \mathbf{Z})$ as

$$\lambda = \lambda_0 \tag{4.14}$$

$$\mathbf{A} = \mathbf{A}_0 \tag{4.15}$$

$$\mathbf{Z} = \begin{bmatrix} \mathbf{I} & \frac{\mathbf{H}_1 \mathbf{A}_0 \mathbf{H}_2^\dagger}{\lambda_0} & \dots & \frac{\mathbf{H}_1 \mathbf{A}_0 \mathbf{H}_K^\dagger}{\lambda_0} \\ \frac{\mathbf{H}_2 \mathbf{A}_0 \mathbf{H}_1^\dagger}{\lambda_0} & \mathbf{I} & \dots & \frac{\mathbf{H}_2 \mathbf{A}_0 \mathbf{H}_K^\dagger}{\lambda_0} \\ \dots & \dots & \dots & \dots \\ \frac{\mathbf{H}_K \mathbf{A}_0 \mathbf{H}_1^\dagger}{\lambda_0} & \frac{\mathbf{H}_K \mathbf{A}_0 \mathbf{H}_2^\dagger}{\lambda_0} & \dots & \mathbf{I} \end{bmatrix}. \tag{4.16}$$

As long as this choice of \mathbf{Z} is positive definite, it can be verified by the method used below that this set is feasible for (4.12) and that the objective functions of both minimizations are the same. Thus we have constructed the worst case noise \mathbf{Z} for the Sato upper bound and have shown (4.10), but only for the case when $\mathbf{Z} > 0$. However, in many practical cases this choice of \mathbf{Z} is singular, and hence, not a feasible choice of \mathbf{Z} for (4.12).

To circumvent this singularity, we construct instead a family of feasible points (i.e $\mathbf{Z} > 0$)

by introducing an arbitrary parameter $\delta > 0$. This family of values of $(\lambda, \mathbf{A}, \mathbf{Z})$ is given by

$$\lambda = \lambda_0 + \delta \quad (4.17)$$

$$\mathbf{A} = \mathbf{A}_0 \quad (4.18)$$

$$\mathbf{Z} = \begin{bmatrix} \mathbf{I} & \frac{\mathbf{H}_1 \mathbf{A}_0 \mathbf{H}_2^\dagger}{\lambda_0 + \delta} & \cdots & \frac{\mathbf{H}_1 \mathbf{A}_0 \mathbf{H}_K^\dagger}{\lambda_0 + \delta} \\ \frac{\mathbf{H}_2 \mathbf{A}_0 \mathbf{H}_1^\dagger}{\lambda_0 + \delta} & \mathbf{I} & \cdots & \frac{\mathbf{H}_2 \mathbf{A}_0 \mathbf{H}_K^\dagger}{\lambda_0 + \delta} \\ \cdots & \cdots & \cdots & \cdots \\ \frac{\mathbf{H}_K \mathbf{A}_0 \mathbf{H}_1^\dagger}{\lambda_0 + \delta} & \frac{\mathbf{H}_K \mathbf{A}_0 \mathbf{H}_2^\dagger}{\lambda_0 + \delta} & \cdots & \mathbf{I} \end{bmatrix}. \quad (4.19)$$

We need to ensure that this set is feasible for (4.12). Since $(\lambda_0, \mathbf{A}_0)$ are an optimizing solution of (4.13), $(\lambda_0, \mathbf{A}_0)$ must satisfy the constraints in (4.13). Therefore we have that $\lambda = \lambda_0 + \delta > 0$ and $\mathbf{A} = \mathbf{A}_0 \geq 0$. Since the matrix \mathbf{Z} has the identity matrix along its block diagonal and is symmetric by construction, we see that if $\mathbf{Z} > 0$ then $\mathbf{Z} \in S$. We thus need to verify that $\mathbf{Z} > 0$ and that $\lambda \mathbf{Z} \geq \mathbf{H} \mathbf{A} \mathbf{H}^\dagger$.

Note that $\lambda_0 + \delta > 0$ and

$$\begin{aligned} (\lambda_0 + \delta) \mathbf{Z} - \mathbf{H} \mathbf{A}_0 \mathbf{H}^\dagger &= \text{diag}[(\lambda_0 + \delta) \mathbf{I} - \mathbf{H}_i \mathbf{A}_0 \mathbf{H}_i^\dagger] \\ &= \text{diag}[\lambda_0 \mathbf{I} - \mathbf{H}_i \mathbf{A}_0 \mathbf{H}_i^\dagger] + \delta \mathbf{I}. \end{aligned} \quad (4.20)$$

Since $(\lambda_0, \mathbf{A}_0)$ are an optimizing solution of (4.13), we have $\lambda_0 \mathbf{I} - \mathbf{H}_i \mathbf{A}_0 \mathbf{H}_i^\dagger \geq 0$ for all i . This implies that $\text{diag}[\lambda_0 \mathbf{I} - \mathbf{H}_i \mathbf{A}_0 \mathbf{H}_i^\dagger] \geq 0$. Since $\delta > 0$, we have

$$\lambda \mathbf{Z} - \mathbf{H} \mathbf{A}_0 \mathbf{H}^\dagger = \text{diag}[\lambda_0 \mathbf{I} - \mathbf{H}_i \mathbf{A}_0 \mathbf{H}_i^\dagger] + \delta \mathbf{I} > 0. \quad (4.21)$$

This implies that $\lambda \mathbf{Z} > \mathbf{H} \mathbf{A}_0 \mathbf{H}^\dagger = \mathbf{H} \mathbf{A} \mathbf{H}^\dagger$. It thus remains to show that $\mathbf{Z} > 0$. Since $\mathbf{A} \geq 0$, we also have that $\mathbf{H} \mathbf{A} \mathbf{H}^\dagger \geq 0$. This implies that $\lambda \mathbf{Z} > 0$. Since $\lambda > 0$, we then get $\mathbf{Z} > 0$. Hence $(\lambda, \mathbf{A}, \mathbf{Z})$ form a feasible set of values for (4.12). Since the Sato upper bound is equal to the infimum (over the feasible set) of the objective function, we have

$$\begin{aligned} \mathcal{C}_{\text{Sato}}(\mathbf{H}_1, \dots, \mathbf{H}_K, P) &\leq -\log |\mathbf{A}| + \text{Tr}(\mathbf{A}) + \lambda P - M \\ &= -\log |\mathbf{A}_0| + \text{Tr}(\mathbf{A}_0) + \lambda_0 P - M + \delta P \\ &= \mathcal{C}_{\text{union}}^{\text{sumrate}}(\mathbf{H}_1^\dagger, \dots, \mathbf{H}_K^\dagger, P) + \delta P. \end{aligned} \quad (4.22)$$

Since this holds for any $\delta > 0$, we get $\mathcal{C}_{\text{Sato}}(\mathbf{H}_1, \dots, \mathbf{H}_K, P) \leq \mathcal{C}_{\text{union}}^{\text{sumrate}}(\mathbf{H}_1^\dagger, \dots, \mathbf{H}_K^\dagger, P)$, which completes the proof of the theorem. \square .

A nice property of the proof of the sum rate capacity proof is that it is *constructive* in the sense that the proof generates worst-case noise covariances for the Sato upper bound, assuming that the optimizing solution to the MIMO MAC sum rate problem is known. Specifically, in Equation (4.19), we explicitly construct a noise covariance for which the

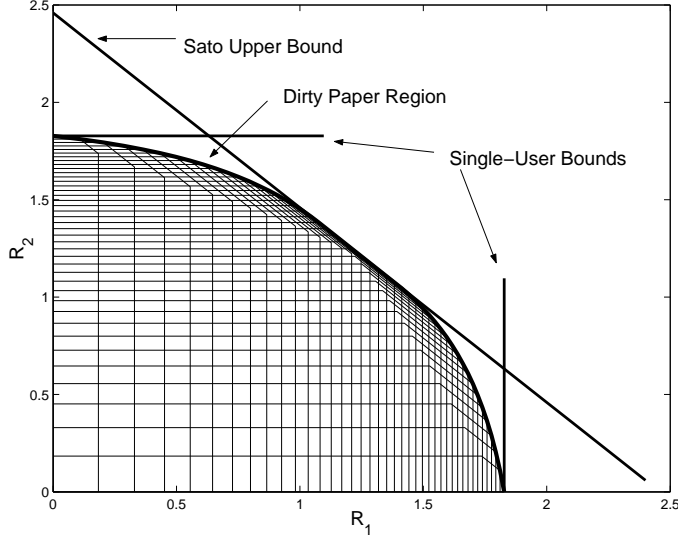


Figure 4.1: Dirty paper broadcast region: $K = 2$, $M = 2$, $r_1 = r_2 = 1$,
 $H_1 = [1 \ .4]$, $H_2 = [.4 \ 1]$, $P = 10$

cooperative capacity is larger than the MIMO MAC sum rate capacity by an arbitrarily small amount δP . Though we show that the constructed matrix $\mathbf{Z} > 0$ when $\delta > 0$, as noted earlier when $\delta \geq 0$ we still are guaranteed $\mathbf{Z} \geq 0$. If the constructed matrix \mathbf{Z} with $\delta = 0$ is strictly non-singular (i.e. $\mathbf{Z} > 0$), then the cooperative capacity with noise covariance \mathbf{Z} is *equal* to the MIMO MAC sum rate capacity. Therefore, in these cases \mathbf{Z} is in fact a worst case noise covariance for the Sato upper bound. Numerically, we also find \mathbf{Z} to be a worst case noise covariance for cases when \mathbf{Z} is singular when $\delta = 0$, as shown in Example 2 below.

The dirty paper BC region and the capacity regions of the dual MAC, along with the Sato upper bound and single-user bounds, are illustrated for a symmetric two user channel in Fig. 4.1. The dirty paper region is the union of the pentagons in the figure because the dirty paper region is formed as a union of the individual power constraint MAC regions (via Theorem 3.6). Since each receiver has only a single antenna, the dual MIMO MAC region with individual power constraints is a simple pentagon. The capacity upper bound is obtained by taking the intersection of the regions formed by the two single user optimum corner points (which are parallel to the axes) and the Sato upper bound, which is tight at the sum rate capacity. Note that the region formed by all three upper bounds is in fact quite close to the dirty paper achievable region. Also note that the boundary of the dirty paper achievable region has a straight line segment at the sum rate point. This characteristic of possessing a straight line segment (i.e. a time-division portion) at sum rate is also true for the MIMO MAC capacity region when the transmitters have more than one antenna [83].

4.2.1 Numerical Examples

In this section we provide two numerical examples to better illustrate the concepts discussed in the paper.

Example 1: Consider a two user broadcast channel with $P = 1$ and channel matrices

$$\mathbf{H}_1 = \begin{bmatrix} 1 & .8 \\ .5 & 2 \end{bmatrix}, \quad \mathbf{H}_2 = \begin{bmatrix} .2 & 1 \\ 2 & .5 \end{bmatrix}. \quad (4.23)$$

The dirty paper achievable region is very difficult to compute without employing duality, as discussed in Chapter 2.2.5. Thus, we find the dual MAC region using convex optimization techniques to obtain the achievable region in Figure 4.2.

To compute the Sato upper bound for the problem, we solve the dual problem to the MIMO MAC. Note that this problem is a convex problem with linear matrix inequality constraints. There are many techniques in the convex optimization literature to solve such problems. We use a readily available software package called SDPSOL, developed by Boyd and Wu [64], to get that $\mathcal{C}_{\text{union}}^{\text{sumrate}}(\mathbf{H}_1^\dagger, \dots, \mathbf{H}_K^\dagger, P) = 2.2615$ nats/sec and obtain \mathbf{A}_0, λ_0 to be

$$\mathbf{A}_0 = \begin{bmatrix} 3.231 & 1.43 \\ 1.43 & 3.603 \end{bmatrix}$$

$$\lambda_0 = 1.2879.$$

From these, we obtain the worst case noise (using Equation (4.19) with $\delta = 0$)

$$\mathbf{Z} = \begin{bmatrix} 1 & 0 & .1332 & .4446 \\ 0 & 1 & .4478 & .0613 \\ .1332 & .4478 & 1 & 0 \\ .4446 & .0613 & 0 & 1 \end{bmatrix}$$

which is non-singular. Therefore, we find that $\mathcal{C}_{\text{coop}}(\mathbf{Z}^{-1/2}\mathbf{H}, P) = \mathcal{C}_{\text{Sato}}(\mathbf{H}_1, \dots, \mathbf{H}_K, P) = \mathcal{C}_{\text{union}}^{\text{sumrate}}(\mathbf{H}_1^\dagger, \dots, \mathbf{H}_K^\dagger, P)$. The corresponding upper bound to the capacity region is shown in Figure 4.2.

The sum rate maximizing covariance matrices in the MAC are

$$\mathbf{Q}_1 = \begin{bmatrix} .0720 & .1827 \\ .1827 & .4634 \end{bmatrix}, \quad \mathbf{Q}_2 = \begin{bmatrix} 0 & .0026 \\ .0026 & .4646 \end{bmatrix}.$$

Notice that the sum rate is not maximized at a single point on the boundary of the capacity region, but it is actually maximized along a line segment. The corner points of this line segment are circled in Figure 4.2. In the MAC, the lower corner point of this line segment can be achieved using the above covariance matrices $\mathbf{Q}_1, \mathbf{Q}_2$ and by decoding User 1 last.

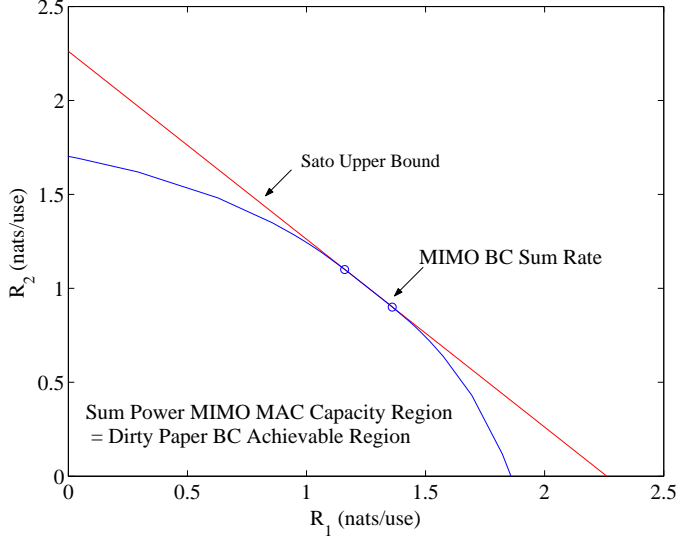


Figure 4.2: Achievable region and Sato upper bound for Example 1

The upper corner point of the line segment can be achieved using the *same* covariance matrices, but the *opposite* decoding order (i.e. decode User 2 last). Any other point on the line segment can be achieved by time-sharing between these two decoding orders.

We can use the MAC-BC transformations in (3.24) to find the corresponding sum rate capacity-achieving BC covariance matrices. Note, however, that the transformations depend on the decoding order in the MAC. If we assume that User 1 is decoded last in the MAC, the transformed BC covariances are:

$$\Sigma_1 = \begin{bmatrix} .0746 & .1932 \\ .1932 & .5004 \end{bmatrix}, \quad \Sigma_2 = \begin{bmatrix} .4104 & -.0776 \\ -.0776 & .0147 \end{bmatrix}.$$

The lower corner point of the sum rate line segment is then achievable in the BC using these covariance matrices and by encoding User 2 last (i.e using dirty paper coding for User 2 to cancel out the signal of User 1). To achieve the upper corner point of the sum rate line segment, we must perform the MAC-BC transformations using the opposite order in the MAC. We then get

$$\Sigma_1 = \begin{bmatrix} .0001 & -.0069 \\ -.0069 & .4841 \end{bmatrix}, \quad \Sigma_2 = \begin{bmatrix} .4849 & .1225 \\ .1225 & .0309 \end{bmatrix}.$$

Clearly, these BC covariance matrices are different than those used to achieve the other corner point of the sum rate line segment. Therefore, we see that in the MAC the corner points of the sum rate boundary can be achieved by using the same set of covariance matrices and different decoding orders. In the BC, however, a different decoding order and different covariance matrices are needed to achieve the corner points of the sum rate boundary.

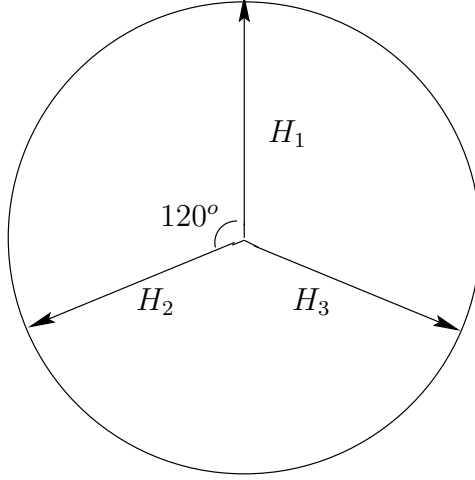


Figure 4.3: Channel Parameters for Example 2

Example 2: Consider a three user broadcast channel, with two antennas at the transmitter ($M = 2$) and one antenna each per receiver ($r_1 = r_2 = r_3 = 1$). The channel matrices are given by $\mathbf{H}_1 = [0 \ 1]$, $\mathbf{H}_2 = [-\sqrt{3}/2 \ -1/2]$, $\mathbf{H}_3 = [\sqrt{3}/2 \ -1/2]$ and the total power constraint is $P = 1$. Note that the channels are unit vectors in Euclidean space, and are spaced 120 degrees apart, as shown in Figure 4.3. Also note that the channel matrix \mathbf{H}

$$\mathbf{H} = \begin{bmatrix} 0 & 1 \\ -\sqrt{3}/2 & -1/2 \\ \sqrt{3}/2 & -1/2 \end{bmatrix} \quad (4.24)$$

has rank two, and that $\mathbf{H}_1 = -(\mathbf{H}_2 + \mathbf{H}_3)$.

First, let us consider the dual MAC problem. By the symmetric structure of these channels, it is clear that allocating equal power to each user maximizes the sum rate of this system. Thus sum rate capacity is achieved with $Q_1 = Q_2 = Q_3 = 1/3$ and any MAC decoding order.

Using the MAC-to-BC transformations in (3.24), we find covariances in the broadcast (corresponding to encoding User 1 last, User 2 second, and User 3 first) that achieve the same sum rate point on the capacity region to be

$$\Sigma_1 = \begin{bmatrix} 0 & 0 \\ 0 & .2857 \end{bmatrix}, \Sigma_2 = \begin{bmatrix} .2187 & .1623 \\ .1623 & .1205 \end{bmatrix} \quad (4.25)$$

$$\Sigma_3 = \begin{bmatrix} .2812 & -.1624 \\ -.1624 & .0937 \end{bmatrix} \quad (4.26)$$

and the sum rate capacity equals

$$\log \left| \mathbf{I} + \frac{1}{3}(\mathbf{H}_1^\dagger \mathbf{H}_1 + \mathbf{H}_2^\dagger \mathbf{H}_2 + \mathbf{H}_3^\dagger \mathbf{H}_3) \right| = .8109 \text{ nats/use.}$$

Now, let us find the worst case noise for the Sato upper bound. Note that, if $n_1 = -(n_2 + n_3)$, then $y_1 = -(y_2 + y_3)$. This implies that the received signal at one of the antennas is a linear combination of the signal at the other two antennas. Therefore, one receive antenna can be eliminated from the system without any loss in the cooperative capacity. Since $\mathbb{E}(n_1^2) = \mathbb{E}(n_2^2) = \mathbb{E}(n_3^2) = 1$, we require that $\mathbb{E}(n_i n_j) = -.5 \quad \forall i \neq j$. Thus, a noise covariance matrix given by

$$\mathbf{Z}_{\text{cand}} = \begin{bmatrix} 1 & -.5 & -.5 \\ -.5 & 1 & -.5 \\ -.5 & -.5 & 1 \end{bmatrix} \quad (4.27)$$

corresponds to $n_1 = -(n_2 + n_3)$, which allows us to eliminate one receive antenna. This noise covariance is a candidate for the worst-case noise covariance for the Sato upper bound. Note that this noise covariance is singular. If we eliminate the third antenna output, we are left with the following two input, two output channel:

$$\mathbf{G} = \begin{bmatrix} 0 & 1 \\ -\sqrt{3}/2 & -1/2 \end{bmatrix}. \quad (4.28)$$

The cooperative capacity with this noise covariance is then

$$\max_{\mathbf{\Sigma}} \log \left| \mathbf{I} + \begin{bmatrix} 1 & -.5 \\ -.5 & 1 \end{bmatrix}^{-1} \mathbf{G} \mathbf{\Sigma} \mathbf{G}^\dagger \right|. \quad (4.29)$$

To evaluate the expression above, we use the standard waterfilling technique [61] and find the optimizing $\mathbf{\Sigma}$ to be $\begin{bmatrix} .5 & 0 \\ 0 & .5 \end{bmatrix}$. The corresponding cooperative capacity is thus equal to .8109 nats/use. Since the cooperative capacity with noise covariance \mathbf{Z}_{cand} equals the MIMO MAC sum rate capacity, \mathbf{Z}_{cand} is a worst case noise for this problem.

Now, let us use the method for obtaining the worst case noise introduced in the proof of Theorem 4.1. Using SDPSOL we get $\mathbf{A}_0 = \begin{bmatrix} 1.5 & 0 \\ 0 & 1.5 \end{bmatrix}$ and $\lambda_0 = 2/3$. From (4.16) we

can construct the worst case noise covariance to be

$$\mathbf{Z}_0 = \begin{bmatrix} \mathbf{I} & \frac{\mathbf{H}_1 \mathbf{A}_0 \mathbf{H}_2^\dagger}{\lambda_0} & \frac{\mathbf{H}_1 \mathbf{A}_0 \mathbf{H}_3^\dagger}{\lambda_0} \\ \frac{\mathbf{H}_2 \mathbf{A}_0 \mathbf{H}_1^\dagger}{\lambda_0} & \mathbf{I} & \frac{\mathbf{H}_2 \mathbf{A}_0 \mathbf{H}_3^\dagger}{\lambda_0} \\ \frac{\mathbf{H}_3 \mathbf{A}_0 \mathbf{H}_1^\dagger}{\lambda_0} & \frac{\mathbf{H}_3 \mathbf{A}_0 \mathbf{H}_2^\dagger}{\lambda_0} & \mathbf{I} \end{bmatrix} \quad (4.30)$$

$$= \begin{bmatrix} 1 & -.5 & -.5 \\ -.5 & 1 & -.5 \\ -.5 & -.5 & 1 \end{bmatrix}. \quad (4.31)$$

We immediately notice that $\mathbf{Z}_{\text{cand}} = \mathbf{Z}_0$. Thus, for this case, the singular noise covariance constructed from (4.16) actually is a worst case noise covariance, even though we are not guaranteed this when the noise is singular.

Note: The fact that dirty paper coding achieves the sum rate capacity of the multiple-antenna broadcast channel was also proven in parallel in [82] and [73].

4.3 Computation of Sum Rate Capacity

In the previous section, we showed that dirty paper coding achieves the sum rate capacity of the multiple-antenna broadcast channel. Using the expression for the DPC rate region given in (2.17) and (2.19), the sum rate capacity is equal to:

$$\begin{aligned} \mathcal{C}_{\text{BC}}(\mathbf{H}_1, \dots, \mathbf{H}_K, P) &= \mathcal{C}_{\text{DPC}}^{\text{sumrate}}(\mathbf{H}_1, \dots, \mathbf{H}_K, P) \\ &= \max_{\sum_{i=1}^K \text{Tr}(\mathbf{\Sigma}_i) \leq P, \mathbf{\Sigma}_i \geq 0, i=1, \dots, K} \log \frac{|\mathbf{I} + \mathbf{H}_i(\sum_{j \geq i} \mathbf{\Sigma}_j) \mathbf{H}_i^\dagger|}{|\mathbf{I} + \mathbf{H}_i(\sum_{j > i} \mathbf{\Sigma}_j) \mathbf{H}_i^\dagger|}. \end{aligned} \quad (4.32)$$

In this section we are interested in determining the optimal covariance matrices $\mathbf{\Sigma}_1, \dots, \mathbf{\Sigma}_K$ that achieve the sum rate capacity, i.e. that achieve the maximum above. If a direct maximization of (4.32) is attempted, one will immediately note that the objective function is not a concave function of the covariance matrices $\mathbf{\Sigma}_1, \dots, \mathbf{\Sigma}_K$. Thus, convex optimization algorithms cannot be used, making it extremely difficult to numerically solve.

There is, however, an alternative way of finding the optimal covariance matrices that achieve the sum rate capacity. Note that by duality, the sum rate capacity of the broadcast channel is equal to the sum rate capacity of the dual multiple-access channel. Thus, we can alternatively express the sum rate capacity of the broadcast channel as

$$\begin{aligned} \mathcal{C}_{\text{BC}}(\mathbf{H}_1, \dots, \mathbf{H}_K, P) &= \mathcal{C}_{\text{union}}^{\text{sumrate}}(\mathbf{H}^\dagger, P) \\ &= \max_{\{\mathbf{Q}_j \geq 0, \sum_{i=1}^K \text{Tr}(\mathbf{Q}_i) \leq P\}} \log \left| \mathbf{I} + \sum_{i=1}^K \mathbf{H}_i^\dagger \mathbf{Q}_i \mathbf{H}_i \right|. \end{aligned} \quad (4.33)$$

The objective function in (4.33) is easily seen to be a concave function of the covariance matrices $\mathbf{Q}_1, \dots, \mathbf{Q}_K$. Furthermore, the MAC-BC transformations given in Chapter 3.1.4 provide a simple mapping from the maximum achieving uplink covariance matrices $\mathbf{Q}_1, \dots, \mathbf{Q}_K$ to the sum capacity achieving downlink covariance matrices $\mathbf{\Sigma}_1, \dots, \mathbf{\Sigma}_K$, i.e. the inputs that maximize (4.32). Since the MAC formulation is the maximization of a concave function, there exist standard interior point convex optimization algorithms [4] that solve the sum power MAC problem. A new interior point based method has also been found in [76]. However, employing an interior point convex optimization algorithm to tackle as well structured a problem as sum capacity is inefficient.

In this section, we exploit the structure in the sum capacity problem to obtain a simple iterative algorithm for calculating sum capacity. More precisely, we propose an iterative algorithm that solves (4.33). This algorithm is inspired by and is very similar to an iterative algorithm for the conventional individual power constraint MAC problem by Yu, Rhee, Boyd, and Cioffi [83]. In the following section, we describe the algorithm in [83]. We then propose our algorithm and show that a simple modification provably converges to the optimum.

4.3.1 Iterative Water-Filling with Individual Power Constraints

The iterative water-filling algorithm for the conventional MIMO MAC problem was obtained by Yu, Rhee, Boyd, and Cioffi in [84]. This algorithm finds the sum capacity of a MIMO MAC with *individual* power constraints P_1, \dots, P_K on each user, which is equal to:

$$\mathcal{C}_{\text{MAC}}(\mathbf{H}_1^\dagger, \dots, \mathbf{H}_K^\dagger, P_1, \dots, P_K) = \max_{\{\mathbf{Q}_i \geq 0, \text{Tr}(\mathbf{Q}_i) \leq P_i\}} \log \left| \mathbf{I} + \sum_{i=1}^K \mathbf{H}_i^\dagger \mathbf{Q}_i \mathbf{H}_i \right|. \quad (4.34)$$

This differs from (4.33) only in the power constraint structure. Notice that the objective is a concave function of the covariance matrices, and that the constraints in (4.34) are separable because there is an individual trace constraint on *each* covariance matrix. In such situations, it is generally sufficient to optimize with respect to the first variable while holding all other variables constant, then optimize with respect to the second variable, etc., in order to reach a globally optimum point. This is referred to as the block-coordinate ascent algorithm and convergence can be shown under relatively general conditions [3, Section 2.7]. If we define the function $f(\cdot)$ as

$$f(\mathbf{Q}_1, \dots, \mathbf{Q}_K) \triangleq \log \left| \mathbf{I} + \sum_{i=1}^K \mathbf{H}_i^\dagger \mathbf{Q}_i \mathbf{H}_i \right|, \quad (4.35)$$

then in the $(l + 1)$ -th iteration of the block-coordinate ascent algorithm,

$$\mathbf{Q}_j^{(l+1)} \triangleq \arg \max_{\mathbf{Q}_j \geq 0, \text{Tr}(\mathbf{Q}_j) \leq P_j} f(\mathbf{Q}_1^{(l)}, \dots, \mathbf{Q}_{j-1}^{(l)}, \mathbf{Q}_j, \mathbf{Q}_{j+1}^{(l)}, \dots, \mathbf{Q}_K^{(l)}) \quad (4.36)$$

for $j = (l \bmod K) + 1$ and $\mathbf{Q}_j^{(l+1)} = \mathbf{Q}_j^{(l)}$ for all other j . Notice that only one of the covariances is updated in each iteration.

The key to the iterative water-filling algorithm is noticing that $f(\mathbf{Q}_1, \dots, \mathbf{Q}_K)$ can be rewritten as:

$$\begin{aligned} f(\mathbf{Q}_1, \dots, \mathbf{Q}_K) &= \log \left| \mathbf{I} + \sum_{i \neq j} \mathbf{H}_i^\dagger \mathbf{Q}_i \mathbf{H}_i + \mathbf{H}_j^\dagger \mathbf{Q}_j \mathbf{H}_j \right| \\ &= \log \left| \mathbf{I} + \sum_{i \neq j} \mathbf{H}_i^\dagger \mathbf{Q}_i \mathbf{H}_i \right| + \\ &\quad \log \left| \mathbf{I} + \left(\mathbf{I} + \sum_{i \neq j} \mathbf{H}_i^\dagger \mathbf{Q}_i \mathbf{H}_i \right)^{-1/2} \mathbf{H}_j^\dagger \mathbf{Q}_j \mathbf{H}_j \left(\mathbf{I} + \sum_{i \neq j} \mathbf{H}_i^\dagger \mathbf{Q}_i \mathbf{H}_i \right)^{-1/2} \right| \end{aligned}$$

for any j . Thus, the iteration in (4.36) can be rewritten as:

$$\mathbf{Q}_j^{(l+1)} = \arg \max_{\mathbf{Q}_j \geq 0, \text{Tr}(\mathbf{Q}_j) \leq P_j} \log \left| \mathbf{I} + \mathbf{G}_j^\dagger \mathbf{Q}_j \mathbf{G}_j \right| \quad (4.37)$$

where $\mathbf{G}_j = \mathbf{H}_j \left(\mathbf{I} + \sum_{i \neq j} \mathbf{H}_i^\dagger \mathbf{Q}_i^{(l)} \mathbf{H}_i \right)^{-1/2}$. This maximization is clearly equal to the expression for the capacity of a point-to-point MIMO channel with channel matrix \mathbf{G}_j and power constraint P_j . It is well known that the capacity of such a MIMO channel is achieved by choosing the input covariance along the eigenvectors of the channel matrix and by water-filling on the eigenvalues of the channel matrix [61]. Thus, $\mathbf{Q}_j^{(l+1)}$ should be chosen as a *water-fill* of the channel \mathbf{G}_j , i.e. the eigenvectors of $\mathbf{Q}_j^{(l+1)}$ should equal the left eigenvectors of \mathbf{G}_j , with the eigenvectors chosen by the water-filling procedure.

At each step of the algorithm, exactly one user optimizes his covariance matrix while treating the signals from all other users as noise. In the next step, the next user (in numerical order) optimizes his covariance while treating all other signals, including the updated covariance of the previous user, as noise. This intuitively appealing algorithm can easily be shown to satisfy the conditions of [3, Section 2.7] and thus provably converges. Furthermore, the optimization in each step of the algorithm simplifies to water-filling over an effective channel, which is computationally efficient.

If we let $\mathbf{Q}_1^*, \dots, \mathbf{Q}_K^*$ denote the optimal covariances, notice that

$$f(\mathbf{Q}_1^*, \dots, \mathbf{Q}_K^*) = \max_{\mathbf{Q}_j \geq 0, \text{Tr}(\mathbf{Q}_j) \leq P_j} f(\mathbf{Q}_1^*, \dots, \mathbf{Q}_{j-1}^*, \mathbf{Q}_j, \mathbf{Q}_{j+1}^*, \dots, \mathbf{Q}_K^*). \quad (4.38)$$

Thus, \mathbf{Q}_1^* is a water-fill of the noise and the signals from all other users, and simultaneously \mathbf{Q}_2^* is a water-fill of the noise and the signals from all other users, and so on. Thus, the sum capacity achieving covariance matrices simultaneously water-fill each of their respective effective channels (which for User j depends on the covariance matrices of all other users) [84], with the water-filling levels (i.e. the eigenvectors) of each user determined by the power constraints P_j . In the next subsection, we will see that similar intuition describes the sum capacity achieving covariance matrices in the MIMO MAC when there is a sum power constraint instead of individual power constraints.

4.3.2 Sum Power Iterative Water-Filling

In the previous section we described an iterative water-filling algorithm that computes the sum capacity of a MIMO MAC subject to individual power constraints. We are instead concerned with computing the sum capacity, along with the corresponding optimal covariance matrices, of a MIMO BC. As stated earlier, this is equivalent to computing the sum capacity (and the corresponding optimal covariance matrices) of a MIMO MAC subject to a sum power constraint, i.e. computing:

$$\mathcal{C}_{\text{MAC}}(\mathbf{H}_1^\dagger, \dots, \mathbf{H}_K^\dagger, P) = \max_{\{\mathbf{Q}_i \geq 0, \sum_{i=1}^K \text{Tr}(\mathbf{Q}_i) \leq P\}} \log \left| \mathbf{I} + \sum_{i=1}^K \mathbf{H}_i^\dagger \mathbf{Q}_i \mathbf{H}_i \right|. \quad (4.39)$$

If we let $\mathbf{Q}_1^*, \dots, \mathbf{Q}_K^*$ denote a set of covariance matrices that achieve the above maximum, it is easy to see that similar to the individual power constraint problem, each covariance must be a water-fill of the noise and signals from all other users. More precisely, this means that for every j , the eigenvectors of \mathbf{Q}_j^* are aligned with the left eigenvectors of $\mathbf{H}_j \left(\mathbf{I} + \sum_{i \neq j} \mathbf{H}_i^\dagger \mathbf{Q}_i^* \mathbf{H}_i \right)^{-1/2}$. However, since there is a *sum* power constraint on the covariances, the water level of all users must be equal. This is akin to saying that no advantage will be gained by transferring power from one user with a higher water-filling level to another user with a lower water-filling level. In the individual power constraint channel, since each user's water-filling level was determined by his own power constraint, the covariances of each user could be updated one at a time. With a sum power constraint, however, we must update all covariances *simultaneously* to maintain a constant water-level.

Motivated by the individual power algorithm, we propose the following algorithm in which all K covariances are simultaneously updated during each step, based on the covariance matrices from the previous step. This is a natural extension of the per-user sequential update described in Chapter 4.3.1. At each iteration step we generate an effective channel for *each* user based on the covariances of all other users. In order to maintain a common water-level, we simultaneously water-fill across all K effective channels, i.e. we maximize the sum of rates on the K effective channels. The $(l + 1)$ -th iteration of the algorithm is described by the following:

1. Generate effective channels $\mathbf{G}_j = \mathbf{H}_j(\mathbf{I} + \sum_{i \neq j} \mathbf{H}_i^\dagger \mathbf{Q}_i^{(l)} \mathbf{H}_i)^{-1/2}$ for $j = 1, \dots, K$.
2. Treating these effective channels as parallel, non-interfering channels, obtain the new covariance matrices $\{\mathbf{Q}_i^{(l+1)}\}_{i=1}^K$ by water-filling with total power P :

$$\{\mathbf{Q}_i^{(l+1)}\}_{i=1}^K = \arg \max_{\mathbf{Q}_i \geq 0, \sum_{i=1}^K \text{Tr}(\mathbf{Q}_i) \leq P} \sum_{i=1}^K \log \left| \mathbf{I} + \mathbf{G}_i^\dagger \mathbf{Q}_i \mathbf{G}_i \right|.$$

This maximization is equivalent to water-filling the block diagonal channel with diagonals equal to $\mathbf{G}_1, \dots, \mathbf{G}_K$. If the SVD of $\mathbf{G}_j \mathbf{G}_j^\dagger$ is written as $\mathbf{G}_j \mathbf{G}_j^\dagger = \mathbf{U}_j \mathbf{D}_j \mathbf{U}_j^\dagger$ with \mathbf{U}_j unitary and \mathbf{D}_j square and diagonal, then the new covariance matrices are given by:

$$\mathbf{Q}_j^{(l+1)} = \mathbf{U}_j \mathbf{\Lambda}_j \mathbf{U}_j^\dagger \quad (4.40)$$

where $\mathbf{\Lambda}_j = [\mu \mathbf{I} - (\mathbf{D}_j)^{-1}]^+$ and the operation $[\mathbf{A}]^+$ denotes a component-wise minimum with zero. Here the water-filling level μ is chosen such that $\sum_{i=1}^K \text{Tr}(\mathbf{\Lambda}_i) = P$.

Perhaps surprisingly, this algorithm does not always lead to an increase in the objective function and does not always converge to the optimum when $K > 2$. Even though the algorithm converges to the maximum sum rate for a two-user channel, the algorithm needs to be modified to guarantee convergence when there are more than two users. In the following section we discuss the modification and the proof of convergence.

4.3.3 Convergence Proof

In this section we show that the sum power iterative water-filling algorithm converges when $K = 2$, but does not always converge when $K > 2$. For $K > 2$, we describe a modified version of the algorithm that provably converges to the optimum.

Two User Analysis

In order to prove convergence of the algorithm for $K = 2$, let us consider the following optimization problem:

$$\begin{aligned} \max_{\text{Tr}(\mathbf{A}_1 + \mathbf{A}_2) \leq P, \text{Tr}(\mathbf{B}_1 + \mathbf{B}_2) \leq P} & \frac{1}{2} \log \left| \mathbf{I} + \mathbf{H}_1^\dagger \mathbf{A}_1 \mathbf{H}_1 + \mathbf{H}_2^\dagger \mathbf{B}_2 \mathbf{H}_2 \right| \\ & + \frac{1}{2} \log \left| \mathbf{I} + \mathbf{H}_1^\dagger \mathbf{B}_1 \mathbf{H}_1 + \mathbf{H}_2^\dagger \mathbf{A}_2 \mathbf{H}_2 \right|. \end{aligned} \quad (4.41)$$

We first show that the solutions to the original sum rate maximization problem in (4.39) and (4.41) are the same. If we let $\mathbf{A}_1 = \mathbf{B}_1 = \mathbf{Q}_1$ and $\mathbf{A}_2 = \mathbf{B}_2 = \mathbf{Q}_2$, we see that any sum rate achievable in (4.39) is also achievable in the modified sum rate in (4.41). Also, since

the $\log(\det(\cdot))$ function is concave we have

$$\log \left| \mathbf{I} + \mathbf{H}_1^\dagger \mathbf{Q}_1 \mathbf{H}_1 + \mathbf{H}_2^\dagger \mathbf{Q}_2 \mathbf{H}_2 \right| \geq \frac{1}{2} \log \left| \mathbf{I} + \mathbf{H}_1^\dagger \mathbf{A}_1 \mathbf{H}_1 + \mathbf{H}_2^\dagger \mathbf{B}_2 \mathbf{H}_2 \right| + \frac{1}{2} \log \left| \mathbf{I} + \mathbf{H}_1^\dagger \mathbf{B}_1 \mathbf{H}_1 + \mathbf{H}_2^\dagger \mathbf{A}_2 \mathbf{H}_2 \right|$$

if we let $\mathbf{Q}_1 = \frac{1}{2}(\mathbf{A}_1 + \mathbf{B}_1)$ and $\mathbf{Q}_2 = \frac{1}{2}(\mathbf{A}_2 + \mathbf{B}_2)$. Since $\text{Tr}(\mathbf{Q}_1) + \text{Tr}(\mathbf{Q}_2) = \frac{1}{2}\text{Tr}(\mathbf{A}_1 + \mathbf{A}_2 + \mathbf{B}_1 + \mathbf{B}_2) \leq P$, any sum rate achievable in (4.41) is also achievable in the original (4.39). Thus, every set of maximizing covariances $(\mathbf{A}_1, \mathbf{A}_2, \mathbf{B}_1, \mathbf{B}_2)$ map directly to a set of maximizing $(\mathbf{Q}_1, \mathbf{Q}_2)$. Therefore, we can equivalently solve (4.41) to find the uplink covariances that maximize the sum-rate expression in (4.39).

Now notice that the maximization in (4.41) has separable constraints on $(\mathbf{A}_1, \mathbf{A}_2)$ and $(\mathbf{B}_1, \mathbf{B}_2)$. Thus, we can use the block coordinate ascent method in which we maximize with respect to $(\mathbf{A}_1, \mathbf{A}_2)$, then with respect to $(\mathbf{B}_1, \mathbf{B}_2)$, and so on. The maximization of (4.41) with respect to $(\mathbf{A}_1, \mathbf{A}_2)$ can be written as:

$$\max_{\text{Tr}(\mathbf{A}_1 + \mathbf{A}_2) \leq P} \log \left| \mathbf{I} + \mathbf{G}_1^\dagger \mathbf{A}_1 \mathbf{G}_1 \right| + \log \left| \mathbf{I} + \mathbf{G}_2^\dagger \mathbf{A}_2 \mathbf{G}_2 \right| \quad (4.42)$$

where $\mathbf{G}_1 = \mathbf{H}_1(\mathbf{I} + \mathbf{H}_2^\dagger \mathbf{B}_2 \mathbf{H}_2)^{-1/2}$ and $\mathbf{G}_2 = \mathbf{H}_2(\mathbf{I} + \mathbf{H}_1^\dagger \mathbf{B}_1 \mathbf{H}_1)^{-1/2}$. Clearly, this is equivalent to the iterative water-filling step described in the previous section where $\mathbf{B}_1, \mathbf{B}_2$ play the role of the covariance matrices from the previous step. Similarly, when maximizing with respect to $\mathbf{B}_1, \mathbf{B}_2$, the covariances $\mathbf{A}_1, \mathbf{A}_2$ are the covariance matrices from the previous step. Therefore, performing the cyclic coordinate ascent algorithm on (4.41) is exactly equivalent to the sum power iterative water-filling algorithm described in Chapter 4.3.2.

Furthermore, notice that each iteration is equal to the calculation of the capacity of a point-to-point MIMO channel. Water-filling is known to be optimal in this setting, and in Chapter 4.6.2 we show that the water-filling solution is also the unique solution. Therefore, by [85, pg. 228] [3, Chapter 2.7], the block coordinate ascent algorithm converges because at each step of the algorithm there is a unique maximizing solution. Thus, the iterative water-filling algorithm given in Chapter 4.3.2 converges to the maximum sum rate when $K = 2$.

More Than Two Users

If there are more than two users, the original algorithm is easily shown by example not to always converge. Thus, the algorithm needs to be slightly modified in order to guarantee convergence. For simplicity, we consider three users and then generalize. Similar to the

previous section, consider the following maximization:

$$\begin{aligned} \max \quad & \frac{1}{3} \log \left| \mathbf{I} + \mathbf{H}_1^\dagger \mathbf{A}_1 \mathbf{H}_1 + \mathbf{H}_2^\dagger \mathbf{B}_2 \mathbf{H}_2 + \mathbf{H}_3^\dagger \mathbf{C}_3 \mathbf{H}_3 \right| \\ & + \frac{1}{3} \log \left| \mathbf{I} + \mathbf{H}_1^\dagger \mathbf{C}_1 \mathbf{H}_1 + \mathbf{H}_2^\dagger \mathbf{A}_2 \mathbf{H}_2 + \mathbf{H}_3^\dagger \mathbf{B}_3 \mathbf{H}_3 \right| \\ & + \frac{1}{3} \log \left| \mathbf{I} + \mathbf{H}_1^\dagger \mathbf{B}_1 \mathbf{H}_1 + \mathbf{H}_2^\dagger \mathbf{C}_2 \mathbf{H}_2 + \mathbf{H}_3^\dagger \mathbf{A}_3 \mathbf{H}_3 \right| \end{aligned} \quad (4.43)$$

subject to the constraints $\text{Tr}(\mathbf{A}_1 + \mathbf{A}_2 + \mathbf{A}_3) \leq P$, $\text{Tr}(\mathbf{B}_1 + \mathbf{B}_2 + \mathbf{B}_3) \leq P$, and $\text{Tr}(\mathbf{C}_1 + \mathbf{C}_2 + \mathbf{C}_3) \leq P$. By the same argument used for the two user case, any set of covariances is a solution to the original optimization problem in (4.39) if and only if it is a solution to the above problem (with $\mathbf{A}_i = \mathbf{B}_i = \mathbf{C}_i$ for $i = 1, 2, 3$). In order to maximize (4.43), we can again use the cyclic coordinate ascent algorithm. We first maximize with respect to $(\mathbf{A}_1, \mathbf{A}_2, \mathbf{A}_3)$, then with respect to $(\mathbf{B}_1, \mathbf{B}_2, \mathbf{B}_3)$, and so on. As before, convergence is guaranteed by [3, Section 2.7]. In the two user case, the cyclic coordinate ascent method applied to the modified optimization problem yields the same iterative water-filling algorithm proposed in Chapter 4.3.2 where the effective user of each channel was based on the covariance matrices from the previous step. If there are more than two users, however, the effective channel of each user depends on covariances that are up to $K - 1$ steps old, instead of just one step old. It is easily seen that the effective channel of User j in the n -th step is:

$$\mathbf{G}_j^{(n)} = \mathbf{H}_j \left(\mathbf{I} + \sum_{i=1}^{K-1} \mathbf{H}_{[j+i]K}^\dagger \mathbf{Q}_{[j+i]K}^{(n-K+i)} \mathbf{H}_{[j+i]K} \right)^{-1/2} \quad (4.44)$$

where $[x]_K = x + lK$ where l is an integer such that $1 \leq x + lK \leq K$. For the three user case, the update of $\mathbf{Q}_1^{(n)}$ depends on $\mathbf{Q}_2^{(n-2)}$ and $\mathbf{Q}_3^{(n-1)}$, $\mathbf{Q}_2^{(n)}$ depends on $\mathbf{Q}_3^{(n-2)}$ and $\mathbf{Q}_1^{(n-1)}$, and $\mathbf{Q}_3^{(n)}$ depends on $\mathbf{Q}_1^{(n-2)}$ and $\mathbf{Q}_2^{(n-1)}$. Thus, the previous $K - 1$ states of the algorithm must be stored. If (4.44) is used to generate each effective channel in step 1 of the sum power iterative water-filling algorithm in Chapter 4.3.2, then the algorithm provably converges to the optimum due to the convergence of the block coordinate ascent method.

Numerical Results

In Figures 4.4 and 4.5, plots of sum rate vs. iteration number are provided for a randomly chosen 10 user channel with 4 transmit and receive antennas. In Fig. 4.4 the original algorithm converges to the optimum, and is seen to converge considerably faster than the modified, provably convergent algorithm. Given that the original algorithm converges in this scenario, it is not surprising that its convergence rate is much faster. The modified algorithm is intuitively slower because updates are based on covariance matrices from up to $K - 1$ iterates ago, as opposed to only the previous iterate. In Fig. 4.5, however, the original algorithm diverges, and oscillates between two sub-optimal points. In general, it

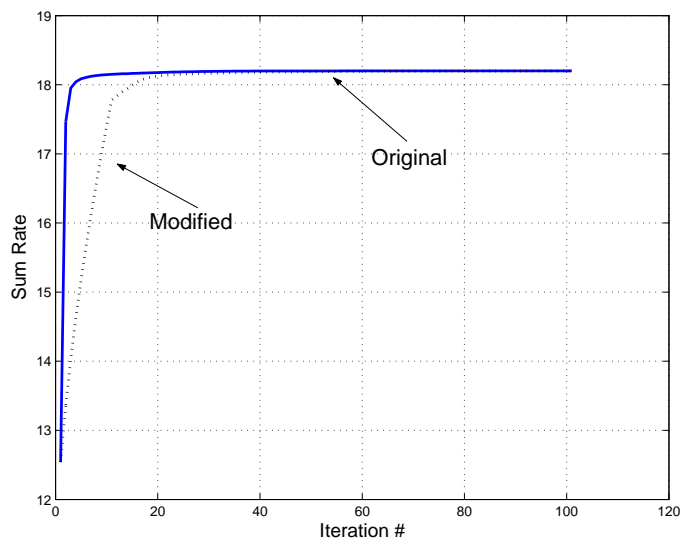


Figure 4.4: Algorithm comparison for convergent scenario

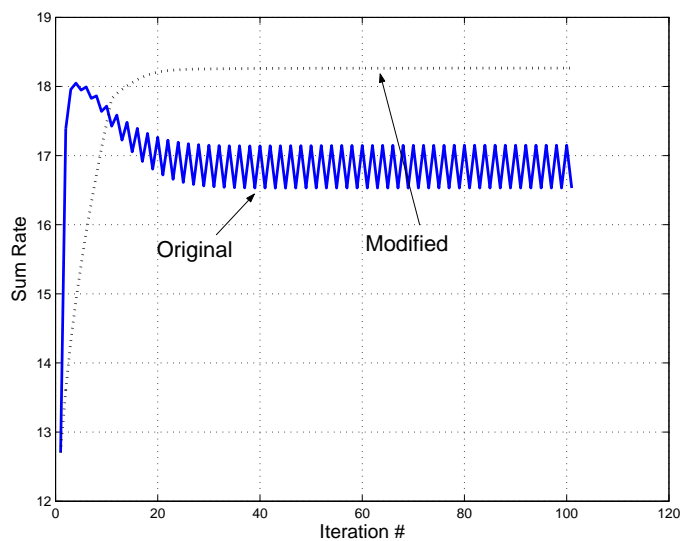


Figure 4.5: Algorithm comparison for divergent scenario

is not difficult to find similar examples of divergence for a large number of users. When convergence speed is of concern, it appears to be beneficial to use the original algorithm for the first few iterations (or until sum rate is decreased in the next iteration) and then use the modified algorithm thereafter. The modified algorithm converges from any starting point, and thus convergence is still guaranteed.

4.4 DPC and TDMA Comparison

Earlier in this chapter, we proved that dirty paper coding achieves the sum rate capacity of the multiple antenna broadcast channel. However, dirty paper coding is a rather new and complicated scheme that has yet to be implemented in practical systems. Current wireless systems such as Qualcomm’s High Data Rate (HDR) system [27] use the much simpler technique of time-division multiple-access (TDMA) in which the base station transmits to only one user at a time. Considering the difficulty in implementing dirty-paper coding, we answer the following question in this section: How large of a performance boost does dirty-paper coding provide over TDMA in terms of sum-rate?

If dirty paper coding is used in a K -user broadcast channel, any rate vector in the K -dimensional dirty paper coding achievable region can be achieved. Similarly, if TDMA is used, any rate vector in the K -dimensional TDMA rate region can be achieved. It is easy to see that the dirty paper coding achievable region is larger than the TDMA rate region. However, defining a meaningful metric that quantifies the difference between two K -dimensional regions for $K \geq 2$ is quite difficult. Viswanathan, Venkatesan, and Huang [76] first investigated the above question by considering different operating points (i.e. rate vectors in the DPC and TDMA rate regions) that are reasonable for cellular systems, and numerically comparing the rates achievable with DPC and TDMA.

In this section we focus exclusively on the sum rate capacity, or maximum throughput, achievable using DPC and TDMA. This operating point is quite reasonable when users have channels with roughly equivalent quality (i.e. no large SNR imbalances), but may not be as fair for asymmetric channels because we would expect users with higher SNR’s to receive a disproportionate fraction of the total data rate. However, the sum capacity is in general an important figure of merit because it quantifies how much total data flow is possible in a broadcast channel. Furthermore, comparing the maximum throughput achievable with DPC and TDMA gives a reasonable estimate of how much “larger” the DPC rate region is compared to the TDMA rate region.

By establishing upper and lower bounds to the DPC sum-rate capacity and the maximum TDMA sum-rate, respectively, we are able to analytically upper bound the ratio of sum-rate capacity to the maximum TDMA sum rate. Furthermore, we characterize the DPC gain at asymptotically high and low SNR. We also investigate the DPC gain in a time-varying, Rayleigh-fading channel in which the transmitter and receiver have perfect channel

knowledge. Using the same techniques as for the downlink, we are also able to upper bound the sum-rate gain that successive decoding provides over TDMA on the uplink (multiple-access) channel.

The remainder of this section is organized as follows. In Chapter 4.4.1 we define the DPC gain, which is the quantity of interest. In Chapter 4.4.2 we develop an analytical bound on the DPC gain and we investigate the asymptotic behavior of the DPC gain at low and high SNR in Chapter 4.4.3. We study the behavior of the DPC gain in Rayleigh fading channels in Chapter 4.4.4. In Chapter 4.4.5 we attempt to bound the DPC rate region in terms of the TDMA rate region. In Chapter 4.4.6 we consider the DPC gain in a frequency-selective broadcast channel and in Chapter 4.4.7 we briefly compare dirty paper coding to transmitter beamforming, another sub-optimal transmission strategy for the broadcast channel. We end by applying our analytical bounds to the multiple-antenna multiple-access channel in Chapter 4.4.8.

4.4.1 Definition of DPC Gain

As shown earlier in this chapter, the sum rate capacity of the MIMO broadcast channel is achievable by dirty paper coding. Due to the MAC-BC duality, the sum-rate capacity of the MIMO BC is equal to the sum-rate capacity of the dual MAC with sum power constraint P :

$$\begin{aligned} C_{BC}(\mathbf{H}_1, \dots, \mathbf{H}_K, P) &= C_{MAC}(\mathbf{H}_1^\dagger, \dots, \mathbf{H}_K^\dagger, P) \\ &= \max_{\{\mathbf{Q}_i: \mathbf{Q}_i \geq 0, \sum_{i=1}^K \text{Tr}(\mathbf{Q}_i) \leq P\}} \log \left| \mathbf{I} + \sum_{i=1}^K \mathbf{H}_i^\dagger \mathbf{Q}_i \mathbf{H}_i \right| \end{aligned} \quad (4.45)$$

where each of the matrices \mathbf{Q}_i is an $N \times N$ positive semi-definite covariance matrix. Note that the previous section provides an algorithm that computes this expression.

The time-division rate region \mathcal{R}_{TDMA} is defined as the set of average rates that can be achieved by time-sharing between single-user transmissions using constant power P :

$$\mathcal{R}_{TDMA}(\mathbf{H}_1, \dots, \mathbf{H}_K, P) \triangleq \left\{ (R_1, \dots, R_K) : \sum_{i=1}^K \frac{R_i}{C(\mathbf{H}_i, P)} \leq 1 \right\} \quad (4.46)$$

where $C(\mathbf{H}_i, P)$ denotes the single-user capacity of the i -th user subject to power constraint P . The single-user capacity of a MIMO channel is given by the following expression¹:

$$C(\mathbf{H}_i, P) = \max_{\{\mathbf{Q}_i: \mathbf{Q}_i \geq 0, \text{Tr}(\mathbf{Q}_i) \leq P\}} \log \left| \mathbf{I} + \mathbf{H}_i^\dagger \mathbf{Q}_i \mathbf{H}_i \right|. \quad (4.47)$$

¹The expression in (4.47) is the capacity of the point-to-point channel with channel matrix \mathbf{H}_i^\dagger . However, the capacity of the dual (or reciprocal) point-to-point channel with channel \mathbf{H}_i is the same [61].

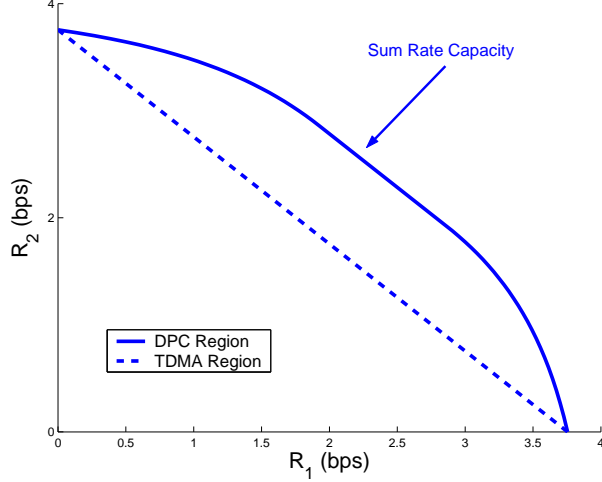


Figure 4.6: DPC and TDMA rate regions for a 2 user system with 2 transmit antennas

The maximum is achieved by choosing the covariance matrix \mathbf{Q}_i to be along the eigenvectors of the channel matrix $\mathbf{H}_i\mathbf{H}_i^\dagger$ and by choosing the eigenvalues according to a water-filling procedure [61].

It is easy to see that the maximum sum-rate in \mathcal{R}_{TDMA} is the largest single-user capacity of the K users:

$$\mathcal{C}_{TDMA}(\mathbf{H}_1, \dots, \mathbf{H}_K, P) \triangleq \max_{\mathbf{R} \in \mathcal{R}_{TDMA}(\mathbf{H}_1, \dots, \mathbf{H}_K, P)} \sum_{i=1}^K R_i = \max_{i=1, \dots, K} C(\mathbf{H}_i, P) \quad (4.48)$$

and is achieved by transmitting only to the user with the largest capacity. We will refer to this quantity as the TDMA sum-rate.

We are interested in quantifying the advantage that DPC gives over TDMA in terms of total throughput. Thus, the performance metric analyzed in this paper is the DPC gain $G(\mathbf{H}_1, \dots, \mathbf{H}_K, P)$, which we define to be the ratio of sum-rate capacity to TDMA sum-rate:

$$G(\mathbf{H}_1, \dots, \mathbf{H}_K, P) \triangleq \frac{\mathcal{C}_{BC}(\mathbf{H}_1, \dots, \mathbf{H}_K, P)}{\mathcal{C}_{TDMA}(\mathbf{H}_1, \dots, \mathbf{H}_K, P)}. \quad (4.49)$$

Since $\mathcal{C}_{BC}(\mathbf{H}_1, \dots, \mathbf{H}_K, P) \geq \mathcal{C}_{TDMA}(\mathbf{H}, P)$ by definition, the DPC gain is always greater than or equal to one. Notice that the DPC gain is a function of the channels $\mathbf{H}_1, \dots, \mathbf{H}_K$ and the SNR P .

In Fig. 4.6, the DPC and TDMA rate regions are shown for a two user broadcast channel with two transmit antennas and single receive antennas. In this symmetric channel the TDMA sum rate is equal to the single-user capacity of either user (3.75 bps), while the sum rate capacity is equal to 4.79 bps. Thus, the DPC gain is equal to 1.28. In the following section, we develop an analytical upper bound to the DPC gain.

4.4.2 Bounds on Sum-Rate Capacity and DPC Gain

In this section we develop a precise analytical upper bound to the DPC gain defined in (4.49). In order to do so, we upper bound the sum-rate capacity of the MIMO BC and lower bound the TDMA sum-rate.

Theorem 4.2 *The sum-rate capacity of the multiple-antenna downlink is upper-bounded as:*

$$\mathcal{C}_{BC}(\mathbf{H}_1, \dots, \mathbf{H}_K, P) \leq M \log \left(1 + \frac{P}{M} \|\mathbf{H}\|_{max}^2 \right) \quad (4.50)$$

where $\|\mathbf{H}\|_{max} = \max_{i=1, \dots, K} \|\mathbf{H}_i\|$ and $\|\cdot\|$ denotes the matrix norm (i.e. the largest singular value).

Proof: We prove this result using the fact that the BC sum rate capacity is equal to the dual MAC sum-rate capacity with power constraint P . The received signal in the dual MAC is $\mathbf{y}_{MAC} = \sum_{i=1}^K \mathbf{H}_i^\dagger \mathbf{x}_i + \mathbf{n}$. The received covariance is given by $\mathbf{\Sigma}_y = E[\mathbf{y}\mathbf{y}^\dagger] = E[\mathbf{n}\mathbf{n}^\dagger] + \sum_{i=1}^K \mathbf{H}_i^\dagger E[\mathbf{x}_i \mathbf{x}_i^\dagger] \mathbf{H}_i = \mathbf{I} + \sum_{i=1}^K \mathbf{H}_i^\dagger \mathbf{Q}_i \mathbf{H}_i$. Notice that the argument of the maximization in the expression of the sum rate capacity of the dual MAC in (4.45) is $\log |\mathbf{\Sigma}_y|$.

The received signal power is given by $E[\mathbf{y}^\dagger \mathbf{y}] = \sum_{i=1}^K E[\mathbf{x}_i^\dagger \mathbf{H}_i \mathbf{H}_i^\dagger \mathbf{x}_i] + E[\mathbf{n}^\dagger \mathbf{n}]$. Since $\mathbf{x}_i^\dagger \mathbf{H}_i \mathbf{H}_i^\dagger \mathbf{x}_i \leq \|\mathbf{H}_i^\dagger\|^2 \|\mathbf{x}_i\|^2 = \|\mathbf{H}_i\|^2 \|\mathbf{x}_i\|^2$ by the definition of matrix norm, we have

$$E[\mathbf{y}^\dagger \mathbf{y}] \leq \sum_{i=1}^K \|\mathbf{H}_i\|^2 E[\mathbf{x}_i^\dagger \mathbf{x}_i] + E[\mathbf{n}^\dagger \mathbf{n}] \quad (4.51)$$

$$\leq \|\mathbf{H}\|_{max}^2 \sum_{i=1}^K E[\mathbf{x}_i^\dagger \mathbf{x}_i] + M \quad (4.52)$$

$$\leq \|\mathbf{H}\|_{max}^2 P + M \quad (4.53)$$

where (4.52) follows from the definition of $\|\mathbf{H}\|_{max}$ and the fact that $E[\mathbf{n}^\dagger \mathbf{n}] = M$ and (4.53) follows from the sum power constraint on the transmitters in the dual MAC (i.e. $\sum_{i=1}^K E[\mathbf{x}_i^\dagger \mathbf{x}_i] \leq P$). Since $E[\mathbf{y}^\dagger \mathbf{y}] = \text{Tr}(E[\mathbf{y}\mathbf{y}^\dagger]) = \text{Tr}(\mathbf{\Sigma}_y)$, this implies that $\text{Tr}(\mathbf{\Sigma}_y) \leq P \|\mathbf{H}\|_{max}^2 + M$. By [13, Theorem 16.8.4], for any positive definite $M \times M$ matrix \mathbf{K} , $|\mathbf{K}| \leq (\frac{\text{Tr}(\mathbf{K})}{M})^M$. Therefore $|\mathbf{\Sigma}_y| \leq (1 + \frac{P}{M} \|\mathbf{H}\|_{max}^2)^M$, from which we get $\mathcal{C}_{BC}(\mathbf{H}_1, \dots, \mathbf{H}_K, P) = \max_{\mathbf{\Sigma}_y} \log |\mathbf{\Sigma}_y| \leq M \log(1 + \frac{P}{M} \|\mathbf{H}\|_{max}^2)$. \square

The upper bound is equal to the sum-rate capacity of a system with M spatially orthogonal eigenmodes (distributed in any manner between the K users), each with norm equal to $\|\mathbf{H}\|_{max}$. Interestingly, users need not be spatially orthogonal for the bound to be achieved with equality. If $N = 1$ and there are more receivers than transmit antennas ($K > M$), then if the users' channels are Welch-bound equality sequences [54] (i.e. $\|\mathbf{H}_i\| = 1$ for all i and $\mathbf{H}^\dagger \mathbf{H} = \frac{K}{M} \mathbf{I}$), then the bound is also met with equality by allocating equal power (choosing $\mathbf{Q}_i = \frac{P}{K}$ in (4.45)) to each user in the dual MAC. Since $K > M$, it is not possible for the K channels (which are the $1 \times M$ rows of the matrix \mathbf{H}) to be mutually orthogonal.

However, the Welch-bound condition requires the M columns of \mathbf{H} to be orthogonal. The i -th column of \mathbf{H} refers to the channel gains from the i -th base station antenna to each of the K mobiles.

We now proceed by lower bounding the TDMA sum-rate.

Theorem 4.3 *The TDMA sum-rate is lower bounded by the rate achieved by transmitting all power in the direction of the largest eigenmode:*

$$\mathcal{C}_{TDMA}(\mathbf{H}_1, \dots, \mathbf{H}_K, P) \geq \log(1 + P\|\mathbf{H}\|_{max}^2). \quad (4.54)$$

Proof: For each user, $C(\mathbf{H}_i, P) \geq \log(1 + P\|\mathbf{H}_i\|^2)$ because single-user capacity is achieved by water-filling over *all* eigenmodes instead of allocating all power to the best eigenmode. Since the TDMA sum-rate is the maximum of the single-user capacities, the result follows. \square

This bound is tight when $N = 1$, but is generally not tight for $N > 1$ because each user has $\min(M, N)$ eigenmodes to water-fill over.

By combining Theorems 4.2 and 4.3, we can upper bound the DPC gain:

$$\frac{\mathcal{C}_{BC}(\mathbf{H}_1, \dots, \mathbf{H}_K, P)}{\mathcal{C}_{TDMA}(\mathbf{H}_1, \dots, \mathbf{H}_K, P)} \leq \frac{M \log(1 + \frac{P}{M}\|\mathbf{H}\|_{max}^2)}{\log(1 + P\|\mathbf{H}\|_{max}^2)} \quad (4.55)$$

$$\leq M \quad (4.56)$$

where we used Theorems 4.2 and 4.3 to get (4.55). Furthermore, since each user's rate in a broadcast channel can be no larger than his respective single-user capacity,

$$\begin{aligned} \mathcal{C}_{BC}(\mathbf{H}_1, \dots, \mathbf{H}_K, P) &\leq \sum_{i=1}^K C(\mathbf{H}_i, P) \\ &\leq K \cdot \mathcal{C}_{TDMA}(\mathbf{H}_1, \dots, \mathbf{H}_K, P). \end{aligned} \quad (4.57)$$

Combining the upper bounds in (4.56) and (4.57) gives the following result:

Theorem 4.4 *The DPC gain is upper bounded by M , the number of transmit antennas, and K , the number of users.*

$$G(\mathbf{H}_1, \dots, \mathbf{H}_K, P) \leq \min(M, K). \quad (4.58)$$

This bound is valid for any set of channels $\mathbf{H}_1, \dots, \mathbf{H}_K$, any number of receive antennas N , any number of users K , and any SNR P . When we consider DPC and TDMA from a signaling dimensions perspective, the upper bound is in fact quite intuitive. In the lower bound on TDMA in Theorem 4.3, only one spatial dimension (corresponding to the largest eigenmode amongst all users) is used. Dirty paper coding, on the other hand, can utilize

up to M dimensions² (Theorem 4.2). Since the TDMA lower bound uses the strongest eigenmode, the quality of each of these M spatial dimensions can be no better than the quality of the dimension used in the TDMA lower bound. Thus the rate on each of the M dimensions can be no larger than the TDMA lower bound, which implies that DPC gives a sum rate no larger than M times the TDMA capacity.

Note: A bound similar to Theorem 4.2 for the single receive antenna ($N = 1$) downlink when users have the same channel norm and are mutually orthogonal was independently derived in an earlier paper by Viswanathan and Kumaran [74, Proposition 2].

4.4.3 Asymptotic DPC Gain

If we consider a system with more transmit antennas than receive antennas ($M \geq N$) in the regimes of high and low SNR, we can establish that the DPC gain converges to $\min\left(\frac{M}{N}, K\right)$ at asymptotically high SNR. Additionally, we can show that the DPC gain converges to unity at low SNR, i.e. that DPC gives no throughput gain at low SNR. We present these results in the following theorems (proofs are given in Chapter 4.6.3 and 4.6.4):

Theorem 4.5 *If the concatenated channel matrix \mathbf{H} has at least $\min(M, NK)$ linearly independent rows and at least one of the channel matrices \mathbf{H}_i is full row rank (i.e. has N linearly independent rows), as $P \rightarrow \infty$ we have*

$$\lim_{P \rightarrow \infty} G(\mathbf{H}_1, \dots, \mathbf{H}_K, P) = \min\left(\frac{M}{N}, K\right). \quad (4.59)$$

Theorem 4.6 *For any channel matrix \mathbf{H} , dirty paper coding and TDMA are equivalent at asymptotically low SNR:*

$$\lim_{P \rightarrow 0} G(\mathbf{H}_1, \dots, \mathbf{H}_K, P) = 1. \quad (4.60)$$

The DPC gain of $\min\left(\frac{M}{N}, K\right)$ at high SNR can be intuitively explained from a dimension counting argument as follows. At high SNR, it is easy to show that the capacity of a MIMO channel grows as $L \log(P)$ (ignoring additive constants), where L is the number of spatial dimensions available in the channel, which is equal to the rank of the channel matrix. Therefore, only the number of spatial dimensions is important at high SNR and

²The term “dimensions” is used rather loosely when applied to DPC. In a single-user non-time varying MIMO channel, spatial dimensions correspond to purely orthogonal signaling directions (generally corresponding to the right eigenvectors of the channel gain matrix). When using DPC, signaling dimensions are generally not orthogonal because orthogonal signaling generally leads to much lower data rates. Thus, the number of spatial dimensions is more accurately interpreted as the rank of the transmit covariance matrix when using DPC.

the quality of these spatial dimensions (i.e. the channel gain) is unimportant. This is expected since as P becomes large, $\log(1 + \alpha P) \approx \log(P) + \log(\alpha) \approx \log(P)$. When using TDMA, there are $\min(M, N)$ dimensions available. This is equal to the number of dimensions available in an M transmit, N receive antenna MIMO channel. When using DPC, each linearly independent row (i.e. each received signal that is not equal to a linear combination of some other received signals) gives a spatial signaling dimension. Assuming \mathbf{H} has at least $\min(M, NK)$ linearly independent rows, DPC can utilize $\min(M, NK)$ spatial dimensions. When $M \geq N$, the ratio of spatial dimensions using DPC vs. TDMA is given by: $\frac{\min(M, NK)}{N} = \min\left(\frac{M}{N}, K\right)$, and thus DPC gives a sum rate equal to $\min\left(\frac{M}{N}, K\right)$ times the sum rate in TDMA.

Since the sum rate capacity grows as $\min(M, NK) \log(P)$ for large P , it is also easy to show that the sum rate capacity upper bound given in Theorem 4.2 is asymptotically tight when $M \leq NK$, or that

$$\lim_{P \rightarrow \infty} \frac{\mathcal{C}_{BC}(\mathbf{H}_1, \dots, \mathbf{H}_K, P)}{M \log\left(1 + \frac{P}{M} \|\mathbf{H}\|_{max}^2\right)} = 1. \quad (4.61)$$

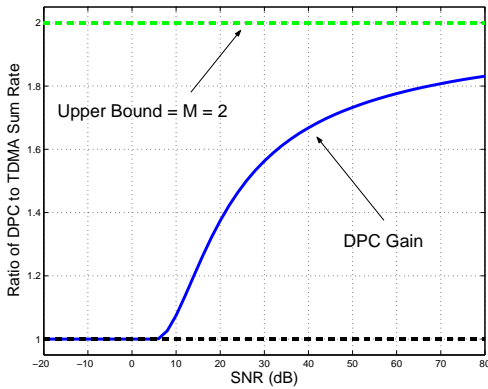
Interestingly, the TDMA sum capacity lower bound in Theorem 4.3 is a factor of N times smaller than the actual TDMA sum capacity in the asymptotic limit:

$$\lim_{P \rightarrow \infty} \frac{\mathcal{C}_{TDMA}(\mathbf{H}_1, \dots, \mathbf{H}_K, P)}{\log\left(1 + P \|\mathbf{H}\|_{max}^2\right)} = N. \quad (4.62)$$

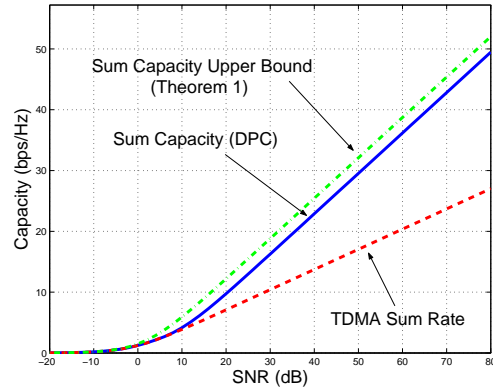
However, this factor of N does not preclude the general upper bound of $\min(M, K)$ on the DPC gain.

We can also compare the high SNR behavior of the sum rate capacity with that of the cooperative-receiver channel. Since receiver cooperation can only increase the capacity of the broadcast channel, the sum capacity $\mathcal{C}_{BC}(\mathbf{H}_1, \dots, \mathbf{H}_K, P)$ is upper bounded by the capacity of the system in which the K receivers fully cooperate, i.e. the capacity of the M transmit, NK receive antenna MIMO channel, which is given by $C(\mathbf{H}, P)$ as defined in (4.47). The cooperative upper-bound MIMO channel also has $\min(M, NK)$ spatial dimensions. Thus, at high SNR the ratio of sum capacity of the broadcast channel to the capacity of the cooperative channel converges to unity. In fact, an even tighter result shows that the difference between the sum capacity with DPC and the cooperative upper bound converges to zero as SNR goes to infinity [5, Theorem 3].

The intuition behind the low SNR result in Theorem 4.6 is exactly the opposite of the high SNR scenario. At low SNR only the quality of the best signaling dimension is important and the number of available signaling dimensions is unimportant. To see this, note that for P small, $\mathcal{C}_{BC}(\mathbf{H}_1, \dots, \mathbf{H}_K, P) \leq M \log\left(1 + \frac{P}{M} \|\mathbf{H}\|_{max}^2\right) \approx M \frac{P}{M} \|\mathbf{H}\|_{max}^2 = P \|\mathbf{H}\|_{max}^2 \approx \mathcal{C}_{TDMA}(\mathbf{H}_1, \dots, \mathbf{H}_K, P)$. DPC allows for simultaneous transmission over all of the different spatial dimensions. Since only the best signaling dimension is of importance



(a) DPC gain



(b) Sum rate plots

Figure 4.7: Plots of DPC gain and sum rate for a 2 user, 2 transmit antenna, 1 receive antenna channel

at low SNR, this option is of no use and DPC and TDMA are equivalent at low enough SNR.

In Fig. 4.7(a), the DPC gain $G(\mathbf{H}_1, \dots, \mathbf{H}_K, P)$ is plotted as a function of SNR for a 2-user channel with 2 transmit antennas and single receive antennas. The upper bound ($= M = 2$) on the DPC gain is also included. Notice the monotonicity of the DPC gain and convergence of the gain at both low and high SNR. When $N = 1$, we conjecture that $G(\mathbf{H}_1, \dots, \mathbf{H}_K, P)$ is in fact a monotonically non-decreasing function of P . Showing that $\mathcal{C}_{BC}(\mathbf{H}_1, \dots, \mathbf{H}_K, P)$ and $\mathcal{C}_{TDMA}(\mathbf{H}, P)$ are increasing functions of P is trivial, but it appears difficult to show the monotonicity of the ratio of these quantities for even the 2-user, $N = 1$ scenario for which an exact expression for $\mathcal{C}_{BC}(\mathbf{H}_1, \dots, \mathbf{H}_K, P)$ is known [5, Theorem 1]. In Fig. 4.7(b), the DPC and TDMA sum rate ($\mathcal{C}_{BC}(\mathbf{H}_1, \dots, \mathbf{H}_K, P)$ and $\mathcal{C}_{TDMA}(\mathbf{H}, P)$, respectively) are plotted for the same system, along with the sum rate capacity upper bound $M \log(1 + \frac{P}{M} \|\mathbf{H}\|_{max}^2)$ from Theorem 4.2. Note that the sum rate capacity upper bound becomes tight (in the ratio sense only) as $P \rightarrow \infty$. Furthermore, notice that the slope of the sum rate capacity curve is approximately twice the slope of the TDMA sum rate curve, leading to the convergence of the DPC gain to two.

In Fig. 4.8(a), the DPC gain is plotted as a function of SNR for a 2-user channel with 2 transmit antennas and 2 receive antennas per user. Notice that the DPC gain converges to $\frac{M}{N} = 1$ at both extremes, but takes its maximum at a finite SNR. When $M = N > 1$, $G(\mathbf{H}_1, \dots, \mathbf{H}_K, P)$ is generally not non-decreasing and actually achieves its maximum at a finite SNR. When $M = N$ as in the figure, both TDMA ($\min(M, N) = M$) and DPC ($\min(M, NK) = M$) can use M spatial dimensions. When using TDMA, the transmitter must choose to use one of the K user's M spatial dimensions. When using DPC, the transmitter can choose M spatial dimensions from all NK available dimensions instead of

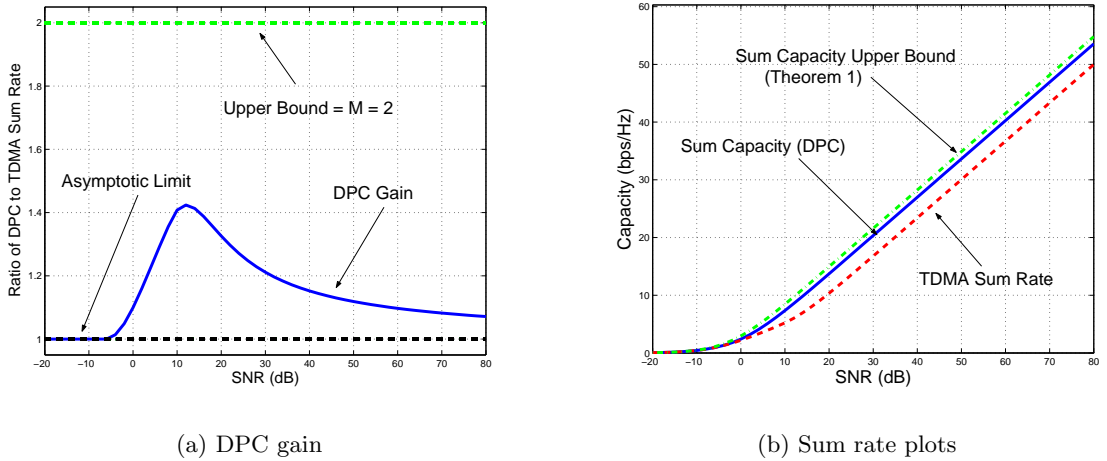


Figure 4.8: Plots of DPC gain and sum rate for a 2 user, 2 transmit antenna, 2 receive antenna channel

being forced to choose one of the K sets (corresponding to each user) of N dimensions. This is not important at high SNR, where only the number of dimensions is relevant, or at low SNR, where only the strongest spatial dimension is relevant. However, this improvement in the quality of dimensions leads to a strict DPC gain at finite SNR. In Fig. 4.8(b) the DPC and TDMA sum rate are plotted for the same system, along with the sum rate capacity upper bound from Theorem 4.2. In this channel, it is easy to see that all three curves have the same growth rate, i.e. are asymptotically equivalent in the ratio sense.

4.4.4 Tightness of Bound in Rayleigh Fading

In this section we consider the downlink sum-rate capacity in uncorrelated Rayleigh fading, i.e. where each entry of \mathbf{H}_k is independently and identically distributed as a complex circularly symmetric Gaussian with unit variance. Here we consider a time-varying system, but we assume the transmitter and receiver have perfect and instantaneous channel state information (CSI), and thus can adapt to the channel in each fading state. We also assume that the transmitter (the base station) is subject to a short-term power constraint, so that the base station must satisfy power constraint P in every fading state. This implies that there can be no adaptive power allocation over time³. Assuming that the fading process is ergodic, the sum-rate is equal to the expected value of the sum-rate in each fading state. Therefore, a reasonable performance metric is the ratio of the average sum rate using DPC to the average sum rate using TDMA, i.e. $\frac{\mathbb{E}_{\mathbf{H}}[C_{BC}(\mathbf{H}_1, \dots, \mathbf{H}_K, P)]}{\mathbb{E}_{\mathbf{H}}[C_{TDMA}(\mathbf{H}_1, \dots, \mathbf{H}_K, P)]}$. Note that this is not the

³If the transmitter is subject to an average power constraint instead of a peak power constraint, the fading channel is theoretically equivalent to the frequency-selective broadcast channel model discussed in Chapter 4.4.6. In the frequency-selective scenario, we show that the DPC gain is also upper bounded by $\min(M, K)$.

same as the quantity $\mathbb{E}_{\mathbf{H}}[G(\mathbf{H}_1, \dots, \mathbf{H}_K, P)]$, which is not as meaningful when considering average rates achievable in a fading channel.

In the previous sections we were able to establish bounds and asymptotic limits for the DPC gain for a fixed channel \mathbf{H} . In this section, we attempt to gain some intuition about the “average” DPC gain, where we average rates over Rayleigh fading channels and then calculate the ratio. By Theorem 4.4, we have $\mathcal{C}_{BC}(\mathbf{H}_1, \dots, \mathbf{H}_K, P) \leq \min(M, K) \cdot \mathcal{C}_{TDMA}(\mathbf{H}_1, \dots, \mathbf{H}_K, P)$ for each instantiation of \mathbf{H} . By taking the expectation of both sides, we get

$$\frac{\mathbb{E}_{\mathbf{H}}[\mathcal{C}_{BC}(\mathbf{H}_1, \dots, \mathbf{H}_K, P)]}{\mathbb{E}_{\mathbf{H}}[\mathcal{C}_{TDMA}(\mathbf{H}_1, \dots, \mathbf{H}_K, P)]} \leq \min(M, K). \quad (4.63)$$

In this section we show that this bound can be tightened to $\min(\frac{M}{N}, K)$ in the limit of high SNR, in the limit of a large number of transmit antennas, and in the limit of a large number of users. Note that the same limiting behavior occurs for the DPC gain of each channel instantiation in the limit of high SNR (Theorem 4.5). We also provide numerical results that show the DPC gain for non-asymptotic systems. To compute the sum rate capacity for each channel instantiation, we use the algorithm provided in Chapter 4.3. Furthermore, we use the standard Monte Carlo method to approximate the expected value of sum rate over the distribution of \mathbf{H} .

High SNR

We first consider the scenario where M , N , and K are fixed, but the SNR P is taken to infinity. Furthermore, we assume $K \geq M \geq N$, which is quite reasonable for practical systems. In this scenario, the DPC gain is shown to asymptotically equal $\frac{M}{N}$, or that:

$$\lim_{P \rightarrow \infty} \frac{\mathbb{E}_{\mathbf{H}}[\mathcal{C}_{BC}(\mathbf{H}_1, \dots, \mathbf{H}_K, P)]}{\mathbb{E}_{\mathbf{H}}[\mathcal{C}_{TDMA}(\mathbf{H}_1, \dots, \mathbf{H}_K, P)]} = \frac{M}{N}. \quad (4.64)$$

We show convergence by establishing upper and lower bounds on TDMA and DPC sum-rate⁴.

Similar to Theorem 4.2, we can upper bound the single-user capacity $C(\mathbf{H}_i, P)$ by $N \log(1 + \frac{P}{N} \|\mathbf{H}_i\|^2)$. Then, using Jensen’s inequality, the TDMA sum-rate can be bounded as:

$$\begin{aligned} \mathbb{E}_{\mathbf{H}}[\mathcal{C}_{TDMA}(\mathbf{H}_1, \dots, \mathbf{H}_K, P)] &\leq N \mathbb{E}_{\mathbf{H}} \left[\log \left(1 + \frac{P}{N} \|\mathbf{H}\|_{max}^2 \right) \right] \\ &\leq N \log \left(1 + \frac{P}{N} \mathbb{E}_{\mathbf{H}}[\|\mathbf{H}\|_{max}^2] \right). \end{aligned}$$

⁴Note that the high SNR result in Theorem 4.5 cannot be extended in a straightforward manner here because the theorem only gives convergence for each instantiation of \mathbf{H} and we require some uniformity of convergence for the result to hold in an expected value sense across instantiations.

Since $\mathcal{C}_{TDMA}(\mathbf{H}_1, \dots, \mathbf{H}_K, P) \geq \mathcal{C}(\mathbf{H}_1, P)$, we can lower bound the TDMA capacity as:

$$\begin{aligned} \mathbb{E}_{\mathbf{H}}[\mathcal{C}_{TDMA}(\mathbf{H}_1, \dots, \mathbf{H}_K, P)] &\geq \mathbb{E}_{\mathbf{H}_1}[C(\mathbf{H}_1, P)] \\ &\geq \mathbb{E}_{\mathbf{H}} \left[\log \left| \mathbf{I} + \frac{P}{N} \mathbf{H}_1^\dagger \mathbf{H}_1 \right| \right] \\ &= N \mathbb{E}_{\mathbf{H}} \left[\log \left(1 + \frac{P}{N} \lambda_i \right) \right] \\ &\geq N \left(\log \left(\frac{P}{N} \right) + \mathbb{E}_{\mathbf{H}} [\log(\lambda_i)] \right). \end{aligned}$$

where λ_i is an unordered eigenvalue of the Wishart matrix $\mathbf{H}_1 \mathbf{H}_1^\dagger$ and the single-user capacity is lower bounded by transmitting equal power (as opposed to the optimal water-filling power allocation) on each of the N eigenmodes of User 1.

Using Theorem 4.2 and Jensen's inequality, we can upper bound the sum-rate capacity as:

$$\begin{aligned} \mathbb{E}_{\mathbf{H}}[\mathcal{C}_{BC}(\mathbf{H}_1, \dots, \mathbf{H}_K, P)] &\leq M \mathbb{E}_{\mathbf{H}} \left[\log \left(1 + \frac{P}{M} \|\mathbf{H}\|_{max}^2 \right) \right] \\ &\leq M \log \left(1 + \frac{P}{M} \mathbb{E}_{\mathbf{H}} [\|\mathbf{H}\|_{max}^2] \right). \end{aligned}$$

We can also lower bound the sum-rate capacity by choosing $\mathbf{Q}_i = \frac{P}{KN} \mathbf{I}$ in (4.45) for each user:

$$\begin{aligned} \mathbb{E}_{\mathbf{H}}[\mathcal{C}_{BC}(\mathbf{H}_1, \dots, \mathbf{H}_K, P)] &\geq \mathbb{E}_{\mathbf{H}} \left[\log \left| \mathbf{I} + \frac{P}{KN} \mathbf{H}^\dagger \mathbf{H} \right| \right] \\ &= M \mathbb{E}_{\mathbf{H}} \left[\log \left(1 + \frac{P}{KN} \lambda_i \right) \right] \\ &\geq M \left(\log \left(\frac{P}{KN} \right) + \mathbb{E}_{\mathbf{H}} [\log(\lambda_1)] \right) \end{aligned}$$

where λ_i is distributed as an unordered eigenvalue of the $M \times M$ Wishart matrix $\mathbf{H}^\dagger \mathbf{H}$.

Using these bounds, as P becomes large, we can upper and lower bound the ratio $\frac{\mathbb{E}_{\mathbf{H}}[\mathcal{C}_{BC}(\mathbf{H}_1, \dots, \mathbf{H}_K, P)]}{\mathbb{E}_{\mathbf{H}}[\mathcal{C}_{TDMA}(\mathbf{H}_1, \dots, \mathbf{H}_K, P)]}$ by $\frac{M}{N}$. It then follows that $\frac{\mathbb{E}_{\mathbf{H}}[\mathcal{C}_{BC}(\mathbf{H}_1, \dots, \mathbf{H}_K, P)]}{\mathbb{E}_{\mathbf{H}}[\mathcal{C}_{TDMA}(\mathbf{H}_1, \dots, \mathbf{H}_K, P)]}$ converges to $\frac{M}{N}$ in the limit of high SNR. This result is intuitively closely related to Theorem 4.5.

In Fig. 4.9, the ratio of sum-rate capacity to the TDMA sum-rate (i.e. $\frac{\mathbb{E}_{\mathbf{H}}[\mathcal{C}_{BC}(\mathbf{H}_1, \dots, \mathbf{H}_K, P)]}{\mathbb{E}_{\mathbf{H}}[\mathcal{C}_{TDMA}(\mathbf{H}_1, \dots, \mathbf{H}_K, P)]}$) is plotted for a system with 10 users. The ratio is plotted for $M = 4$ and $N = 1$, $N = 2$, and $N = 4$. In each case the DPC gain converges to $\frac{M}{N}$, though it does so quite slowly for the $N = 1$ case.

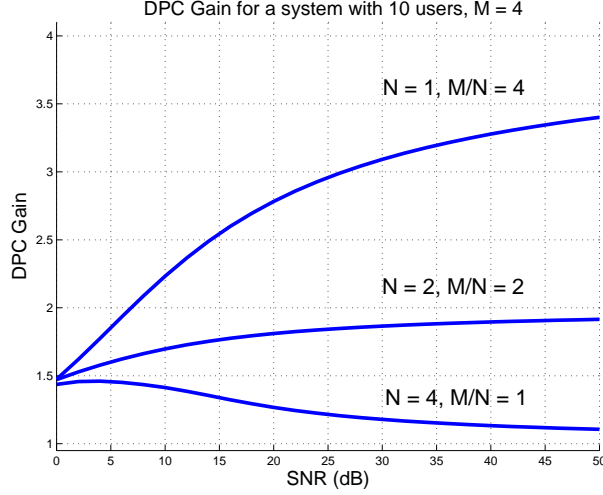


Figure 4.9: DPC Gain as a function of SNR for a 10 user system

Large M

In this section we examine the scenario where the number of users (K), number of receive antennas (N), and SNR (P) are fixed but the number of transmit antennas (M) is taken to be large. We will show that the DPC gain converges to K in this case, i.e.:

$$\lim_{M \rightarrow \infty} \frac{\mathbb{E}_{\mathbf{H}} [\mathcal{C}_{BC}(\mathbf{H}_1, \dots, \mathbf{H}_K, P)]}{\mathbb{E}_{\mathbf{H}} [\mathcal{C}_{TDMA}(\mathbf{H}_1, \dots, \mathbf{H}_K, P)]} = K. \quad (4.65)$$

As in the previous section, we lower bound the sum rate capacity by choosing $\mathbf{Q}_i = \frac{P}{KN} \mathbf{I}$ in (4.45) for each user and in each fading state. Since the identity covariance is optimal for point-to-point MIMO channels in Rayleigh fading [61], with the above choice of \mathbf{Q}_i the lower bound is equal to the point-to-point capacity of a KN transmit, M receive MIMO channel where only the receiver has channel knowledge. If the number of receive antennas in this point-to-point link is allowed to become large (i.e. $M \rightarrow \infty$) but the number of transmit antennas in this point-to-point model (KN) is kept fixed, then the capacity of the point-to-point system grows as $KN \log(1 + \frac{MP}{KN})$ [23].

As in the previous section, the TDMA sum-rate is upper bounded as $\mathbb{E}_{\mathbf{H}} [\mathcal{C}_{TDMA}(\mathbf{H}_1, \dots, \mathbf{H}_K, P)] \leq N \mathbb{E}_{\mathbf{H}} [\log(1 + \frac{P}{N} \|\mathbf{H}\|_{max}^2)]$. Using standard probability arguments, we can upper bound $\mathbb{E}_{\mathbf{H}} [\mathcal{C}_{TDMA}(\mathbf{H}_1, \dots, \mathbf{H}_K, P)]$ by $N \log(1 + \frac{P}{N} M(1 + \alpha))$, where α is any strictly positive number.

If we now take the ratio of DPC sum-rate capacity to TDMA sum-rate as $M \rightarrow \infty$, we get

$$\begin{aligned} \lim_{M \rightarrow \infty} \frac{\mathbb{E}_{\mathbf{H}} [\mathcal{C}_{BC}(\mathbf{H}_1, \dots, \mathbf{H}_K, P)]}{\mathbb{E}_{\mathbf{H}} [\mathcal{C}_{TDMA}(\mathbf{H}_1, \dots, \mathbf{H}_K, P)]} &\geq \lim_{M \rightarrow \infty} \frac{KN \log(1 + \frac{MP}{KN})}{N \log(1 + \frac{P}{N} M(1 + \alpha))} \\ &= K. \end{aligned} \quad (4.66)$$

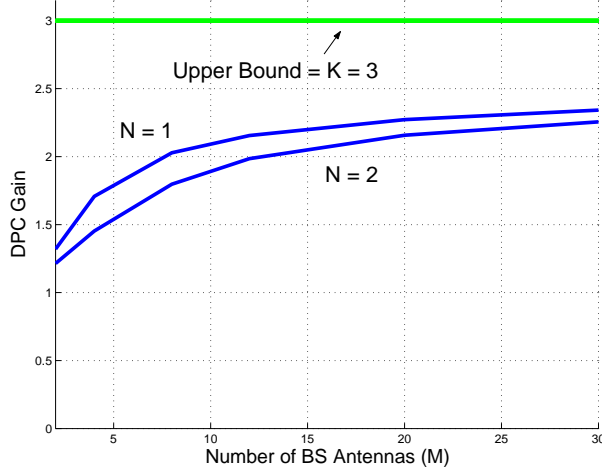


Figure 4.10: DPC Gain as a function of M for a system with 3 users at 10 dB

By Theorem 4.4, this ratio is also upper-bounded by K for all M . Thus, in the limit of many transmit antennas and with a fixed number of receivers, the DPC gain goes to K . Intuitively, as M becomes large, the NK rows of \mathbf{H} become mutually orthogonal because each row is a random vector in \mathbb{C}^M . Using TDMA, signaling can be done over N roughly orthogonal dimensions, whereas DPC allows signaling over NK dimensions. Thus, DPC can use K times as many signaling dimensions. Furthermore, the received SNR increases linearly with M . Thus, we are effectively in the high SNR regime when considering asymptotically large M , which implies that the factor of K increase in the number of spatial dimensions gained by using DPC translates to a factor of K increase in rate.

In Figure 4.10 the DPC gain is plotted as a function of the number of transmit antennas for a system with 3 users, each with 10 dB average SNR. Notice that for both $N = 1$ and $N = 2$, slow convergence to $K = 3$ is observed as M becomes large.

Large K

If the number of antennas and the SNR are kept fixed and the number of users is taken to be large, it is shown in [60] that the dirty paper gain converges to $\frac{M}{N}$, i.e.:

$$\lim_{K \rightarrow \infty} \frac{\mathbb{E}_{\mathbf{H}} [C_{BC}(\mathbf{H}_1, \dots, \mathbf{H}_K, P)]}{\mathbb{E}_{\mathbf{H}} [C_{TDMA}(\mathbf{H}_1, \dots, \mathbf{H}_K, P)]} = \frac{M}{N} \quad (4.67)$$

More specifically, the authors show that the sum rate capacity and the TDMA sum-rate grow as $M \log \log(K)$ and $N \log \log(K)$, respectively. The intuition in this scenario is that as the number of users grows large, you can find a roughly orthogonal set (of size M or N) of channels to transmit over. Furthermore, the quality of these channels (i.e. the channel gain) grows roughly as $\log(K)$ because the maximum of independent exponential random variables grows logarithmically. Thus, the approximate rate is equal to (# of dimensions)

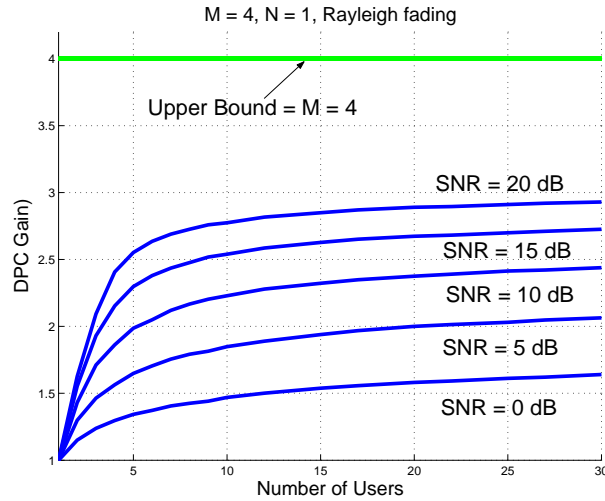


Figure 4.11: DPC Gain as a function of # of users for a system with 4 TX antennas and 1 RX antenna

$\cdot \log \log(K)$.

Numerical Results

In this section we provide plots and analysis of the DPC gain in Rayleigh fading for more realistic system parameters. In Fig. 4.11, the DPC gain is plotted as a function of the number of users for a system with four transmit antennas and one receive antenna. Plots are provided for different average SNR values. The DPC gain converges to four in the limit of a large number of users (i.e. each SNR curve converges to four), but convergence occurs extremely slow, particularly for the lower SNR values. However, a factor of 2 to 3 increase in sum rate is possible for systems with 20 users and average SNR's ranging from 5 to 20 dB.

In Figure 4.12 the DPC gain is plotted against SNR for systems with single receive antennas and differing numbers of transmit antennas. Each curve converges to M at very high SNR, and convergence occurs relatively quickly, unlike in the previous figure. Notice that at 0 dB, the DPC gain is larger than two only when there are eight transmit antennas. However, at 10 to 20 dB, gains of 2 to 5 are feasible if four or more antennas are used.

In general, note that the largest DPC gain occurs in systems with a large number of users relative to the number of transmit antennas operating at a high average SNR. Cellular systems typically have a large number of users per cell (i.e. 20 - 30), which is large compared to reasonable base station antenna deployments, but SNR's are typically quite low.

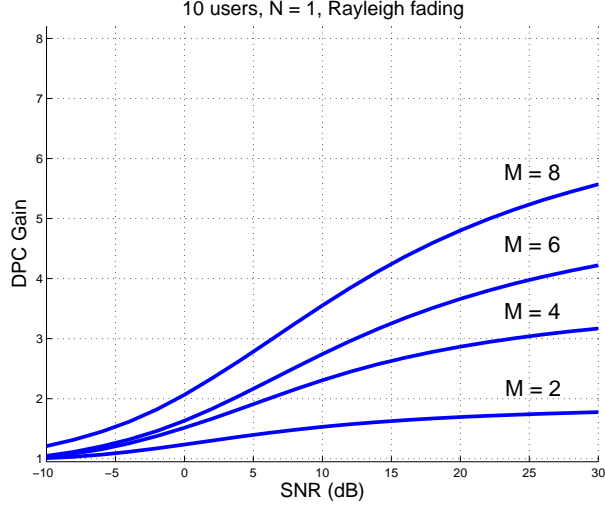


Figure 4.12: DPC Gain as a function of SNR for a 10 user system with 1 RX antenna

4.4.5 Rate Region Bounds

Given that the sum-rate gain of DPC over TDMA can be elegantly upper bounded by $\min(M, K)$, a natural question to ask is whether the entire DPC rate region can be upper bounded by the same factor $\min(M, K)$ times the TDMA rate region, i.e. is $\mathcal{R}_{DPC}(\mathbf{H}_1, \dots, \mathbf{H}_K, P) \subseteq \min(M, K) \cdot \mathcal{R}_{TDMA}(\mathbf{H}_1, \dots, \mathbf{H}_K, P)$? We have thus far investigated the gain DPC provides when all users' rates are weighted equally, but such a result would bound the total gain DPC can provide for *any* weighting of transmission rates.

By single-user capacity bounds, we know that $\mathbf{R} \in \mathcal{R}_{DPC}(\mathbf{H}_1, \dots, \mathbf{H}_K, P)$ implies $\mathbf{R}_i \leq C(\mathbf{H}_i, P)$ for $i = 1, \dots, K$. Thus, $\frac{1}{K} \sum_{i=1}^K \mathbf{R}_i \leq \sum_{i=1}^K \frac{1}{K} C(\mathbf{H}_i, P)$, which by the definition of $\mathcal{R}_{TDMA}(\mathbf{H}_1, \dots, \mathbf{H}_K, P)$ in (4.46) implies $\frac{1}{K} \mathbf{R} \in \mathcal{R}_{TDMA}(\mathbf{H}_1, \dots, \mathbf{H}_K, P)$. Thus, it follows that $\mathcal{R}_{DPC}(\mathbf{H}_1, \dots, \mathbf{H}_K, P) \subseteq K \cdot \mathcal{R}_{TDMA}(\mathbf{H}_1, \dots, \mathbf{H}_K, P)$. However, it is in fact surprisingly simple to show that it is *not always true* that $\mathcal{R}_{DPC}(\mathbf{H}_1, \dots, \mathbf{H}_K, P) \subseteq M \cdot \mathcal{R}_{TDMA}(\mathbf{H}_1, \dots, \mathbf{H}_K, P)$. Consider a single transmit and single receive antenna broadcast channel ($M = N = 1$). As long as each of the channel gains are not equal, the capacity region (which is equal to the DPC region for the scalar broadcast channel) of the scalar broadcast channel is strictly larger than the TDMA region [13], i.e. $\mathcal{R}_{DPC}(\mathbf{H}_1, \dots, \mathbf{H}_K, P) \supset \mathcal{R}_{TDMA}(\mathbf{H}_1, \dots, \mathbf{H}_K, P)$. Interestingly, for symmetric channels (i.e. single user capacities of all users are equal $C(\mathbf{H}_1, P) = C(\mathbf{H}_2, P) = \dots = C(\mathbf{H}_K, P)$), the $\min(M, K)$ bound on the DPC gain implies that for any \mathbf{R} in the DPC region, $\sum_{i=1}^K R_i \leq \mathcal{C}_{BC}(\mathbf{H}_1, \dots, \mathbf{H}_K, P) \leq \min(M, K) \cdot C(\mathbf{H}_1, P)$. Therefore, it follows that $\mathcal{R}_{DPC}(\mathbf{H}_1, \dots, \mathbf{H}_K, P) \subseteq \min(M, K) \cdot \mathcal{R}_{TDMA}(\mathbf{H}_1, \dots, \mathbf{H}_K, P)$ for symmetric channels. However, this result is not true in general.

4.4.6 Frequency Selective Broadcast Channels

A frequency selective multiple-antenna broadcast channel can be decomposed into a set of parallel, independent flat-fading multiple-antenna broadcast channels [21]. In practical systems, orthogonal frequency division multiplexing (OFDM) can be used to reduce a frequency-selective channel into a finite number of parallel, frequency-flat MIMO broadcast channels (corresponding to each frequency tone). Dirty paper coding could be used separately on each of these frequency tones, or TDMA could be used on each tone (i.e. choose only user per tone to transmit to). If DPC is used on each tone, power can optimally be allocated to different tones to meet an average power constraint. If this same per-tone power allocation is used in conjunction with TDMA instead of DPC (transmitting to only the strongest user on each tone), Theorem 4.4 can be used to upper bound the DPC gain in each tone by $\min(M, K)$. Therefore, the total sum rate achieved using DPC (and optimal allocation of power across tones) is still at most $\min(M, K)$ times larger than the rate achievable using TDMA on each tone. However, if only one user was selected for transmission across all tones, which implies that this user may not be the best user for each tone, the gain of DPC is no longer upper bounded by M , but is still upper bounded by K , the number of users.

4.4.7 Transmitter Beamforming

Transmitter beamforming⁵ is a sub-optimal technique that supports simultaneous transmission to multiple users on a broadcast channel. Each active user is assigned a beamforming direction by the transmitter and multi-user interference is treated as noise. Transmit beamforming is actually quite similar to dirty paper coding, but with DPC some multi-user interference is “pre-subtracted” at the transmitter, thus increasing the rates of some users. In [73] it is shown that transmitter beamforming for the broadcast channel without pre-coding is dual to receiver beamforming in the multiple-access channel without successive interference cancellation. As a result, when $N = 1$, the maximum sum rate using beamforming can be written as [65]:

$$C_{BF}(\mathbf{H}_1, \dots, \mathbf{H}_K, P) = \max_{\{P_i: \sum_{i=1}^K P_i \leq P\}} \sum_{j=1}^K \log \frac{|\mathbf{I} + \sum_{i=1}^K \mathbf{H}_i^\dagger P_i \mathbf{H}_i|}{|\mathbf{I} + \sum_{i \neq j} \mathbf{H}_i^\dagger P_i \mathbf{H}_i|} \quad (4.68)$$

This optimization cannot be cast in a convex form, and does not lend itself to numerical computation. However, we are able to analytically show that beamforming and DPC are equivalent at low and high SNR.

Theorem 4.7 *If \mathbf{H} has at least M independent rows, beamforming performs as well as*

⁵Transmitter beamforming is also referred to as SDMA, or space-division multiple access.

DPC in the ratio sense at both asymptotically low and high SNR.

$$\lim_{P \rightarrow \infty} \frac{C_{BC}(\mathbf{H}_1, \dots, \mathbf{H}_K, P)}{C_{BF}(\mathbf{H}_1, \dots, \mathbf{H}_K, P)} = \lim_{P \rightarrow 0} \frac{C_{BC}(\mathbf{H}_1, \dots, \mathbf{H}_K, P)}{C_{BF}(\mathbf{H}_1, \dots, \mathbf{H}_K, P)} = 1. \quad (4.69)$$

Proof: By Theorem 1, we have $C_{BC}(\mathbf{H}_1, \dots, \mathbf{H}_K, P) \leq M \log(1 + \frac{P}{M} \|\mathbf{H}\|_{max}^2)$. For simplicity, assume that the first M rows of \mathbf{H} are linearly independent. In the proof of Theorem 4.5, we show that the sum rate achievable using channel inversion is at least as large as $\sum_{i=1}^M \log(1 + \alpha_i^2 \frac{P}{M})$. Channel inversion is a particular method of transmitter beamforming (zero-forcing beamforming), and thus $C_{BF}(\mathbf{H}_1, \dots, \mathbf{H}_K, P) \geq \sum_{i=1}^M \log(1 + \alpha_i^2 \frac{P}{M})$. Therefore we have:

$$\begin{aligned} \lim_{P \rightarrow \infty} \frac{C_{BC}(\mathbf{H}_1, \dots, \mathbf{H}_K, P)}{C_{BF}(\mathbf{H}_1, \dots, \mathbf{H}_K, P)} &\leq \lim_{P \rightarrow \infty} \frac{M \log(1 + \frac{P}{M} \|\mathbf{H}\|_{max}^2)}{\sum_{i=1}^M \log(1 + \alpha_i^2 \frac{P}{M})} \\ &= 1 \end{aligned}$$

The low SNR result follows directly from Theorem 4.6 and the fact that $C_{BF}(\mathbf{H}, P) \geq C_{TDMA}(\mathbf{H}_1, \dots, \mathbf{H}_K, P)$. \square

The equivalence of transmitter beamforming and DPC at high SNR follows from the fact that both DPC and transmitter beamforming can use $\min(M, NK)$ signaling dimensions. However, the use of dirty paper coding reduces interference seen at the receivers and therefore improves the quality of each of the signaling dimensions, leading to an increase in sum rate at finite SNR. Thus, an interesting open problem is to analytically bound the gain that DPC provides over transmitter beamforming. We conjecture that the ratio $\frac{C_{BC}(\mathbf{H}_1, \dots, \mathbf{H}_K, P)}{C_{BF}(\mathbf{H}_1, \dots, \mathbf{H}_K, P)}$ is bounded by a constant ($< M$) independent of the number of antennas and the channel \mathbf{H} for all P , but we have been unable to prove this due to the difficulty of working with the beamforming sum-rate expression in (4.68). Viswanathan and Venkatesan [75] recently characterized the performance of downlink beamforming and dirty paper coding as M and K both grow to infinity at some fixed ratio $\frac{M}{K} = \alpha$. In this asymptotic regime, the ratio $\frac{C_{BC}(\mathbf{H}_1, \dots, \mathbf{H}_K, P)}{C_{BF}(\mathbf{H}_1, \dots, \mathbf{H}_K, P)}$ is bounded by 2 for all values of α and P .

4.4.8 Bound on Sum-Rate Gain of Successive Decoding for Uplink

Successive decoding is a capacity-achieving scheme for the multiple-access channel (uplink) in which multiple users simultaneously transmit to the base station and the receiver successively decodes and subtracts out the signals of different users. This technique achieves the sum-rate capacity of the MIMO MAC [13, Chapter 14], but is difficult to implement in practice. The sum-rate capacity of the MAC with transmitter power constraints

$\mathbf{P} = (P_1, \dots, P_K)$ is given by:

$$\mathcal{C}_{MAC}(\mathbf{H}_1, \dots, \mathbf{H}_K, \mathbf{P}) = \max_{\{\text{Tr}(\mathbf{Q}_i) \leq P_i \ \forall i\}} \log \left| \mathbf{I} + \sum_{i=1}^K \mathbf{H}_i^\dagger \mathbf{Q}_i \mathbf{H}_i \right|.$$

Notice that the sum-rate capacity of the MAC is identical to the BC sum-rate capacity expression in (4.45) except that the MAC expression has *individual* power constraints instead of a sum constraint.

Using the proof technique of Theorem 4.2 on the dual uplink (K transmitters with N antennas each and a single receiver with M antennas) modified for individual power constraints $\mathbf{P} = (P_1, \dots, P_K)$, it is easy to see that the following holds:

$$\mathcal{C}_{MAC}(\mathbf{H}_1, \dots, \mathbf{H}_K, \mathbf{P}) \leq M \log \left(1 + \frac{\sum_{i=1}^K P_i \|\mathbf{H}_i\|^2}{M} \right). \quad (4.70)$$

A sub-optimal transmission scheme is to allow only one user to transmit at a time. Since each user in the uplink has an individual power constraint, users are allocated orthogonal time slots in which they transmit. Thus, the TDMA rate region is defined as:

$$\mathcal{R}_{TDMA}(\mathbf{H}_1, \dots, \mathbf{H}_K, \mathbf{P}) \triangleq \bigcup_{\alpha_i \geq 0, \sum_{i=1}^K \alpha_i = 1} \left(\alpha_1 C \left(\mathbf{H}_1, \frac{P_1}{\alpha_1} \right), \dots, \alpha_K C \left(\mathbf{H}_K, \frac{P_K}{\alpha_K} \right) \right).$$

As before, the TDMA sum-rate is defined as the maximum sum of rates in this region. As used in the proof of Theorem 4.3, for each user $C(\mathbf{H}_i, \frac{P_i}{\alpha_i}) \geq \log(1 + \frac{P_i}{\alpha_i} \|\mathbf{H}_i\|^2)$ for any α_i . Thus,

$$\mathcal{C}_{TDMA}(\mathbf{H}_1, \dots, \mathbf{H}_K, \mathbf{P}) \geq \max_{\alpha_i \geq 0, \sum_{i=1}^K \alpha_i = 1} \sum_{i=1}^K \alpha_i \log \left(1 + \frac{P_i}{\alpha_i} \|\mathbf{H}_i\|^2 \right).$$

The RHS of this expression corresponds to the TDMA region of a *scalar* MAC with channel gains $\|\mathbf{H}_1\|, \dots, \|\mathbf{H}_K\|$. It is easy to verify that this expression is maximized by choosing $\alpha_i = \frac{P_i \|\mathbf{H}_i\|^2}{\sum_{j=1}^K P_j \|\mathbf{H}_j\|^2}$. With this choice of α_i , we get the following upper bound:

$$\mathcal{C}_{TDMA}(\mathbf{H}_1, \dots, \mathbf{H}_K, \mathbf{P}) \geq \log \left(1 + \sum_{i=1}^K P_i \|\mathbf{H}_i\|^2 \right). \quad (4.71)$$

Combining (4.70) and (4.71) we get $\frac{\mathcal{C}_{MAC}(\mathbf{H}_1, \dots, \mathbf{H}_K, \mathbf{P})}{\mathcal{C}_{TDMA}(\mathbf{H}_1, \dots, \mathbf{H}_K, \mathbf{P})} \leq M$. As before, the single-user capacity of each user also upper bounds this ratio by K . Thus, we finally get

$$\frac{\mathcal{C}_{MAC}(\mathbf{H}_1, \dots, \mathbf{H}_K, \mathbf{P})}{\mathcal{C}_{TDMA}(\mathbf{H}_1, \dots, \mathbf{H}_K, \mathbf{P})} \leq \min(M, K) \quad (4.72)$$

or that performing optimal successive decoding at the base station offers a gain of at most

$\min(M, K)$ over TDMA.

4.5 Summary

Throughout this chapter, one unifying theme has been the use of duality. The dirty paper coding achievable region of the multiple-antenna broadcast channel is extremely difficult to deal with, both analytically and numerically. However, the dual multiple-access capacity region is considerably easier to work with in both regards due to its convex properties. We first used the dual form of the dirty paper region to analytically prove achievability of the sum rate capacity. We then exploited the convex structure of the multiple-access sum capacity to develop an intuitive algorithm that calculates the sum capacity of the multiple-antenna broadcast channel. Finally, we again used the expression for multiple-access sum capacity to analytically compare the sum rate capacity to the maximum sum rate achievable using time division multiple-access, which is a sub-optimal technique for the downlink. Interestingly, after completion of this work, duality was again used to show that the dirty paper coding region is optimal if Gaussian inputs are capacity achieving for the multiple-antenna broadcast channel [70] [72]. Furthermore, the optimality of Gaussian inputs has recently been shown [77], which finally settles the question of the optimality of dirty paper coding for the multiple-antenna broadcast channel.

4.6 Appendix

4.6.1 Lagrangian Dual Problem

We first find the dual problem of the maximum sum-rate of the MIMO MAC: ⁶

$$\max_{\mathbf{Q}_i \in S} \log \left| \mathbf{I} + \sum_{i=1}^K \mathbf{H}_i^\dagger \mathbf{Q}_i \mathbf{H}_i \right| \quad (4.73)$$

over the convex set $S = \{\mathbf{Q}_i : \mathbf{Q}_i \geq 0 \forall i, \sum_{i=1}^K \text{Tr}(\mathbf{Q}_i) \leq P\}$.

The problem given by (4.73) is a convex optimization problem, i.e., it has a concave objective function and a convex constraint set. Hence a convex Lagrangian dual minimization problem can be obtained that achieves the same optimum value at (4.73). For this, we rewrite (4.73) as

$$\begin{aligned} & \min_{\mathbf{X}, \mathbf{Q}_i} \quad -\log |\mathbf{X}| \\ \text{such that} \quad & \mathbf{X} = \mathbf{I} + \sum_{i=1}^K \mathbf{H}_i^\dagger \mathbf{Q}_i \mathbf{H}_i, \quad \sum_{i=1}^K \text{Tr}(\mathbf{Q}_i) \leq P, \quad \mathbf{Q}_i \geq 0. \end{aligned}$$

⁶This derivation is based on the dual problem found in [83]

Note that matrix inequalities are associated with dual variables that are matrices, while scalar inequalities are associated with scalar dual variables. The Lagrangian for this problem is:

$$\begin{aligned} \mathcal{L}(\mathbf{X}, \mathbf{Q}_i, \mathbf{A}, \mathbf{S}_i, \lambda) &= -\log |\mathbf{X}| + \text{Tr}[\mathbf{A}(\mathbf{X} - \mathbf{I} - \sum_{i=1}^K \mathbf{H}_i^\dagger \mathbf{Q}_i \mathbf{H}_i)] \\ &\quad + \lambda(\sum_{i=1}^K \text{Tr}(\mathbf{Q}_i) - P) + \sum_{i=1}^K \text{Tr}(\mathbf{S}_i \mathbf{Q}_i). \end{aligned} \quad (4.74)$$

The dual function is found by minimizing with respect to the primal variables \mathbf{X}, \mathbf{Q}_i :

$$g(\mathbf{A}, \mathbf{S}_i, \lambda) = \inf_{\mathbf{X}, \mathbf{Q}_i} \mathcal{L}(\mathbf{X}, \mathbf{Q}_i, \mathbf{A}, \mathbf{S}_i, \lambda). \quad (4.75)$$

We obtain the optimality conditions by differentiating the Lagrangian (4.74) with respect to the primal variables to get

$$\begin{aligned} \lambda \mathbf{I} &= \mathbf{H}_i \mathbf{A} \mathbf{H}_i^\dagger + \mathbf{S}_i \quad \forall i \\ \mathbf{X}^{-1} &= \mathbf{A}. \end{aligned}$$

For any Lagrangians not satisfying these conditions, we get $g(\mathbf{A}, \mathbf{S}_i, \lambda) = -\infty$. For Lagrangians that do satisfy these conditions, we get

$$g(\mathbf{A}, \mathbf{S}_i, \lambda) = \log |\mathbf{A}| - \text{Tr}(\mathbf{A}) - \lambda P + t. \quad (4.76)$$

The dual problem is then obtained by maximizing the dual function $g(\mathbf{A}, \mathbf{S}_i, \lambda)$ with respect to the dual variables:

$$\begin{aligned} &\max_{\mathbf{A}, \lambda} \log |\mathbf{A}| - \text{Tr}(\mathbf{A}) - \lambda P + t && (4.77) \\ \text{such that} &\quad \mathbf{A} \geq 0, \lambda \geq 0 \\ &\quad \lambda \mathbf{I} \geq \mathbf{H}_i \mathbf{A} \mathbf{H}_i^\dagger \quad \forall i. \end{aligned}$$

Due to the convexity of the original optimization, the sum rate capacity of the MAC is equal to the solution of the dual problem above (4.77).

We now use Lagrangian duality to find an alternative form for the Sato upper bound. The Sato upper bound is originally defined in (4.6) as:

$$\mathcal{C}_{\text{Sato}}(\mathbf{H}_1, \dots, \mathbf{H}_K, P) \triangleq \inf_{\mathbf{Z} \in \mathcal{S}} \max_{\mathbf{\Sigma} \geq 0, \text{Tr}(\mathbf{\Sigma}) \leq P} \log \left| \mathbf{I} + \mathbf{Z}^{-1} \mathbf{H} \mathbf{\Sigma} \mathbf{H}^\dagger \right|. \quad (4.78)$$

We will find an alternate form for this upper bound by considering the Lagrangian dual of only the inner maximization (and not of the entire expression). For any $\mathbf{Z} > 0$, consider

the inner maximization:

$$\max_{\mathbf{\Sigma} \geq 0, \text{Tr}(\mathbf{\Sigma}) \leq P} \log \left| \mathbf{I} + \mathbf{Z}^{-1} \mathbf{H} \mathbf{\Sigma} \mathbf{H}^\dagger \right|. \quad (4.79)$$

Note that the maximization in (4.79) is the capacity of a multi-antenna system with channel given by $\mathbf{Z}^{-1/2} \mathbf{H}$ and additive white Gaussian noise [61]. Therefore, (4.79) is equivalent to:

$$\max_{\mathbf{Q} \geq 0, \text{Tr}(\mathbf{Q}) \leq P} \log \left| \mathbf{I} + \mathbf{H}^\dagger \mathbf{Z}^{-1/2} \mathbf{Q} \mathbf{Z}^{-1/2} \mathbf{H} \right|. \quad (4.80)$$

Notice that this maximization is equivalent to the form of the MAC sum-rate maximization in (4.73) with $K = 1$, $\mathbf{H}_1^\dagger = \mathbf{H}^\dagger \mathbf{Z}^{-1/2}$, and $\mathbf{Q}_1 = \mathbf{Q}$. Therefore, the above maximization (4.80) is equivalent to:

$$\begin{aligned} & \max_{\mathbf{A}, \lambda} \log |\mathbf{A}| - \text{Tr}(\mathbf{A}) - \lambda P + t \quad (4.81) \\ \text{such that} \quad & \mathbf{A} \geq 0, \lambda \geq 0 \\ & \lambda \mathbf{I} \geq \mathbf{Z}^{-1/2} \mathbf{H} \mathbf{A} \mathbf{H}^\dagger \mathbf{Z}^{-1/2}. \end{aligned}$$

Clearly, we can multiply the last inequality by the term $\mathbf{Z}^{-1/2}$ on both sides and negate the objective function to get:

$$\begin{aligned} & \min_{\mathbf{A}, \lambda} -\log |\mathbf{A}| + \text{Tr}(\mathbf{A}) + \lambda P - M \quad (4.82) \\ \text{such that} \quad & \mathbf{A} \geq 0, \lambda \geq 0 \\ & \lambda \mathbf{Z} \geq \mathbf{H} \mathbf{A} \mathbf{H}^\dagger. \end{aligned}$$

Since this is equivalent to the inner maximization of the Sato upper bound for every $\mathbf{Z} \in S$, we can rewrite the Sato upper bound as:

$$\begin{aligned} \mathcal{C}_{\text{Sato}}(\mathbf{H}_1, \dots, \mathbf{H}_K, P) &= \inf_{\mathbf{Z} \in S} \min_{\mathbf{A}, \lambda} -\log |\mathbf{A}| + \text{Tr}(\mathbf{A}) + \lambda P - M \\ & \text{such that} \quad (4.83) \\ & \lambda \geq 0, \mathbf{A} \geq 0 \\ & \lambda \mathbf{Z} \geq \mathbf{H} \mathbf{A} \mathbf{H}^\dagger. \end{aligned}$$

4.6.2 Uniqueness of Water-Filling Solution

In this appendix we show that there is a unique solution to the following problem:

$$\max_{\mathbf{Q} \geq 0, \text{Tr}(\mathbf{Q}) \leq P} \log \left| \mathbf{I} + \mathbf{H} \mathbf{Q} \mathbf{H}^\dagger \right| \quad (4.84)$$

for any non-zero $\mathbf{H} \in \mathbb{C}^{N \times M}$ for arbitrary M, N . This proof is identical to the proof of optimality of water-filling in [61, Section 3.2], with the addition of a simple proof of

uniqueness.

Since $\mathbf{H}^\dagger \mathbf{H} \in \mathbb{C}^{M \times M}$ is Hermitian and positive semi-definite, we can diagonalize it and write $\mathbf{H}^\dagger \mathbf{H} = \mathbf{U} \mathbf{D} \mathbf{U}^\dagger$ where \mathbf{U} is unitary and \mathbf{D} is diagonal with non-negative entries. Using the identity $|\mathbf{I} + \mathbf{A} \mathbf{B}| = |\mathbf{I} + \mathbf{B} \mathbf{A}|$, we can rewrite the objective function as

$$\log |\mathbf{I} + \mathbf{H} \mathbf{Q} \mathbf{H}^\dagger| = \log |\mathbf{I} + \mathbf{Q} \mathbf{H}^\dagger \mathbf{H}| = \log |\mathbf{I} + \mathbf{Q} \mathbf{U} \mathbf{D} \mathbf{U}^\dagger| = \log |\mathbf{I} + \mathbf{U}^\dagger \mathbf{Q} \mathbf{U} \mathbf{D}|. \quad (4.85)$$

Let $\tilde{\mathbf{Q}} = \mathbf{U}^\dagger \mathbf{Q} \mathbf{U}$. Clearly $\mathbf{Q} = \mathbf{U} \tilde{\mathbf{Q}} \mathbf{U}^\dagger$. Since $\text{Tr}(\mathbf{A} \mathbf{B}) = \text{Tr}(\mathbf{B} \mathbf{A})$ and \mathbf{U} is unitary, we have $\text{Tr}(\tilde{\mathbf{Q}}) = \text{Tr}(\mathbf{U}^\dagger \mathbf{Q} \mathbf{U}) = \text{Tr}(\mathbf{Q} \mathbf{U} \mathbf{U}^\dagger) = \text{Tr}(\mathbf{Q})$. Furthermore, $\tilde{\mathbf{Q}} \geq 0$ if and only if $\mathbf{Q} \geq 0$. Therefore, the maximization can equivalently be carried out over $\tilde{\mathbf{Q}}$, i.e.:

$$\max_{\tilde{\mathbf{Q}} \geq 0, \text{Tr}(\tilde{\mathbf{Q}}) \leq P} \log |\mathbf{I} + \tilde{\mathbf{Q}} \mathbf{D}|. \quad (4.86)$$

with $\mathbf{D} \in \mathcal{R}^{M \times M}$ diagonal and non-negative. In addition, any solution to (4.84) corresponds to a solution of (4.86) via the invertible mapping $\tilde{\mathbf{Q}} = \mathbf{U}^\dagger \mathbf{Q} \mathbf{U}$. Thus, if the maximization in (4.84) has multiple solutions, the maximization in (4.86) must also have multiple solutions. Therefore, it is sufficient to show that (4.86) has a unique solution, which we prove next.

First notice that Haddamard's inequality [13] gives the following upper bound $|\mathbf{I} + \tilde{\mathbf{Q}} \mathbf{D}| \leq \prod_{i=1}^K (1 + \mathbf{Q}_{ii} \mathbf{D}_{ii})$, which is achievable if and only if \mathbf{Q} is diagonal. Since $\text{Tr}(\mathbf{Q}) = \sum_{i=1}^K \mathbf{Q}_{ii} \leq P$ and $\mathbf{Q}_{ii} \geq 0$ for $i = 1, \dots, K$ by the positive semi-definite condition, for any feasible non-diagonal \mathbf{Q} there exists a diagonal \mathbf{Q} corresponding to a strictly larger objective value. Therefore, the optimal solution must be diagonal. If \mathbf{Q} is diagonal, the objective function is equal to $\sum_{i=1}^M \log(1 + \mathbf{Q}_{ii} \mathbf{D}_{ii})$. Since we can ignore entries of \mathbf{D} that are zero and the assumption that \mathbf{H} is not the zeroes matrix insures that at least one diagonal entry of \mathbf{D} is non-zero, we can without loss of generality assume $\mathbf{D}_{ii} > 0$ for $i = 1, \dots, M$. Therefore, the objective is a strictly concave function of $\mathbf{Q}_{11}, \dots, \mathbf{Q}_{MM}$, and thus (4.86) has a unique solution.

4.6.3 Proof of Theorem 4.5

The basic premise is to show that $C_{BC}(\mathbf{H}_1, \dots, \mathbf{H}_K, P)$ grows as $\min(M, NK) \log(P)$ and $C_{TDMA}(\mathbf{H}_1, \dots, \mathbf{H}_K, P)$ grows as $N \log(P)$. We first consider a channel with $M < NK$. Note that by Theorem 1, $C_{BC}(\mathbf{H}_1, \dots, \mathbf{H}_K, P) \leq M \log(1 + \frac{P}{M} \|\mathbf{H}\|_{max}^2)$. Furthermore, we form a matrix (denoted by $\mathbf{H}^{M,M}$) consisting of any set of M linearly independent rows of \mathbf{H} . By the linear independence of the rows, $\mathbf{H}^{M,M}$ is strictly positive definite. Therefore, we can invert the channel at the transmitter to give M independent and parallel non-zero channels, though there is a power penalty involved in channel inversion. The result is M independent and parallel channels with strictly non-zero channel gains $\alpha_1, \dots, \alpha_M$. Thus, we have $C_{BC}(\mathbf{H}_1, \dots, \mathbf{H}_K, P) \geq \sum_{i=1}^M \log(1 + \alpha_i^2 \frac{P}{M})$, because allocating equal power on the

parallel channels is sub-optimal.

Without loss of generality, assume \mathbf{H}_1 has full row rank. Then a lower bound to $C_{TDMA}(\mathbf{H}_1, \dots, \mathbf{H}_K, P)$ is arrived at by:

$$C_{TDMA}(\mathbf{H}_1, \dots, \mathbf{H}_K, P) \geq C(\mathbf{H}_1, P) \geq \sum_{i=1}^N \log \left(1 + \lambda_i \frac{P}{N} \right), \quad (4.87)$$

where $(\lambda_1, \dots, \lambda_N)$ are the eigenvalues of $\mathbf{H}_1 \mathbf{H}_1^\dagger$. Similar to Theorem 4.2, we can upper bound $C_{TDMA}(\mathbf{H}_1, \dots, \mathbf{H}_K, P)$ by assuming there exists a user with N eigenmodes with eigenvalues equal to $\|\mathbf{H}\|_{max}$: $C_{TDMA}(\mathbf{H}_1, \dots, \mathbf{H}_K, P) \leq N \log \left(1 + \|\mathbf{H}\|_{max}^2 \frac{P}{N} \right)$. Combining these bounds, we can establish that $\lim_{P \rightarrow \infty} \frac{C_{BC}(\mathbf{H}_1, \dots, \mathbf{H}_K, P)}{C_{TDMA}(\mathbf{H}_1, \dots, \mathbf{H}_K, P)}$ is bounded above and below by $\frac{M}{N}$.

If $KN \leq M$ (i.e. $K \leq \frac{M}{N}$), we can similarly show that DPC grows as $KN \log(P)$ while TDMA grows as $N \log(P)$. Thus, the DPC gain is asymptotically equal to K .

4.6.4 Proof of Theorem 4.6

Without loss of generality, assume that $|\mathbf{H}_1| \geq |\mathbf{H}_2| \cdots \geq |\mathbf{H}_K|$. First notice that on the dual MAC we have:

$$\log \left| \mathbf{I} + \sum_{i=1}^K \mathbf{H}_i^\dagger \mathbf{Q}_i \mathbf{H}_i \right| = I(X_1, \dots, X_K; Y) \quad (4.88)$$

$$= \sum_{i=1}^K I(X_i; Y | X_1, \dots, X_{i-1}) \quad (4.89)$$

$$\leq \sum_{i=1}^K I(X_i; Y | X_1, \dots, X_{i-1}, X_{i+1}, \dots, X_K) \quad (4.90)$$

$$= \sum_{i=1}^K \log \left| \mathbf{I} + \mathbf{H}_i^\dagger \mathbf{Q}_i \mathbf{H}_i \right| \quad (4.91)$$

where we have used the chain rule for mutual information in (4.89) and the fact that X_1, \dots, X_K are independent to get $I(X_i; Y | X_1, \dots, X_{i-1}, X_{i+1}, \dots, X_K) \geq I(X_i; Y | X_1, \dots, X_{i-1})$ in (4.90). Thus we can upper bound the sum capacity of the dual MIMO MAC by the sum capacity of a multiple-access channel where each transmitter has an independent channel (\mathbf{H}_i^\dagger) to the receiver. By diagonalizing each \mathbf{H}_i , we can write the sum capacity of this upper bound as:

$$\max_{P_{i,j} \geq 0: \sum_{i,j} P_{i,j} \leq P} \sum_{i,j} \log(1 + P_{i,j} \lambda_{i,j}) \quad (4.92)$$

where $\lambda_{i,j}$ is the j -th eigenvalue of $\mathbf{H}_i \mathbf{H}_i^\dagger$. Assume that $\lambda_{i,j} \geq \lambda_{i,k}$ for all $k > j$. Notice that the optimal power allocation maximizing (4.92) is found by the standard water-filling procedure for parallel Gaussian channels [13, Chapter 10.4].

We must separately consider two different cases: $|\mathbf{H}_1| > |\mathbf{H}_2|$ and $|\mathbf{H}_1| = |\mathbf{H}_2|$. First consider $|\mathbf{H}_1| > |\mathbf{H}_2|$, which implies $\lambda_{1,1} > \lambda_{2,1}$. From the water-filling procedure, we know that for $P \leq \frac{1}{\lambda_{1,1}} - \frac{1}{\lambda_{2,1}}$, there is not enough power to fill any of the channels of Users 2, \dots , K . Therefore, the maximum in (4.92) is achieved by only allocating power to User 1, i.e. TDMA is optimal, for small enough P . Thus, for $P \leq \frac{1}{\lambda_{1,1}} - \frac{1}{\lambda_{2,1}}$, we have $C_{BC}(\mathbf{H}_1, \dots, \mathbf{H}_K, P) = C_{TDMA}(\mathbf{H}_1, \dots, \mathbf{H}_K, P)$.

Now consider the scenario where $|\mathbf{H}_1| = |\mathbf{H}_2| = \dots = |\mathbf{H}_L|$, i.e. where L users have the same largest eigenvalue. Let m_i be the multiplicity of the largest eigenvalue of the i -th user, and assume $\sum_{i=1}^L m_i = J$. Then for $P \leq J(\frac{1}{\lambda_{1,1}} - \frac{1}{\lambda^*})$, where λ^* is the second largest eigenvalue amongst all users, the maximum in (4.92) is achieved by allocating equal power to the J eigenmodes with the largest eigenvalue. The corresponding capacity is $J \log(1 + |\mathbf{H}_1|^2 \frac{P}{J})$. In this case, note that

$$\lim_{P \rightarrow 0} \frac{J \log(1 + |\mathbf{H}_1|^2 \frac{P}{J})}{\log(1 + |\mathbf{H}_1|^2 P)} = 1. \quad (4.93)$$

Thus, in the limit of small P , the ratio of the sum capacity of the upper bound to the TDMA capacity goes to one.

Chapter 5

Fading Multi-User Channels

Due to user mobility, wireless channels are typically time-varying. In the past, wireless engineers typically built in a large fade margin in systems to allow for a certain amount of channel degradation. However, this is clearly a sub-optimal method of dealing with fading channels. Instead, more intelligent system architectures provide receivers and transmitters with the capability to adapt power and rate in response to changing channel conditions. In this chapter, we characterize the optimum power and rate allocation policies for fading single-antenna broadcast channels with respect to different performance metrics.

In [20], Goldsmith and Varaiya derived the optimum power and rate allocation strategy that maximizes the long-term average rate in a single-user fading channel with perfect and instantaneous channel knowledge at both the transmitter and receiver. In [41], Li and Goldsmith extended this work to fading broadcast channels. As one would intuitively expect, the optimal strategy involves increasing both power and rate for users with good channel conditions, and decreasing both quantities for users with poor channel conditions. Though such a strategy may maximize the average rate of transmission, it may come at the expense of transmitting at extremely low or zero data rate to users for a long period of time while their channel quality is poor. Since this may not be permissible in delay-sensitive applications such as video transmission, it is also useful to consider different performance metrics for fading channels.

In the first section, we consider a fading broadcast channel and maximize the average rate of transmission while maintaining some minimum rate in every fading state, i.e. while maintaining some minimum level of service in each fading state. Thus, regardless of how poor the channel quality is, each user must be served at some minimum rate. Such a policy is appropriate for transmission of a mixture of delay-sensitive traffic (such as video) corresponding to the minimum rate and delay-insensitive traffic (such as data) being transmitted at any excess rate possible beyond the minimum rate. We show that the minimum rate capacity region can be written in terms of the ergodic capacity region of a broadcast channel with effective noises determined by the minimum rate requirements. This allows us to

use previously known results on the ergodic capacity region of the broadcast channel [41] to find the optimum power allocation policy. Though we only directly find the optimum power allocation policy for the fading broadcast channel, we are able to use duality to also find the minimum rate capacity region and the corresponding optimal power allocation policies for the fading multiple-access channel.

In the final section of the chapter, we consider a fading broadcast channel in which the transmitter can send independent messages to each of the receivers as well as a common message that must be received by both of the receivers. In a cellular setting, for example, this might correspond to separate data file transmission to individual users while simultaneously multi-casting a news update to every user. We are able to derive the optimal rate and power allocation scheme that maximizes long-term average rates in this scenario. Unlike the optimal power allocation schemes for the fading broadcast channel without common messages, a water-filling like interpretation is not possible when there are both common and independent messages. Material in this chapter also appears in [29] [30] [32].

5.1 Broadcast Channels with Minimum Rate Constraints

In this section we characterize the minimum rate capacity region of the fading broadcast channel. We assume that the transmitter and all receivers can track the channel fade perfectly, or in other words that the transmitter and all receivers have perfect channel state information (CSI). Furthermore, we assume the channel is *slowly fading* relative to codeword length, i.e. the channel is constant during transmission of a codeword.

Two notions of Shannon capacity have been developed for multi-user fading channels: ergodic capacity and outage capacity. Ergodic capacity is concerned with achieving long-term rates averaged over all fading states [63], [62], [41], while outage capacity achieves a constant rate in all non-outage fading states subject to an outage probability [42], [43]. Zero-outage capacity refers to outage capacity with zero outage probability [22].

The ergodic capacity of a fading broadcast channel determines the maximum achievable long-term rates averaged over all fading states. The optimal resource allocation scheme for rates in the ergodic capacity region is found in [25, 41] and corresponds to multi-level water-filling over both time (i.e. fading states) and users. As intuition would suggest, users are allocated the most power when their channels are strong, and little, if any, power when their channels are weak. Such an allocation scheme maximizes long-term average rates, but may result in long delays for users in deep channel fades. This clearly may not be reasonable for delay-sensitive applications such as video or voice transmission.

In the outage capacity region of a broadcast channel, each user maintains a constant rate some percentage of the time and no data is transmitted (i.e. an outage is declared) the rest of the time. In essence, no data is transmitted to a user when his channel is weak because it takes a great deal of power to transmit data over a weak channel. Constant rates

are maintained in all other states. The optimal power allocation scheme is essentially a multi-user extension of channel inversion. This scheme eliminates all channel variation seen by the receivers by scaling the transmitted signal to invert fading so constant rates can be maintained during non-outage. Because constant rate transmission requires more power in a weak channel than in a strong channel, users are allocated the most power when their channels are weak. This is in sharp contrast to the allocation scheme used to maximize ergodic rates, where users are allocated the most power when their channels are strongest. It is therefore clear that stronger channel states are not truly taken advantage of and as a result the outage capacity region may be significantly smaller than the ergodic capacity region. Zero-outage capacity is a special case of outage capacity in which no outage is allowed and constant rates must be maintained in all fading states.

Ergodic and outage capacity are clearly two very different performance measures, as reflected by their contrasting power allocation strategies. In ergodic capacity, the transmitter *takes advantage* of time-variation in the channel by transmitting more data to users with strong channels, while in outage capacity the transmitter *equalizes* time-variation by transmitting at constant rates in all non-outage states. For a system that simultaneously transmits delay-sensitive and delay-insensitive data, neither of these approaches appears optimal. It is not desirable to shut off users for long periods of time as is possible in the ergodic capacity region, but forcing constant rates to be maintained subject only to an outage probability as is done in the outage capacity region severely reduces the set of achievable rates.

In this section we combine the notions of ergodic and zero-outage capacity by maximizing the ergodic capacity subject to minimum rate requirements for all users in all fading states. Thus, some power is used to maintain the minimum rates in all fading states while the remaining power is used to maximize the average rates in excess of the minimum rates. Users are never completely cut-off due to the minimum rate requirements, but time-variation of the channel is still taken advantage of by transmitting to users at rates higher than the minimum rates when their channels are strong and at exactly the minimum rates when their channels are poor. Clearly, the minimum rate requirement must be in the zero-outage capacity region for the rates to be achievable in all states.

We consider a slowly fading channel that is assumed to be constant over the duration of each codeword. Thus, we associate an instantaneous rate with each user in every fading state. The minimum rate capacity region is defined as the set of all average rates achievable subject to an average power constraint such that the instantaneous rates in each fading state do not violate a minimum rate constraint. We show that the minimum rate capacity region is equal to the sum of the minimum rate vector plus the *ergodic* capacity region of an effective noise channel, where the effective noise depends on the minimum rate requirements. This relationship allows us to easily characterize the boundary of the minimum rate capacity

region and the optimal power allocation policies in terms of known results for ergodic capacity [25, 41, 63].

We then extend these results to find the minimum rate capacity region subject to a peak power constraint instead of an average power constraint, and also subject to both a peak and average power constraint. Furthermore, the problem of minimum rates with outage is also addressed. When outage is allowed, ergodic capacity is maximized with the constraint that minimum rates must be satisfied at least a certain percentage of time. This is a combination of ergodic capacity and outage capacity, as opposed to non-outage minimum rate capacity, which is a combination of ergodic and zero-outage capacity. A similar notion of minimum-rate outage capacity was independently proposed by Luo et. al. in [46, 47] for single-user channels. Finally, we use the duality relationship of the Gaussian MAC-BC established in Chapter 3.1 to derive the minimum rate capacity region of the fading multiple-access channel.

The remainder of this section is organized as follows. Chapter 5.1.1 describes the flat-fading broadcast channel model and Chapter 5.1.2 defines ergodic and zero-outage capacity. In Chapter 5.1.3 we precisely define the minimum rate capacity region. In Chapter 5.1.4 we characterize the minimum rate capacity region in terms of the ergodic capacity region and find the optimal power allocation schemes. In Chapter 5.1.5 we find the minimum rate capacity region with peak power constraints and in Chapter 5.1.6 we find the minimum rate outage capacity region. Numerical results are presented in Chapter 5.1.7, followed by a derivation of the MAC minimum rate capacity region in Chapter 5.1.8.

5.1.1 System Model

We consider a fading Gaussian broadcast channel, as described in Chapter 2.2.3:

$$Y_j[i] = \sqrt{h_j[i]}X[i] + n_j[i] \quad j = 1, \dots, K.$$

where $n_j[i]$ is normally distributed with unit variance and the channel gains $h_1[i], \dots, h_K[i]$ vary according to some ergodic process. For simplicity, we incorporate the channel gain into the noise term and define an effective noise density¹ $n_j[i] = 1/g_j[i]$. Thus, an equivalent form for the received signal is given by:

$$Y_j[i] = X[i] + z_j[i] \quad j = 1, \dots, K \tag{5.1}$$

where $z_j[i]$ is Gaussian noise with power $n_j[i]$.

We assume that the noise density vector $\mathbf{n}[i] = (n_1[i], n_2[i], \dots, n_K[i])$ is known to the transmitter and all K receivers at time instant i . The transmitter can therefore vary the

¹Notice that the noise density is the instantaneous power of the noise and is not the instantaneous noise sample.

power of the signal transmitted to each user $P_j[z]$ as a function of the noise vector $\mathbf{n}[z]$ subject to an average power constraint \bar{P} . Since all receivers have knowledge of \mathbf{n} , each receiver can perform successive decoding in which the decoding order depends on the ordering of \mathbf{n} .

As the noise density vector incorporates the effects of the channel gain, we will alternatively refer to \mathbf{n} as the *fading state* throughout this paper.

5.1.2 Ergodic & Zero Outage Capacity Regions

In this section we present results from [41, 42] on the ergodic and zero-outage capacity of the fading broadcast channel.

Ergodic Capacity Region

The ergodic capacity region is defined as the set of all long-term average rates achievable in a fading channel with arbitrarily small probability of error. In [41], the ergodic capacity region and optimal power allocation scheme for the fading broadcast channel is found by decomposing the fading channel into a parallel set of constant broadcast channels, one for each fading state \mathbf{n} . In Chapter 2.2.3 an expression for the ergodic capacity region was given in (2.12). We now restate the expression for the ergodic capacity region, denoted by $\mathcal{C}_{ergodic}(\bar{P}; \mathbf{n})$, in terms of the noise vector \mathbf{n} :

$$\mathcal{C}_{ergodic}(\bar{P}; \mathbf{n}) = \bigcup_{\mathcal{P} \in \mathcal{F}} \mathcal{C}_{BC}(\mathcal{P}; \mathbf{n}). \quad (5.2)$$

where \mathcal{F}_{BC} is the set of power policies meeting the power constraint $\mathcal{F}_{BC} = \{\mathcal{P}_{BC} : \mathbb{E}_{\mathbf{n}}[\sum_{j=1}^K P_j^B(\mathbf{n})] \leq \bar{P}\}$ and $\mathcal{C}_{BC}(\mathcal{P})$ defined as

$$\mathcal{C}_{BC}(\mathcal{P}; \mathbf{n}) = \{R_j : R_j \leq \mathbb{E}_{\mathbf{n}}[R_j(\mathbf{P}(\mathbf{n}))], \quad j = 1, 2, \dots, K\}$$

with $R_j(\mathbf{P}(\mathbf{n}))$ given by:

$$R_j(\mathbf{P}(\mathbf{n})) = \log \left(1 + \frac{P_j(\mathbf{n})}{n_j + \sum_{k=1}^K P_k(\mathbf{n}) \mathbf{1}[n_j > n_k]} \right) \quad (5.3)$$

where $\mathbf{1}[\cdot]$ is the indicator function.

The optimal power allocation scheme that achieves the boundary points of the ergodic capacity region is a multi-level extension of water-filling. Because the data rate varies from state to state, a different codebook (a codebook is assumed to have codewords for all K users) is used in every joint fading state, as in the multiplexing strategy described in [20, 41]. This coding scheme works in either a slow-fading or fast-fading environment, but the decoding delay is highly dependent on the correlation time of the channel because of the multiplexing structure. An achievability proof and a converse are provided in [41].

Zero-Outage Capacity Region

For the K -user broadcast channel, a rate vector $\mathbf{R} = (R_1, R_2, \dots, R_K)$ is in the zero-outage capacity region if and only if the rate vector can be achieved in all fading states while meeting the average power constraint. The zero-outage capacity region (also referred to as the *delay-limited capacity*) for the multiple-access channel is derived in [22]. In [42] it is shown that rates in the zero-outage capacity region of the broadcast channel can be achieved using superposition coding and successive decoding.

From Eq. 3 of [42], the minimum power to support a rate vector \mathbf{R} in fading state \mathbf{n} is:

$$P^{min}(\mathbf{R}, \mathbf{n}) = \sum_{k=1}^K \left[e^{\sum_{j=k+1}^K R_{\pi(j)}} (e^{R_{\pi(k)}} - 1) n_{\pi(k)} \right] + (e^{R_{\pi(K)}} - 1) n_{\pi(K)} \quad (5.4)$$

where $\pi(\cdot)$ is the permutation such that $n_{\pi(1)} < n_{\pi(2)} < \dots < n_{\pi(K)}$. Therefore, the zero-outage capacity region is the set of all rate vectors that meet the average power constraint:

$$\mathcal{C}_{zero}(\bar{P}; \mathbf{n}) = \{(R_1, R_2, \dots, R_K) : \mathbb{E}_{\mathbf{n}}[P^{min}(\mathbf{R}, \mathbf{n})] \leq \bar{P}\}. \quad (5.5)$$

The boundary of the capacity region is the set of all rate vectors \mathbf{R} such that the power constraint is met with equality [42]. The zero-outage capacity region is more formally defined as the set of rate vectors for which there exists codebooks that can be decoded with a delay *independent* of the channel correlation structure (i.e. the speed of the fading) for any desired non-zero probability of error. This is in stark contrast to the ergodic capacity, in which the decoding delay is highly dependent on the channel correlation.

5.1.3 Minimum Rate Capacity Region

Definition of Capacity Region

We define the minimum rate capacity region of a K -user broadcast channel to be the region of all achievable average rate vectors subject to an average power constraint \bar{P} and minimum rate constraints $\mathbf{R}^* = (R_1^*, R_2^*, \dots, R_K^*)$. The minimum rate constraint forces the instantaneous rate of each user to be at least as large as its corresponding minimum rate in all fading states, i.e. we require $R_j(\mathbf{n}) \geq R_j^* \quad j = 1, \dots, K \quad \forall \mathbf{n}$. Since we are dealing with slowly fading channels that are assumed to be constant over the length of a codeword, the notion of an instantaneous rate $R_j(\mathbf{n})$ in each fading state is reasonable. Moreover, the set of achievable instantaneous rates in each fading state is equal to the capacity region of the constant Gaussian broadcast channel defined by the joint fading state and the amount of power allocated to each user.

Using the previously stated notion of a power allocation scheme, let $\mathcal{C}_{min}(\mathcal{P})$ denote the

set of achievable long-term average rates in excess of the minimum rates for power policy \mathcal{P} :

$$\mathcal{C}_{min}(\mathcal{P}) = \{R_j : R_j^* \leq R_j \leq \mathbb{E}_{\mathbf{n}}[R_j(\mathbf{P}(\mathbf{n}))] \quad j = 1, \dots, K\}$$

where $R_j(\mathbf{P}(\mathbf{n}))$ is defined in (5.3). Notice this definition is slightly different than the definition of $\mathcal{C}(\mathcal{P})$ in Chapter 5.1.2. The set $\mathcal{C}_{min}(\mathcal{P})$ does not include the rates below the minimum rates because if the average rates are less than the minimum rates, then the minimum rates must be violated in some fading states.

To ensure that the minimum rates are satisfied, we must restrict the set of feasible power policies more tightly than in the case of ergodic capacity. Let \mathcal{F}' denote the set of all power policies that satisfy the minimum rate constraints in every fading state and the average power constraint \bar{P} :

$$\mathcal{F}' \equiv \left\{ \mathcal{P} : \mathbb{E}_{\mathbf{n}} \left[\sum_{j=1}^K P_j(\mathbf{n}) \right] \leq \bar{P}, \quad R_j(\mathbf{P}(\mathbf{n})) \geq R_j^* \quad \forall j, \mathbf{n} \right\}$$

The additional constraint ensures that the minimum rates can be maintained for all K users in every fading state for any power policy in \mathcal{F}' .

Definition 5.1 *The minimum rate capacity region of a fading broadcast channel with perfect CSI at the transmitter and receivers, average power constraint \bar{P} , and minimum rate constraint $\mathbf{R}^* = (R_1^*, R_2^*, \dots, R_K^*) \in \mathcal{C}_{zero}(\mathbf{n}, \bar{P})$ is:*

$$\mathcal{C}_{min}(\bar{P}, \mathbf{R}^*; \mathbf{n}) = Co \left(\bigcup_{\mathcal{P} \in \mathcal{F}'} \mathcal{C}_{min}(\mathcal{P}) \right) \quad (5.6)$$

where $Co(\cdot)$ denotes the convex hull operation. The achievability of this region follows from the achievability proof for ergodic capacity given in [41] and standard timesharing arguments.

Remarks on Coding

In the slowly fading channel model that we consider, the channel is assumed to be constant over the duration of a codeword. If the transmitter and receivers use a multiplexing strategy similar to that of [20], then a different rate vector and a different set of codebooks is associated with every joint fading state. In this context, minimum rate capacity is the set of all achievable average rates such that the instantaneous rates in every fading state meet the minimum rate requirements. The associated decoding delay at each user is equal to the codeword length, which can be arbitrarily long due to our slow fading assumption.

Since our definition of minimum rate capacity explicitly mentions instantaneous rates (i.e. rates associated with each fading state), no converse seems to exist for this formulation. A more Shannon theoretic formulation of minimum rate capacity that would not

require the slow fading assumption might consider transmitting delay-sensitive data at the minimum rate with a delay independent of the channel variation (similar to zero-outage capacity), while simultaneously maximizing transmission of delay-insensitive data with no delay requirement (similar to ergodic capacity). In this setting it appears natural to transmit using two independent codebooks, one for the delay-sensitive data and one for the delay-insensitive data. However, as we discuss below, it appears to be quite difficult to apply this approach to the broadcast channel.

In Chapter 5.1.4 we discuss a coding strategy for the single-user channel such that the minimum rate data (i.e. the codeword from the minimum rate codebook) can be decoded before the codeword from the excess rate codebook. This allows the minimum rate data to be decoded with a delay that is independent of the rate of channel variation, but the decoding delay associated with the excess rate (i.e. above the minimum rate) data can be infinite. This coding strategy works in both slow-fading and fast-fading environments. However, this scheme does not generalize to the multi-user broadcast channel because the successive decoding structure, which is capacity-achieving for the broadcast channel, essentially precludes the possibility of all users having finite delays associated with their minimum rate data and infinite delays associated with their excess rate data. Since successive decoding is needed in the broadcast channel, strong users are required to decode and cancel out the codewords intended for weaker users before being able to decode their own codewords. This must include a cancellation of the minimum rate data and the excess rate data of other users. Thus, the decoding delay of the strongest user is at least as large as the maximum of the decoding delay of all other users. If users have a possibly infinite delay associated with decoding the excess rate data, then the decoding delay associated with the minimum rate codebook of the strongest user will also be infinite. One possibility is for all users to treat all excess rate codewords (including their own) as noise while decoding their minimum rate codewords, but this appears to be quite sub-optimal. In this section we concentrate solely on the slow-fading channel in which coding can be performed in each fading state and we leave the subject of minimum rate capacity for fast-fading channels as a topic for future research.

Relationship with Ergodic and Zero-Outage Capacity Regions

The minimum rate capacity region is closely related to the zero-outage and ergodic capacity regions because minimum rate capacity is essentially a combination of these two capacities. Some fraction of the available power is used to achieve the minimum rates in all fading states, while the remaining power is used to maximize the long-term rates achievable in excess of the minimum rates. For the minimum rate problem to be feasible, the minimum rate vector must be in the zero-outage capacity region of the channel in order for the rates to be achievable in all fading states. For any $\mathbf{R}^* \in \mathcal{C}_{zero}(\bar{P}; \mathbf{n})$, the boundary of the minimum

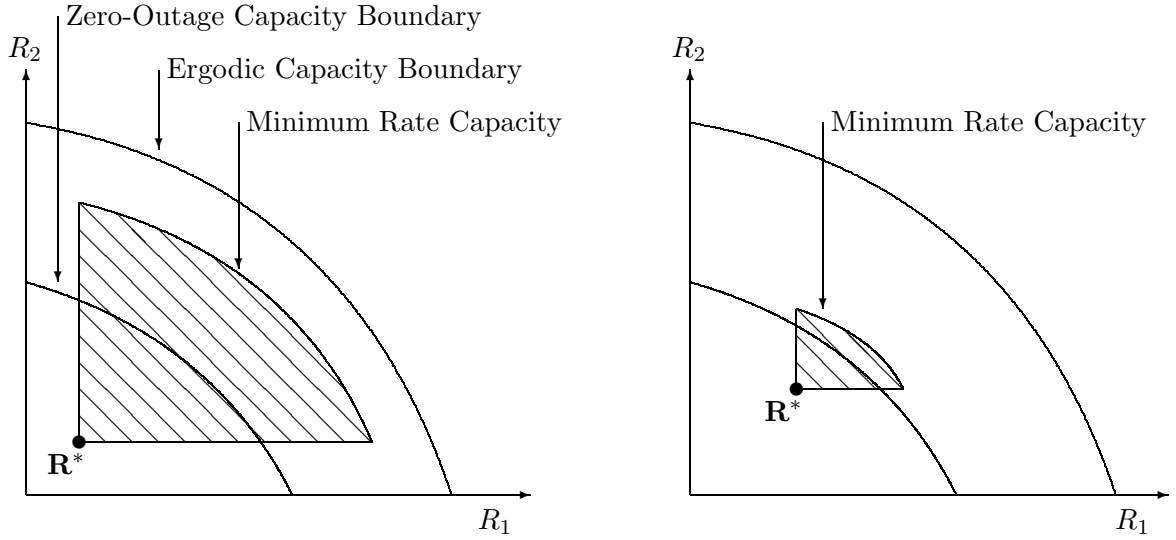


Figure 5.1: Ergodic, zero-outage, and minimum rate capacity regions for small (left) and large (right) minimum rates.

rate capacity region lies between the boundaries of the zero-outage capacity region and the ergodic capacity region:

$$\mathcal{C}_{zero}(\bar{P}; \mathbf{n}) \subseteq \mathbf{Boundary}\{\mathcal{C}_{min}(\bar{P}, \mathbf{R}^*; \mathbf{n})\} \subseteq \mathcal{C}_{ergodic}(\bar{P}; \mathbf{n}) \quad (5.7)$$

This follows from the definition of zero-outage capacity as the set of rates achievable in all fading states and from the definition of ergodic capacity as the set of achievable average rates, without any minimum rate constraints. If the minimum rates of all users are zero, the minimum rate capacity region is the same as the ergodic capacity region. If the minimum rate vector \mathbf{R}^* is on the boundary of the zero-outage capacity region, achieving the minimum rate vector in all states consumes all available power and rates in excess of the minimum rates are not possible. In this situation the minimum rate capacity region consists of only one point, \mathbf{R}^* . When \mathbf{R}^* is non-zero and not on the boundary of the zero-outage capacity region, the boundary of the minimum rate capacity region lies strictly between $\mathcal{C}_{zero}(\bar{P}; \mathbf{n})$ and $\mathcal{C}_{ergodic}(\bar{P}; \mathbf{n})$.

To illustrate the relationship between the different capacity regions, Fig. 5.1 shows the ergodic, zero-outage, and minimum rate capacity regions for two different minimum rate constraints. The corner point of the minimum rate capacity region corresponds to \mathbf{R}^* . In the graph on the left, the minimum rate vector is well within the zero-outage capacity region and as a result the minimum rate capacity region extends significantly past the zero-outage capacity region. In the second graph, the minimum rate vector is close to the boundary of the zero-outage capacity region and therefore a large fraction of the power is used to simply

achieve the minimum rates. Thus there is little power left over to exceed the minimum rates and as a result the boundary of the minimum rate capacity region does not extend much further out than the boundary of the zero-outage capacity region. Notice that in all cases the minimum rate capacity region does not extend to the axes due to the minimum rate constraints.

Since the minimum rate boundary lies between the ergodic and zero-outage boundaries, the difference between the ergodic and zero-outage capacity regions is a good indicator of the degradation in capacity (i.e. the difference between $\mathcal{C}_{ergodic}(\bar{P}; \mathbf{n})$ and $\mathcal{C}_{min}(\bar{P}, \mathbf{R}^*; \mathbf{n})$) due to minimum rates. If the zero-outage capacity region is much smaller than the ergodic capacity region, the minimum rate capacity region is generally much smaller than the ergodic capacity region. Alternatively, if the zero-outage capacity region is not much smaller than the ergodic capacity region, the minimum rate capacity region is generally quite close to the ergodic capacity region.

5.1.4 Explicit Characterization of Minimum Rate Capacity Region

In this section we explicitly characterize the boundary of the minimum rate capacity region of a K -user broadcast channel and find the corresponding optimal power allocation scheme. Directly characterizing the minimum rate capacity region yields a rather non-intuitive solution, but we show that the minimum rate capacity region can be written in terms of the *ergodic* capacity region of a related broadcast channel. This characterization is intuitively easy to understand and allows the minimum rate capacity region to be calculated using only the ergodic capacity techniques of [41].

Derivation of Minimum Rate Capacity Region

Due to the convexity of the minimum rate capacity region, for any $\mathbf{R}^* \in \mathcal{C}_{zero}(\bar{P}; \mathbf{n})$ and power constraint \bar{P} , the boundary of the region can be traced out by the following maximization:

$$\max_{\mathbf{R}} \boldsymbol{\mu} \cdot \mathbf{R} \quad \text{subject to} \quad \mathbf{R} \in \mathcal{C}_{min}(\bar{P}, \mathbf{R}^*; \mathbf{n}) \quad (5.8)$$

over all priority vectors $\boldsymbol{\mu} = (\mu_1, \dots, \mu_K)$ such that $\sum_{i=1}^K \mu_i = 1$. By the definition of $\mathcal{C}_{min}(\bar{P}, \mathbf{R}^*; \mathbf{n})$, the following is an equivalent maximization:

$$\begin{aligned} & \max_{\mathbf{P}(\mathbf{n})} \mathbb{E}_{\mathbf{n}} \left[\sum_{i=1}^K \mu_i R_i(\mathbf{P}(\mathbf{n})) \right] \\ & \text{subject to:} \quad \mathbb{E}_{\mathbf{n}} \left[\sum_{i=1}^K P_i(\mathbf{n}) \right] \leq \bar{P}, \quad R_i(\mathbf{P}(\mathbf{n})) \geq R_i^*, \forall i, \mathbf{n} \end{aligned} \quad (5.9)$$

where $R_i(\mathbf{P}(\mathbf{n}))$ is defined in (5.3).

For each fading state \mathbf{n} , let $\pi(\cdot)$ be the permutation such that $n_{\pi(1)} \leq n_{\pi(2)} \cdots \leq n_{\pi(K)}$. Since successive decoding is performed at each receiver in which the weakest user (i.e. the user with the largest noise power), or User $\pi(K)$) is decoded first, $R_i(\mathbf{P}(\mathbf{n}))$ can be defined as:

$$\begin{aligned} R_{\pi(i)}(\mathbf{P}(\mathbf{n})) &= \log \left(1 + \frac{P_{\pi(i)}(\mathbf{n})}{n_{\pi(i)} + \sum_{j<i} P_{\pi(j)}(\mathbf{n})} \right) \\ &= C \left(\frac{P_{\pi(i)}(\mathbf{n})}{n_{\pi(i)} + \sum_{j<i} P_{\pi(j)}(\mathbf{n})} \right) \end{aligned} \quad (5.10)$$

where $C(\cdot)$ is defined as $C(x) = \log(1 + x)$.

In order for each user to achieve their respective minimum rates in each state, a minimum amount of power must be allocated to each user in each fading state. We use $P_i^*(\mathbf{n})$ to denote the minimum power that User i must be allocated in fading state \mathbf{n} in order to exactly achieve R_i^* . We define the minimum powers such that if all users are allocated their minimum powers in a fading state, then all users will exactly achieve their respective minimum rates. From the definition of $R_i(\mathbf{P}(\mathbf{n}))$ in (5.10) it follows that the minimum power of each user is given by:

$$P_{\pi(i)}^*(\mathbf{n}) \triangleq \left(n_{\pi(i)} + \sum_{j<i} P_{\pi(j)}^*(\mathbf{n}) \right) \left(e^{R_{\pi(i)}^*} - 1 \right). \quad (5.11)$$

We define $\hat{P}_i(\mathbf{n})$ as the power allocated to User i in excess of the minimum power. The total power allocated to each user in fading state \mathbf{n} is thus $P_i(\mathbf{n}) = P_i^*(\mathbf{n}) + \hat{P}_i(\mathbf{n})$. The minimum rate constraints clearly imply $P_i(\mathbf{n}) \geq P_i^*(\mathbf{n})$, which implies $\hat{P}_i(\mathbf{n}) \geq 0$.

Since the rates are direct functions of the power allocation, we can replace the rate constraints in (5.9) with a power constraint to result in the following equivalent maximization:

$$\begin{aligned} &\max_{\hat{\mathbf{P}}(\mathbf{n})} \mathbb{E}_{\mathbf{n}} \left[\sum_{i=1}^K \mu_i C \left(\frac{P_{\pi(i)}^*(\mathbf{n}) + \hat{P}_{\pi(i)}(\mathbf{n})}{n_{\pi(i)} + \sum_{j<i} P_{\pi(j)}(\mathbf{n})} \right) \right] \\ \text{subject to: } &\mathbb{E}_{\mathbf{n}} \left[\sum_{i=1}^K \hat{P}_i(\mathbf{n}) \right] \leq P', \quad \hat{P}_{\pi(i)}(\mathbf{n}) \geq (e^{R_i^*} - 1) \sum_{j<i} \hat{P}_{\pi(j)}(\mathbf{n}) \quad \forall i, \mathbf{n} \end{aligned} \quad (5.12)$$

where $P' \triangleq \bar{P} - \mathbb{E}_{\mathbf{n}} \left[\sum_{i=1}^K P_i^*(\mathbf{n}) \right]$ is the total excess power. Notice that the maximization is over the excess power allocation $\hat{\mathbf{P}}(\mathbf{n})$ only. The minimum rate constraints make this problem more difficult than maximizing ergodic capacity. However, with some algebraic manipulation we will see that the minimum rate capacity maximization is equivalent to a related ergodic capacity maximization.

Using the rate-splitting identity (i.e. $C(\frac{a+b}{n}) = C(\frac{a}{n}) + C(\frac{b}{a+n})$), we can simplify the

rate equation in (5.10). We have omitted the dependence on the fading state \mathbf{n} for brevity.

$$\begin{aligned}
R_{\pi(i)}(\mathbf{P}(\mathbf{n})) &= C \left(\frac{P_{\pi(i)}^* + \hat{P}_{\pi(i)}}{n_{\pi(i)} + \sum_{j<i} P_{\pi(j)}} \right) \\
&= C \left(\frac{P_{\pi(i)}^* + (e^{R_{\pi(i)}^*} - 1) \sum_{j<i} \hat{P}_{\pi(j)}}{n_{\pi(i)} + \sum_{j<i} P_{\pi(j)}} \right) + \\
&\quad C \left(\frac{\hat{P}_{\pi(i)} - (e^{R_{\pi(i)}^*} - 1) \sum_{j<i} \hat{P}_{\pi(j)}}{n_{\pi(i)} + \sum_{j<i} P_{\pi(j)} + P_{\pi(i)}^* + (e^{R_{\pi(i)}^*} - 1) \sum_{j<i} \hat{P}_{\pi(j)}} \right) \\
&= C \left(\frac{P_{\pi(i)}^* + (e^{R_{\pi(i)}^*} - 1) \sum_{j<i} \hat{P}_{\pi(j)}}{n_{\pi(i)} + \sum_{j<i} P_{\pi(j)} + \sum_{j<i} \hat{P}_{\pi(j)}} \right) + \\
&\quad C \left(\frac{\hat{P}_{\pi(i)} - (e^{R_{\pi(i)}^*} - 1) \sum_{j<i} \hat{P}_{\pi(j)}}{n_{\pi(i)} + \sum_{j \leq i} P_{\pi(j)}^* + e^{R_{\pi(i)}^*} \sum_{j<i} \hat{P}_{\pi(j)}} \right) \\
&= R_{\pi(i)}^* + C \left(\frac{\hat{P}_{\pi(i)} - (e^{R_{\pi(i)}^*} - 1) \sum_{j<i} \hat{P}_{\pi(j)}}{n_{\pi(i)} + \sum_{j \leq i} P_{\pi(j)}^* + e^{R_{\pi(i)}^*} \sum_{j<i} \hat{P}_{\pi(j)}} \right)
\end{aligned}$$

where we have used the definition of $P_i^*(\mathbf{n})$ to obtain the final step. From this simplification it should be clear that power $P_{\pi(i)}^* + (e^{R_i^*} - 1) \sum_{j<i} \hat{P}_{\pi(j)}$ maintains the minimum rate of each user, while power $\hat{P}_{\pi(i)} - (e^{R_i^*} - 1) \sum_{j<i} \hat{P}_{\pi(j)}$ (which is non-negative by the power constraint in (5.12)) increases the rate above the minimum rate. Let us introduce the following effective noise and power terms (for each joint fading state), denoted by $P_i^e(\mathbf{n})$ and n_i^e :

$$n_{\pi(i)}^e \triangleq \left(n_{\pi(i)} + \sum_{j \leq i} P_{\pi(j)}^*(\mathbf{n}) \right) e^{\sum_{j>i} R_{\pi(j)}^*} \quad (5.13)$$

$$P_{\pi(i)}^e(\mathbf{n}) \triangleq \left(\hat{P}_{\pi(i)}(\mathbf{n}) - (e^{R_{\pi(i)}^*} - 1) \sum_{j<i} \hat{P}_{\pi(j)}(\mathbf{n}) \right) e^{\sum_{j>i} R_{\pi(j)}^*} \quad (5.14)$$

Substituting these terms into our previous expression, we get

$$R_{\pi(i)}(\mathbf{P}(\mathbf{n})) = R_{\pi(i)}^* + C \left(\frac{P_{\pi(i)}^e(\mathbf{n})}{n_{\pi(i)}^e + e^{\sum_{j \geq i} R_{\pi(j)}^*} \sum_{j<i} \hat{P}_{\pi(j)}(\mathbf{n})} \right).$$

In Chapter 5.4.1 we show that $\sum_{j<i} P_{\pi(j)}^e(\mathbf{n}) = e^{\sum_{j \geq i} R_{\pi(j)}^*} \sum_{j<i} \hat{P}_{\pi(j)}(\mathbf{n})$. Thus we can

finally rewrite the rate expression as:

$$R_{\pi(i)}(\mathbf{P}(\mathbf{n})) = R_{\pi(i)}^* + C \left(\frac{P_{\pi(i)}^e(\mathbf{n})}{n_{\pi(i)}^e + \sum_{j<i} P_{\pi(j)}^e(\mathbf{n})} \right), \quad (5.15)$$

which is identical to the rate equations for ergodic capacity for a channel with noises n_1^e, \dots, n_K^e . Since the rate of each user can be written explicitly in terms of effective power and effective noise, we can in fact maximize the weighted sum rate as a function of only the effective noises and effective powers. In Chapter 5.4.2 we show that every set of excess powers satisfying the minimum rate constraints in (5.12) maps uniquely to a set of non-negative effective powers, and vice versa. In Chapter 5.4.3, we show that the mapping from noise state to effective noise state is one-to-one for a fixed minimum rate vector and strictly unequal noise powers (which is true with probability 1 for a continuous fading distribution). Thus, we can write the effective power allocation as a function of the joint effective noise state instead of the joint noise state. Furthermore, $\sum_{i=1}^k P_i^e(\mathbf{n}) = \sum_{i=1}^K \hat{P}_i(\mathbf{n})$ by Chapter 5.4.1. Therefore, the maximization in (5.12) is equivalent to:

$$\begin{aligned} & \sum_{i=1}^K \mu_i R_i^* + \max_{\mathbf{P}^e(\mathbf{n})} \mathbb{E}_{\mathbf{n}} \left[\sum_{i=1}^K \mu_i C \left(\frac{P_{\pi(i)}^e(\mathbf{n})}{n_{\pi(i)}^e + \sum_{j<i} P_{\pi(j)}^e(\mathbf{n})} \right) \right] \\ & \text{subject to: } \mathbb{E}_{\mathbf{n}} \left[\sum_{i=1}^K P_i^e(\mathbf{n}) \right] \leq P', \quad P_i^e(\mathbf{n}) \geq 0 \quad \forall i, \mathbf{n}. \end{aligned} \quad (5.16)$$

In Chapter 5.4.4 we show that the ordering of the effective noises is the same as the ordering of the actual noises, i.e. $n_{\pi(1)}^e \leq \dots \leq n_{\pi(K)}^e$. Thus, the above maximization is identical to the problem of maximizing $\boldsymbol{\mu} \cdot \mathbf{R}$ in the ergodic capacity region of the channel with noises defined as in (5.13) and power P' . We refer to the channel with noises n_i^e and power P' as the *effective channel*. The joint distribution of \mathbf{n}^e can be derived from the mapping in (5.13).

Without the constant term $\sum_{i=1}^K \mu_i R_i^*$, (5.16) is identical to the ergodic capacity maximization expression of the effective broadcast channel [25, 41]. Therefore the average rates achievable *in excess* of the minimum rates are equal to the rates achievable in the effective channel, or to the ergodic capacity region of the effective channel. The minimum rate capacity region is therefore equal to the ergodic capacity region of the effective channel plus the minimum rates²:

$$\mathcal{C}_{min}(\bar{P}, \mathbf{R}^*; \mathbf{n}) = \mathbf{R}^* + \mathcal{C}_{ergodic}(P'; \mathbf{n}^e) \quad (5.17)$$

where $\mathcal{C}_{ergodic}(P'; \mathbf{n}^e)$ refers to the ergodic capacity of the effective channel. In Figure 5.2 the ergodic capacity region of the effective channel and the minimum rate capacity region

²The sum here refers to the set found by adding \mathbf{R}^* to every element in $\mathcal{C}_{ergodic}(P'; n_1^e, \dots, n_K^e)$.

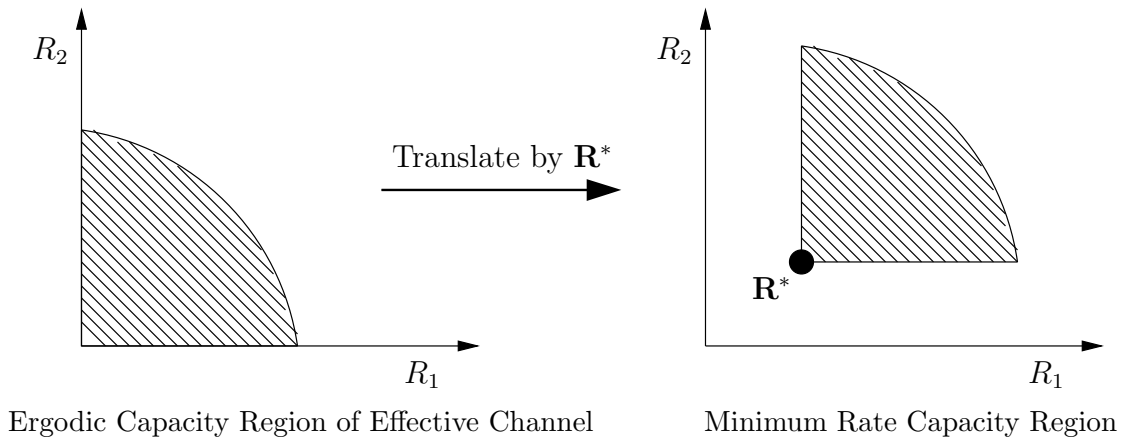


Figure 5.2: Ergodic capacity of effective channel and minimum rate capacity region

are plotted as an example of this relationship.

Optimal Power Allocation Policies

The optimal power allocation scheme to achieve the boundary of the minimum rate capacity region can be found by finding the optimal power allocation to achieve the boundary of the ergodic capacity region of the effective channel. The allocation of minimum power is pre-determined by the minimum rate requirements and the noise powers, while the optimal allocation of excess power is related to the optimal power allocation to achieve the ergodic capacity region of the effective channel. More specifically, to find the optimal power allocation policy that maximizes $\boldsymbol{\mu} \cdot \mathbf{R}$ in $\mathcal{C}_{min}(\bar{P}, \mathbf{R}^*; \mathbf{n})$ for some fixed priority vector $\boldsymbol{\mu}$, we define the optimal allocation of effective power (i.e. $P_i^e(\mathbf{n}^e)$) to be the optimal power allocation policy that maximizes $\boldsymbol{\mu} \cdot \mathbf{R}$ in $\mathcal{C}_{ergodic}(P'; \mathbf{n}^e)$ for the same priority vector $\boldsymbol{\mu}$. We can then transform the effective power allocation $P_i^e(\mathbf{n}^e)$ to the excess power allocation $\hat{P}_i(\mathbf{n})$ by the relationships given in (5.13) and (5.14). The minimum power allocation $P_i^*(\mathbf{n})$ is defined in (5.11), and the total power allocated to each user in every fading state is $P_i(\mathbf{n}) = P_i^*(\mathbf{n}) + \hat{P}_i(\mathbf{n})$.

The optimal power allocation scheme for ergodic capacity maximization is described in [41, Chapter III]. We briefly discuss the power allocation here, but we defer the reader to [41] for a more complete description. The optimal power allocation is a more complicated version of the single-user waterfilling algorithm derived in [20]. In each fading state, power can be allocated to any of the K users, or none at all. The total amount of power allocated

to each fading state can be described in the following compact form:

$$\sum_{i=1}^K P_i^e(\mathbf{n}) = \left[\max_{i=1, \dots, K} \left(\frac{\mu_i}{\lambda} - n_i^e \right) \right]^+ \quad (5.18)$$

where $[x]^+ \triangleq \max(x, 0)$ and $\frac{1}{\lambda}$ is the water-filling level chosen such that the power constraint P' is met with equality. This is akin to waterfilling to the “best” user in each fading state, where the notion of best user depends not only on the noise power but also on the user-by-user priorities. Notice, however, that this is only the allocation of *total* power to each fading state. The actual distribution of power between users in each fading state is rather involved and we defer the reader to [41] for more details. A greedy algorithm to find the optimal power allocation policy (over fading states and users) can also be found in [41, 63]

If the maximum sum rate of the minimum rate capacity region is being found (i.e. $\mu_1 = \dots = \mu_K$), then from results on ergodic capacity we know that it is optimal to only allocate effective power to the user with the smallest noise power. Thus, at most one user per fading state strictly exceeds his minimum rate requirement. However, for general priorities this is not true. Note that we are discussing only the allocation of effective power, which relates directly to the excess power. Of course, each user must be allocated the minimum power in every fading state, so all K users are active in every fading state.

Figure 5.3 illustrates the optimal amount of effective power in a two-user system that is allocated to each fading state for a discrete, four state fading distribution where $\mu_2 > \mu_1$. Note that the breakdown of power between the two users, which requires the iterative algorithm of [41], is not indicated in this figure. Water-level $\frac{\mu_1}{\lambda}$ is used for channels that are allocated excess power on n_1^e and $\frac{\mu_2}{\lambda}$ is used for channels allocated excess power on n_2^e . Water-filling is done on the effective noise-level that corresponds to the largest power allocation in that state. In the first state water-filling is done on n_2^e because although $n_2^e > n_1^e$, the higher water-level of n_2^e compensates for this difference. Because $\mu_2 > \mu_1$ in the figure, water-filling is done on n_1^e only when $n_1^e \ll n_2^e$, as in state 2. In states 3 and 4, water-filling is done on n_2^e .

Interpretation of Effective Channel

The effective channel encapsulates how power allocated to one user manifests itself into additional required power for other users due to the minimum rate requirements. Consider the power allocated to each user as consisting of two components: a part that achieves the minimum rate, and the part that leads to excess rate above the minimum rate. The minimum power $P_i^*(\mathbf{n})$ allocated to each user leads to the minimum rates of each user only if all other users are allocated exactly their minimum power levels. The minimum power does not take into account excess power allocated to users who are seen as interference. Every increment of power δP allocated to User $\pi(i)$ forces User $\pi(i+1)$ to allocate $\delta P \cdot (e^{R_{\pi(i+1)}^*} - 1)$

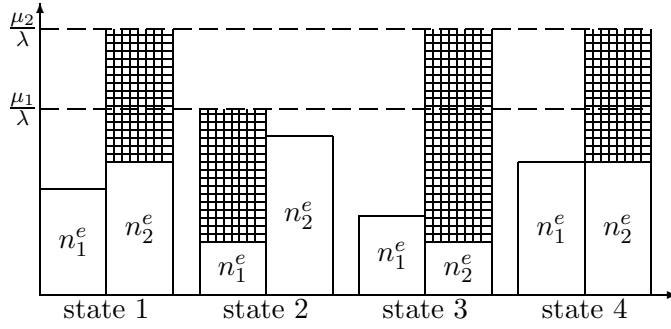


Figure 5.3: Water-filling diagram for two-user channel with minimum rates

to maintain his minimum rate. User $\pi(i+2)$ must then compensate for power δP and power $\delta P \cdot (e^{R_{\pi(i+1)}^*} - 1)$. This forces User $\pi(i+2)$ to allocate $\delta P \cdot e^{R_{\pi(i+1)}^*} (e^{R_{\pi(i+2)}^*} - 1)$ to maintain his minimum rate. This process continues up to the weakest user. In total, every increment of power δP allocated to User $\pi(i)$ corresponds to a total allocation of power $\delta P \cdot e^{\sum_{j>i} R_{\pi(j)}^*}$ to Users $\pi(i), \dots, \pi(K)$. Thus, allocation of excess power must capture two elements. First, excess power allocated to stronger users (i.e. $\sum_{j<i} \hat{P}_{\pi(j)}$) must be compensated for. The left-over excess power of User $\pi(i)$ after compensating for the excess power of stronger users thus is $\hat{P}_{\pi(i)}(\mathbf{n}) - (e^{R_{\pi(i)}^*} - 1) \sum_{j<i} \hat{P}_{\pi(j)}$. However, this left-over excess power must be multiplied by the factor $e^{\sum_{j>i} R_{\pi(j)}^*}$ to account for the fact that weaker users must compensate for any left-over excess power allocated to User $\pi(i)$. Therefore, the effective power of User i is $\left(\hat{P}_{\pi(i)}(\mathbf{n}) - (e^{R_{\pi(i)}^*} - 1) \sum_{j<i} \hat{P}_{\pi(j)}(\mathbf{n}) \right) e^{\sum_{j>i} R_{\pi(j)}^*}$. It seems that the effective noise of each user should be equal to the actual noise plus the minimum power allocated to stronger users. However, the actual effective noise is multiplied by the factor $e^{\sum_{j>i} R_{\pi(j)}^*}$ to compensate for the fact that the effective power of User i is multiplied by the same factor.

Single User Channel

A single user channel can be viewed as the broadcast channel described in Chapter 5.1.1 with $K = 1$. Thus, the characterization of minimum rate capacity derived in Chapter 5.1.4 can be applied to the single-user channel as well. Clearly, the minimum power for each state is defined as $P^*(n) \triangleq n(e^{R^*} - 1)$. As before, the minimum rate capacity can be found by solving the ergodic capacity of the effective channel. From the expressions in (5.13) and (5.14), we see that $n^e = n + P^*(n)$ and $P^e(n) = \hat{P}(n)$. The power constraint of the effective channel is $P' = \bar{P} - \mathbb{E}_n[P^*(n)]$. Since waterfilling over time achieves ergodic capacity of a single-user fading channel [20], the optimal allocation of effective power is

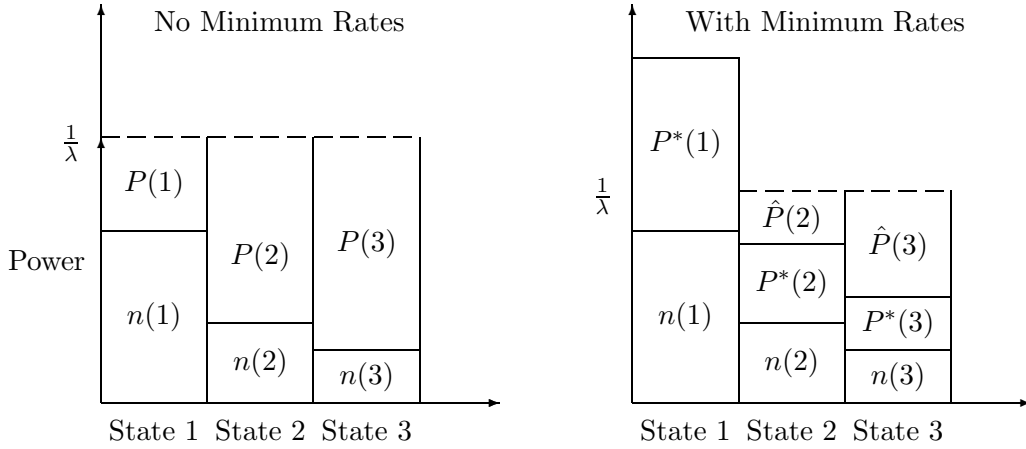


Figure 5.4: Water-filling diagram for a single-user channel

found by waterfilling over the effective noise n^e :

$$\hat{P}(n) = \begin{cases} \frac{1}{\lambda} - (n + P^*(n)) & n + P^*(n) \leq \frac{1}{\lambda} \\ 0 & n + P^*(n) > \frac{1}{\lambda} \end{cases}$$

where $\frac{1}{\lambda}$ is the water-filling level satisfying the excess power constraint P' .

This simple power allocation scheme yields a closed-form expression for the capacity of a single-user channel with power constraint \bar{P} and minimum rate R^* :

$$\mathcal{C}_{min}(\bar{P}, R^*; n) = R^* \Pr \left[n \geq \frac{1}{\lambda} e^{-R^*} \right] + \int_0^{\frac{1}{\lambda} e^{-R^*}} \log \left(\frac{1}{\lambda n} \right) p(n) dn$$

In this expression we use the fact that $n + P^*(n) = n e^{R^*}$.

Figure 5.4 illustrates the water-filling procedure for zero and non-zero minimum rates for a single-user three state channel. State 1 is the weakest of the three channels. The graph on the left shows the power allocation scheme without minimum rates. We see that all three channels are allocated power, but the rate achieved in states 1 and 2 may be quite small. When minimum rates are applied, the minimum power P^* becomes an additional source of noise. Because $P^*(n)$ is an increasing function of n , the effective noise term of state 1 becomes much larger than the other two terms. When water-filling is done on the effective noise terms, additional power is only allocated to states 2 and 3 because the effective noise term of state 1 is too large and because much of the power was used to simply achieve the minimum rates in all three states. In state 1 transmission will be done at exactly R^* , whereas the minimum rate will be exceeded in the other two states due to the excess power allocated to those states.

As briefly mentioned earlier, in a single-user channel data can be transmitted at the

minimum rate with a decoding delay that is independent of the rate of channel variation while simultaneously transmitting delay-insensitive data that takes advantage of the ergodic nature of the channel. This can be accomplished through the use of a separate minimum rate codebook and an ergodic rate codebook and the idea of rate-splitting [53]. Notice that the rate in each fading state can be expanded as:

$$\begin{aligned}
R(n) &= C\left(\frac{P^*(n) + \hat{P}(n)}{n}\right) \\
&= C\left(\frac{\hat{P}(n)e^{-R^*}}{n}\right) + C\left(\frac{P^*(n) + \hat{P}(n)(1 - e^{-R^*})}{n + \hat{P}(n)e^{-R^*}}\right) \\
&= \hat{R}(n) + R^*(n)
\end{aligned}$$

where the excess rate is $\hat{R}(n) = C\left(\frac{\hat{P}(n)e^{-R^*}}{n}\right) = C\left(\frac{\hat{P}(n)}{n + P^*(n)}\right)$.

A minimum rate codebook of size $2^{n_{min}R^*}$ with blocklength n_{min} can be used to transmit data at the minimum rate, while a codebook of size $2^{n\mathbb{E}[\hat{R}(n)]}$ with blocklength n that is an integer multiple of n_{min} can be used to transmit data at the excess rate. Codewords from both codebooks are simultaneously sent. The minimum rate codeword is scaled by the quantity $P^*(n) + \hat{P}(1 - e^{-R^*})$, while the ergodic codeword is scaled by $\hat{P}(n)e^{-R^*}$. Treating the ergodic codeword as interference, it is easy to show that the received SINR of the minimum rate codeword is exactly $e^{R^*} - 1$, as required to transmit at rate R^* . Thus, the minimum rate codeword can be successfully decoded while treating the ergodic codeword as interference. After decoding and subtracting out the minimum rate codewords, the ergodic codeword can be decoded at the end of the ergodic blocklength, since only the actual noise remains in the channel.

This two-codebook strategy cannot be used for the broadcast channel because the strongest user must decode both the ergodic and minimum rate codeword of every other weaker user before being able to decode his own minimum rate codeword. This eliminates the possibility of decoding the minimum rate codewords before the ergodic codewords.

5.1.5 Alternative Constraints on Transmitted Power

We have derived the minimum rate capacity region of a broadcast channel subject to an average power constraint. The optimal transmitted power is a function of the joint fading state and can be quite large in some fading states. In practical broadcast situations, there is generally a peak power constraint and there may or may not be an average power constraint. In this section we characterize the minimum rate capacity region of a K -user broadcast channel subject to two different constraint sets: a peak power constraint only, and both a peak and an average power constraint.

Peak Power Constraint

We now consider the problem of maximizing minimum rate capacity subject to only a peak power constraint P_{peak} in each fading state. The capacity region can then be defined as the set of all achievable average rates subject to minimum rate, peak, and power constraints as it was for the average power constraint case in Chapter 5.1.3. We let \mathcal{F}'' denote the set of feasible power policies satisfying the peak power constraint and the minimum rate constraint in all fading states:

$$\mathcal{F}'' \equiv \left\{ \mathcal{P} : \sum_{j=1}^K P_j(\mathbf{n}) \leq P_{peak}, \quad R_j(\mathbf{P}(\mathbf{n})) \geq R_j^* \quad \forall j, \mathbf{n} \right\}.$$

The capacity region subject to peak power constraint P_{peak} is then:

$$C_{min}^{peak}(P_{peak}, \mathbf{R}^*; \mathbf{n}) = C_o \left(\bigcup_{\mathcal{P} \in \mathcal{F}''} C_{min}(\mathcal{P}) \right). \quad (5.19)$$

To find the boundary of the capacity region, we perform a maximization similar to (5.9), except with a peak power constraint replacing the average power constraint.

Since the weighted sum of the rates is an increasing function of the total power allocated to each fading state, each fading state should be allocated the peak power. Clearly the minimum rates must be achievable in each state under the peak power constraint P_{peak} which implies $P_{peak} \geq \sum_{i=1}^K P_i^*(\mathbf{n}) \quad \forall \mathbf{n}$. Given that each fading state is allocated the peak power, the remaining task is to optimally allocate P_{peak} between the K users in each fading state. We may first allocate the minimum power required to achieve the minimum rates in each state, leaving excess power $P_{peak} - \sum_{i=1}^K P_i^*(\mathbf{n})$ in each fading state. The excess power must then be optimally distributed between the K users to maximize the weighted sum of their rates in excess of the minimum rates. The set of achievable excess rates is equal to the capacity region of the effective broadcast channel, which takes the form of a constant broadcast channel in each fading state. However, maximizing weighted sum rate for a constant channel turns out to be nearly as difficult as maximizing weighted sum rate for a fading channel. First, a different waterfilling level $\frac{1}{\lambda(\mathbf{n})}$ must be chosen for *each* fading state to satisfy:

$$P_{peak} - \sum_{i=1}^K P_i^*(\mathbf{n}) = \max_{i=1, \dots, K} \left(\frac{\mu_i}{\lambda(\mathbf{n})} - n_i^e \right).$$

The effective power $P_{peak} - \sum_{i=1}^K P_i^*(\mathbf{n})$ is then allocated to the K users in each fading state according to the procedure detailed in [41, Section III]. As before, the actual excess power allocation policy can be inferred from the allocation of effective power by the relationship in (5.13) and (5.14).

Peak and Average Power Constraint

In this section we find the minimum rate capacity subject to average power constraint \bar{P} and peak power constraint P_{peak} . We assume $P_{peak} > \bar{P}$. If this condition is not satisfied, the average power constraint is meaningless. The capacity region can be defined as it was for the average power constraint case in Chapter 5.1.3. We let \mathcal{F}''' denote the set of feasible power policies:

$$\mathcal{F}''' \equiv \left\{ \mathcal{P} : \mathbb{E}_{\mathbf{n}} \left[\sum_{j=1}^K P_j(\mathbf{n}) \right] \leq \bar{P}, \sum_{j=1}^K P_j(\mathbf{n}) \leq P_{peak} \quad \forall \mathbf{n}, R_j(\mathbf{P}(\mathbf{n})) \geq R_j^* \quad \forall j, \mathbf{n} \right\}.$$

The capacity region subject to peak power constraint P_{peak} can then be characterized as:

$$\mathcal{C}_{min}^{peak+avg}(\bar{P}, P_{peak}, \mathbf{R}^*; \mathbf{n}) = \mathcal{C}o \left(\bigcup_{\mathcal{P} \in \mathcal{F}'''} \mathcal{C}_{min}(\mathcal{P}) \right). \quad (5.20)$$

To find the boundary of the K -user capacity region, we perform a maximization similar to (5.9) with the addition of a state-by-state peak power constraint. We can therefore allocate minimum power to both users and reduce the problem to an ergodic capacity maximization problem. As stated before, the minimum power required in each state to meet the minimum rate requirements must not violate the peak power constraint. However, we must maximize the ergodic capacity of the effective channel subject to average power constraint $P' \triangleq \bar{P} - \mathbb{E}_{\mathbf{n}} \left[\sum_{i=1}^K P_i^*(\mathbf{n}) \right]$ and peak power constraint $P_{peak} - \sum_{i=1}^K P_i^*(\mathbf{n})$ in each fading state. The optimal power allocation with both average and peak power constraints is simply a truncated version of the optimal power allocation policy with only an average power constraint. This is easiest to see by considering the greedy algorithm [63, Section 3.2] [41, Section III.A] to allocate power with only an average power constraint. In the greedy algorithm, each user is represented via a utility function which is a function of the amount of power allocated in each fading state. The peak power constraint effectively truncates the utility functions of all users at $z = P_{peak} - \sum_{i=1}^K P_i^*(\mathbf{n})$ in each fading state. Then it is easy to show that the total effective power allocated to each fading state is given by:

$$\sum_{i=1}^K P_i^e(\mathbf{n}) = \min \left(P_{peak} - \sum_{i=1}^K P_i^*(\mathbf{n}), \left[\max_{i=1, \dots, K} \left(\frac{\mu_i}{\lambda} - n_i^e \right) \right]^+ \right)$$

The only difference between this scheme and the optimal excess power allocation scheme without the peak power constraint is that the excess power allocated to a state is truncated at $P_{peak} - \sum_{i=1}^K P_i^*(\mathbf{n})$, which in turn affects the optimal water-filling level $\frac{1}{\lambda}$. The distribution of excess power to the K users within each fading state follows the procedure detailed in [41, Section III], with the simple caveat that the total effective power allocated to each fading state cannot be larger than $P_{peak} - \sum_{i=1}^K P_i^*(\mathbf{n})$.

5.1.6 Minimum Rate Outage Capacity

In this section we discuss minimum rate capacity with outage subject to an average power constraint. In minimum rate capacity, minimum rates must be maintained in all fading states. With outage, however, this constraint is loosened slightly and the minimum rate of every user must only be met subject to outage probabilities $\mathbf{P}^{out} = (P_1^{out}, \dots, P_K^{out})$. In other words, ergodic capacity is maximized subject to the constraint that the minimum rate of user k must be met with at least probability $(1 - P_k^{out})$ for $k = 1, \dots, K$. Minimum rate outage allows minimum rate transmission to be suspended to users when their channels are very poor. Transmission is allowed during outages, but minimum rates are not required to be met during these times. In more practical terms, delay-sensitive data must be transmitted at the minimum rates a certain percentage of the time, whereas delay-insensitive data has no such constraint. This is different than the definition of outage capacity [42, 43] in which no data is transmitted during outages and the only concern is the constant channel achievable during non-outages.

In certain severe fading distributions (i.e. Rayleigh fading), it is not possible to maintain a constant data rate at all times with an average power constraint. This implies that channels with such distributions have no zero-outage capacity region and therefore have no minimum rate capacity region. However, most fading channels can support a constant rate with outage and thus have a minimum-rate outage capacity region.

In this section we analyze the scenario where outage is declared on a user-by-user basis as opposed to declaring a common outage during which no user is required to meet his minimum rate [42]. We will see that the case of common outage is a special case of the more general independent outage formulation.

Minimum Rate Outage Capacity Region with Independent Outage

To find the minimum rate outage capacity, we first define the outage function $\mathbf{w}(\mathbf{n}) = (w_1(\mathbf{n}), \dots, w_K(\mathbf{n}))$ over all fading states where $w_k(\mathbf{n}) = 1$ for fading states in which the minimum rate of User k must be satisfied and $w_k(\mathbf{n}) = 0$ otherwise³. Due to the outage constraints, the outage function must satisfy $\mathbb{E}_{\mathbf{n}}[w_k(\mathbf{n})] \geq (1 - P_k^{out})$ for each user. The outage function is an indicator function that determines which states are required to maintain the minimum rates of the different users. Maximizing ergodic capacity given outage function $\mathbf{w}(\mathbf{n})$ is very similar to finding non-outage minimum rate capacity, except with *time-varying* minimum rates $\mathbf{R}^*(\mathbf{n}, w(\mathbf{n}))$. We define $\mathbf{R}^*(\mathbf{n}, w_k(\mathbf{n}))$ as:

$$R_k^*(\mathbf{n}, w_k(\mathbf{n})) = \begin{cases} 0 & w_k(\mathbf{n}) = 0 \\ R_k^* & w_k(\mathbf{n}) = 1 \end{cases} \quad (5.21)$$

³We need not consider $0 < w_k(\mathbf{n}) < 1$ since we are only concerned with continuous fading distributions

where R_k^* is assumed to be the actual desired minimum rate of User k . We then write the time-varying minimum rates as $\mathbf{R}^*(\mathbf{n}, \mathbf{w}(\mathbf{n})) = (R_1^*(\mathbf{n}, w_1(\mathbf{n})), \dots, R_K^*(\mathbf{n}, w_K(\mathbf{n})))$.

Though the minimum rates were assumed to be constant in the original minimum rate capacity formulation, time-varying minimum rates can be handled using almost the identical solution. To achieve the minimum rate capacity with time-varying minimum rates $\mathbf{R}^*(\mathbf{n}, \mathbf{w}(\mathbf{n}))$, we simply need to replace \mathbf{R}^* with $\mathbf{R}^*(\mathbf{n}, \mathbf{w}(\mathbf{n}))$ in the optimal power allocation scheme derived in Chapter 5.1.4. The fact that the fading broadcast channel was decomposed into a parallel set of constant broadcast channels, one for each fading state, allows us to optimally deal with time-varying minimum rates using this simple substitution.

With this in mind, we define $\mathcal{C}_{min}(\bar{P}, \mathbf{R}^*(\mathbf{n}, \mathbf{w}(\mathbf{n})); \mathbf{n})$ to be the minimum rate capacity of the broadcast channel with time-varying minimum rates $\mathbf{R}^*(\mathbf{n}, \mathbf{w}(\mathbf{n}))$. For each outage function $\mathbf{w}(\mathbf{n})$ satisfying the outage constraints, $\mathcal{C}_{min}(\bar{P}, \mathbf{R}^*(\mathbf{n}, \mathbf{w}(\mathbf{n})); \mathbf{n})$ defines an achievable rate region that satisfies both the average power constraint and the outage constraints.

Definition 5.2 *The minimum rate outage capacity of a fading broadcast channel with perfect CSI at the transmitter and receivers, average power constraint \bar{P} , minimum rate constraint $\mathbf{R}^* = (R_1^*, R_2^*, \dots, R_K^*) \in \mathcal{C}_{out}(\bar{P}, \mathbf{P}^{out})$, and outage probabilities $\mathbf{P}^{out} = (P_1^{out}, \dots, P_K^{out})$ is:*

$$\mathcal{C}_{min}^{outage}(\bar{P}, \mathbf{R}^*, \mathbf{P}^{out}; \mathbf{n}) = Co \left(\bigcup_{\mathbf{w}(\mathbf{n})} \mathcal{C}_{min}(\bar{P}, \mathbf{R}^*(\mathbf{n}, \mathbf{w}(\mathbf{n})); \mathbf{n}) \right)$$

where the union is over all $\mathbf{w}(\mathbf{n})$ satisfying $\mathbb{E}_{\mathbf{n}}[w_k(\mathbf{n})] \geq (1 - P_k^{out}) \forall k = 1, \dots, K$.

Notice that the minimum rate vector \mathbf{R}^* must be in the independent outage capacity region [42], i.e. $\mathbf{R}^* \in \mathcal{C}_{out}(\bar{P}, \mathbf{P}^{out})$, for the minimum rates to be achievable with the given outage probability.

Minimum Rate Outage Capacity Region with Common Outage

The minimum rate outage capacity with common outage can be characterized using the expression for minimum rate outage capacity with independent outage. With common outage, the outage function $\mathbf{w}(\mathbf{n})$ must satisfy the additional constraint $w_1(\mathbf{n}) = w_2(\mathbf{n}) = \dots = w_K(\mathbf{n}) \forall \mathbf{n}$. In addition, the vector outage constraint becomes a scalar outage probability P^{out} . The capacity region then is:

$$\mathcal{C}_{min}^{outage}(\bar{P}, \mathbf{R}^*, P^{out}) = Co \left(\bigcup_{\mathbf{w}(\mathbf{n})} \mathcal{C}_{min}(\bar{P}, \mathbf{R}^*(\mathbf{n}, \mathbf{w}(\mathbf{n}))) \right)$$

where the union is over all $\mathbf{w}(\mathbf{n})$ satisfying $\mathbb{E}_{\mathbf{n}}[w_1(\mathbf{n})] \geq (1 - P^{out})$. Notice that the minimum rate vector \mathbf{R}^* must be in the common outage capacity region [42], i.e. $\mathbf{R}^* \in \mathcal{C}_{out}(\bar{P}, P^{out})$,

for the minimum rates to be achievable with common outage and with the given outage probability.

Minimum Rate Outage Capacity for a Single-User Channel

The definition of minimum rate outage capacity given in Definition 5.2 applies to single-user channels as well, but the expression can be simplified significantly in the single-user case. For a single-user channel, the outage function $w(n)$ is only a function of the fading state because there is only one user and the capacity region is one-dimensional. Finding the largest achievable rate subject to the power and outage constraint therefore is equivalent to finding the outage function that corresponds to the largest achievable rate. In [46], the concept of minimum rate capacity with outage was independently proposed and the optimal outage function $w^*(n)$ was found to be:

$$w^*(n) = \begin{cases} 1 & n < s^* \\ 0 & n \geq s^* \end{cases} \quad (5.22)$$

where the threshold s^* is chosen to satisfy $\mathbb{E}_n[w^*(n)] = Pr\{n < s^*\} = 1 - P^{out}$.

The optimal scheme is therefore seen to be a threshold policy: minimum rates must be maintained in all states better (i.e. smaller noise values) than the threshold, while minimum rates need not be maintained in states worse than the threshold. This is very similar to the solution to the minimum outage probability problem under a long-term average power constraint for a single user channel solved in [6]. When maximizing outage capacity, all power available goes towards maintaining a constant rate in non-outage states. In minimum rate outage capacity, however, some fraction of the power maintains the minimum rate in non-outage states. The excess power, however, is water-filled over the fading states with respect to the effective channel to maximize rates achieved in excess of the minimum rates.

Unfortunately, the multi-user broadcast channel does not appear to have such a simple solution for either common outage or independent outage because the relationship between the minimum power allocation, effective noise terms, and the effectiveness of each fading state and user is much more complicated than the single-user case.

5.1.7 Numerical Results

In this section we present numerical results on the capacity of a two user broadcast channel with minimum rate constraints with an average power constraint and no outage. In all plots the total transmitted power is 10 mW, the bandwidth is 100 kHz, and the noise distribution is symmetric. Furthermore, the minimum rates are symmetric in Figs. 5.5-5.8.

In Fig. 5.5 the capacity region of a two-user channel with very different noise levels is plotted. In one fading state, n_1 is 40 dB less than n_2 (i.e. the SNR of user 1 would be

40 dB larger than the SNR of user 2 assuming each user was allocated the same power), and vice versa in the second fading state. Without minimum rates, capacity is achieved by allocating almost all power to the better of the two users in each channel state. This causes the capacity region to be highly convex. When minimum rate constraints are applied, however, power must also be allocated to the weaker user in every fading state to satisfy the minimum rates, leading to a large capacity reduction. It is clear from Fig. 5.5 that the minimum rate capacity region is significantly smaller than the ergodic capacity region, especially for large minimum rates.

The zero-outage capacity region in Fig. 5.5 is significantly smaller than the ergodic capacity region. As expected, the minimum rate capacity region is significantly smaller than the ergodic capacity region. We will see a similar relationship between the zero-outage and minimum rate capacity regions for the other channel models.

The capacity region of a channel where n_1 and n_2 differ by 20 dB in each fading state is plotted in Fig. 5.6. The ergodic capacity region is much less convex than in Fig. 5.5 because the channels of the two users are more similar in each state. This is because the optimal power allocation scheme is not so heavily weighted towards the better user in each state so even the poorer user is allocated significant power in each state. Minimum rate constraints force allocation of additional power to the poorer user in each fading state, but this is not as sub-optimal as it is for the first example. We see in Fig. 5.6 that the minimum rate capacity region is smaller than the ergodic capacity region, but not by as much as in Fig. 5.5.

In the final two plots, results for more realistic channel models are presented. Independent fading is assumed for both receivers and the channel gain is incorporated into the noise power, as described in Chapter 5.1.1. Rician fading with $K = 1$ is modeled in Fig. 5.7. This is not as severe as Rayleigh fading, which has no zero-outage capacity region, but the power of the multipath component is equal to the power of the line-of-sight component. The noise levels take on a wide range of values, as they do in the channel plotted in Fig. 5.5. As expected by our earlier results, minimum rates reduce capacity significantly. Once again we see that the zero-outage capacity region is much smaller than the ergodic capacity region.

In Fig. 5.8, Rician fading with $K = 5$ is modeled. Because the power of the line of sight component is five times as strong as the multipath component, both users generally have strong channels and this channel resembles the channel plotted in Fig. 5.6. As expected, minimum rates do not reduce capacity significantly.

Finally, in Fig. 5.9, the capacity regions of a Rician fading channel with $K = 1$ and asymmetric minimum rates are plotted. In the graph the capacity regions for minimum rates of (100 kbps, 100 kbps), (100 kbps, 50 kbps), and (100 kbps, 0 kbps) are shown. This relates to a scenario where one user has stricter requirements than the other or only one of

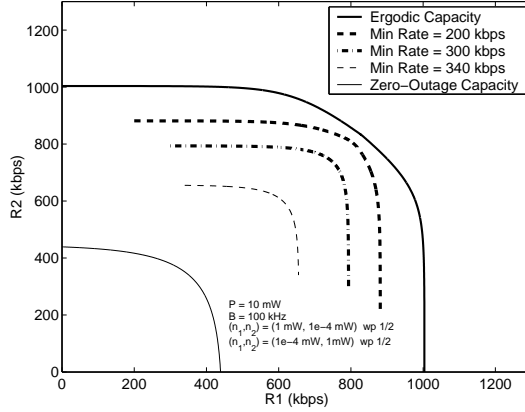


Figure 5.5: Capacity of symmetric channel with 40 dB difference in SNR

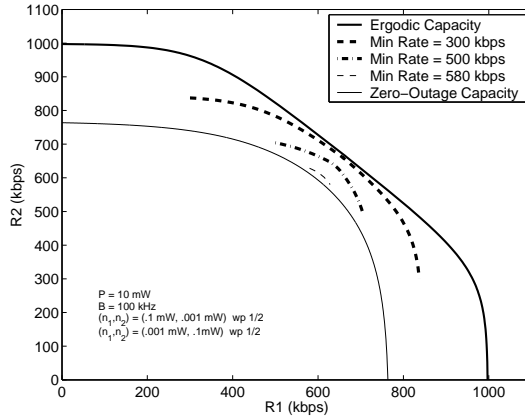


Figure 5.6: Capacity of symmetric channel with 20dB difference in SNR

the two users requires a minimum rate. We see that the capacity region for the asymmetric minimum rate pair is considerably larger than the capacity region for the symmetric rate pair. Notice that reducing the minimum rate of user 2 increases the capacity of both users, not just user 2, because reducing R_2^* frees up power that can be allocated to either user.

From these results it is clear that minimum rates decrease the capacity regions of fading channels in which the noise levels of the users differ significantly in many channel states, i.e. when either of the two users has a significantly larger channel gain than the other user in many channel states. When the channels of the users do not differ significantly, minimum rates do not reduce the capacity region significantly.

5.1.8 Multiple-Access Channel with Minimum Rate Constraints

In this section we derive the minimum rate capacity region of the fading multiple-access channel using the concept of duality. We define the minimum rate capacity region to be the set of achievable average rates, subject to minimum rate constraints $\mathbf{R}^* = (R_1^*, \dots, R_K^*)$

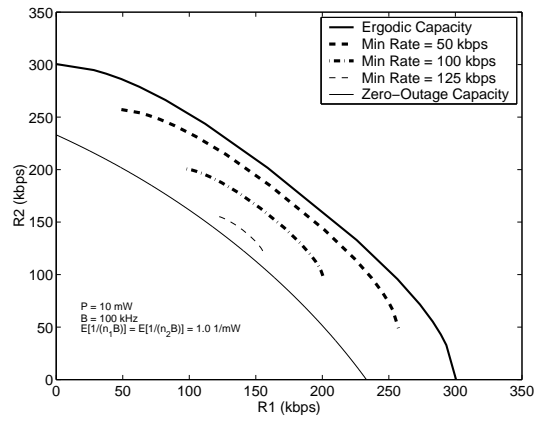


Figure 5.7: Rician fading with $K = 1$, Average SNR = 10 dB

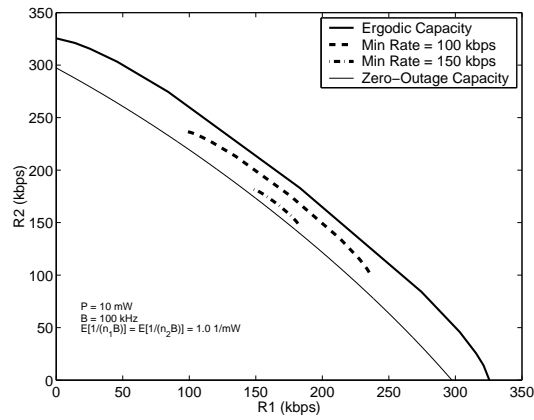


Figure 5.8: Rician fading with $K = 5$, Average SNR = 10 dB

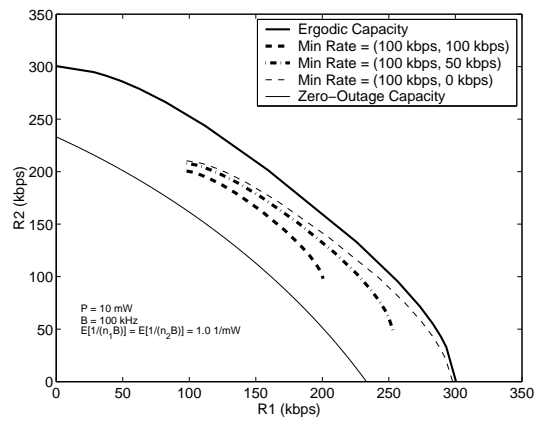


Figure 5.9: Rician fading with $K = 1$, Average SNR = 10 dB, Asymmetric Minimum Rates

in each fading state. From this definition and the characterization of the ergodic capacity region of the fading MAC given in Chapter 2.2.4, it follows that a rate vector \mathbf{R} is in $\mathcal{C}_{MAC}^{min}(\mathbf{P}, \mathbf{R}^*; \mathbf{n})$ if and only if there exists $\mathbf{R}(\mathbf{n})$ such that $\mathbf{R} \leq \mathbb{E}_{\mathbf{n}}[\mathbf{R}(\mathbf{n})]$ with $\mathbf{R}(\mathbf{n}) \in \mathcal{C}_{MAC}(\sum_{i=1}^K \mathbf{P}_i^M(\mathbf{n}); \mathbf{n}) \quad \forall \mathbf{n}$ and $\mathbf{R}(\mathbf{n}) \geq \mathbf{R}^*$ for all \mathbf{n} , for some power policy $\mathbf{P}^M(\mathbf{n})$ satisfying the power constraints. Using the methodology from the proof of Theorem 3.4, it is easy to see that the BC minimum rate capacity region equals the sum power MAC minimum rate capacity region:

$$\mathcal{C}_{BC}^{min}(\bar{\mathbf{P}}, \mathbf{R}^*; \mathbf{n}) = \bigcup_{\{\mathbf{P}: \mathbf{1} \cdot \mathbf{P} = \bar{\mathbf{P}}\}} \mathcal{C}_{MAC}^{min}(\mathbf{P}, \mathbf{R}^*; \mathbf{n}). \quad (5.23)$$

The most interesting application of duality to minimum rate capacity is characterizing the minimum rate capacity region of the MAC via the dual BC. Directly finding the minimum rate capacity of the MAC appears to be quite difficult⁴, but duality allows us to do so directly from the dual BC. A straightforward application of Theorem 3.2 gives:

$$\mathcal{C}_{MAC}^{min}(\mathbf{P}, \mathbf{R}^*; \mathbf{n}) = \bigcap_{\alpha > 0} \mathcal{C}_{BC}^{min}\left(\mathbf{1} \cdot \frac{\mathbf{P}}{\alpha}, \mathbf{R}^*; \alpha \mathbf{n}\right). \quad (5.24)$$

Since every point on the boundary of the MAC minimum rate capacity region is also on the boundary of the scaled BC minimum rate capacity region, we can also find the optimal power policy and decoding order for the MAC. As always in the BC, users are decoded in order of increasing channel gain. In the case of a scaled channel, this corresponds to decoding in order of *increasing* $\frac{h_i}{\lambda_i^*}$. By duality, users in the MAC should be decoded in order of *decreasing* $\frac{h_i}{\lambda_i^*}$. The optimal MAC power allocation policy can be derived from the optimal power policy of the scaled BC.

The MAC minimum rate capacity region for a discrete fading distribution channel is plotted in Figure 5.10. In the figure, the MAC ergodic, zero-outage, and minimum rate capacity region boundaries are all shown. The corresponding dual BC capacity region (ergodic, zero-outage, and minimum rate) boundaries are indicated with dotted lines. The minimum rate capacity region is shown for symmetric minimum rates of 200 Kbps for each user. In the figure, all three MAC capacity regions were calculated using duality, i.e. by taking the intersection of scaled BC capacity regions. However, we show only the unscaled BC capacity regions in the plot for simplicity. Note that the MAC minimum rate capacity region lies between the zero-outage and ergodic capacity regions as it does for the BC minimum rate capacity region [30].

⁴Even given the MAC decoding order (which duality provides), it still does not seem possible to determine the optimal power policy that maximizes the weighted sum rate while satisfying the minimum rate constraints. This is related to the difficulty in finding the zero-outage capacity. The zero-outage capacity region has only been characterized implicitly by minimizing the weighted sum power needed to achieve a rate vector [22].

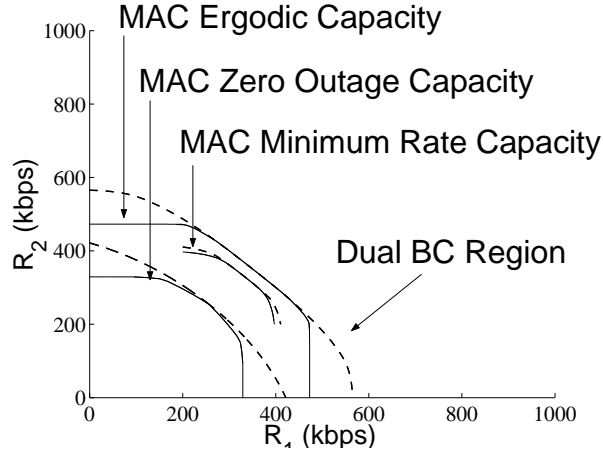


Figure 5.10: MAC Minimum Rate (200 Kbps Min Rate), Ergodic, and Zero-Outage Capacity Regions

5.2 Broadcast Channels with Common Messages

In the previous portion of this chapter, we considered a fading broadcast channel in which the transmitter only wished to send independent information to each of the users. However, as wireless networks evolve, it is becoming apparent that multi-cast (i.e. sending a common message to all users on a downlink channel) is an important mode of communication that systems will require in the future. In cellular networks, for example, multi-cast information could be common information such as news updates or location-based information. It is reasonable to assume that networks will want to transmit a mixture of common information to all users and independent information to each of the users. With this in mind, we consider broadcast channels with both common and independent information.

We consider parallel two-user Gaussian broadcast channels, where the transmitter wants to send independent information to users 1 and 2 at rates R_1 and R_2 , respectively, and a common message (i.e. a message decodable by both users) at rate R_0 . For degraded broadcast channels, the common message rate and the independent information rate to the degraded user are interchangeable, because the strongest user can decode anything that the degraded user can. However, we consider parallel channels where in some channels User 1 is the degraded user, but in other channels User 2 is the degraded user. The capacity region of this channel (for both discrete memoryless channels and for Gaussian channels) was characterized in [18] in terms of a union of regions, where the union was taken over different power distributions between the different channels. We first derive an equivalent expression for this capacity region that is more amenable to optimization techniques. We then pose the problem of characterizing the optimal power and rate allocation schemes that achieve the boundary of the three-dimensional region using Lagrangian techniques. We then apply the utility function approach used for the broadcast channel [63] without

common information, but we find that this approach does not work in general. We use a more direct approach to maximize the Lagrangian function and obtain the capacity region with common messages using this approach. Using this method, the optimal allocation is found by performing a finite maximization in each channel.

Finally, we consider MIMO broadcast channels, which in general are not degraded. Thus, the capacity region with or without common messages is not known for this channel. We propose an achievable region based on dirty paper coding. We also consider the maximum common rate achievable on these channels, i.e. the common message capacity.

The remainder of this section is organized as follows. In Chapter 5.2.1 we describe the system model, followed by the capacity region of the broadcast channel in 5.2.2. In Chapter 5.2.3 we describe the Lagrangian formulation used to find the optimal power allocation, along with a method to maximize the Lagrangian. In Chapter 5.2.5 we describe a simple procedure to find the optimal Lagrangian multipliers, followed by some numerical results in 5.2.6. Finally, we discuss MIMO broadcast channels in Chapter 5.2.7.

5.2.1 System Model

We consider a set of N parallel two user broadcast channels, which can be viewed as a discrete approximation of a fading channel. As in the previous section (Chapter 5.1.1), we incorporate the channel gain into the noise power to get:

$$y_j(i) = x(i) + z_j(i) \quad i = 1, \dots, N \quad (5.25)$$

for $j = 1, 2$ and where $z_1(i) \sim N(0, N_1(i))$ and $z_2(i) \sim N(0, N_2(i))$. If $N_1(i) \leq N_2(i)$ for all i , then this is a *degraded* broadcast channel. For such a channel, the common message and independent message sent to User 2 are interchangeable, and the optimal power allocation is essentially equivalent to that for channels with only independent information [41, 63]. We will only consider the non-degraded case, i.e. where for some i we have $N_1(i) \leq N_2(i)$ and for some other i we have $N_2(i) \leq N_1(i)$. The resultant channel is referred to as a product of reversely degraded, or unmatched, broadcast channels [18]. We impose an average power constraint P on the input, i.e. $\sum_{i=1}^N E[x(i)^2] \leq P$.

5.2.2 Capacity Region Characterization

In [18], the capacity region for two parallel Gaussian broadcast channels (non-degraded) with a common message and independent messages for both users is given. This characterization can be extended to $N > 2$ parallel channels and given in the following simplified form.

Theorem 5.1 *The capacity region $C_{BC}(\bar{P})$ of N parallel two-user broadcast channels is*

equal to the convex hull of all rate triplets (R_0, R_1, R_2) satisfying

$$R_0 \leq \min \left(\sum_{i=1}^N C \left(\frac{P_0(i)}{P_1(i) + P_2(i) + N_1(i)} \right), \sum_{i=1}^N C \left(\frac{P_0(i)}{P_1(i) + P_2(i) + N_2(i)} \right) \right) \quad (5.26)$$

$$R_1 \leq \sum_{i \in A} C \left(\frac{P_1(i)}{N_1(i)} \right) + \sum_{i \in B} C \left(\frac{P_1(i)}{P_2(i) + N_1(i)} \right) \quad (5.27)$$

$$R_2 \leq \sum_{i \in A} C \left(\frac{P_2(i)}{P_1(i) + N_2(i)} \right) + \sum_{i \in B} C \left(\frac{P_2(i)}{N_2(i)} \right) \quad (5.28)$$

for some $P_0(i), P_1(i), P_2(i)$ such that $\sum_{i=1}^N P_0(i) + P_1(i) + P_2(i) \leq \bar{P}$. Here A denotes the set of $i \in 1, \dots, N$ such that $N_1(i) \leq N_2(i)$ and B is the complementary set, i.e. the set of i such that $N_2(i) < N_1(i)$, and $C(x) = \log(1 + x)$.

Proof: See Chapter 5.4.5. \square

The powers $(P_0(i), P_1(i), P_2(i))$ can be interpreted as the power allocated to send the common message, the independent message to user 1, and the independent message to user 2, respectively. The common message is decoded first, with the powers $P_1(i) + P_2(i)$ treated as interference, followed by the independent messages. For $i \in A$, User 1 can decode and subtract out the codeword intended for User 2 before decoding his own codeword. For $i \in B$, User 1 must treat $P_2(i)$ as interference while decoding his independent message. Similarly, User 2 can decode and subtract out the codeword intended for User 1 for $i \in B$, but must treat User 1's codeword as interference for $i \in A$.

For transmission of the independent messages, separate codebooks and rates are used for each user on each of the N channels. These codewords are decoded *independently* on each channel. However, the common message codebook cannot be broken into different codebooks for each channel, i.e. joint encoding and joint decoding must be performed across the channels to achieve capacity. If the common message was broken into different codebooks for each channel, the common rate transmitted on each channel would be limited by the weakest user in *each* channel. The corresponding common rate would be given by $\sum_{i=1}^N C \left(\frac{P_0(i)}{P_1(i) + P_2(i) + \max(N_1(i), N_2(i))} \right)$. This is highly sub-optimal, and much higher common message rates can be achieved by jointly decoding. Each user extracts a different amount of information about the common message from each of the channels due to the different noise powers of the users on each channel, and we consider the total amount of mutual information across all channels.

5.2.3 Formulation of Optimization

From Theorem 5.1, the capacity region can be defined as the convex hull of all rate points satisfying the inequalities in (5.26) - (5.28) for any power allocation satisfying the average

power constraint. Since the capacity region is convex, we can fully characterize it by maximizing the weighted sum of rates. We wish to find the optimal power allocation policy that maximizes the weighted sum of rates for all possible weights. This is given by the following problem;

$$\max_{(R_0, R_1, R_2) \in C_{BC}(\bar{P})} \mu_1 R_1 + \mu_2 R_2 + \mu_0 R_0. \quad (5.29)$$

Using standard convex optimization techniques, for the optimal λ , this is equivalent to:

$$\begin{aligned} \max_{\mathbf{P}(i)} \quad & \mu_1 R_1(\mathbf{P}(i)) + \mu_2 R_2(\mathbf{P}(i)) + \\ & \mu_0 (\min(R_{01}(\mathbf{P}(i)), R_{02}(\mathbf{P}(i)))) - \lambda \left(\sum_{i=1}^N P(i) - \bar{P} \right) \end{aligned} \quad (5.30)$$

where $R_1(\mathbf{P}(i))$ and $R_2(\mathbf{P}(i))$ are defined as:

$$\begin{aligned} R_1(\mathbf{P}(i)) &= \sum_{i=1}^N C \left(\frac{P_1(i)}{N_1(i) + P_2(i) \mathbf{1}[i \in B]} \right) \\ R_2(\mathbf{P}(i)) &= \sum_{i=1}^N C \left(\frac{P_2(i)}{N_2(i) + P_1(i) \mathbf{1}[i \in A]} \right) \end{aligned}$$

and $R_{0j}(\mathbf{P}(i))$ is defined as:

$$R_{0j}(\mathbf{P}(i)) = \sum_{i=1}^N C \left(\frac{P_0(i)}{N_j(i) + P_1(i) + P_2(i)} \right)$$

for $j = 1, 2$, and $P(i) \triangleq P_0(i) + P_1(i) + P_2(i)$. Through a standard convex optimization procedure, the minimum operation can be replaced by a weighted sum of the two common rates. It then follows that the optimal power allocation policy solves

$$\begin{aligned} \max_{\mathbf{P}(i)} \quad & \mu_1 R_1(\mathbf{P}(i)) + \mu_2 R_2(\mathbf{P}(i)) + \lambda_1 R_{01}(\mathbf{P}(i)) + \\ & \lambda_2 R_{02}(\mathbf{P}(i)) - \lambda \left(\sum_{i=1}^N P(i) - \bar{P} \right) \end{aligned} \quad (5.31)$$

for the optimal Lagrangian multipliers $(\lambda, \lambda_1, \lambda_2)$, which each must be non-negative and satisfy $\lambda_1 + \lambda_2 = \mu_0 = (1 - \mu_1 - \mu_2)$. Furthermore, for any λ , the solution to (5.30) is equal to the solution to (5.31) for λ_1 and λ_2 such that the optimizing power allocation yields either $R_{01} = R_{02}$ or $\lambda_i = 0$ for one of the users.

In the next section we describe how to solve (5.31) for any $(\lambda, \lambda_1, \lambda_2)$. In section 5.2.5 we describe a simple method to find the optimal Lagrange multipliers.

5.2.4 Maximization of Lagrangian

In this section we describe a method to solve (5.31), i.e. maximize the weighted sum of rates given the power price λ and the Lagrangian's λ_1 and λ_2 . First note that a power allocation solves (5.31) if and only if it is the solution to

$$\begin{aligned} \max_{P_0(i), P_1(i), P_2(i)} \quad & \mu_1 R_1(P(i)) + \mu_2 R_2(P(i)) + \lambda_1 R_{01}(P(i)) \\ & + \lambda_2 R_{02}(P(i)) - \lambda (P_0(i) + P_1(i) + P_2(i)) \end{aligned} \quad (5.32)$$

for each $i = 1, \dots, N$. When there is no common message (i.e. $\lambda_1 = \lambda_2 = 0$), this can be solved using an intuitive utility function approach [41, 63]. In Chapter 5.2.4 we show that this approach does not work in general when there is a common message, and we must instead use a more direct method.

Utility Function Approach

In this section we attempt to use the utility function approach developed in [63] to determine the optimal power allocation policy given the Lagrangian multipliers, i.e. to solve (5.32). In [63], utility functions were used to find the optimal power allocation for parallel broadcast channels with only independent messages. Without loss of generality, we consider states where $N_1(i) < N_2(i)$. We define the following utility functions:

$$\begin{aligned} u_1(z) &= \frac{\mu_1}{N_1(i) + z} - \lambda \\ u_2(z) &= \frac{\mu_2}{N_2(i) + z} - \lambda \\ u_0(z) &= \frac{\lambda_1}{N_1(i) + z} + \frac{\lambda_2}{N_2(i) + z} - \lambda \end{aligned}$$

If we let J^* denote the solution to (5.32) and J^* is achieved by $(P_0(i), P_1(i), P_2(i))$, then we have

$$\begin{aligned} J^* &= \int_{z=0}^{P_1(i)} u_1(z) dz + \int_{z=P_1(i)}^{P_1(i)+P_2(i)} u_2(z) dz + \int_{z=P_1(i)+P_2(i)}^{P_0(i)+P_1(i)+P_2(i)} u_0(z) dz \\ &\leq \int_{z=0}^{\infty} \left[\max_i u_i(z) \right]^+ dz \end{aligned}$$

where the argument of the final integral is a pointwise maximum of the utility functions. This upper bound is achievable if the maximum of the utility functions is in order of decreasing channel gains (i.e. $u_1(z)$ is the maximum function initially, followed by $u_2(z)$ and then $u_0(z)$). When there is no common message, then this condition is satisfied and the upper bound is achievable [63]. Thus, the optimum power allocation can be found by taking the pointwise maximum of the utility functions corresponding to both users. However, for

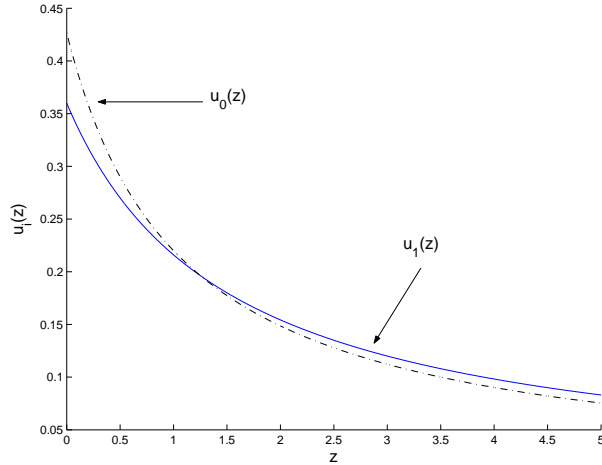


Figure 5.11: Utility Functions for a sample channel with $\mu_2 = 0$

common messages, the ordering of the utility functions does not always satisfy this condition and thus the utility function approach can not be used in general. There are a number of interesting scenarios where the utility function approach does work:

1. $\mu_0 < \mu_1$ and $\mu_0 < \mu_2$: If this condition is satisfied, then $u_0(z) \leq u_j(z)$ for all $z \geq 0$, where User j is the user with the smaller noise power. Thus, no common message is transmitted in each state and the utility function $u_0(z)$ can be ignored. The situation then simplifies to the standard independent messages BC, for which the utility function approach works.
2. $\mu_0 \geq \mu_1$ and $\mu_0 \geq \mu_2$: In this scenario, $u_0(z) \geq u_j(z)$ for all $z \geq 0$, where User j is the user with the larger noise power. Thus we are left with the common rate user and the better of two users. In this scenario it can be shown that the utility functions are ordered correctly such that the upper bound is achievable. This includes the interesting case when $\mu_0 \geq \mu_1 = \mu_2$.

Interestingly, the utility function approach does not in general work when either $\mu_1 = 0$ or $\mu_2 = 0$. In Fig. 5.2.4, utility functions are shown for a channel where $N_1 = 1.5$, $N_2 = 1$, $\mu_1 = .54$, $\lambda_1 = .1$, and $\lambda_2 = .36$. For $0 \leq z \leq 1.25$, $u_0(z)$ is the largest utility function, but for $z > 1.25$, $u_1(z)$ is the largest function. Therefore, the upper bound J^* can not be achieved, because User 0 must be allocated power after (i.e. for larger z) User 1 is allocated power. It is also possible to find counter examples for situations where all three priorities are non-zero.

Direct Approach

Since the utility function approach does not work in general, we must consider a more direct approach to maximize the Lagrangian function. The most straightforward way of maximizing a continuous function is to consider the points where the derivatives of the function are zero. The only complication is that the powers $P_0(i)$, $P_1(i)$, and $P_2(i)$ must all be non-negative. Thus, for $j = 1, 2, 3$, the derivative of the objective function with respect to $P_j(i)$ must be equal to 0 if the optimal $P_j(i)$ is strictly positive. Additionally, if $P_j^*(i) = 0$ for some j , then the derivative with respect to $P_j(i)$ at $P_j(i) = 0$ must be less than or equal to zero. The simple structure of the objective function implies that each partial derivative is equal to zero at only one point. Thus, it is sufficient to consider the 8 different combinations of power allocations. The maximum of the objective function is then equal to the maximum of these 8 possible combinations.

Without loss of generality, consider a state where $N_1(i) \leq N_2(i)$. The partial derivatives of (5.32) are given by:

$$\begin{aligned} \frac{\partial J}{\partial P_1} &= \frac{\mu_1}{P_1 + N_1} + \frac{\mu_2}{P_1 + P_2 + N_2} - \frac{\mu_2}{P_1 + N_2} + \frac{\lambda_1}{P_0 + P_1 + P_2 + N_1} \\ &\quad - \frac{\lambda_1}{P_1 + P_2 + N_1} + \frac{\lambda_2}{P_0 + P_1 + P_2 + N_2} - \frac{\lambda_2}{P_1 + P_2 + N_2} - \lambda \\ \frac{\partial J}{\partial P_2} &= \frac{\mu_2}{P_1 + P_2 + N_2} + \frac{\lambda_1}{P_0 + P_1 + P_2 + N_1} - \frac{\lambda_1}{P_1 + P_2 + N_1} + \\ &\quad \frac{\lambda_2}{P_0 + P_1 + P_2 + N_2} - \frac{\lambda_2}{P_1 + P_2 + N_2} - \lambda \\ \frac{\partial J}{\partial P_0} &= \frac{\lambda_1}{P_0 + P_1 + P_2 + N_1} + \frac{\lambda_2}{P_0 + P_1 + P_2 + N_2} - \lambda. \end{aligned}$$

Since there are three different powers to be allocated, there are three different sets of partial derivatives to consider. First consider the four cases corresponding to $P_0 = 0$. By setting some of these derivatives to zero (i.e. the partials corresponding to users with non-zero power), we find the optimal allocations are given by the following when $P_0 = 0$:

1. $P_1 = P_2 = 0$
2. $P_1 > 0, P_2 = 0$: $P_1 = \frac{\mu_1}{\lambda} - N_1$
3. $P_2 > 0, P_1 = 0$: $P_2 = \frac{\mu_2}{\lambda} - N_2$
4. $P_1 > 0, P_2 > 0$: $P_1 = \frac{\mu_1 N_2 - \mu_2 N_1}{\mu_2 - \mu_1}$, $P_2 = \frac{\mu_2}{\lambda} - N_2 - P_1$.

When $P_0 > 0$ the power allocations are given by:

1. $P_0 > 0, P_1 = P_2 = 0$: $P_0 = P_{thresh}$
2. $P_0, P_1 > 0, P_2 = 0$: $P_1 = \frac{\lambda_2 N_1 - (\mu_1 - \lambda_1) N_2}{\mu_1 - \mu_0}$, $P_0 = P_{thresh} - P_1$

3. $P_0, P_2 > 0, P_1 = 0$: $P_2 = \frac{\lambda_1 N_2 - (\mu_2 - \lambda_2) N_1}{\mu_2 - \mu_0}$, $P_0 = P_{thresh} - P_2$
4. $P_0, P_1, P_2 > 0$: $P_1 = \frac{\mu_1 N_2 - \mu_2 N_1}{\mu_2 - \mu_1}$, $P_2 = \frac{\lambda_1 N_2 - (\mu_2 - \lambda_2) N_1}{\mu_2 - \mu_0} - P_1$, $P_0 = P_{thresh} - P_1 - P_2$

where

$$P_{thresh} = \frac{1}{2\lambda} (\mu_0 - \lambda(N_1 + N_2) + \sqrt{(\lambda(N_1 + N_2) - \mu_0)^2 + 4\lambda(\lambda_1 N_2 + \lambda_2 N_1 - \lambda N_1 N_2)}).$$

One of these 8 power allocations is guaranteed to achieve the maximum of (5.32). Thus we can find the maximum of the Lagrangian in each state by evaluating all eight power allocations, checking for non-negativity of powers, and then choosing the allocation that maximizes the objective.

When there is only independent information, it can be shown that only one of the four cases is feasible for different values of λ , i.e. the space $\lambda > 0$ can be decomposed into four mutually exclusive intervals corresponding to the four different allocations. Thus, a closed form solution for the optimal power allocation can be given in terms of λ . However, no such simplification can be done for the situation when there is a common message. Thus, in general, the maximum amongst the eight allocations must be taken.

5.2.5 Optimal Lagrange Multipliers

By the KKT conditions, the solution to the original Lagrangian characterization in (5.30) for the optimal $(\lambda, \lambda_1, \lambda_2)$ will satisfy the power constraint with equality. It is easy to see that the power allocation solving (5.30) is a decreasing function of λ . Thus, the optimal λ can be found by solving (5.30) for different values of λ determined by the bisection method (over λ).

To maximize the Lagrangian function in (5.30), we work with the simplified maximization in (5.31), where the minimum is replaced with a weighted sum of the common message rates. It can be shown that for any λ , the solution to (5.30) is equal to the solution of (5.31) for λ_1 and λ_2 such that the optimizing power allocation yields $R_{01} = R_{02}$ or $\lambda_i = 0$ for one of the two users. This follows intuitively because for any power allocation that yields $R_{01} \neq R_{02}$, we can reallocate $P_0(i)$ over different channels without increasing the sum of power to increase the smaller of the two common rates slightly, and thus increase the objective function. However, this is not possible if the allocation of power $P_0(i)$ is already single-user optimal for the user with the smaller common rate (i.e. no reallocation of $P_0(i)$ increases the common rate of the user with the smaller common rate). This corresponds to the scenario where either $\lambda_1 = 0$ or $\lambda_2 = 0$ ⁵. Furthermore, it can also be shown that the optimizing R_{01} in (5.30) is an increasing function of λ_1 and the optimizing R_{02} is a decreasing function of λ_2 .

⁵In general, the minimum of two concave functions occurs at a point where the two functions meet, unless the minimum of the two functions is equal to the maximum of one of the functions.

Thus, the following procedure can be used to find the optimal Lagrange multipliers $(\lambda, \lambda_1, \lambda_2)$. First choose an initial positive value for λ . Then repeat the following algorithm:

1. Solve (5.30) by the following procedure:
 - (a) Solve (5.31) with $(\lambda_1 = 0, \lambda_2 = \mu_0)$. If $R_{01} \geq R_{02}$ for the optimizing solution, proceed to Step 2.
 - (b) Solve (5.31) with $(\lambda_1 = \mu_0, \lambda_2 = 0)$. If $R_{02} \geq R_{01}$ for the optimizing solution, proceed to Step 2.
 - (c) Use the bisection method to find λ_1 such that the optimizing solution of (5.31) satisfies $R_{01} = R_{02}$.
2. If the solution of (5.30) exactly meets the power constraint, then exit. Otherwise, if the solution of (5.30) is strictly larger/smaller than the power constraint, then increase/decrease λ and return to Step 1.

Note that the update of λ can be performed using a one-dimensional bisection method, and Step 1(c) can be performed with a one-dimensional bisection method on λ_1 . This procedure is implemented in order to find numerical results in the next section.

5.2.6 Numerical Results

In this section we present numerical results on the capacity region of a two-user broadcast channel. In Fig. 5.12 the capacity region of a two user channel is shown for $N = 2$. In state 1, user 1 has an average SNR of 10 dB and user 2 has an SNR of -10 dB. In state 2, the SNR's of the users are reversed from state 1. Notice that due to the large difference in SNR of the two users, the capacity region when $R_0 = 0$ (i.e. no common message) is far from the straight line segment connecting the maximum single-user rate to users 1 and 2. However, if $R_2 = 0$ (or $R_1 = 0$ by symmetry), the region is quite close to time-sharing between transmitting only a common message and transmitting only independent information to User 1. In Fig. 5.13 the capacity region of a two-user channel is shown where in state 1, user 1 has an SNR of 0 dB while user 2 has an SNR of -10 dB. In state 2, the roles of the users are reversed. We again see that the capacity region is relatively flat in the direction of the common message (R_0), which implies that time-sharing between sending common messages and independent information comes quite close to the actual capacity-achieving strategy.

5.2.7 MIMO Channels

In this section we consider multiple-input, multiple-output (MIMO) broadcast channels. Since MIMO broadcast channels are not in general degraded, the capacity region with

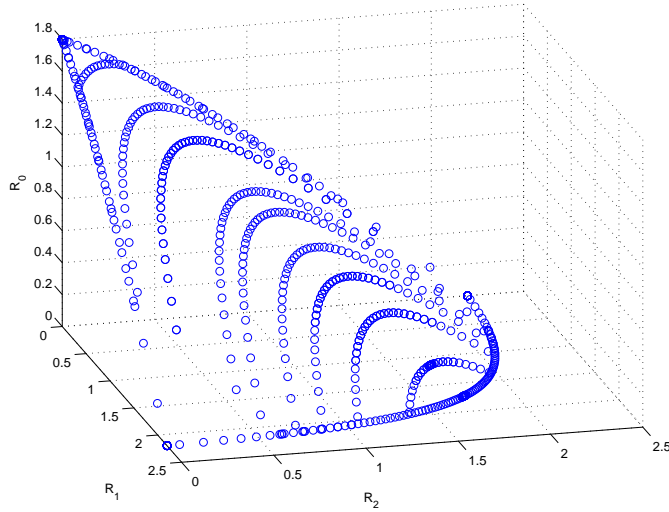


Figure 5.12: Plot of capacity region channel with 20 dB SNR difference between the two users

common and independent messages is unknown even for a single constant channel (i.e. $N = 1$). In the following sections we discuss an achievable region, followed by discussion of transmitting only common messages over a multiple-input, single-output channel.

Achievable Region

An achievable region for the common and independent messages MIMO broadcast channel can be established using dirty paper coding [8]. Dirty paper coding was shown to achieve the sum rate capacity of the MIMO broadcast channel (i.e. the maximum of $R_0 + R_1 + R_2$ in the capacity region) in [5, 69, 73, 82].

By first encoding the common message followed by the independent messages, the following rate triplet is achievable:

$$R_0 = \min_{j=1,2} \log \frac{|\mathbf{I} + \mathbf{H}_j(\Sigma_0 + \Sigma_1 + \Sigma_2)\mathbf{H}_j^T|}{|\mathbf{I} + \mathbf{H}_j(\Sigma_1 + \Sigma_2)\mathbf{H}_j^T|} \quad (5.33)$$

$$R_1 = \log \frac{|\mathbf{I} + \mathbf{H}_1(\Sigma_1 + \Sigma_2)\mathbf{H}_1^T|}{|\mathbf{I} + \mathbf{H}_1\Sigma_2\mathbf{H}_1^T|} \quad (5.34)$$

$$R_2 = \log |\mathbf{I} + \mathbf{H}_2\Sigma_2\mathbf{H}_2^T| \quad (5.35)$$

for any set of positive semi-definite covariances satisfying $Tr(\Sigma_0 + \Sigma_1 + \Sigma_2) \leq P$. Additionally, the ordering of users 1 and 2 can be switched so that user 1 sees no interference and user 2 views Σ_1 as interference. Notice the similarity between this region and the dirty paper coding region for the MIMO broadcast channel with only independent messages given in Chapter 2.2.5. As in the independent information scenario, the rate equations are

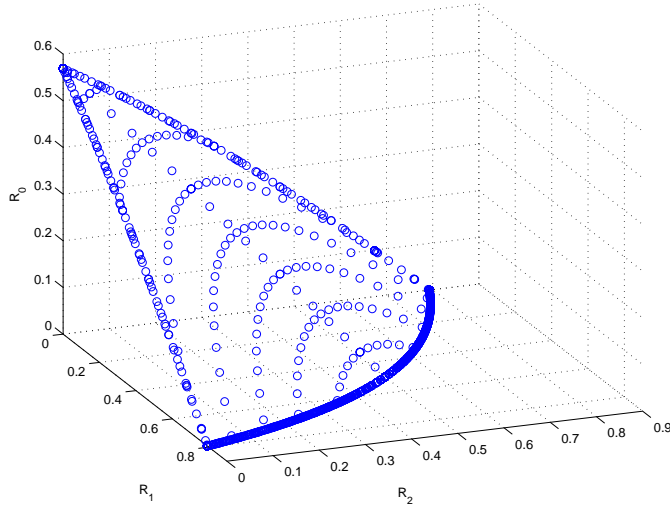


Figure 5.13: Plot of capacity region channel with 10 dB SNR difference between the two users

not concave functions of the input covariances, and thus finding the boundary region of this achievable region (even for $N = 1$) seems to be difficult from a numerical perspective. Furthermore, no apparent duality seems to hold when common messages are added to the broadcast channel. An intuitive dual of the broadcast channel with common messages is the multiple-access channel with correlated sources [12]. However, the common message requirement actually reduces the achievable rates in the broadcast channel, while correlation actually increases the capacity of the multiple-access channel.

Common Message Capacity

Though the above achievable region appears to be difficult to compute, it is far easier to calculate the common message capacity (i.e. the maximum common rate) of a MIMO broadcast channel. Since Gaussian inputs are optimal for MIMO channels, the common rate capacity of a K -use broadcast channel is given by:

$$\mathcal{C}_0 = \max_{p(x): E[|x|^2] \leq P} \min_{i=1, \dots, K} I(X; Y_i) = \max_{\mathbf{\Sigma} \geq 0, \text{Tr}(\mathbf{\Sigma}) \leq P} \min_{i=1, \dots, K} \log |\mathbf{I} + \mathbf{H}_i \mathbf{\Sigma} \mathbf{H}_i^T|. \quad (5.36)$$

The objective function of this maximization is a minimum of concave functions, and thus is a concave function. Therefore, standard convex optimization techniques can be applied to perform the maximization.

For the case of multiple-input, single-output channels (i.e. single antennas at each of the receivers), it can be shown that a rank-one covariance matrix (i.e. beamforming) achieves the common message capacity when there are two users. Interestingly, beamforming does not in general achieve the common message capacity for more than two users. Consider a

system of K unit norm users, each equally spaced around the unit circle. For any $\epsilon > 0$, we can find large enough K such that for any choice of a direction vector \mathbf{v} , $\min_{i=1,\dots,K} |\mathbf{H}_i \mathbf{v}| < \epsilon$, since any direction is nearly orthogonal to at least one user because users are equally spaced around the unit circle. The common rate when using covariance $\Sigma = \frac{P}{M} \mathbf{v} \mathbf{v}^T$ is equal to $\min_{i=1,\dots,K} \log(1 + \frac{P}{M} \mathbf{H}_i \mathbf{v} \mathbf{v}^T \mathbf{H}_i^T)$. Thus, using beamforming, the common rate goes to 0 as $K \rightarrow \infty$. However, by using an identity covariance, i.e. $\Sigma = \frac{1}{M} \mathbf{I}_M$, the mutual information of *each* user is $\log(1 + \frac{1}{M} \|\mathbf{H}_i\|^2) = \log(1 + \frac{1}{M})$ which is independent of K . Thus, the common message capacity is not achieved by beamforming for large enough K .

5.3 Summary

In this chapter we analyzed time-varying broadcast channels and derived the optimal adaptive transmission policy for two different settings. We first considered a flat-fading broadcast channel in which we wished to maximize long-term average rates subject to a lower bound on the instantaneous rate of each user in every fading state. We termed this the minimum rate capacity, and found that the optimal power allocation scheme can be characterized in terms of the optimal power policy achieving the ergodic capacity (i.e. long-term average rates only) of a related effective channel. Furthermore, we were able to exploit the duality relationship established in Chapter 3 to find the minimum rate capacity region of the fading multiple-access channel using our characterization of the minimum rate capacity region of the dual broadcast channel.

In addition to minimum rate capacity, we considered parallel broadcast channels in which there are both independent and common messages. In the two-user scenario, this corresponds to independent messages for each of the two users, and a common message that must be decodable by both users. We found that the addition of common messages significantly changes the structure of the optimal power allocation policy. Most importantly, the intuitive water-filling and utility function interpretations that applied to the broadcast channel with independent messages do not apply when common messages are included. We also briefly considered MIMO broadcast channels with common information and proposed an achievable region for such channels based on dirty paper coding. In general, it seems that the broadcast channel with common and independent messages has been largely ignored and seems ripe for further research activity.

5.4 Appendix

5.4.1 Proof of Excess and Effective Power Relationship

In this section we prove the following result:

$$\sum_{j < i} P_{\pi(j)}^e = e^{\sum_{j \geq i} R_{\pi(j)}^*} \sum_{j < i} \hat{P}_{\pi(j)} \quad (5.37)$$

for $i = 2, \dots, K + 1$ by induction. First notice that for $i = 2$, we have $P_{\pi(1)}^e = \hat{P}_{\pi(1)} e^{\sum_{i=2}^K R_i^*}$ by the definition of $P_{\pi(i)}^e$ in (5.14). Assume (5.37) holds for i . We will show it holds for $i + 1$ as well. Using the inductive hypothesis to get the second line, we have:

$$\begin{aligned} \sum_{j \leq i} P_{\pi(j)}^e &= P_{\pi(i)}^e + \sum_{j < i} P_{\pi(j)}^e \\ &= e^{\sum_{j > i} R_{\pi(j)}^*} \left(\hat{P}_{\pi(i)}(\mathbf{n}) - \left(e^{R_{\pi(i)}^*} - 1 \right) \sum_{j < i} \hat{P}_{\pi(j)}(\mathbf{n}) \right) + e^{\sum_{j \geq i} R_{\pi(j)}^*} \sum_{j < i} \hat{P}_{\pi(j)} \\ &= e^{\sum_{j > i} R_{\pi(j)}^*} \left(\hat{P}_{\pi(i)}(\mathbf{n}) - \left(e^{R_{\pi(i)}^*} - 1 \right) \sum_{j < i} \hat{P}_{\pi(j)}(\mathbf{n}) + e^{R_{\pi(i)}^*} \sum_{j < i} \hat{P}_{\pi(j)} \right) \\ &= e^{\sum_{j > i} R_{\pi(j)}^*} \sum_{j \leq i} \hat{P}_{\pi(j)} \\ &= e^{\sum_{j \geq i+1} R_{\pi(j)}^*} \sum_{j < i+1} \hat{P}_{\pi(j)} \end{aligned}$$

Notice that for $i = K + 1$, this implies $\sum_{j=1}^K P_{\pi(j)}^e = \sum_{j=1}^K \hat{P}_{\pi(j)}$, or that the sum of effective powers equals the sum of excess powers.

5.4.2 Proof that Excess to Effective Power Transformation is One-to-One

In this section we show that every set of non-negative *effective* powers $(P_1^e(\mathbf{n}), \dots, P_K^e(\mathbf{n}))$ corresponds uniquely to a valid (i.e. powers that meet or exceed all minimum rate constraints) set of excess powers $(\hat{P}_1(\mathbf{n}), \dots, \hat{P}_K(\mathbf{n}))$, and vice versa. This property is required so that the maximization over non-negative effective powers in (5.16) is equivalent to the original maximization over excess powers in (5.12).

First, by the definition of effective power given in (5.14) it is easy to see that any set of excess powers $(\hat{P}_1(\mathbf{n}), \dots, \hat{P}_K(\mathbf{n}))$ that meet the constraints of (5.12) map to non-negative effective powers. Note also that the transformation preserves sum power in each fading state, and thus preserves average power as well.

To show equivalence in the other direction, first note that the effective power transformation in (5.14) can be written in matrix form as $\mathbf{P}^e(n) = \mathbf{A}\hat{\mathbf{P}}(n)$ where \mathbf{A} is a $K \times K$ matrix with $\mathbf{A}(i, i) = e^{\sum_{j > i} R_{\pi(j)}^*} > 0$ and $\mathbf{A}(i, j) = -e^{\sum_{j > i} R_{\pi(j)}^*} (e^{R_{\pi(i)}^*} - 1) \leq 0$ for all

$j < i$. Thus \mathbf{A} is lower-triangular with strictly positive diagonal entries (which ensures invertibility) and negative entries below the diagonal. It is straightforward to show that the inverse of such a matrix is lower-triangular with all non-negative entries. Thus, by using \mathbf{A}^{-1} , we can map uniquely from non-negative effective powers to non-negative excess powers. Furthermore, since the powers satisfy (5.14) by definition, for all i and \mathbf{n} we have

$$\begin{aligned} \hat{P}_{\pi(i)}(\mathbf{n}) - (e^{R_{\pi(i)}^*} - 1) \sum_{j < i} \hat{P}_{\pi(j)}(\mathbf{n}) &= \frac{P_{\pi(i)}^e(\mathbf{n})}{e^{\sum_{j > i} R_{\pi(j)}^*}} \\ &\geq 0 \end{aligned}$$

since $\mathbf{P}^e(\mathbf{n}) \geq 0$ by assumption. Also, as noted earlier, the sum of the effective powers equals the sum of the excess powers in each fading state. Thus, the excess powers corresponding to any non-negative set of effective powers satisfy all constraints in the original rate maximization in (5.12).

5.4.3 Proof that Noise to Effective Noise Transformation is One-to-One

Here we show that the transformation from noise state \mathbf{n} to effective noise state \mathbf{n}^e is a one-to-one transformation by showing that the map from \mathbf{n} to \mathbf{n}^e is an invertible linear transformation from \mathfrak{R}^K to \mathfrak{R}^K . The effective noise is defined in (5.13) as:

$$n_{\pi(i)}^e \triangleq \left(n_{\pi(i)} + \sum_{j \leq i} P_{\pi(j)}^*(\mathbf{n}) \right) e^{\sum_{j > i} R_{\pi(j)}^*}$$

One can inductively show that

$$\sum_{j \leq i} P_{\pi(j)}^*(\mathbf{n}) = \sum_{k=1}^i n_{\pi(k)} (e^{R_{\pi(k)}^*} - 1) e^{\sum_{l=k+1}^i R_{\pi(l)}^*}. \quad (5.38)$$

Substituting this expression into the definition of effective noise, we get:

$$n_{\pi(i)}^e = n_{\pi(i)} e^{\sum_{j \geq i} R_{\pi(j)}^*} + \sum_{k=1}^{i-1} n_{\pi(k)} (e^{R_{\pi(k)}^*} - 1) e^{\sum_{j > k} R_{\pi(j)}^*}. \quad (5.39)$$

In matrix terms, we can write the effective noise as $\mathbf{n}^e = \mathbf{B}\mathbf{n}$ where \mathbf{B} is a lower-triangular $K \times K$ matrix defined by the coefficients given in (5.39). Notice that $\mathbf{B}(i, i) = e^{\sum_{j \geq i} R_{\pi(j)}^*} > 0$, which implies that the matrix \mathbf{B} is invertible and thus the transformation is one-to-one.

5.4.4 Proof of Effective Noise Ordering Equivalence

In this section we prove that the effective noise terms n_1^e, \dots, n_K^e have the same ordering as the original noises n_1, \dots, n_K . Since $n_{\pi(1)} \leq n_{\pi(2)} \leq \dots \leq n_{\pi(K)}$ by the definition of $\pi(\cdot)$,

we wish to show that $n_{\pi(1)}^e \leq n_{\pi(2)}^e \leq \dots \leq n_{\pi(K)}^e$, or that $n_{\pi(i)}^e \leq n_{\pi(i+1)}^e$. We can expand $n_{\pi(i+1)}^e$ as

$$\begin{aligned}
n_{\pi(i+1)}^e &= \left(\sum_{j \leq i+1} P_{\pi(j)}^* + n_{\pi(i+1)} \right) e^{\sum_{j > i+1} R_{\pi(j)}^*} \\
&= \left(\sum_{j \leq i} P_{\pi(j)}^* + n_{\pi(i+1)} + P_{\pi(i+1)}^* \right) e^{\sum_{j > i+1} R_{\pi(j)}^*} \\
&= \left(\sum_{j \leq i} P_{\pi(j)}^* + n_{\pi(i+1)} \right) e^{R_{\pi(i+1)}^*} e^{\sum_{j > i+1} R_{\pi(j)}^*} \\
&= \left(\sum_{j \leq i} P_{\pi(j)}^* + n_{\pi(i+1)} \right) e^{\sum_{j > i} R_{\pi(j)}^*} \\
&= n_{\pi(i)}^e + (n_{\pi(i+1)} - n_{\pi(i)}) e^{\sum_{j > i} R_{\pi(j)}^*}.
\end{aligned}$$

Since $n_{\pi(i+1)} \geq n_{\pi(i)}$ by our choice of $\pi(\cdot)$, we have $n_{\pi(i+1)}^e \geq n_{\pi(i)}^e$.

5.4.5 Proof of Theorem 5.1

In this section we prove that the capacity region of N parallel Gaussian broadcast channels is given by the expression in Theorem 5.1. First note that the capacity region of N parallel Gaussian broadcast channels is equal to all rate triples (R_0, R_1, R_2) that satisfy the following

set of inequalities:

$$R_0 \leq \sum_{i=1}^N C \left(\frac{\bar{\alpha}_i P(i)}{N_1(i) + \alpha_i P(i)} \right) \quad (5.40)$$

$$R_0 \leq \sum_{i=1}^N C \left(\frac{\bar{\alpha}_i P(i)}{N_2(i) + \alpha_i P(i)} \right) \quad (5.41)$$

$$R_0 + R_1 \leq \sum_{i \in A} C \left(\frac{P(i)}{N_1(i)} \right) + \sum_{i \in B} C \left(\frac{\bar{\alpha}_i P(i)}{N_1(i) + \alpha_i P(i)} \right) \quad (5.42)$$

$$R_0 + R_2 \leq \sum_{i \in B} C \left(\frac{P(i)}{N_2(i)} \right) + \sum_{i \in A} C \left(\frac{\bar{\alpha}_i P(i)}{N_2(i) + \alpha_i P(i)} \right) \quad (5.43)$$

$$\begin{aligned} R_0 + R_1 + R_2 &\leq \sum_{i \in A} C \left(\frac{P(i)}{N_1(i)} \right) + \sum_{i \in B} \left(C \left(\frac{\bar{\alpha}_i P(i)}{N_1(i) + \alpha_i P(i)} \right) \right. \\ &\quad \left. + C \left(\frac{\alpha_i P(i)}{N_2(i)} \right) \right) \end{aligned} \quad (5.44)$$

$$\begin{aligned} R_0 + R_1 + R_2 &\leq \sum_{i \in B} C \left(\frac{P(i)}{N_2(i)} \right) + \sum_{i \in A} \left(C \left(\frac{\bar{\alpha}_i P(i)}{N_2(i) + \alpha_i P(i)} \right) \right. \\ &\quad \left. + C \left(\frac{\alpha_i P(i)}{N_1(i)} \right) \right) \end{aligned} \quad (5.45)$$

for some choice of $\alpha_i \in [0, 1]$ and $P(i) \geq 0$ such that $\sum_{i=1}^N P(i) = P$.

Note that this is a generalization of Theorem 2 in [18] to $N > 2$ parallel channels. Achievability follows from the argument in [18]. The converse mirrors the converse for the $N = 2$ case given in [18] except for the addition of one extra step when using the entropy power inequality (EPI). Without loss of generality, assume $N_1(i) \leq N_2(i)$ for $1 \leq i \leq L < N$, and $N_2(i) < N_1(i)$ for $L+1 \leq i \leq N$. Note that we use $Y = Y_1, \dots, Y_N$ and $Z = Z_1, \dots, Z_N$. Furthermore, we let $A = \{1, \dots, L\}$ and $B = \{L+1, \dots, N\}$, and thus $Y_A = Y_1, \dots, Y_L$, $Y_B = Y_{L+1}, \dots, Y_N$, $Z_A = Z_1, \dots, Z_L$, and $Z_B = Z_{L+1}, \dots, Z_N$. Furthermore, all quantities of the form Y_i or Z_i are in fact n -vectors, where n is the block-length. With this notation, the converse is nearly identical to the converse in [18] if $Y_A, Y_B, Z_A, Z_B, X_A, X_B$ are substituted for $Y_1, Y_2, Z_1, Z_2, X_1, X_2$. The only difference is in the use of the EPI going from (5.53) to (5.58).

First, by Fano's inequality we have:

$$H(W_0, W_1|Y) \leq P_e n(R_0 + R_1) + 1 \triangleq n\epsilon_{1n} \quad (5.46)$$

$$H(W_0, W_2|Z) \leq P_e n(R_0 + R_2) + 1 \triangleq n\epsilon_{2n}. \quad (5.47)$$

Then

$$\begin{aligned}
nR_0 &= H(W_0) = I(W_0; Y) + H(W_0|Y) \leq I(W_0; Y) + n\epsilon_{1n} \\
&= I(W_0; Y_B) + I(W_0; Y_A|Y_B) + n\epsilon_{1n} \\
&\leq I(W_0, W_1, Z_A; Y_B) + H(Y_A|Y_B) - H(Y_A|Y_B, W_0) + n\epsilon_{1n} \\
&\leq I(W_0, W_1, Z_A; Y_B) + H(Y_A) - H(Y_A|Y_B, W_0, W_2) + n\epsilon_{1n} \\
&= I(W_0, W_1, Z_A; Y_B) + I(W_0, W_2, Y_B; Y_A) + n\epsilon_{1n} \\
&= H(Y_B) - H(Y_B|W_0, W_1, Z_A) + H(Y_A)H(Y_A|W_0, W_2, Y_B) + n\epsilon_{1n} \quad (5.48)
\end{aligned}$$

Due to the entropy-maximizing property of Gaussian random variables, we have

$$H(Y_A) \leq \sum_{i \in A} H(Y_i) \leq \frac{n}{2} \sum_{i \in A} \log 2\pi e(N_1(i) + P(i)) \quad (5.49)$$

$$H(Y_B) \leq \sum_{i \in B} H(Y_i) \leq \frac{n}{2} \sum_{i \in B} \log 2\pi e(N_1(i) + P(i)) \quad (5.50)$$

$$H(Z_A) \leq \sum_{i \in A} H(Z_i) \leq \frac{n}{2} \sum_{i \in A} \log 2\pi e(N_2(i) + P(i)) \quad (5.51)$$

$$H(Z_B) \leq \sum_{i \in B} H(Z_i) \leq \frac{n}{2} \sum_{i \in B} \log 2\pi e(N_2(i) + P(i)) \quad (5.52)$$

where $\sum_{i=1}^N P(i) \leq P$ due to the power constraint.

Now, it is easy to see that there exist $\alpha_1, \dots, \alpha_N \in [0, 1]$ such that:

$$\exp((2/n)H(Z_j|W_0, W_1, Z_A, Z_{L+1}, \dots, Z_{j-1})) = 2\pi e(N_2(j) + \alpha_j P_j) \quad (5.53)$$

for $j = L + 1, \dots, N$, and

$$\exp((2/n)H(Y_i|W_0, W_2, Y_B, Y_1, \dots, Y_{i-1})) = 2\pi e(N_1(i) + \alpha_i P(i)) \quad (5.54)$$

for $i = 1, \dots, N$. Notice the extra conditioning on $(Z_{L+1}, \dots, Z_{j-1})$ and on (Y_1, \dots, Y_{i-1}) is not present in Equations 44-45 of [18].

We now have

$$\begin{aligned}
H(Z_B|W_0, W_1, Z_A) &= \sum_{j=L+1}^N H(Z_j|W_0, W_1, Z_A, Z_{L+1}, \dots, Z_{j-1}) \\
&= \frac{n}{2} \sum_{j=L+1}^N \log 2\pi e(N_2(j) + \alpha_j P_j)
\end{aligned} \tag{5.55}$$

$$\begin{aligned}
H(Y_A|W_0, W_2, Y_B) &= \sum_{i=1}^L H(Y_i|W_0, W_2, Y_B, Y_1, \dots, Y_{i-1}) \\
&= \frac{n}{2} \sum_{i=1}^L \log 2\pi e(N_1(i) + \alpha_i P(i))
\end{aligned} \tag{5.56}$$

Using the conditional form of the entropy power inequality, we get:

$$\begin{aligned}
\exp((2/n)H(Y_j|W_0, W_1, Z_A, Z_{L+1}, \dots, Z_{j-1})) &\geq \exp((2/n) \cdot \\
&\quad H(Z_j|W_0, W_1, Z_A, Z_{L+1}, \dots, Z_{j-1})) \\
&\quad + 2\pi e(N_1(j) - N_2(j)) \\
&= 2\pi e(\alpha_j P_j + N_1(j)) \\
\exp((2/n)H(Z_i|W_0, W_2, Y_B, Y_1, \dots, Y_{i-1})) &\geq \exp((2/n) \cdot \\
&\quad H(Y_i|W_0, W_2, Y_B, Y_1, \dots, Y_{i-1})) \\
&\quad + 2\pi e(N_2(i) - N_1(i)) \\
&= 2\pi e(\alpha_i P(i) + N_2(i))
\end{aligned}$$

for $i = 1, \dots, L$ and $j = L + 1, \dots, N$. Therefore we get

$$\begin{aligned}
H(Y_B|W_0, W_1, Z_A) &= \sum_{j=L+1}^N H(Y_j|W_0, W_1, Z_A, Y_{L+1}, \dots, Y_{j-1}) \\
&\geq \sum_{j=L+1}^N H(Y_j|W_0, W_1, Z_A, Z_{L+1}, \dots, Z_{j-1}) \\
&\geq \frac{n}{2} \sum_{j=L+1}^N \log 2\pi e(\alpha_j P_j + N_1(j))
\end{aligned} \tag{5.57}$$

where we used the degradedness of the channel from Z_3 to Y_3 in the second line. Similarly

we get

$$\begin{aligned}
H(Z_A|W_0, W_2, Y_B) &= \sum_{i=1}^L H(Z_i|W_0, W_2, Y_B, Z_1, \dots, Z_{i-1}) \\
&\geq \sum_{i=1}^L H(Z_i|W_0, W_2, Y_B, Y_1, \dots, Y_{i-1}) \\
&\geq \frac{n}{2} \sum_{i=1}^L \log 2\pi e(\alpha_i P(i) + N_2(i))
\end{aligned} \tag{5.58}$$

Plugging (5.49), (5.50), (5.56), and (5.57) into (5.48) we get

$$\begin{aligned}
nR_0 &\leq \frac{n}{2} \sum_{i \in A} \log 2\pi e(N_1(i) + P(i)) - \frac{n}{2} \sum_{i=1}^L \log 2\pi e(N_1(i) + \alpha_i P(i)) \\
&\quad + \frac{n}{2} \sum_{i \in B} \log 2\pi e(N_1(i) + P(i)) - \frac{n}{2} \sum_{j=L+1}^N \log 2\pi e(\alpha_j P_j + N_1(j)) + n\epsilon_{1n} \\
&= n \sum_{i=1}^N C \left(\frac{\bar{\alpha}_i P(i)}{N_1(i) + \alpha_i P(i)} \right) + n\epsilon_{1n}
\end{aligned} \tag{5.59}$$

where we let $C(x) = \frac{1}{2} \log(1+x)$. Similarly, we can get

$$nR_0 \leq n \sum_{i=1}^N C \left(\frac{\bar{\alpha}_i P(i)}{N_2(i) + \alpha_i P(i)} \right) + n\epsilon_{2n} \tag{5.60}$$

Furthermore, using Fano's again we have

$$\begin{aligned}
n(R_0 + R_1) &\leq I(W_0, W_1; Y) + n\epsilon_{1n} \\
&= I(W_0, W_1; Y_B) + I(W_0, W_1; Y_A|Y_B) + n\epsilon_{1n} \\
&= I(W_0, W_1; Y_B) + H(Y_A|Y_B) - H(Y_A|W_0, W_1, Y_B) + n\epsilon_{1n} \\
&\leq I(W_0, W_1; Y_B) + H(Y_A) - H(Y_A|X_A) + n\epsilon_{1n} \\
&\leq I(W_0, W_1, Z_A; Y_B) + I(X_A; Y_A) + n\epsilon_{1n}
\end{aligned} \tag{5.61}$$

where we used $H(Y_A|X_A) \leq H(Y_A|W_0, W_1, Y_B)$ (due to the memoryless nature of the channel) in the fourth line.

From earlier inequalities we have

$$\begin{aligned}
I(W_0, W_1, Z_A; Y_B) &\leq \frac{n}{2} \sum_{i \in B} \log 2\pi e(N_1(i) + P(i)) - \frac{n}{2} \sum_{i \in B} \log 2\pi e(\alpha_i P(i) + N_1(i)) \\
&= \sum_{i \in B} nC \left(\frac{\bar{\alpha}_i P(i)}{N_1(i) + \alpha_i P(i)} \right)
\end{aligned} \tag{5.62}$$

We also have

$$\begin{aligned}
I(X_A; Y_A) &= H(Y_A) - H(Y_A|X_A) \\
&= H(Y_A) - \frac{n}{2} \sum_{i=1}^L \log 2\pi e N_1(i) \\
&\leq \frac{n}{2} \sum_{i \in A} \log 2\pi e (N_1(i) + P(i)) - \frac{n}{2} \sum_{i \in A} \log 2\pi e N_1(i) \\
&= \sum_{i \in A} nC \left(\frac{P(i)}{N_1(i)} \right). \tag{5.63}
\end{aligned}$$

Thus, $R_0 + R_1$ must satisfy:

$$R_0 + R_1 \leq \sum_{i \in A} C \left(\frac{P(i)}{N_1(i)} \right) + \sum_{i \in B} C \left(\frac{\bar{\alpha}_i P(i)}{N_1(i) + \alpha_i P(i)} \right) + \epsilon_{1n} \tag{5.64}$$

Similarly, we can show $R_0 + R_2$ must satisfy:

$$R_0 + R_2 \leq \sum_{i \in B} C \left(\frac{P(i)}{N_2(i)} \right) + \sum_{i \in A} C \left(\frac{\bar{\alpha}_i P(i)}{N_2(i) + \alpha_i P(i)} \right) + \epsilon_{2n} \tag{5.65}$$

From Equation (30) of [18] we have

$$\begin{aligned}
n(R_0 + R_1 + R_2) &\leq I(W_0, W_1, Z_A; Y_B) + I(X_A; Y_A) \\
&\quad + I(W_2; Z_B|W_0, W_1, Z_A) + n\epsilon_{1n} + n\epsilon_{2n}. \tag{5.66}
\end{aligned}$$

Notice that

$$\begin{aligned}
I(W_2; Z_B|W_0, W_1, Z_A) &= H(Z_B|W_0, W_1, Z_1, Z_2) - H(Z_B|W_0, W_1, W_2, Z_A) \\
&\leq H(Z_B|W_0, W_1, Z_A) - H(Z_B|X_B) \\
&= \frac{n}{2} \sum_{j=L+1}^N \log 2\pi e (N_2(j) + \alpha_j P_j) - \frac{n}{2} \sum_{j=L+1}^N \log 2\pi e N_2(j) \\
&= \sum_{i \in B} nC \left(\frac{\alpha_i P(i)}{N_2(i)} \right) \tag{5.67}
\end{aligned}$$

where we used $H(Z_B|W_0, W_1, W_2, Z_A) \geq H(Z_B|X_B)$ (due to the memoryless nature of the channel) to get the second line. Plugging in the expressions in (5.62), (5.63), and (5.67) into the upper bound in (5.66) we get

$$R_0 + R_1 + R_2 \leq \sum_{i \in A} C \left(\frac{P(i)}{N_1(i)} \right) + \sum_{i \in B} C \left(\frac{\bar{\alpha}_i P(i)}{N_1(i) + \alpha_i P(i)} \right) + \sum_{i \in B} C \left(\frac{\alpha_i P(i)}{N_2(i)} \right).$$

Equation (31) of [18] similarly gives us

$$\begin{aligned} n(R_0 + R_1 + R_2) &\leq I(W_0, W_2, Y_B; Z_A) + I(X_B; Z_B) \\ &\quad + I(W_1; Y_A | W_0, W_2, Y_B) + n\epsilon_{1n} + n\epsilon_{2n}. \end{aligned} \quad (5.68)$$

which yields

$$R_0 + R_1 + R_2 \leq \sum_{i \in B} C \left(\frac{P(i)}{N_2(i)} \right) + \sum_{i \in A} C \left(\frac{\bar{\alpha}_i P(i)}{N_2(i) + \alpha_i P(i)} \right) + \sum_{i \in A} C \left(\frac{\alpha_i P(i)}{N_1(i)} \right).$$

This completes the proof of the converse of the region specified by the inequalities in (5.40) - (5.45).

Now it is only left to show that the capacity region specified by the six inequalities is equivalent to the region given in Theorem 5.1, which we refer to as Region B. Since it is easy to show that any rate triplet in Region B is achievable, we only need to show that any rate triplet in the capacity region (i.e. any rate triplet satisfying (5.40) - (5.45)) is also in Region B.

For fixed values of α_i and $P(i)$, the inequalities in (5.40) - (5.45) define a polyhedron. Due to the convexity of Region B, it is sufficient to show that the corner points of the polyhedron are in Region B. Let C_{0a} , C_{0b} , C_{01} , C_{02} , C_{012a} , C_{012b} denote the six inequalities, respectively. Furthermore, let $C_0 = \min(C_{0a}, C_{0b})$ and $C_{012} = \min(C_{012a}, C_{012b})$. It is easy to see that $C_{0a} \leq C_{01} \leq C_{012a}$, $C_{0b} \leq C_{02} \leq C_{012b}$, $C_{01} + C_{02} \leq C_{012a}$, and $C_{01} + C_{02} \leq C_{012b}$.

We consider two cases, $C_{012a} = C_{012b}$ and $C_{012a} \neq C_{012b}$. Let us first assume $C_{012a} = C_{012b}$. Notice that

$$\begin{aligned} C_{012a} &= \sum_{i \in A} C \left(\frac{P(i)}{N_1(i)} \right) + \sum_{i \in B} \left(C \left(\frac{\bar{\alpha}_i P(i)}{N_1(i) + \alpha_i P(i)} \right) + C \left(\frac{\alpha_i P(i)}{N_2(i)} \right) \right) \\ &= \sum_{i \in A} \left(C \left(\frac{\alpha_i P(i)}{N_1(i)} \right) + C \left(\frac{\bar{\alpha}_i P(i)}{N_1(i) + \alpha_i P(i)} \right) \right) \\ &\quad + \sum_{i \in B} \left(C \left(\frac{\bar{\alpha}_i P(i)}{N_1(i) + \alpha_i P(i)} \right) + C \left(\frac{\alpha_i P(i)}{N_2(i)} \right) \right) \\ &= C_{0a} + \sum_{i \in A} C \left(\frac{\alpha_i P(i)}{N_1(i)} \right) + \sum_{i \in B} C \left(\frac{\alpha_i P(i)}{N_2(i)} \right) \end{aligned}$$

Similarly, $C_{012b} = C_{0b} + \sum_{i \in A} C \left(\frac{\alpha_i P(i)}{N_1(i)} \right) + \sum_{i \in B} C \left(\frac{\alpha_i P(i)}{N_2(i)} \right)$, which implies $C_{0a} = C_{0b}$.

The corner points of the polyhedron lie in either the $R_0 = 0$ plane or the $R_0 = C_0$ plane. Since $C_{01} + C_{02} \geq C_{012a} = C_{012b}$ and $C_{01} \leq C_{012a}$ and $C_{02} \leq C_{012a}$, the polyhedron has four corner points along the $R_0 = 0$ plane: $(R_1 = C_{01}, R_2 = 0)$, $(R_1 = C_{01}, R_2 = C_{012} - C_{01})$, $(R_1 = C_{012} - C_{02}, R_2 = C_{02})$, and $(R_1 = 0, R_2 = C_{02})$. Clearly we need only consider the

middle two of these four points. First consider $(R_1 = C_{01}, R_2 = C_{012} - C_{01})$. We have

$$\begin{aligned} R_1 &= C_{01} = \sum_{i \in A} C \left(\frac{P(i)}{N_1(i)} \right) + \sum_{i \in B} C \left(\frac{\bar{\alpha}_i P(i)}{N_1(i) + \alpha_i P(i)} \right) \\ R_2 &= C_{012} - C_{01} = C_{012a} - C_{01} \\ &= \sum_{i \in B} C \left(\frac{\alpha_i P(i)}{N_2(i)} \right) \end{aligned}$$

Let $P_1(i) = P(i)$ and $P_2(i) = 0$ for $i \in A$, and $P_1(i) = \bar{\alpha}_i P(i)$ and $P_2(i) = \alpha_i P(i)$ for $i \in B$. Plugging into (5.27) and (5.28), we can see that $(R_0 = 0, R_1 = C_{01}, R_2 = C_{012a} - C_{01})$ is in Region B. Similarly, we can show that $(R_0 = 0, R_1 = C_{012b} - C_{02}, R_2 = C_{02})$ is in Region B. Thus, the four corner points along the $R_0 = 0$ plane are contained in Region B.

It is easy to show that there are only three corner points along the $R_0 = C_0$ plane (i.e. the face is a rectangle instead of a pentagon), which are $(R_0 = C_0, R_1 = C_{01} - C_0, R_2 = 0)$, $(R_0 = C_0, R_1 = C_{01} - C_0 = C_{012} - C_{02}, R_2 = C_{012} - C_{01} = C_{02} - C_0)$, and $(R_0 = C_0, R_1 = 0, R_2 = C_{02} - C_0)$. Clearly, we need only consider the middle of these three points, i.e. $(R_0 = C_0, R_1 = C_{01} - C_0, R_2 = C_{012} - C_{01})$. Note that the rate triplet

$$\begin{aligned} R_0 &= C_0 = \sum_{i=1}^N C \left(\frac{\bar{\alpha}_i P(i)}{N_1(i) + \alpha_i P(i)} \right) = \sum_{i=1}^N C \left(\frac{\bar{\alpha}_i P(i)}{N_2(i) + \alpha_i P(i)} \right) \\ R_1 &= C_{01} - C_0 = C_{01} - C_{0a} = \sum_{i \in A} C \left(\frac{\alpha_i P(i)}{N_1(i)} \right) \\ R_2 &= C_{012} - C_{01} = C_{012a} - C_{01} = \sum_{i \in B} C \left(\frac{\alpha_i P(i)}{N_2(i)} \right) \end{aligned}$$

is achievable if we choose $P_0(i) = \bar{\alpha}_i P(i)$ for all i , $P_1(i) = \alpha_i P(i)$ for $i \in A$ and $P_1(i) = 0$ for $i \in B$, and $P_2(i) = \alpha_i P(i)$ for $i \in B$ and $P_2(i) = 0$ for $i \in A$. Thus, we have shown that the polyhedron defined by the six inequalities is contained in Region B whenever $C_{012a} = C_{012b}$.

Now let us consider the other case, i.e. $C_{012a} \neq C_{012b}$. Without loss of generality, assume $C_{012a} > C_{012b}$. Notice that C_{012a} is a decreasing function of $\bar{\alpha}_i$ for $i \in B$ because $N_1(i) \geq N_2(i)$ for $i \in B$. However, C_{0a} , C_{0b} , and C_{01} are increasing functions of $\bar{\alpha}_i$ for $i \in B$ and C_{02} and C_{012b} are not affected by $\bar{\alpha}_i$ for $i \in B$. Thus, we can increase $\bar{\alpha}_i$ for $i \in B$ until we have $C_{012a} = C_{012b}$. Since the five inequalities other than C_{012a} increased, this corresponds to a larger region of rates. Furthermore, we previously showed that the corner points of the polyhedron are contained in Region B whenever $C_{012a} = C_{012b}$, which implies that the original polyhedron, corresponding to the original values of α_i , is also in Region B.

Notice, however, that there is the possibility that $C_{012a} > C_{012b}$ even if $\bar{\alpha}_i = 1$ for all $i \in B$. Again, this clearly corresponds to a larger polyhedron than with the original choice of α_i , but we must explicitly show the corner points are contained in Region B. With $\bar{\alpha}_i = 1$

for all $i \in B$, we have

$$\begin{aligned}
C_{012a} &= \sum_{i \in A} C \left(\frac{P(i)}{N_1(i)} \right) + \sum_{i \in B} \left(C \left(\frac{\bar{\alpha}_i P(i)}{N_1(i) + \alpha_i P(i)} \right) + C \left(\frac{\alpha_i P(i)}{N_2(i)} \right) \right) \\
&= \sum_{i \in A} C \left(\frac{P(i)}{N_1(i)} \right) + \sum_{i \in B} C \left(\frac{P(i)}{N_1(i)} \right) \\
&= C_{01}.
\end{aligned}$$

Thus $C_{012a} = C_{01} > C_{012b} \geq C_{02}$. Furthermore, from the expansion of C_{012a} in (5.69) it is easy to see that $C_{012a} > C_{012b}$ implies $C_{0a} > C_{0b}$. Also notice that $C_{02} = C_{0b}$. Thus, the following three inequalities define the polyhedron: $R_0 \leq C_{0b}$, $R_0 + R_2 \leq C_{0b}$, and $R_0 + R_1 + R_2 \leq C_{012b}$. Along the $R_0 = 0$ face, there are three corner points: $(R_1 = C_{012b}, R_2 = R_0 = 0)$, $(R_1 = C_{012b} - C_{0b}, R_2 = C_{0b})$, and $(R_0 = R_1 = 0, R_2 = C_{0b})$. Since $R_1 = C_{012a} > C_{012b}$ is clearly achievable by letting $P_1(i) = P(i)$, the first point is achievable. Since $C_{0b} = \sum_{i \in A} C \left(\frac{\bar{\alpha}_i P(i)}{N_2(i) + \alpha_i P(i)} \right) + \sum_{i \in B} C \left(\frac{P(i)}{N_2(i)} \right)$ and $C_{012b} - C_{0b} = \sum_{i \in A} C \left(\frac{\alpha_i P(i)}{N_1(i)} \right)$, the second point is achievable by choosing $P_1(i) = \alpha_i P(i)$ and $P_2(i) = \bar{\alpha}_i P(i)$. This in turn implies that the third point is achievable.

Now consider the $R_0 = C_0 = C_{0b}$ plane. Since $R_0 + R_2 \leq C_{0b}$, this implies $R_2 = 0$. Thus, we need only consider $R_0 = C_{0b}$ and $R_1 = C_{012b} - C_{0b} = \sum_{i \in A} C \left(\frac{\alpha_i P(i)}{N_1(i)} \right)$. By choosing $P_0(i) = \bar{\alpha}_i P(i)$ and $P_1(i) = \alpha_i P(i)$, this rate is achievable. Thus, the entire polyhedron is contained in Region B. Thus, the capacity region is contained in Region B. Since Region B is also achievable, this completes the proof of Theorem 5.1.

Chapter 6

Capacity of Cooperative Ad-Hoc Networks

Sensor networks and ad-hoc networks are receiving more and more attention from the research community. In such networks, it is easy to envision a group of nodes that wish to communicate data to another distant group of nodes. For example, a group of nodes may sense a phenomenon and then wish to communicate their measurements to surrounding sensors. Thus, it is feasible to consider a closely packed group of nodes that wish to transmit information to another group of nodes.

In this chapter, we consider a scenario where there are two independent transmitting nodes, and two independent receivers. Each transmitter wants to send a message to a different receiver. In information theory, this channel is classified as an interference channel [13, Ch. 14], and is one of the most fundamental open problems in multi-user information theory. We attack this problem from a different perspective and ask the following question: How much does allowing cooperation between the transmitters and/or cooperation between the receivers increase the set of achievable data rates? However, we do not allow this cooperation to occur for free and instead explicitly constrict cooperation to consist of transmitting messages between the two transmitters and/or transmitting messages between the two receivers. To capture the cost of cooperation, we place a sum power constraint on the total power transmitted in the system by all nodes.

The notion of cooperative communication has been considered in several recent works. Sendonaris et. al. [57] considered the rates achievable in a channel with two cooperative transmitters and a single receiver. Yazdi et. al. [80] is a more recent work on the same channel model. A channel with two cooperative transmitters (using low-complexity schemes such as amplify-and-forward) and two non-cooperative receivers was considered in terms of outage and diversity for fading channels without transmitter channel state information in [40]. Recent work by Host-Madsen [24] analyzed the same channel without fading, but with more complicated transmitter cooperation schemes involving dirty paper coding. The

cooperative nature of these channels makes them closely related to the classical relay channel [11].

In this chapter we consider the two transmitter, two receiver case from the capacity region perspective for the case of no fading, or slow fading with perfect channel state information at all transmitters and receivers. We are concerned solely with achievable rates, as opposed to outage and diversity as many of the works in this area have considered. For transmitter cooperation we use dirty paper coding, which we earlier showed (Chapter 4.2) achieves the sum capacity of the multiple-antenna broadcast channel. Our work differs from previous research in this area in that 1) we consider cooperation schemes that asymptotically (i.e. as the distance between nodes in a cluster decreases to zero) achieve the information theoretic upper bounds, yet are simple enough to facilitate numerical computation of the achievable rates and therefore give general insight about the underlying problem, and 2) we consider receiver cooperation in addition to transmitter cooperation, which, to the best of our knowledge, no previous work has considered in this setting.

For simplicity and to gain intuition, we consider the scenario where the channel between the two transmitters, the channel between the transmitters and the receivers, and the channel between the two receivers are orthogonal (i.e. on separate frequency bands or time slots). We are most interested in the scenario where the distance between the two transmitters and the distance between the two receivers are small relative to the distance between each transmitter-receiver pair. This allows high-rate communication between the two transmitters or between the two receivers using small amounts of power. We consider the rates achievable without cooperation versus rates achievable with transmitter-only cooperation, receiver-only cooperation, and transmitter and receiver cooperation. We compare these achievable rates to three different information theoretic upper bounds: 1) perfect transmitter cooperation (multiple-antenna broadcast channel [5, 69, 73, 82]), 2) perfect receiver cooperation (multiple-antenna multiple-access channel [61]), and 3) perfect receiver cooperation and perfect transmitter cooperation (multiple-antenna point-to-point channel [61]).

The remainder of this chapter is organized as follows: In Chapter 6.1 we describe the system model. In Chapters 6.4 - 6.6 we describe different cooperation schemes. In Chapter 6.7 we describe upper bounds to the rates achievable using cooperation. Finally, in Chapter 6.8 we give some numerical results. Material in this chapter also appears in [34].

6.1 System Model

Consider a system with two transmitters and two receivers as shown in Fig. 6.1. We assume that the distance between each of the four transmitter-receiver pairs is the same, which is roughly true if the distance between the transmitter and receiver clusters is large. Thus, we assume that the channel gains between every transmitter and receiver has norm one. Thus, the channels between each transmitter-receiver pair are the same, except for random phases,

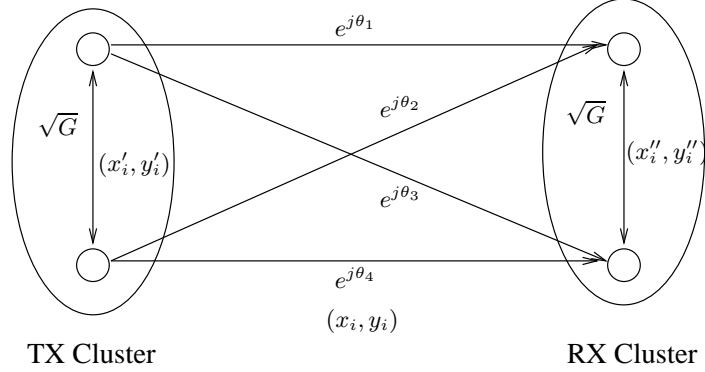


Figure 6.1: System Model

denoted by θ_i , which are assumed to be uniformly distributed in $[0, 2\pi]$. This simplifying assumption is largely made to aid intuition, but can easily be removed so that more general fading processes can be studied as well.

There are three orthogonal communication channels: the channel between the transmitters and receivers, the channel between the two transmitters, and the channel between the two receivers. We first describe the channel connecting the transmitters and receivers. We let x_1 and x_2 denote the two transmit signals, and y_1 and y_2 denote the two corresponding received signals. Transmitter 1 wishes to communicate to receiver 1, and transmitter 2 wishes to communicate to receiver 2. In matrix form, the channel can be written as:

$$\begin{bmatrix} y_1 \\ y_2 \end{bmatrix} = \mathbf{H} \begin{bmatrix} x_1 \\ x_2 \end{bmatrix} + \begin{bmatrix} n_1 \\ n_2 \end{bmatrix} \quad (6.1)$$

where n_1 and n_2 are independent $N(0, 1)$ noises. As shown in Fig. 6.1, the channel gains $H_{i,j}$ are only phases: $H_{1,1} = e^{j\theta_1}$, $H_{1,2} = e^{j\theta_2}$, $H_{2,1} = e^{j\theta_3}$, and $H_{2,2} = e^{j\theta_4}$.

There is also an AWGN channel between the two transmitters, with channel gain equal to \sqrt{G} . If there is only distance based path-loss with $1/d^2$ attenuation, this corresponds to the scenario when the distance between the two clusters is \sqrt{G} times larger than the distance between nodes in a cluster. For simplicity, we assume that the two transmitters can simultaneously transmit and receive on this channel. We let x'_1 denote the signal that transmitter 1 sends to transmitter 2, and we let y'_2 denote the corresponding received signal at transmitter 1. The channels are then defined by $y'_1 = \sqrt{G}x'_2 + n_3$ and $y'_2 = \sqrt{G}x'_1 + n_4$, where n_3 and n_4 are independent unit-variance Gaussian noises. There is an analogous AWGN channel between the two receivers, also with channel gain equal to \sqrt{G} . If we let x''_1 denote the signal that receiver 1 transmits to receiver 2 on this channel, and we let y''_2 denote the corresponding received signal at receiver 2, then this channel is defined by $y''_1 = \sqrt{G}x''_2 + n_5$ and $y''_2 = \sqrt{G}x''_1 + n_6$, where n_5 and n_6 are independent unit-variance Gaussian noises. Here x''_1 and x''_2 are constrained to be functions of the previously received

signals y_1 and y_2 , respectively.

We assume that transmitter 1 has a message intended for receiver 1, and transmitter 2 has a message intended for receiver 2. We impose a total system power constraint of P on the total transmit energy, i.e. we require

$$E[x_1^2 + x_2^2 + x_1'^2 + x_2'^2 + x_1''^2 + x_2''^2] \leq P.$$

This power constraint is intended to capture the system-wide cost of transmitter and receiver cooperation.

Finally, we must specify the bandwidth of each of the transmitter cooperation channel, the receiver cooperation channel, and the direct communication channel. We denote the bandwidths of these three channel as B_1 , B_2 , and B_3 , respectively. We deal with two different models, referred to as bandwidth assumption 1 and 2. Under bandwidth assumption 1, we assume that orthogonal channels have been previously set aside for the three links, and we assume each of the three channels has a bandwidth of 1 Hz ($B_1 = B_2 = B_3 = 1$). Furthermore, the upper bounds are calculated with respect to the 1 Hz direct communication band, i.e. ignoring the cooperation bands. Under bandwidth assumption 2, we assume there is a single 1 Hz channel which must be divided into three different bands. Thus we have the further degree of freedom of choosing B_1 , B_2 , and B_3 such that $B_1 + B_2 + B_3 = 1$. Furthermore, the upper bounds are calculated with respect to the entire 1 Hz band. For this reason, we clearly expect to see larger cooperation gains under bandwidth assumption 1.

Though we work with the simplifying assumptions of equal amplitude channel gains, results generalize to the case of arbitrary channel gains.

6.2 Broadcast and Multiple-Access Channel Background

Throughout this chapter we discuss the broadcast and multiple-access channels implicitly contained in the two transmitter/two receiver channel. If the receivers are assumed to cooperate perfectly, the channel becomes a multiple-access channel (MAC) with two single-antenna transmitters and a two-antenna receiver. The channels of the transmitters are given by the *columns* of the matrix \mathbf{H} . In terms of Fig. 6.1, this corresponds to communicating from the left cluster to the right cluster, with perfectly cooperative nodes in the right cluster (RX cluster). If the transmitters are assumed to cooperate perfectly, the channel becomes a broadcast channel with two single-antenna receivers and a two-antenna transmitter. The channels of the two receivers are equal to the *rows* of the matrix \mathbf{H} . In terms of Fig. 6.1, this corresponds to communicating from the left cluster to the right cluster, with perfectly cooperative nodes in the left cluster (TX cluster).

In Chapter 3 we showed that the broadcast channel is closely related to the *dual* multiple-access channel, which is the MAC where the two nodes in the receiving cluster are the single-antenna independent *transmitters* and the cooperative nodes in the transmitter cluster are the two-antenna *receiver*. In terms of Fig. 6.1, this corresponds to communicating from the right cluster to the left cluster (opposite the normal direction of communication), with perfectly cooperative nodes in the left cluster. The channels of the two transmitters are the transposes of the channels of the two receivers in the broadcast channel. Thus, the transmitter channels correspond to the transpose of the *rows* of \mathbf{H} . It is important to note that the MAC corresponding to perfect receiver cooperation is different from the dual MAC. However, in Chapter 6.5 we show that the capacity regions of these multiple-access channels are the same.

6.3 Non-Cooperative Transmission

Without cooperation on either the transmitter or receiver side, the channel is a Gaussian interference channel, for which the capacity region is in general not known. However, the channel we consider is a “strong” interference channel¹, for which the capacity region is known [56]. The strong interference condition implies that each receiver can decode the transmitted messages of *both* transmitters. Thus, the capacity region is upper bounded by each receiver’s multiple-access channel, and this bound is in fact tight. If transmitter 1 uses power P_1 and transmitter 2 uses power $P_2 = P - P_1$, the multiple-access region is given by the pentagon described by $R_1 \leq \log(1 + P_1)$, $R_2 \leq \log(1 + P_2)$, and $R_1 + R_2 \leq \log(1 + P)$. Since there is a sum power constraint on the transmitters instead of individual power constraints, the non-cooperative capacity region is equal to the set of rates satisfying $R_1 + R_2 \leq \log(1 + P)$. It is easy to see that this set of rates is also achievable using TDMA. We will thus refer to the TDMA rate as a non-cooperative benchmark to compare our cooperative schemes against.

6.4 Transmitter Cooperation

In this section, we describe a transmitter cooperation scheme. If the transmitters were allowed to jointly encode their messages, the channel would be a multiple-antenna broadcast channel. For such a channel, the sum capacity can be achieved by using dirty paper coding. Motivated by this, we consider a strategy where the two transmitters first exchange their intended messages (or codewords, since each transmitter is assumed to know the other transmitter’s codebook) using some fraction of the total power P , and then *jointly* encode

¹A strong interference channel refers to the situation where the channel gain of the interference is as large as the channel gain of the desired signal.

both messages using dirty paper coding (i.e. encode as if they were a joint transmitter) with the remaining power. Causality is not a problem for any of our cooperative schemes since we consider orthogonal channels for cooperation and we can offset communication by one block initially.

Assume power $\frac{P_t}{2}$ is used by each transmitter to send his intended message to the other transmitter. Then the intra-transmitter rate is equal to $R_t = B_1 \log(1 + \frac{P_t}{2}G)$. The remaining power $P - P_t$ is used to jointly encode using dirty-paper coding. We require that R_t is high enough to ensure that each transmitter *fully* knows the intended codeword of the other transmitter (i.e. R_t must be as large as the rate of the message of each user). Since each transmitter knows both messages after this exchange, each user can then perform standard dirty paper coding as if the two antennas were actually cooperative, but then only send the information on one of the two antennas. The sum rate achievable using joint dirty paper coding is equal to the sum-rate capacity of the dual multiple-access channel with power $P - P_t$. Since each element of the channel matrix \mathbf{H} has amplitude one, this is equal to:

$$R_{DPC} = B_2 \log \left| \mathbf{I} + \frac{P - P_t}{2} (\mathbf{H}_1^T \mathbf{H}_1 + \mathbf{H}_2^T \mathbf{H}_2) \right| \quad (6.2)$$

where $\mathbf{H}_i = [H_{i,1} \ H_{i,2}]$ is the row vector representing the received channel of Receiver i . For a given P_t , the achievable sum rate is $\min(2R_t, R_{DPC})$. Thus, the optimal transmission rate while using transmission cooperation is given by:

$$R_{TX} = \max_{0 \leq P_t \leq P, B_1, B_2} \min(2R_t, R_{DPC}), \quad (6.3)$$

where $B_1 = B_2 = 1$ under BW assumption 1 and $B_1 + B_2 \leq 1$ under BW assumption 2. Since R_t is an increasing function of P_t and R_{DPC} is a decreasing function of P_t , the optimum is achieved at the P_t for which $R_t = \frac{1}{2}R_{DPC}$.

6.5 Receiver Cooperation

In this section, we describe a method that allows the receivers to cooperate. Since the channels of each of the signals are equivalent except for the phase differences, the amount of information decodable at each of the receivers is roughly the same. Thus, there is no advantage gained if a receiver attempts to first decode the message intended for the other receiver and then pass it on to the other receiver. With perfect receiver cooperation, receiver 1 would get to see the received signal y_2 in addition to its own signal y_1 . Thus, a logical method for cooperation is for each receiver to amplify-and-forward their received signal to the other receiver, which always results in some noise amplification.

Each receiver uses the fraction of power $\frac{P_r}{2}$ to amplify-and-forward its received signal to the other receiver. Since the transmitters do not cooperate in this mode, the signals x_1

and x_2 are independent and are chosen to be $N(0, \frac{P-P_r}{2})$. The expected received power at y_1 is given by $E[y_1^2] = E[x_1^2] + E[x_2^2] + E[n_1^2] = P - P_r + 1$. Thus, receiver 1 transmits

$$\sqrt{\frac{P_r/2}{P - P_r + 1}} y_1 = \sqrt{\frac{P_r/2}{P - P_r + 1}} (H_{1,1}x_1 + H_{2,1}x_2 + n_1)$$

The corresponding received signal at receiver 2 is given by $\sqrt{G \frac{P_r/2}{P - P_r + 1}} (h_{1,1}x_1 + h_{2,1}x_2 + n_1) + n$, where $n \sim N(0, 1)$. The aggregate signal at receiver 1 is then given by:

$$\tilde{y}_1 = \begin{bmatrix} \mathbf{H}_1 \\ \alpha \mathbf{H}_2 \end{bmatrix} x + \begin{bmatrix} n_1 \\ n_2 \end{bmatrix} \quad (6.4)$$

$$= \mathbf{F}_1 x_1 + \mathbf{F}_2 x_2 + \begin{bmatrix} n_1 \\ n_2 \end{bmatrix} \quad (6.5)$$

where $\alpha = \frac{\sqrt{G \frac{P_r/2}{P - P_r + 1}}}{1 + \sqrt{G \frac{P_r/2}{P - P_r + 1}}}$, $\mathbf{F}_1 = \begin{bmatrix} e^{j\theta_1} \\ \alpha e^{j\theta_3} \end{bmatrix}$, and $\mathbf{F}_2 = \begin{bmatrix} e^{j\theta_2} \\ \alpha e^{j\theta_4} \end{bmatrix}$. Notice that \tilde{y}_1 differs from the pair (y_1, y_2) only due to the α factor, which is caused by noise amplification. By symmetry, the sum rate decodable at each receiver (using aggregate signals \tilde{y}_1 and \tilde{y}_2) are the same. The sum rate decodable at receiver 1 is given by:

$$R_{coop} = B_2 \log \left| \mathbf{I} + \frac{P - P_r}{2} (\mathbf{F}_1 \mathbf{F}_1^T + \mathbf{F}_2 \mathbf{F}_2^T) \right| \quad (6.6)$$

Since α is a function of P_r , this expression must be maximized over P_r to find the largest achievable rate. Thus the maximum data rate while using receiver cooperation is given by:

$$R_{RX} = \max_{0 \leq P_r \leq P} B_2 \log \left| \mathbf{I} + \frac{P - P_r}{2} (\mathbf{F}_1 \mathbf{F}_1^T + \mathbf{F}_2 \mathbf{F}_2^T) \right|. \quad (6.7)$$

It is important to note that the amplify-and-forward technique requires the same amount of bandwidth on the receiver cooperation link as on the direct communication link. Thus, we must have $B_2 = B_3 = \frac{1}{2}$ under BW assumption 2, while $B_2 = B_3 = 1$ as always under BW assumption 1. Furthermore, notice that \mathbf{F}_1 and \mathbf{F}_2 are functions of P_r through the parameter α . When the power gain G is very large (i.e. when the receivers are very close to each other), we get $\alpha \approx 1$ and we expect to come close to the MAC (fully cooperative receivers) upper bound.

6.6 Transmitter Cooperation & Receiver Cooperation

In this section we describe a scheme in which the two transmitters cooperate by exchanging their intended messages and then cooperatively signal using dirty paper coding, and the

two receivers cooperate by amplifying-and-forwarding. We let P_t denote the power used to exchange messages between the transmitter. The corresponding rate is $R_t = B_1 \log(1 + \frac{P_t}{2})$. We again require that each transmitter completely knows the intended message of the other transmitter. Once the transmitters exchange messages, we encode using dirty paper coding, similar to the transmitter cooperation scheme. However, in this case, each user has two receive antennas, where the second antenna is the signal received via the amplify-and-forward channel from the other receiver. Power P_r is used to perform amplify-and-forward between the two receivers. This leaves power $P - P_t - P_r$ to jointly transmit data using dirty paper coding.

Because cooperative dirty paper encoding is performed at the two transmitters, x_1 and x_2 are correlated with covariance matrix Σ_x . The expected received power at y_1 is then equal to $1 + \mathbf{H}_2 \Sigma_x \mathbf{H}_2^T$. As in the case with only amplify-and-forward, the resultant composite signal at receiver 1 is given by

$$\tilde{y}_1 = \begin{bmatrix} \mathbf{H}_1 \\ \beta \mathbf{H}_2 \end{bmatrix} x + \begin{bmatrix} n_1 \\ n_2 \end{bmatrix} \quad (6.8)$$

where $\beta = \frac{\sqrt{G \frac{P_r/2}{\mathbf{H}_2 \Sigma_x \mathbf{H}_2^T + 1}}}{1 + \sqrt{G \frac{P_r/2}{\mathbf{H}_2 \Sigma_x \mathbf{H}_2^T + 1}}}$, For fixed β and P_r and P_t , the sum rate achievable from the cooperative transmitters to the receivers (with composite channels \tilde{y}_1 and \tilde{y}_2) is equal to the sum capacity of the dual multiple-access channel. In the dual multiple-access channel, the composite receivers are the two-antenna transmitters and the cooperative transmitters become the two-antenna receiver. Since each transmitter has two antennas, we are not able to invoke symmetry to find the sum capacity of the dual multiple-access channel as before. Thus, the sum capacity must be characterized in terms of a maximization:

$$R_{coop} = \max_{Tr(\mathbf{Q}_1 + \mathbf{Q}_2) \leq P} B_2 \log \left| \mathbf{I} + \tilde{\mathbf{H}}_1^T \mathbf{Q}_1 \tilde{\mathbf{H}}_1 + \tilde{\mathbf{H}}_2^T \mathbf{Q}_2 \tilde{\mathbf{H}}_2 \right|$$

where the maximization is over covariance matrices \mathbf{Q}_1 and \mathbf{Q}_2 , with $\tilde{\mathbf{H}}_1 \triangleq \begin{bmatrix} \mathbf{H}_1 \\ \beta \mathbf{H}_2 \end{bmatrix}$, and $\tilde{\mathbf{H}}_2 \triangleq \begin{bmatrix} \beta \mathbf{H}_1 \\ \mathbf{H}_2 \end{bmatrix}$. The maximizing covariances can be found using the algorithm in Chapter 4.3. Given \mathbf{Q}_1 and \mathbf{Q}_2 , the sum rate achieving covariance matrix for the downlink (i.e. Σ_x) can be found² [69].

²The sum rate was maximized assuming a fixed value of β , but interestingly, the choice of Σ_x in fact determines the value of β . Thus, we initially assume that Σ_x is a scaled version of the identity when determining β . We then maximize the sum capacity of the broadcast channel assuming this β . After finding the corresponding Σ_x , we re-calculate the value of β . This procedure can be repeated, but we empirically find this to yield a negligible increase in rate.

The maximum rate of transmission using both transmitter and receiver cooperation is thus given by:

$$R_{TX-RX} = \max_{P_r+P_t \leq P, B_1, B_2, B_3} \min(2R_t, R_{coop}) \quad (6.9)$$

Here R_t is an increasing function of P_t and R_{coop} is an increasing function of P_r . Under BW assumption 1 we have $B_1 = B_2 = B_3 = 1$, as always. Under BW assumption 2, notice that the amplify-and-forward technique again requires $B_2 = B_3$. Thus, the bandwidths must satisfy $B_1 + 2B_2 \leq 1$. For fixed P_t and P_r , the achievable sum rate is $\min(2R_t, R_{coop})$. By the same reasoning used for transmitter-only cooperation, for a fixed P_r , the optimal choice of P_t yields $2R_t = R_{coop}$. However, it is necessary to directly maximize the achievable rates over all choices of P_r . When $P_r = 0$ this strategy is identical to the transmitter-only cooperation scheme, and thus this scheme performs at least as well as the transmitter cooperation scheme. Since transmitter cooperation yields higher rates than receiver cooperation, there is a full ordering on the achievable rates of the three different schemes for any channel.

Finally notice that as G becomes very large, the scaling term β can be made close to one. Thus in the limit (i.e. $\beta \rightarrow 1$), the composite channels of both receivers become equal to $[y_1 \ y_2]^T$. Since both received channels are the same, the broadcast channel capacity region is equal to the point-to-point capacity from the cooperative transmitter to either of the receivers, i.e. the point-to-point MIMO capacity of the original channel.

6.7 Upper Bounds

There are three information theoretic upper bounds that bound the rates achievable with transmitter cooperation only, receiver cooperation only, and transmitter and receiver cooperation. Note that for all three bounds, we use a bandwidth of 1 Hz.

First, consider the scenario where only the transmitters attempt to cooperate. The capacity of the channel where the transmitters are allowed to perfectly cooperate (without use of any power), but the receivers are not allowed to cooperate is an upper bound to the rates achievable using only transmitter cooperation. This is not a general upper bound on our system, but is a bound when only transmitter side cooperation is allowed. Since the receivers must decode their messages independently, the channel becomes a two transmit antenna, two receiver (single receive antenna each) broadcast channel with transmit power constraint P . Due to the symmetry of the channel, the sum capacity of the broadcast channel is equal to the sum capacity of the dual multiple-access channel when equal power is allocated to each transmitter:

$$R_{BC} = \log \left| \mathbf{I} + \frac{P}{2} (\mathbf{H}_1^T \mathbf{H}_1 + \mathbf{H}_2^T \mathbf{H}_2) \right|. \quad (6.10)$$

Next consider the scenario where only the receivers attempt to cooperate. In this scenario, an upper bound is reached by allowing the receivers to perfectly cooperate. The channel then becomes a two transmitter (single antenna each), two receive antenna multiple-access channel, for which the capacity region is known. Due to the symmetry of the channels, the sum capacity of the multiple-access channel is given by:

$$R_{MAC} = \log \left| \mathbf{I} + \frac{P - P_r}{2} (\mathbf{F}_1 \mathbf{F}_1^T + \mathbf{F}_2 \mathbf{F}_2^T) \right| \quad (6.11)$$

where $\mathbf{F}_1 = \begin{bmatrix} e^{j\theta_1} \\ e^{j\theta_3} \end{bmatrix}$ and $\mathbf{F}_2 = \begin{bmatrix} e^{j\theta_2} \\ e^{j\theta_4} \end{bmatrix}$. Though the broadcast channel arising from perfect transmitter cooperation and the multiple-access channel arising from perfect receiver cooperation are not duals of each other in the sense of Chapter 3, it can be shown by direct computation that equations (6.10) and (6.11) are equal. Furthermore, the dirty paper achievable region corresponding to transmitter-only cooperation is equal to the multiple-access capacity region which bounds receiver-only cooperation.

A true upper bound to our system is reached by allowing perfect cooperation at the transmitters *and* at the receivers. The channel then becomes a 2×2 MIMO channel, whose capacity is given by water-filling the eigenvalues of the channel matrix \mathbf{H} [61]. Interestingly, Theorem 3 of [5] shows that the difference between the MIMO point-to-point capacity and the sum capacity of the BC goes to zero as the SNR P goes to infinity. Thus, at high SNR we expect cooperation at either the TX or at the RX cluster to be sufficient to come close to the MIMO upper bound.

6.8 Numerical Results

In this section we provide numerical results for both bandwidth assumptions.

6.8.1 Bandwidth Assumption 1

In Fig. 6.2, the upper bounds and achievable rates are plotted for a random channel chosen with an SNR of 0 dB and for $G = 10$ dB. If we assume a path-loss exponent of 2, this corresponds to a physical scenario where the distance between the nodes in the clusters is $\sqrt{10}$ times less than the distance between the two clusters. The rates achievable with TX cooperation and with TX & RX cooperation are identical, and both come extremely close to the broadcast channel upper bound. There is, however, a sizable gap between the BC/MAC upper bound and the MIMO upper bound. The TX & RX cooperation scheme will approach the MIMO upper bound, but only for very large values of G . The rates achievable with RX cooperation do exceed the non-cooperative rates achievable with TDMA, but they are considerably smaller than the TX cooperation rates.

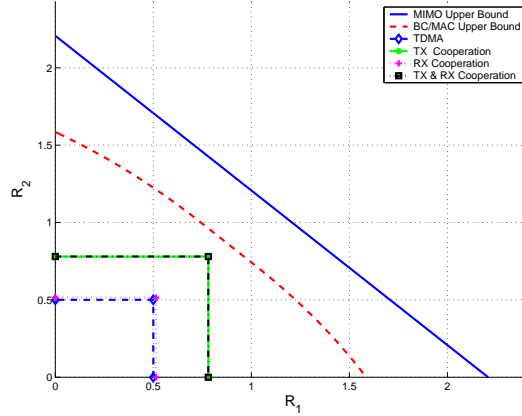


Figure 6.2: Upper bounds and achievable rates for SNR = 0 dB, $G = 10$ dB

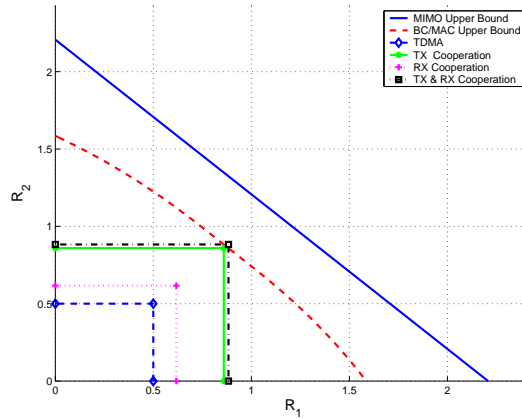


Figure 6.3: Upper bounds and achievable rates for SNR = 0 dB, $G = 20$ dB

In Fig. 6.3, the bounds and rates are plotted for the same channel with $G = 20$ dB. As expected, the achievable rates with cooperation increase. However, the rates achievable with RX cooperation are still quite small, while the rates achievable with TX cooperation are quite large and are very close to the BC/MAC upper bound. Furthermore, the rates achievable with TX & RX cooperation actually exceed those achievable with TX cooperation alone.

In Fig. 6.4, the average achievable sum rates using the different cooperation schemes are plotted versus G for an average SNR of 10 dB. To compute these results, a large sample of channels were instantiated (i.e. different random phases) and the achievable rates were calculated for different values of G , and then an average was taken over the instantiations. Notice that the three upper bounds are independent of G because they assume perfect cooperation. Since the SNR is 10 dB, there is not a very significant gap between the MIMO upper bound and the MAC/BC upper bound. As G increases (i.e. as the nodes within each cluster move closer to each other), the achievable rates approach the upper bounds.

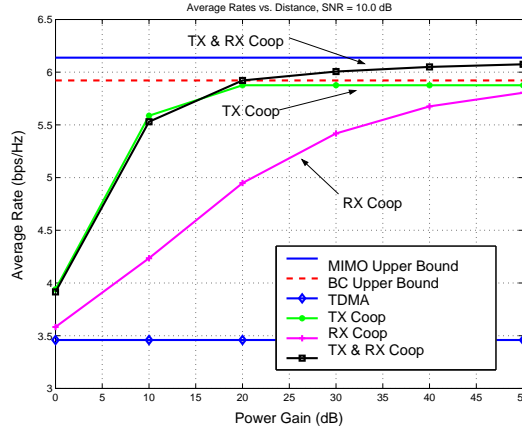


Figure 6.4: Plot of rate vs. gain for SNR = 10 dB

As discussed before, TX & RX cooperation always performs better than TX cooperation, which generally outperforms RX cooperation. However, it is most interesting to note that TX & RX cooperation and TX cooperation are virtually identical for $G \leq 20$ dB. Upon closer examination, one finds that the optimum TX & RX scheme for such values of G is achieved by only using transmitter cooperation, i.e. not having the receivers use any power for amplify-and-forward. For $G > 20$ dB, a gap does open up between the TX & RX scheme and the TX scheme. Interestingly, this gap appears at the point where the TX cooperation scheme achieves the BC upper bound. Thus, up to the BC upper bound it seems that is not worthwhile to do both TX & RX cooperation, but beyond this point (i.e. for larger values of G) it becomes worthwhile to cooperate in both clusters.

In Figure 6.4, there is a significant gap between the rates achievable using TDMA and the rates achievable using TX cooperation, even at relatively small values of G (i.e. 10 dB). Thus, there is in fact a significant advantage to performing cooperation in either or both of the clusters. Another general trend seen in all plots is the poor performance of the RX cooperation scheme relative to the TX cooperation scheme. For all but very small values of G , the RX cooperation scheme performs much poorer than the TX cooperation scheme. Transmitter cooperation allows for joint encoding (similar to coherent combining) of the two messages, while receiver cooperation only provides an additional scaled antenna output, where the scaling is proportional to G . For large enough G , however, the simple amplify-and-forward operation performed at the receivers is sufficient to achieve the MAC/BC upper bound.

6.8.2 Bandwidth Assumption 2

In Fig. 6.5 - 6.7, similar figures are plotted for BW assumption 2. Notice that receiver cooperation performs extremely poorly in general, as does receiver and transmitter cooperation. This is because both RX cooperation and TX & RX cooperation employ the

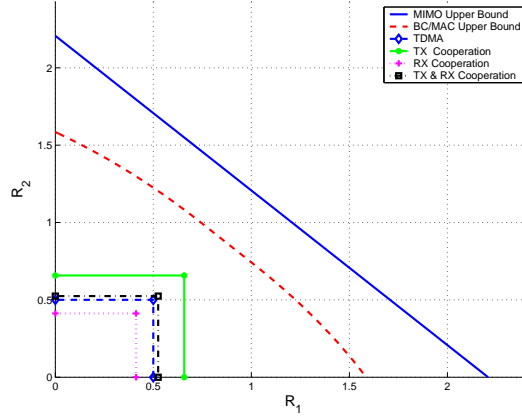


Figure 6.5: Upper bounds and achievable rates for $\text{SNR} = 0$ dB, $G = 10$ dB

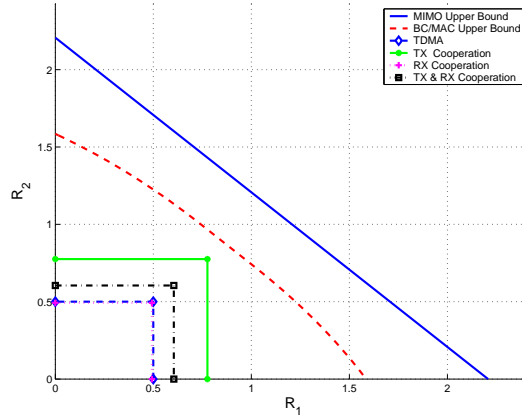


Figure 6.6: Upper bounds and achievable rates for $\text{SNR} = 0$ dB, $G = 20$ dB

amplify-and-forward technique, which forces a great deal of bandwidth to be used for the receiver communication link. When using only TX cooperation, some bandwidth must be allocated, but there is no equal bandwidth requirement as with the amplify-and-forward scheme. Thus, TX cooperation does not do as well under BW assumption 2, but it still provides sizable gains over non-cooperation.

6.9 Summary

In this chapter we quantified the benefits of transmitter and/or receiver cooperation in sensor/ad-hoc network-type settings. This communication setup contained both a multiple-antenna broadcast channel and a multiple antenna multiple-access channel within it, and we were able to make use of some of the earlier results of this thesis. We found that transmitter cooperation or transmitter and receiver cooperation can lead to significant performance improvements in terms of increased data rates. On the other hand, receiver cooperation

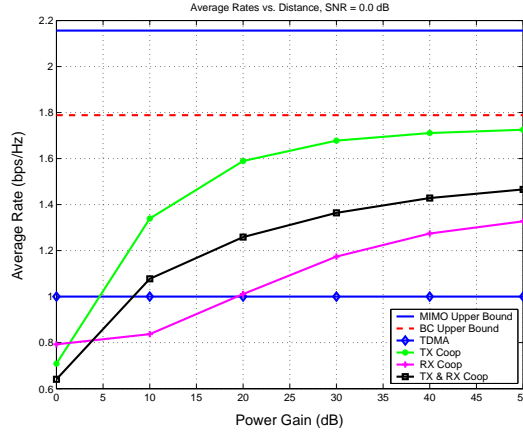


Figure 6.7: Plot of rate vs. gain for SNR = 0 dB, BW assumption 2

without transmitter cooperation does not appear to be very beneficial. Though the model we have worked with in this paper is quite simple, this appears to only be the beginning of a promising line of research examining the benefits of node cooperation.

Chapter 7

Conclusions and Future Work

This thesis has investigated the capacity of multi-user wireless communication channels. In particular, we established a fundamental connection between the two most common multi-user channels, the broadcast channel and the multiple-access channel. This duality relationship is important in and of itself for the insight it gives, but additionally duality leads to a number of interesting results in this thesis. Multiple antenna broadcast channels were also studied, and the duality result played an important role in finding the sum rate capacity of this channel. We also studied the benefit of cooperative communication in an ad-hoc network, and found that transmitter cooperation appears to be an effective way of significantly increasing data rates in such networks.

A large portion of this work concentrated on establishing a relationship between the multiple-access channel and the broadcast channel. This duality relationship was first established for Gaussian versions of the channel, for constant, fading, and multiple antenna channels, and then extended to a class of deterministic, discrete memoryless channels. Duality is of particular importance because it concretely affirms the intuitive similarities between the multiple-access and broadcast channel models. There are a number of interesting and fundamental duality connections in information theory, such as the duality between channel coding and rate distortion [10], source and channel coding [52], and the MAC and Slepian-Wolf region [13, Section 14.5]). It is as of yet unclear if the multiple-access/broadcast channel duality is an equivalently fundamental dual. Given the strong duality between channel coding and rate distortion (i.e lossy source coding) theory, it is also quite possible that there is a more natural duality between the broadcast channel and a distributed source coding problem, or between the multiple-access channel and a multiple description problem. In addition to the insight gained by establishment of duality, we also saw that duality led to a number of important new results for the multiple antenna broadcast channel, and also leads to an expression for the minimum rate capacity region of the fading multiple-access channel.

We also extensively studied multiple user multiple antenna channels, which are of particular importance to increase data rates in next generation wireless systems. Using duality, we were able to establish the optimality of dirty paper coding for the multiple antenna downlink and identify asymptotic regimes in which dirty paper coding provides a particularly large data rate increase over the sub-optimal, albeit more practical, technique of time division multiple access. One surprising conclusion to be drawn from this thesis and related work is that a linear increase in capacity on both the uplink and downlink channels can be achieved by adding multiple base station antennas without adding multiple antennas at mobile devices. This is in stark contrast to point-to-point MIMO channels, in which multiple antennas must be added on both sides to achieve a linear increase in capacity.

Clearly, it is much more economical and practical to add additional antennas (and the corresponding complexity) at wired base stations than at power and space limited mobile terminals. On the downlink channel, dirty paper coding or a sub-optimal technique such as zero-forcing beamforming can be employed to obtain this linear increase. On the uplink channel, multi-user detection is required at the base station. There is, however, the caveat that perfect and instantaneous channel knowledge at all transmitters and receivers (i.e. at the base station and all terminals) has been assumed in establishing these results. Obtaining receiver channel knowledge seems feasible through use of pilot symbols, but transmitter channel knowledge generally requires feedback from the receivers. For multiple-antenna systems, this feedback may require substantial bandwidth and may in fact be difficult to obtain within a fast enough time scale.

If only the receiver has channel knowledge in a downlink channel, then adding multiple base station antennas leads to only a logarithmic, instead of linear, increase in capacity. Thus, it is of great interest to study the large gray area between these two extreme cases, where the receiver has perfect channel knowledge while the transmitter has only partial or imperfect knowledge of the channel. Answering this and related questions will allow us to more fully understand the benefit of adding multiple base station antennas in cellular systems. Interestingly, if each mobile has only a single antenna, then transmitter channel knowledge is not required on the uplink channel. In this situation, since each transmitter has only a single antenna, no adaptation to the channel matrices is necessary and transmission of Gaussian codewords (at the appropriate rate, which may require very limited feedback from the base station) and multi-user detection at the multiple antenna receiver is sufficient to achieve capacity.

We also studied time-varying wireless channels and found optimal power and rate allocation policies for different performance metrics. We first analyzed the minimum rate capacity of the broadcast channel, which is the set of long-term average rates achievable subject to a minimum instantaneous rate in each fading state. We then used the broadcast channel/multiple-access duality to derive the minimum rate capacity region of the

multiple-access channel. In addition to studying minimum rate capacity of the broadcast channel, we also considered the ergodic capacity of the fading broadcast channel in which the transmitter wishes to send a common, or multicast, message in addition to independent messages to each user. We found that the optimal power allocation policy differs significantly from the optimal policy when there is no common message. We also considered the multiple-antenna broadcast channel with common messages, for which the capacity region is unknown. We proposed an extension of the dirty paper coding region to allow for common messages. Given the recent work proving the optimality of dirty paper coding for the multiple antenna broadcast channel without common messages [78], it is natural to ask if this achievable region is the actual capacity region when common messages are added. However, it is easy to see that the proof technique of [78] does not extend to the common message scenario, and thus the optimality of this region is still unclear.

In the final chapter of this thesis we studied the role of cooperation in ad-hoc/sensor networks. We found that relatively simple cooperation schemes, particularly at the transmitter side, can provide rather significant increases in data rates. However, we assumed perfect synchronization and perfect channel knowledge in our model. Neither of these assumptions are very realistic, and thus it is important to study the importance of these assumptions to our results. Synchronization can be obtained in ad-hoc networks, but at a rather large cost of resources such as time and power. Thus consider asynchronous or partially synchronous transmission is an interesting possibility. With regards to channel knowledge, an interesting extension of our work is to consider cooperation in ad-hoc networks without perfect channel information at all transmitters and receivers. Most work in ad-hoc and sensor networks has concentrated on network layer issues such as routing and scheduling, but it is apparent that physical layer issues are of equal importance. A recent paper [26] has studied the physical layer of ad-hoc networks and found that the degree of channel knowledge is crucial in determining optimal transmission strategies, particularly in mobile environments where channels change very rapidly. In such environments, it may not be feasible to track changes in channel conditions and network topology. Thus, it is of critical importance to understand the fundamental limits of ad-hoc networks in such conditions.

Bibliography

- [1] R. Ahlswede. Multi-way communication channels. In *Proceedings 2nd Int. Symp. Information Theory*, pages 23–52, 1973.
- [2] P. Bergmans. A simple converse for broadcast channels with additive white Gaussian noise. *IEEE Trans. Inform. Theory*, 20(2):279 – 280, March 1974.
- [3] D. Bertsekas. *Nonlinear Programming*. Athena Scientific, 1999.
- [4] S. Boyd and L. Vandenberghe. *Introduction to convex optimization with engineering applications*. Course Reader, 2001.
- [5] G. Caire and S. Shamai. On the achievable throughput of a multiantenna Gaussian broadcast channel. *IEEE Trans. Inform. Theory*, 49(7):1691–1706, July 2003.
- [6] G. Caire, G. Taricco, and E. Biglieri. Optimum power control over fading channels. *IEEE Trans. Inform. Theory*, 45(5):1468–1489, July 1999.
- [7] R.S. Cheng and S. Verdu. Gaussian multiaccess channels with ISI: Capacity region and multiuser water-filling. *IEEE Trans. Inform. Theory*, 39(3):773–785, May 1993.
- [8] M. Costa. Writing on dirty paper. *IEEE Trans. Inform. Theory*, 29(3):439–441, May 1983.
- [9] T. Cover. Broadcast channels. *IEEE Trans. Inform. Theory*, 18(1):2–14, Jan. 1972.
- [10] T. Cover and M. Chiang. Duality between channel capacity and rate distortion with two-sided state information. *IEEE Trans. Inform. Theory*, 48(6):1629–1638, June 2002.
- [11] T. Cover and A. El Gamal. Capacity theorems for the relay channel. *IEEE Trans. Inform. Theory*, 25(5):572–584, Sept. 1979.
- [12] T. Cover, A. El Gamal, and M. Salehi. Multiple access channels with arbitrarily correlated sources. *IEEE Trans. Inform. Theory*, 26(6):648–657, Nov 1980.
- [13] T. M. Cover and J. A. Thomas. *Elements of Information Theory*. Wiley, 1991.

- [14] E.C. Van der Muelen. A survey of multiway channels in information theory: 1961-1976. *IEEE Trans. Inform. Theory*, 23:1–37, Jan 1977.
- [15] U. Erez, S. Shamai, and R. Zamir. Capacity and lattice strategies for cancelling known interference. In *Proceedings of Int. Symp. Inform. Theory and its Applications*, pages 681–684, Nov. 2000.
- [16] G. J. Foschini and M. J. Gans. On limits of wireless communications in a fading environment when using multiple antennas. *Wireless Personal Commun. : Kluwer Academic Press*, (6):311–335, 1998.
- [17] R. Gallager. Capacity and coding for degraded broadcast channels. *Problemy Peredachi Informatsii*, 10:3–14, June-Sept 1974.
- [18] A. El Gamal. Capacity of the product and sum of two unmatched broadcast channels. *Probl. Information Transmission*, 6(1):3–23, Jan-March 1980.
- [19] S. I. Gel'fand. Capacity of one broadcast channel. *Probl. Peredachi Inf.*, 13(3):106–108, July-Sept. 1977. Translated in *Probl. Inform. Transm.*, pp. 240-242, July-Sept. 1977.
- [20] A. Goldsmith and P. Varaiya. Capacity of fading channels with channel side information. *IEEE Trans. Inform. Theory*, 43:1986–1992, Nov. 1997.
- [21] A.J. Goldsmith and M. Effros. The capacity region of broadcast channels with intersymbol interference and colored Gaussian noise. *IEEE Trans. Inform. Theory*, 47(1):211–219, Jan. 2001.
- [22] S. Hanly and D.N. Tse. Multiaccess fading channels—Part II: Delay-limited capacities. *IEEE Trans. Inform. Theory*, 44(7):2816–2831, November 1998.
- [23] B. Hochwald, T. L. Marzetta, and V. Tarokh. Multi-antenna channel-hardening and its implications for rate feedback and scheduling. Submitted to *IEEE Trans. Inform. Theory*, 2002, available at <http://mars.bell-labs.com>.
- [24] A. Host-Madsen. A new achievable rate for cooperative diversity based on generalized writing on dirty paper. In *Proceedings of IEEE Int. Symp. Inform. Theory*, page 317, June 2003.
- [25] D. Hughes-Hartog. *The capacity of the degraded spectral Gaussian broadcast channel*. PhD thesis, Stanford University, 1975.
- [26] S. Jafar and A. Goldsmith. Too much mobility limits the capacity of ad-hoc. Submitted to *IEEE Trans. on Information Theory*.

- [27] A. Jalali, R. Padovani, and R. Pankaj. Data throughput of CDMA-HDR: a high efficiency-high data rate personal communication wireless system. In *Proceedings of IEEE Vehicular Tech. Conf.*, May 2000.
- [28] N. Jindal and A. Goldsmith. Dirty paper coding vs. TDMA for MIMO broadcast channels. Submitted to *IEEE Trans. Inform. Theory*, June 2004.
- [29] N. Jindal and A. Goldsmith. Capacity and optimal power allocation for fading broadcast channels with minimum rates. In *Proc. of IEEE Global Commun. Conf.*, pages 1296–1292, November 2001.
- [30] N. Jindal and A. Goldsmith. Capacity and optimal power allocation for fading broadcast channels with minimum rates. *IEEE Trans. Inform. Theory*, 49(11):2895–2909, Nov. 2003.
- [31] N. Jindal and A. Goldsmith. Dirty paper coding vs. TDMA for MIMO broadcast channels. In *Proceedings of Int. Conf. Commun.*, June 2004.
- [32] N. Jindal and A. Goldsmith. Optimal power allocation for parallel broadcast channels with independent and common information. In *Proceedings of Int. Symp. Inform. Theory*, July 2004.
- [33] N. Jindal, S. Jafar, S. Vishwanath, and A. Goldsmith. Sum power iterative water-filling for multi-antenna Gaussian broadcast channels. In *Proceedings of Asilomar Conf. on Signals, Systems, & Comp.*, 2002.
- [34] N. Jindal, U. Mitra, and A. Goldsmith. Capacity of ad-hoc networks with node cooperation. In *Proceedings of Int. Symp. Inform. Theory*, July 2004.
- [35] N. Jindal, S. Vishwanath, and A. Goldsmith. On the duality of multiple-access and broadcast channels. In *Proceedings of Allerton Conf. on Commun., Control, and Comput.*, Oct 2001.
- [36] N. Jindal, S. Vishwanath, and A. Goldsmith. On the duality of Gaussian multiple-access and broadcast channels. In *Proceedings of Int. Symp. Inform. Theory*, page 500, June 2002.
- [37] N. Jindal, S. Vishwanath, and A. Goldsmith. On the duality between general multiple-access/broadcast channels. In *Proceedings of Int. Symp. Inform. Theory*, page 313, July 2003.
- [38] N. Jindal, S. Vishwanath, and A. Goldsmith. On the duality of Gaussian multiple-access and broadcast channels. *IEEE Trans. Inform. Theory*, 50(5):768–783, May 2004.

- [39] E. Jorswieck and H. Boche. Rate balancing for the multi-antenna Gaussian broadcast channel. pages 545–549, 2002.
- [40] N. Laneman, D. N. C. Tse, and G. W. Wornell. Cooperative diversity in wireless networks: Efficient protocols and outage behavior. To appear in *IEEE Trans. Inform. Theory*. Preprint available at <http://www.nd.edu/~jnl/pubs>.
- [41] L. Li and A. Goldsmith. Capacity and optimal resource allocation for fading broadcast channels–Part I: Ergodic capacity. *IEEE Trans. Inform. Theory*, 47(3):1083–1102, March 2001.
- [42] L. Li and A. Goldsmith. Capacity and optimal resource allocation for fading broadcast channels–Part II: Outage capacity. *IEEE Trans. Inform. Theory*, 47(3):1103–1127, March 2001.
- [43] L. Li, N. Jindal, and A. Goldsmith. Outage capacities and optimal power allocation for fading multiple-access channels. Submitted to *IEEE Trans. Inform. Theory*.
- [44] H. Liao. *Multiple access channels*. PhD thesis, Depart. of Electrical Engineering, University of Hawaii, 1972.
- [45] D.G. Luenberger. *Optimization by Vector Space Methods*. Wiley, 1969.
- [46] J. Luo, L. Lin, R. Yates, and P. Spasojevic. Service outage based power and rate allocation. *IEEE Trans. Inform. Theory*, 49(1):323–330, January 2003.
- [47] J. Luo, R. Yates, and P. Spasojevic. Service outage based power and rate allocation for parallel fading channels. In *Proc. of IEEE Global Commun. Conf.*, 2003.
- [48] Jerrold E. Marsden and Michael J. Hoffman. *Elementary Classical Analysis*. W. H. Freeman, 1993.
- [49] K. Marton. The capacity region of deterministic broadcast channels. In *Proceedings of IEEE International Symposium on Information Theory*, 1977.
- [50] K. Marton. A coding theorem for the discrete memoryless broadcast channel. *IEEE Trans. Inform. Theory*, 25(3):306–311, May 1979.
- [51] M.S. Pinsker. Capacity of noiseless broadcast channels. *Probl. Peredachi Inf.*, 14(2):28–34, Apr.-June 1978. Translated in *Probl. Inform. Transm.*, pp. 97-102, Apr.-June 1978.
- [52] S. Pradhan and K. Ramchandran. Duality between source coding and channel coding and its extension to the side information case. *IEEE Trans. Inform. Theory*, 49(5):1181–1203, May 2003.

- [53] B. Rimoldi and R. Urbanke. A rate-splitting approach to the Gaussian multiple-access channel. *IEEE Trans. Inform. Theory*, 42(2):364–375, March 1996.
- [54] M. Rupf and J.L. Massey. Optimum sequence multisets for synchronous code-division multiple-access channels. *IEEE Trans. Inform. Theory*, 40(4):1261 – 1266, July 1994.
- [55] H. Sato. An outer bound on the capacity region of the broadcast channel. *IEEE Trans. Inform. Theory*, 24:374–377, May 1978.
- [56] H. Sato. The capacity of the Gaussian interference channel under strong interference. *IEEE Trans. Inform. Theory*, 27(6):786–788, Nov 1981.
- [57] A. Sendonaris, E. Erkip, and B. Aazhang. User cooperation diversity-part i: system description. *IEEE Trans. Communications*, 51(11):1927–1938, Nov 2003.
- [58] C. Shannon. Two-way communication channels. In *Proceedings of 4th Berkeley Symp. Math. Statist. and Prob.*, 1961. Reprinted in *Key Papers in the Development of Information Theory*, (D. Slepian, Ed.) New York: IEEE Press, 1974, pp. 339-372.
- [59] C. E. Shannon. A mathematical theory of communication. *Bell System Technical Journal*, 27:379 – 423, 623–656, July and October 1948.
- [60] M. Sharif and B. Hassibi. A comparison of time-sharing, DPC, and beamforming for MIMO broadcast channels with many users. Submitted to *IEEE Trans. Commun.*, 2004.
- [61] E. Telatar. Capacity of multi-antenna Gaussian channels. *European Trans. on Telecomm. ETT*, 10(6):585–596, November 1999.
- [62] D.N. Tse and S. Hanly. Multiaccess fading channels–Part I:Polymatroid structure, optimal resource allocation and throughput capacities. *IEEE Trans. Inform. Theory*, 44(7):2796–2815, November 1998.
- [63] D.N.C. Tse. Optimal power allocation over parallel Gaussian broadcast channels. *IEEE Trans. Inform. Theory*, 1998. Submitted for publication.
- [64] L. Vandenberghe, S. Boyd, and S.P. Wu. Determinant maximization with linear matrix inequality constraints. *SIAM Journal on Matrix Anal. and Appl.*, 19(2):499–533, 1998.
- [65] S. Venkatesan and H. Huang. System capacity evaluation of multiple antenna systems using beamforming and dirty paper coding. unpublished manuscript.
- [66] S. Verdú. Multiple-access channels with memory with and without frame synchronism. *IEEE Trans. Inform. Theory*, 35(3):605–619, May 1989.

- [67] S. Vishwanath, S. Jafar, and A. Goldsmith. Optimum power and rate allocation strategies for multiple access fading channels. In *Proceedings of Vehicular Tech. Conf.*, pages 2888–2892, May 2000.
- [68] S. Vishwanath, N. Jindal, and A. Goldsmith. On the capacity of multiple input multiple output broadcast channels. In *Proceedings of Int. Conf. Commun.*, pages 1444–1450, April 2002.
- [69] S. Vishwanath, N. Jindal, and A. Goldsmith. Duality, achievable rates, and sum-rate capacity of MIMO broadcast channels. *IEEE Trans. Inform. Theory*, 49(10):2658–2668, Oct. 2003.
- [70] S. Vishwanath, G. Kramer, S. Shamai(Shitz), S. A. Jafar, and A. Goldsmith. Outer bounds for multi-antenna broadcast channels. In *Proceedings of DIMACS workshop on Sig. Proc. for Wireless Commun.*, Sept. 2002.
- [71] S. Vishwanath, W. Rhee, N. Jindal, S.A. Jafar, and A. Goldsmith. Sum power iterative water-filling for gaussian vector broadcast channels. In *Proceedings of Int. Symp. Inform. Theory*, page 467, July 2003.
- [72] P. Viswanath and D. Tse. On the capacity of the multi-antenna broadcast channel. In *Proceedings of DIMACS workshop on Sig. Proc. for Wireless Commun.*, Sept. 2002.
- [73] P. Viswanath and D. N. Tse. Sum capacity of the vector Gaussian broadcast channel and uplink-downlink duality. *IEEE Trans. Inform. Theory*, 49(8):1912–1921, Aug. 2003.
- [74] H. Viswanathan and K. Kumaran. Rate scheduling in multiple antenna downlink wireless systems. *Lucent Technical Memorandum*, Document No. ITD-01-41685K.
- [75] H. Viswanathan and S. Venkatesan. Asymptotics of sum rate for dirty paper coding and beamforming in multiple-antenna broadcast channels. In *Proceedings of Allerton Conf. on Commun., Control, and Comput.*, Oct. 2003.
- [76] H. Viswanathan, S. Venkatesan, and H. C. Huang. Downlink capacity evaluation of cellular networks with known interference cancellation. *IEEE J. Sel. Areas Commun.*, 21:802–811, June 2003.
- [77] H. Weingarten, Y. Steinberg, and S. Shamai. Capacity region of the degraded mimo broadcast channel. In *Proceedings of Int. Symp. Inform. Theory*, July 2004.
- [78] H. Weingarten, Y. Steinberg, and S. Shamai. The capacity region of the Gaussian MIMO broadcast channel. In *Proceedings of Conference on Information Sciences and Systems*, March 2004.

- [79] J. Wolfowitz. *Coding Theorems of Information Theory*. Springer-Verlang, 1964.
- [80] K. Yazdi, H. El Gamal, and P. Schitner. On the design of cooperative transmission schemes. In *Proceedings of Allerton Commun., Computing, and Control*, Oct 2003.
- [81] W. Yu and J. Cioffi. Trellis precoding for the broadcast channel. In *Proceedings of Global Commun. Conf.*, pages 1344–1348, Oct. 2001.
- [82] W. Yu and J. M. Cioffi. Sum capacity of a Gaussian vector broadcast channel. In *Proc. of Int. Symp. Inform. Theory*, page 498, June 2002.
- [83] W. Yu, W. Rhee, S. Boyd, and J. Cioffi. Iterative water-filling for vector multiple access channels. In *Proceedings of IEEE International Symposium on Information Theory*, page 322, 2001.
- [84] W. Yu, W. Rhee, S. Boyd, and J. Cioffi. Iterative water-filling for Gaussian vector multiple access channels. *IEEE Trans. Inform. Theory*, 50(1):145–152, Jan. 2004.
- [85] W. Zangwill. *Nonlinear Programming: A Unified Approach*. Prentice Hall, 1969.